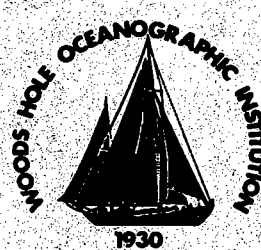


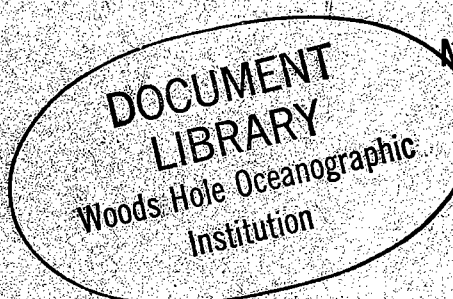
Woods Hole Oceanographic Institution



SOFAR Float Trajectories from an Experiment to Measure the Atlantic Cross Equatorial Flow (1989–1990)

by

Philip L. Richardson
Marguerite E. Zemanovic
Christine M. Wooding
William J. Schmitz, Jr.
and
James F. Price



August 1992

Technical Report

Funding was provided by the National Science Foundation through Grant Nos.

OCE-8521082, OCE-8517375, and OCE-9114656.

Approved for public release; distribution unlimited.

WHOI-92-33

**SOFAR Float Trajectories from an Experiment to Measure
the Atlantic Cross Equatorial Flow (1989-1990)**

by

Philip L. Richardson
Marguerite E. Zemanovic
Christine M. Wooding
William J. Schmitz, Jr.
and
James F. Price

Woods Hole Oceanographic Institution
Woods Hole, Massachusetts 02543



August 1992

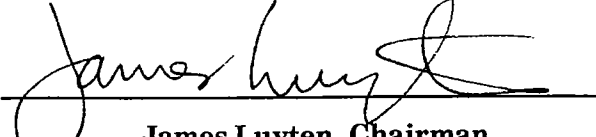
Technical Report

Funding was provided by the National Science Foundation through Grant Nos.
OCE-8521082, OCE-8517375, and OCE-9114656.

Reproduction in whole or in part is permitted for any purpose of the
United States Government. This report should be cited as:
Woods Hole Oceanog. Inst. Tech. Rept., WHOI-92-33.

Approved for publication; distribution unlimited.

Approved for Distribution:



A handwritten signature of James Luyten is written over a horizontal line. Below the signature, the text "James Luyten, Chairman" and "Department of Physical Oceanography" is printed.

James Luyten, Chairman
Department of Physical Oceanography



Abstract

Neutrally buoyant SOFAR floats at nominal depths of 800, 1800, and 3300 m were tracked for 21 months in the vicinity of western boundary currents near 6N and at several sites in the Atlantic near 11N and along the equator. Trajectories at 1800 m show a swift (> 50 cm/sec), narrow (100 km wide) southward-flowing deep western boundary current (DWBC) extending from 7N to the equator. At times (February–March 1989) DWBC water turned eastward and flowed along the equator and at other times (August–September 1990) the DWBC crossed the equator and continued southward. The mean velocity near the equator was eastward from February 1989 to February 1990 and westward from March 1990 to November 1990. Thus the cross-equatorial flow in the DWBC appeared to be linked to the direction of equatorial currents which varied over periods of more than a year. No obvious DWBC nor swift equatorial current was observed by 3300 m floats.

Eight-hundred-meter floats revealed a northwestward intermediate level western boundary current although flow patterns were complicated. Three floats that significantly contributed to the northwestward flow looped in anticyclonic eddies that translated up the coast at 8 cm/sec. Six 800 m floats drifted eastward along the equator between 5S and 6N at a mean velocity of 11 cm/sec; one reached 5W in the Gulf of Guinea, suggesting that the equatorial current extended at least 35–40° along the equator. Three of these floats reversed direction near the end of the tracking period, implying low frequency fluctuations.

Contents

Abstract	i
1 Introduction	1
2 Methods	2
a) Temperature and pressure	2
b) Groundings	7
c) Float tracking and data processing	9
3 1800 m Trajectories	9
a) Deep Western Boundary Current (DWBC) trajectories	9
b) DWBC velocity	15
c) DWBC recirculation	19
d) Equatorial currents	19
e) DWBC-equatorial current connection	21
4 3300 m Trajectories	25
5 800 m Trajectories	25
a) Intermediate Western Boundary Current (IWBC)	25
b) Anticyclonic eddies	30
c) Equatorial currents at 800 m	30
d) Reversal	30
e) Southward velocity	35
f) IWBC-equatorial current connection at 800 m	35
6 Summary and Conclusions	35
Acknowledgments	37
References	38
Appendix A: Summary Composites of Trajectories	39
Appendix B: Plots of Individual Floats	63

List of Tables

I	Summary of SOFAR float data	4
II	Autonomous Listening Station (ALS) moorings	6
III	Slow sinking rate of SOFAR floats	8
IV	Differences between launch position and first tracked position	10
V	Summary of 1800 m deep western boundary current observations . .	18
VI	Northwestward intermediate western boundary current at 800 m . .	29
VII	Summary of eddy characteristics estimated from looping float trajectories at 800 m	33

List of Figures

1	Launch locations of SOFAR floats and Autonomous Listening Stations during January–February 1989	3
2	Summary of 1800 m SOFAR float trajectories and overall displacement vectors	12
3	Individual 1800 m float trajectories along the western boundary	13
4	Summary of 1800 m western boundary current trajectories	14
5	Segments of 1800 m trajectories of floats that drifted faster than 20 cm/sec	16
6	Average along-boundary velocity, transport, and eddy kinetic energy at 1800 m in the vicinity of the deep western boundary current (DWBC), west of 43W	17
7	Profile of velocity (cm/sec) as a function of pressure measured on 17 January 1989 at 0N, 30W	20
8	Individual 1800 m float trajectories along the equator from January 1989 to November 1990	22
9	Time series of 1800 m eastward velocity along the equator	23
10	Schematic diagrams summarizing the 21 months of 1800 m float data	24
11	Summary of 3300 m float trajectories and displacement vectors from January 1989 to October 1990	26
12	Summary of 800 m trajectories and displacement vectors	27
13	Trajectories of four 800 m floats	28
14	Trajectories of 800 m floats trapped in eddies and trajectories of the eddies	31
15	Trajectories of six 800 m floats that drifted eastward in equatorial currents	34
16	Schematic diagram summarizing the 21 months of 800 m float data .	36

1 Introduction

This report describes SOFAR float trajectories in the equatorial Atlantic at depths of 800 m in the Antarctic Intermediate Water and at 1800 m and 3300 m in the North Atlantic Deep Water. The fundamental issue investigated is the exchange of water between the North and South Atlantic Oceans. Water mass properties including freon imply that deep western boundary current (DWBC) water splits near the equator, with part flowing eastward along the equator and part continuing southward along the western boundary. It was not known to what extent the tongue of freon lying along the equator near 1700 m is due to advection or to enhanced mixing. Thus a secondary issue investigated is the nature of the connection between the DWBC and flow along the equator.

The DWBC is the major pathway by which cold deep water flows southward into the South Atlantic and, eventually, into the Pacific and Indian Oceans. The warm upper layer in the Atlantic, including the intermediate water, is thought to flow northward in compensation for the deep water. Schmitz and Richardson (1991) have identified $13 \times 10^6 \text{ m}^3/\text{s}$ of upper level water from the South Atlantic flowing northward across the equator into the Gulf Stream. Neither flow had previously been directly measured crossing the equator. This large-scale thermohaline circulation results in a northward heat flux through the Atlantic which is important for world climate. An improved understanding of the thermohaline circulation and its variability is required in order to design a scheme to measure variations in the meridional flux of heat in the oceans and variations in climate.

The results described here are the first subsurface float trajectories in this region. They reveal new information concerning the thermohaline circulation, including a swift, $\sim 50 \text{ cm/sec}$, southward-flowing DWBC at 1800 m that at times feeds into an eastward equatorial current and at other times crosses the equator directly. These data provide a first direct measurement of the cross-equatorial flow of deep water and its complex patterns. Some floats at 800 m and 1800 m drifted long distances along the equator, up to 38° of longitude, and give a first Lagrangian view of these equatorial currents and their connections to the currents along the western boundary.

The report is divided into two main parts. The first follows this introduction and summarizes the whole experiment. The second part consists of two appendices that show some summary composites of trajectories (Appendix A) and plots of individual floats (Appendix B).

2 Methods

During January and February 1989, 48 SOFAR floats were launched in the tropical Atlantic, 14 at 800 m in the intermediate water, 15 at 1800 m and 15 at 3300 m in the deep water, and 4 by J. Price as engineering tests of a Bobber float, at depths near 300 and 650 db (Figure 1, Tables I and II). The floats were tracked acoustically from January 1989 to November 1990 by means of an array of six moored autonomous listening stations. See Table I for the dates during which each float was tracked. Float tracking is continuing for an additional two years. Thirty-one of the floats were launched along a line spanning the Atlantic between 6N and 11N, with closest spacing between floats near the western boundary off French Guiana, where the velocity is swiftest. Seventeen floats were launched along the equator in the west, where meridional flow is thought to cross the equator and eastward flow along the equator originates. Thus the whole width of the Atlantic between French Guiana and West Africa was instrumented with floats, although sparsely in the eastern region.

All but two of the 800 m and 1800 m floats were tracked for the full 21 months and were heard out to ranges of 3000 km (Table I). One float (28) entered the Caribbean and another (34) faded after six months. Six of the 3300 m floats were never heard, two due to a reduced range of around 1000 km there, four due to unexplained failures. The mean trackable lifetime of 3300 m floats was around a year due to their gradually sinking toward the lower limit of the sound channel. Most of the deep floats that were tracked could be heard by at least one listening station up to October 1990.

a) Temperature and pressure

All floats except the four Bobbers failed to transmit correct temperature and pressure data after they had equilibrated, and they also failed to activate their buoyancy control which keeps them at constant pressure. In order to estimate equilibrium depths at sea, two floats at each level were followed acoustically from the ship as they sank. The floats at the 800 db level equilibrated at 795 db and 800 db; those at the 1800 db level equilibrated at 1825 db and 1770 db. Two deep floats were followed down to 2570 db and 2860 db where their telemetry stopped. An extrapolation of their data to equilibrium pressure showed that the floats reached 3255 db and 3250 db. In the following, the three equilibrium pressures will be referred to as 800 m, 1800 m, and 3300 m, but individual floats could have differed from these nominal depths.

TROPICAL ATLANTIC SOFAR FLOAT EXPERIMENT

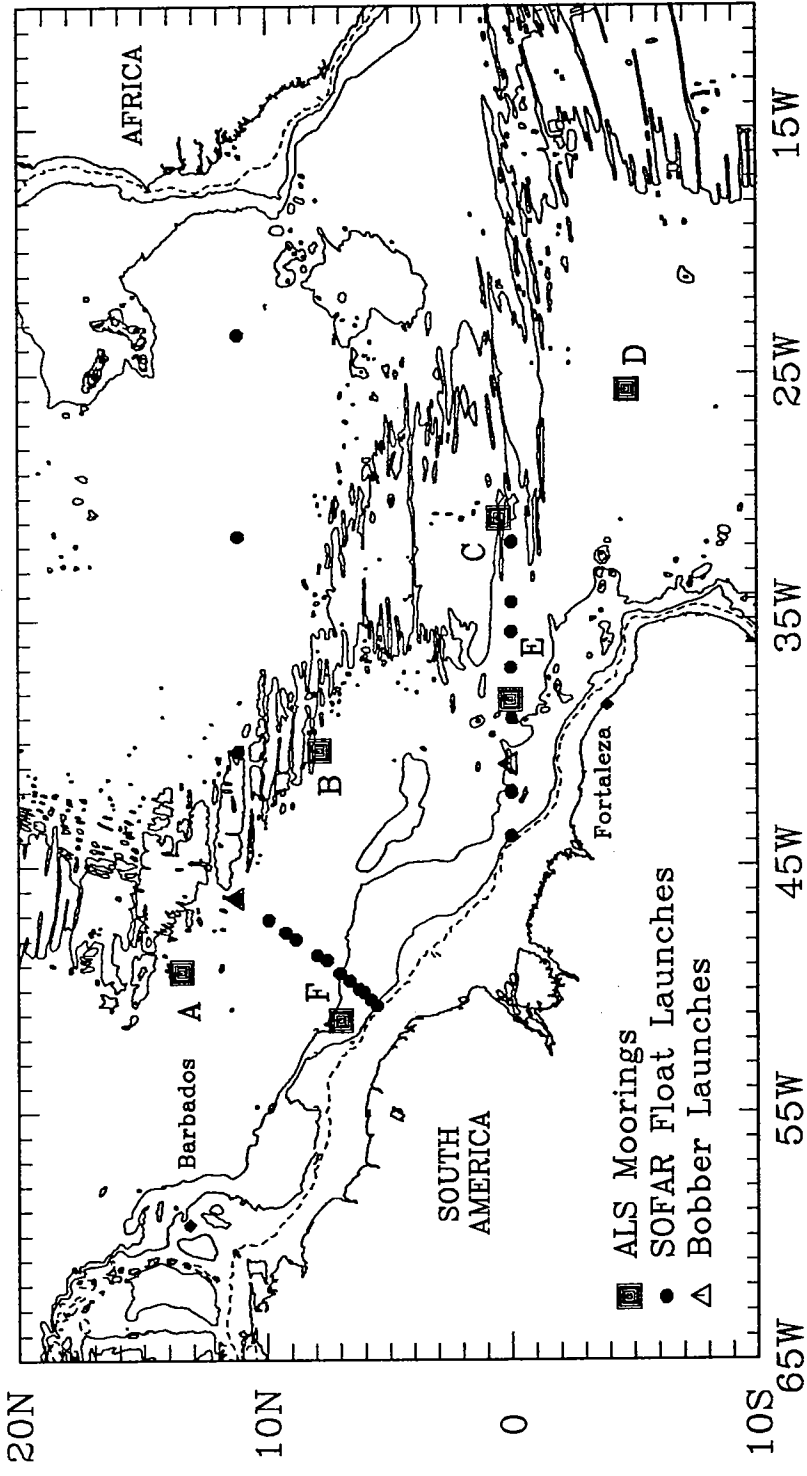


Figure 1: Launch locations of SOFAR floats and Autonomous Listening Stations (ALS) during January–February 1989. Depth contours are from Uchupi (1971): 200 m is dashed, 2000 m and 4000 m are solid lines.

Table I: Summary of SOFAR Float Data^a

Float ID	Pressure (db) ^b	Launch		End		Number of Days Tracked	Mean Velocity (cm/sec) \bar{v}			
		Date yymmdd	Lat. deg. N	Date yymmdd	Lat. deg. N					
1) 800 m Floats										
a) Equatorial										
16	(800)	890125	00.01	43.83	901107	-06.10	28.96			
31	800	890125	00.01	42.01	901102	00.94	36.32			
B63	450-850	890124	00.05	40.94	901030	09.97	49.93			
B62	200-500	890124	00.04	40.86	890827	01.42	42.58			
28	795	890123	00.00	39.00	900422	12.19	61.19			
34	(800)	890122	00.00	35.50	890725	-03.67	19.41			
24	1125 ^c	890121	00.00	31.81	901030	-01.93	09.92			
b) IWBC/Line										
25	(800)	890205	05.52	50.62	901102	03.74	45.34			
21	(800)	890205	05.78	50.40	900928	05.74	48.96			
23	(800)	890206	06.04	50.09	901102	11.55	56.60			
22	(800)	890206	06.62	49.61	901102	15.37	58.72			
20	(800)	890207	07.54	48.78	901030	07.54	44.09			
26	(800)	890207	09.23	47.67	901107	03.32	14.46			
B12	250-350	890208	11.20	46.29	890714	07.30	44.82			
B81	550-700	890208	11.21	46.29	891230	09.94	59.60			
19	(800)	890209	11.15	40.36	901024	05.43	25.83			
18	(800)	890213	11.17	31.57	901111	11.37	34.73			
17	(800)	890215	11.18	23.40	901107	11.40	18.79			
2) 1800 m Floats										
a) Equatorial										
9	(1800)	890125	00.01	43.82	901108	-00.35	31.32			
6	1775	890125	00.01	42.08	901012	-02.77	38.79			
1	1825	890123	00.00	39.03	901103	00.70	17.73			
3 ^d	(1800)	890122	00.01	35.51	—	—	—			
15	(1800)	890121	00.01	31.84	901101	00.14	39.60			

Float ID	Pressure (db) ^b	Launch		End		Number of Days Tracked	Mean Velocity (cm/sec) \bar{v}
		Date yymmdd	Lat. deg. N	Date yymmdd	Lat. deg. N		
2) 1800 m Floats (cont.)							
b) DWBC/Line	10 ^e	(1800)	890205	05.52	50.62	890329	04.41
5	(1800)	890205	05.77	50.39	901102	00.71	48.60
14	(1800)	890206	06.04	50.09	901102	05.98	45.70
2	(1800)	890206	06.63	49.61	901112	-03.26	36.43
8	(1800)	890207	07.54	48.78	901106	-03.95	36.37
13	(1800)	890207	09.23	47.67	901030	03.71	45.63
11	(1800)	890208	11.20	46.30	901106	09.43	46.31
4	(1800)	890209	11.15	40.36	901103	06.93	47.51
12	(1800)	890213	11.17	31.57	901112	10.65	30.82
7	(1800)	890215	11.18	23.40	901112	11.95	25.08
3) 3300 m Floats							
a) Equatorial	41 ^f	(3300)	890125	00.02	42.01	—	—
30	(3300)	890123	00.00	39.02	900925	-04.59	34.66
45	(3300)	890123	00.03	36.95	891017	-01.13	36.71
35	3250	890122	00.00	34.29	901028	00.32	32.95
38	(3300)	890121	-00.01	31.79	900521	-01.46	34.18
b) DWBC/Line							
42	3255	890206	06.25	49.96	891021	07.82	50.93
39	(3300)	890206	06.63	49.62	891205	05.52	46.19
40	(3300)	890206	07.02	49.31	900213	08.81	45.82
36	(3300)	890207	07.95	48.59	890930	09.24	51.04
29 ^f	(3300)	890207	08.82	47.95	—	—	—
37 ^f	(3300)	890207	09.92	47.17	—	—	—
43 ^f	(3300)	890208	11.20	46.29	—	—	—
44	(3300)	890209	11.15	40.37	890522	11.15	41.15
33 ^f	(3300)	890213	11.17	31.57	—	—	—
32 ^f	(3300)	890215	11.18	23.40	—	—	—
						total	57.9 years

a) Floats are sorted by pressure, general location, then by longitude.

b) Initial float pressure was observed for two floats at each level. The range in pressure is given for the four Bobber floats. Target pressures of other floats are shown in parentheses.

c) Ballasted deep to lie in the eastward current jet.

d) Not tracked due to the acoustic signal being overwhelmed by a simultaneous test signal in each listening station.

e) Grounded on continental slope.

f) Never heard by listening stations.

Table II: Autonomous Listening Station (ALS) Moorings

ALS Site	ALS #	ALS Depth (m)	Launch Date yymmdd	Recovery Date yymmdd	Latitude deg. N	Longitude deg. W
A	160A	950	890109	901030	13.453	49.260
B	161A	815	890112	901102	7.845	40.345
C	162A	645	890117	901119	0.519	30.848
D	163A	751	890119	901108	-4.711	25.667
E	164A	751	890123	901112	0.034	38.276
F	159A	756	890108	901028	6.980	51.235

All ALSs functioned normally except for 159A which failed electronically on 890816.

To determine the equilibrium pressure of the deep floats, the linear regression between the square of the float's vertical velocity and the pressure was used to estimate the pressure at the point of zero velocity. Vertical velocity was calculated from the pressure time series telemetered from the floats as they descended. This method assumed that at any instant the drag force on a float, given by $\rho/2(C_D A W^2)$ where C_D is the drag coefficient, A is the area, ρ is the water density, and W is vertical velocity, is balanced by the negative buoyancy force on the float, which is proportional to its height above equilibrium pressure. Calculations using a characteristic CTD profile in the tropical Atlantic show that the negative buoyancy of a deep float is approximately linear from its equilibrium pressure up to a pressure of around 1000 db. The drag coefficient of spheres vs Reynold number is nearly constant over virtually the entire range of vertical velocities experienced by the floats as they descended.

Without active ballasting, SOFAR floats gradually sink due to the slow deformation of their pressure housing, which is aluminum for 800 m and 1800 m floats and glass for 3300 m floats. In order to estimate this sink rate, all available historical float data were examined. Ten aluminum floats and five glass floats were found to give reliable estimates of the long-term sink rate (Table III). The low number is because (1) most floats actively adjusted their buoyancy to maintain a constant pressure, (2) most floats were ballasted too deep and rose toward their target pressure, and (3) many floats were near the Gulf Stream where their pressure varied in time due to the vertical heaving of the water column, which made estimating the sink rate difficult.

The mean sink rate and standard error of aluminum floats was 0.37 ± 0.05 db/d. No obvious relationship was seen between their sink rate and the pressure level, which suggests that the mean sink rate is appropriate for all depths. The mean rate implies that the 800 m and 1800 m floats would have sunk around 230 m over the 21 months discussed here. The mean sink rate of the glass floats was 0.62 ± 0.11 db/d, which implies that the 3300 m floats would have sunk around 220 m over their mean lifetime of 12 months. The gradually decreasing acoustic range observed with the 3300 m floats is inferred to be due to their gradual sinking toward the lower limit of the sound channel.

b) Groundings

A few 1800 m floats on the inshore edge of the DWBC drifted into water shallower than their equilibrium depth and probably dragged along the sea floor. One of these (float 10) clearly went aground after 51 days and remained stuck for the rest of the 21 months. The speed of a few of these DWBC floats seemed to decrease as they

Table III: Slow Sinking Rate of SOFAR Floats

<i>Aluminum floats</i>			
Float ID	Pressure (db)	Days in water	Sink Rate (db/d) ^a
GU 162	2000	278	0.18
GU 156	2000	260	0.36
LD 62	700	147	0.37
GU 167	2000	120	0.22
LD 86	1300	92	0.41
MO 10	1500	72	0.69
LD 51	1300	69	0.22
MO 5	1500	58	0.48
MO 2	1500	52	0.39
LD 65	700	32	0.42
average			0.37±0.05 ^b

<i>Glass floats</i>			
Float ID	Pressure (db)	Days in water	Sink Rate (db/d) ^c
MA 24	2500	1320	0.32
MA 25	2500	1240	0.46
MA 22	2500	740	0.74
MA 26	2500	740	0.70
MA 63	2500	320	0.93
average			0.62 ± 0.11 ^d

- a) Around half of the aluminum floats exhibited a somewhat decreasing sink rate with time. For these, the slower sink rate is given since this would seem to be the best estimate of the long term rate. Only floats that sank longer than 30 days were included because of this variable rate. The wall thickness of the aluminum tubes was 1.59 cm for shallow ones (< 1000 db) and 1.90 cm for deep ones (> 1000) db.
- b) The standard deviation of values is 0.15 db/d and the standard error is 0.05 db/d.
- c) The glass float's sinking rate deviated in curious ways from a constant rate (Rees and Gould, personal communication).
- d) The standard deviation of values is 0.24 db/d and the standard error is 0.11 db/d. The data imply that the longer a float is in the water the slower its sink rate, which results from slower sinking floats taking longer to reach equilibrium pressure than faster sinking ones.

drifted landward, probably due to both friction as the floats dragged on the sea floor and reduced near-bottom water velocity.

The ability of a float to drag upslope along the bottom into water shallower than the equilibrium depth can be understood by a simple calculation. Imagine an 1800 m float that is carried upslope along the sea floor to 1300 db where the float is approximately 0.5 kg negatively buoyant. If we assume that the drag of the sea floor on the bottom of a drifting float is equal to this value, that the float remains vertical, and that its drag coefficient is 1.0, then an average water velocity of \sim 7 cm/sec past the float will provide sufficient drag to force it to drift.

c) Float tracking and data processing

The floats transmitted an 80 sec 250 Hz acoustic signal once per day. Float clock corrections and positions were calculated from the times of arrival of signals received at the moored listening stations. Spurious positions were edited manually, gaps less than 10 days long were linearly interpolated, and the resulting time series were smoothed by means of a Gaussian shaped filter (of weights 0.054, 0.245, 0.403, 0.245, and 0.054) to reduce position errors and tidal and inertial fluctuations. Velocity along trajectories was calculated at each final position by means of a cubic spline function. The average accuracy of a fix was estimated to be less than 10 km based on a comparison of float launch locations and first tracked positions (Table IV).

3 1800 m Trajectories

A summary plot (Figure 2) of 1800 m trajectories shows strikingly different kinds of trajectories in different regions. Eight of the fifteen floats drifted southeastward for various lengths of time in a fast (50–60 cm/sec), narrow (\sim 100 km), deep western boundary current (DWBC). Five floats drifted long eastward distances, up to 25° of longitude, within a few degrees of the equator. Compared to these, the two floats in the eastern Atlantic near 11° N barely moved.

a) DWBC trajectories

The best evidence for a narrow, swift DWBC comes from the first two months, February and March 1989, when three floats (10, 14, and 5) drifted southward (Figures 3, 4). Float 10 grounded on the continental slope after 51 days; the two others reached the equator. Float 14 returned northward and ended up near the

Table IV: Differences Between Launch Position And First Tracked Position

Float	Launch Information			First Tracked Position			Pos. Diff. km.	Lat. Diff. deg.	Long. Diff. deg.	Time Diff. hrs.	Initial Clk. Err. secs.	
	Date ymmdd	Time hhmm	Lat. deg. N	Long. deg. W	Date ymmdd	Time hhmm	Lat. deg. N	Long. deg. W	Pos. Diff. km.	Lat. Diff. deg.	Long. Diff. deg.	
01	890123	2220	0.00	39.03	890126	1	-0.39	38.84	48.7	29.7	0.26	-0.06
02	890206	1524	6.63	49.61	890208	21	6.72	49.47	19.2	17.2	-0.01	-0.15
04	890209	2021	11.15	40.36	890210	101	11.13	40.36	2.0	1.5	0.01	0.00
05	890205	2015	5.77	50.39	890206	121	5.76	50.39	1.6	3.1	-0.02	0.01
06	890125	907	0.01	42.08	890126	141	0.10	41.98	14.8	8.6	-0.07	-0.03
07	890215	2141	11.18	23.40	890216	201	11.30	23.18	27.4	26.9	-0.11	-0.22
08	890207	36	7.54	48.78	890207	221	7.58	48.81	5.2	5.2	-0.03	0.03
09	890125	1945	0.01	43.81	890126	241	-0.02	43.67	16.6	8.3	-0.05	-0.06
10	890205	1743	5.52	50.62	890206	301	5.46	50.56	8.6	1.9	-0.01	0.02
11	890208	809	11.20	46.30	890209	321	11.25	46.17	14.8	12.9	-0.08	-0.09
12	890213	1936	11.17	31.57	890214	341	11.15	31.60	4.4	4.0	0.03	0.03
13	890207	1555	9.23	47.67	890208	401	9.26	47.71	6.0	4.7	-0.01	0.04
14	890206	209	6.04	50.09	890206	421	6.05	50.13	4.0	5.0	-0.01	0.04
15	890121	1910	0.01	31.84	890122	441	-0.05	31.89	9.1	12.2	0.09	0.07
16	890125	2005	0.01	43.83	890126	501	0.08	43.91	12.0	14.0	-0.09	0.09
17	890215	2152	11.18	23.40	890216	521	11.23	23.20	22.8	22.3	-0.05	-0.20
18	890213	1921	11.17	31.57	890214	541	11.14	31.57	3.8	5.6	0.04	-0.02
19	890209	2006	11.15	40.36	890210	601	11.14	40.35	2.4	2.8	0.00	-0.03
20	890207	111	7.54	48.78	890207	621	7.55	48.76	2.5	3.0	-0.02	-0.01
21	890205	2145	5.78	50.40	890207	641	5.86	50.47	11.8	16.4	-0.15	-0.02
22	890206	1543	6.62	49.61	890207	701	6.59	49.60	3.6	6.6	-0.05	-0.04
23	890206	223	6.04	50.09	890206	721	6.06	50.17	8.5	6.7	-0.03	0.05
24	890121	1655	0.00	31.81	890124	741	0.13	31.42	46.1	28.3	-0.23	-0.10
25	890205	1758	5.52	50.62	890206	801	5.55	50.66	5.4	4.9	-0.04	0.03
26	890207	1537	9.23	47.67	890208	821	9.26	47.75	10.1	7.5	0.02	0.07

Table IV: (continued)

Float	Launch Information			First Tracked Position			Pos.	Est.	Lat.	Long.	Time	Initial
	Date yymmdd	Time hhmm	Lat. deg. N	Long. deg. W	Date yyymmdd	Time hhmm	Lat. deg. N	Long. deg. W	Diff. km.	Diff. deg.	Diff. hrs.	Clik. Err. secs.
28	890123	2104	0.00	39.00	890124	901	0.05	39.12	14.4	6.2	-0.04	0.04
30	890123	2117	0.00	39.02	890128	941	0.25	38.94	28.5	44.9	-0.38	-0.13
31	890125	725	0.01	42.01	890125	1001	0.10	42.01	9.8	10.0	-0.09	0.00
34	890122	2012	0.00	35.50	890124	1101	-0.11	35.42	14.8	2.5	0.00	-0.02
35	890122	941	0.00	34.29	890123	1121	-0.05	34.29	5.3	14.2	0.09	0.09
36	890207	439	7.95	48.59	890207	1141	8.00	48.64	7.9	7.3	-0.05	0.05
38	890121	1427	0.015	31.79	890123	1221	-0.01	31.79	0.6	2.1	-0.02	0.01
39	890206	1457	6.63	49.62	890207	1241	6.69	49.59	6.9	7.3	-0.06	0.03
40	890206	1937	7.02	49.31	890207	1301	7.07	49.28	6.5	6.2	-0.05	-0.02
42	890206	610	6.25	49.96	890206	1341	6.28	49.90	6.6	5.2	-0.03	0.03
												7.5
												-1.3
44	890209	1941	11.15	40.37	890212	1421	11.27	40.29	15.7	29.7	-0.24	-0.11
45	890123	720	0.03	36.95	890123	1441	0.10	36.94	7.6	8.1	-0.07	-0.01
B12	890208	901	11.20	46.29	890208	1501	11.21	46.30	1.1	1.9	-0.02	0.00
B62	890124	1046	0.04	40.87	890125	1541	0.15	40.78	15.4	7.3	0.00	-0.07
B63	890124	2004	0.05	40.94	890126	1601	0.19	40.71	30.0	9.8	-0.01	-0.09
B81	890208	824	11.21	46.29	890208	1621	11.19	46.30	2.0	1.5	0.01	0.01
												8.0
												-2.9
Average differences												
												20.0
												11.8 10.3

The average difference between the launch position and the first tracked position for all floats is 11.8 km. The floats with the largest difference in positions often have large differences in time between launch and first tracked position. When we include only those floats whose first position falls within 24 hours of the time of launch, the average difference in position is reduced to 8.3 km. The difference is reduced further to 7.4 km when the position at the time of launch, estimated from the first two tracked positions, is used. Thus a significant part of the mean difference in position for all floats is due to the float drift between launch and first tracked position. An additional part of the average difference is due to the inaccuracy of the estimated launch positions which were based on GPS fixes, satellite navigation fixes, and dead reckoning between satellite fixes.

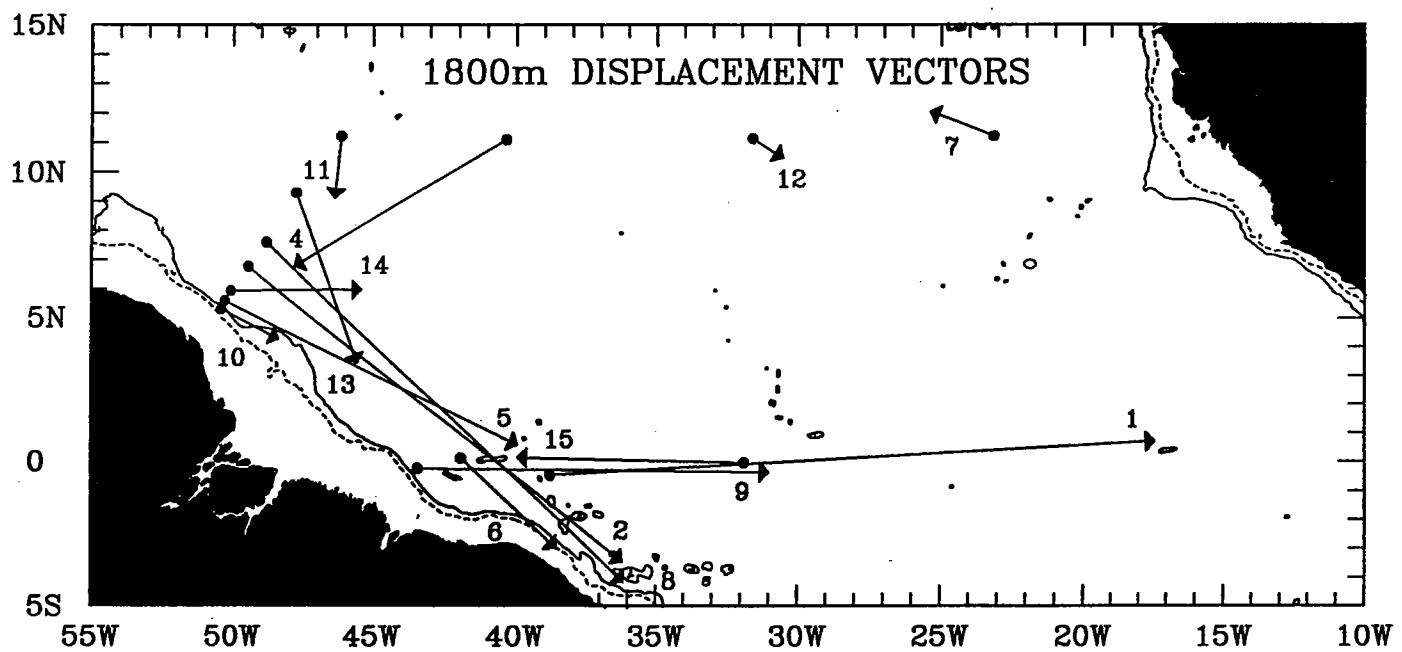
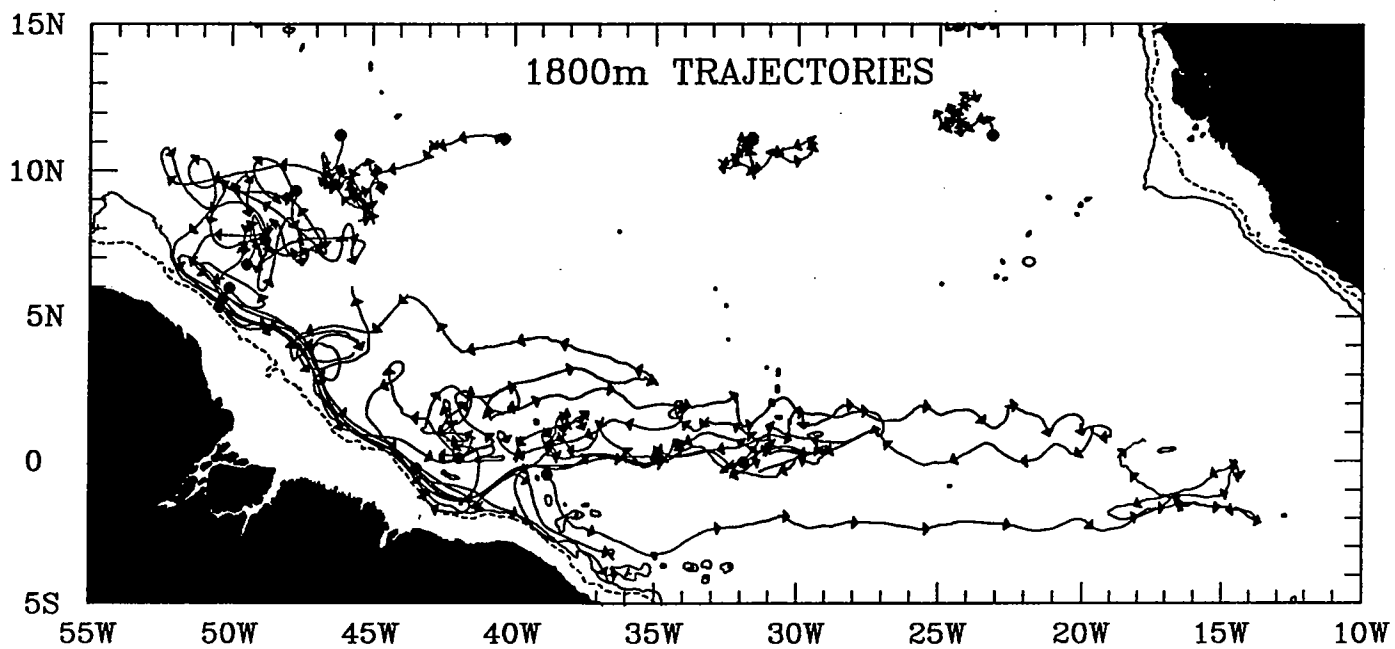


Figure 2: Summary of 1800 m SOFAR float trajectories and overall displacement vectors from January 1989 to November 1990. Arrowheads are spaced at intervals of 30 days along trajectories.

1800m WESTERN BOUNDARY CURRENT TRAJECTORIES

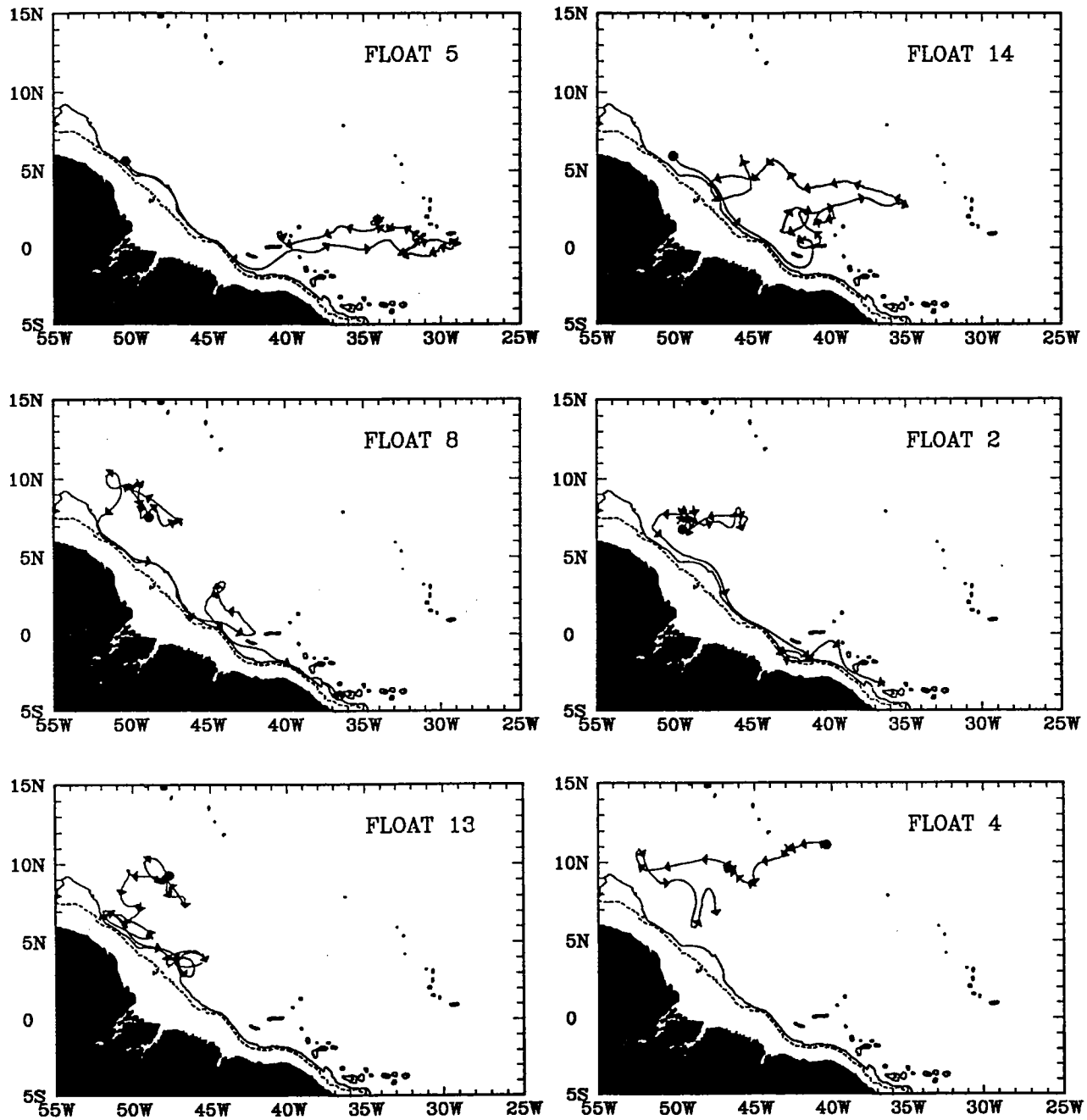


Figure 3: Individual 1800 m float trajectories along the western boundary from January 1989 to November 1990. Arrowheads are spaced at 30 day intervals. Upper panels show floats 5 and 14 launched directly into the DWBC in early February 1989. Middle panels show floats 2 and 8 that were entrained into the DWBC in January 1990 (5) and March 1990 (2). Lower panels show float 13, which remained in the vicinity of the western boundary from February 1990 to November 1990, and float 4, which meandered southeastward offshore of the mean DWBC.

1800m WESTERN BOUNDARY CURRENT FLOATS

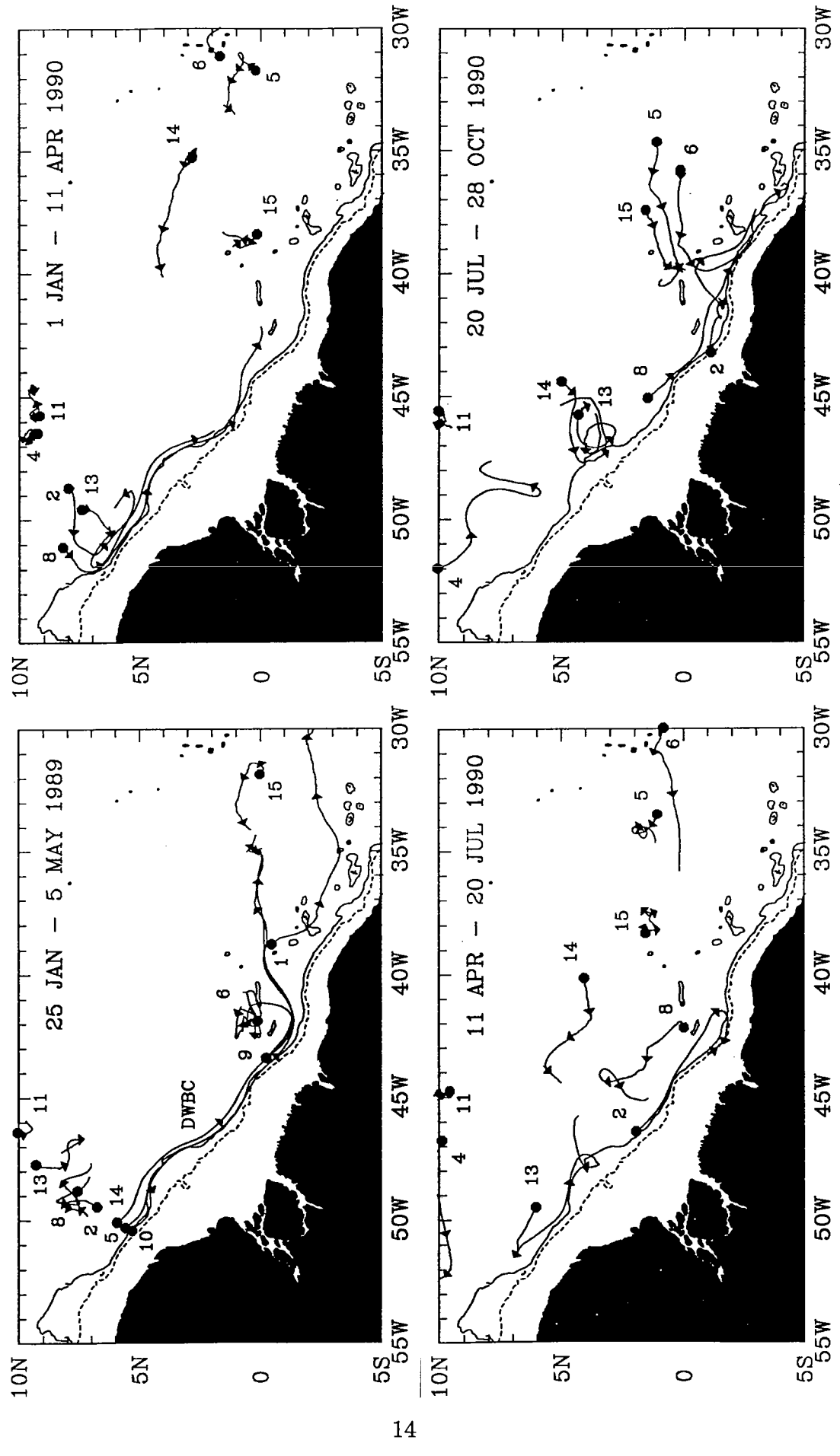


Figure 4: Summary of 1800 m western boundary current trajectories. Each panel shows 100-day subsets of data.
No floats drifted in the western boundary current from April to December 1989.

DWBC near 6N in November 1990. Float 5 drifted eastward along the equator to 29W (July 1989), and then westward, ending near 1N, 40W.

The next three floats (2, 8, and 13) drifted westward from offshore launch positions and were entrained into the DWBC near 7N. Floats 2 and 8 drifted southward in the DWBC during January–April 1990. Float 8 reached the equator in April, recirculated to the north, was re-entrained into the DWBC in July, crossed the equator in August, and reached 4S by October, the farthest south of any 1800 m float. Float 2 crossed the equator in April 1990, recirculated inshore during May–July, and then continued southward to 3S at the end. Float 13 entered the DWBC in February 1990, where it made numerous loops and reached as far south as 4N by November 1990. This float plus float 14 looped in a 200 km diameter cyclonic eddy centered near 4.5N, 46.5W next to the western boundary (July–October 1990).

Three other floats were briefly in the DWBC south of the equator. Float 9, launched in the DWBC near the equator, exited and drifted eastward along the equator. Float 6 drifted near the equator for most of the 21 months, entered the DWBC in October 1990 and drifted south to 2.5S. Float 1, launched on the equator near 39W, briefly drifted southeastward in the DWBC, then eastward to 14W, then north across the equator near 18W. This path showed that a float crossing the equator in the DWBC may return northward again, although the float ended up near the equator. Out of the six floats in the DWBC, two (2 and 8) crossed the equator within 21 months.

b) DWBC velocity

Most 1800 m floats drifted southeastward paralleling the 1800 m depth contour while they were in the DWBC (Figure 5). In order to calculate the cross- and along-stream characteristics of this current, float positions and velocities were converted to distances seaward of the 1800 m contour and velocity components normal and parallel to the contour. The mean velocity and transport of the DWBC as measured by 1800 m floats in this coordinate system are shown in Figure 6 and values tabulated in Table V. Only floats west of 43W were included in this composite in order to screen out floats in swift equatorial currents. Figure 6 is noteworthy because it represents a space (0N–7N) and time (12 months) average that shows the horizontal structure of this portion of the DWBC. Individual along-boundary velocity values peaked at around 55 cm/sec and 10 km bin averages reached 26 cm/sec. The DWBC was bounded by a flanking counterflow or recirculation; the width of the DWBC is 100 km as measured between points of zero velocity, and the width of the recirculation is at least 600 km.

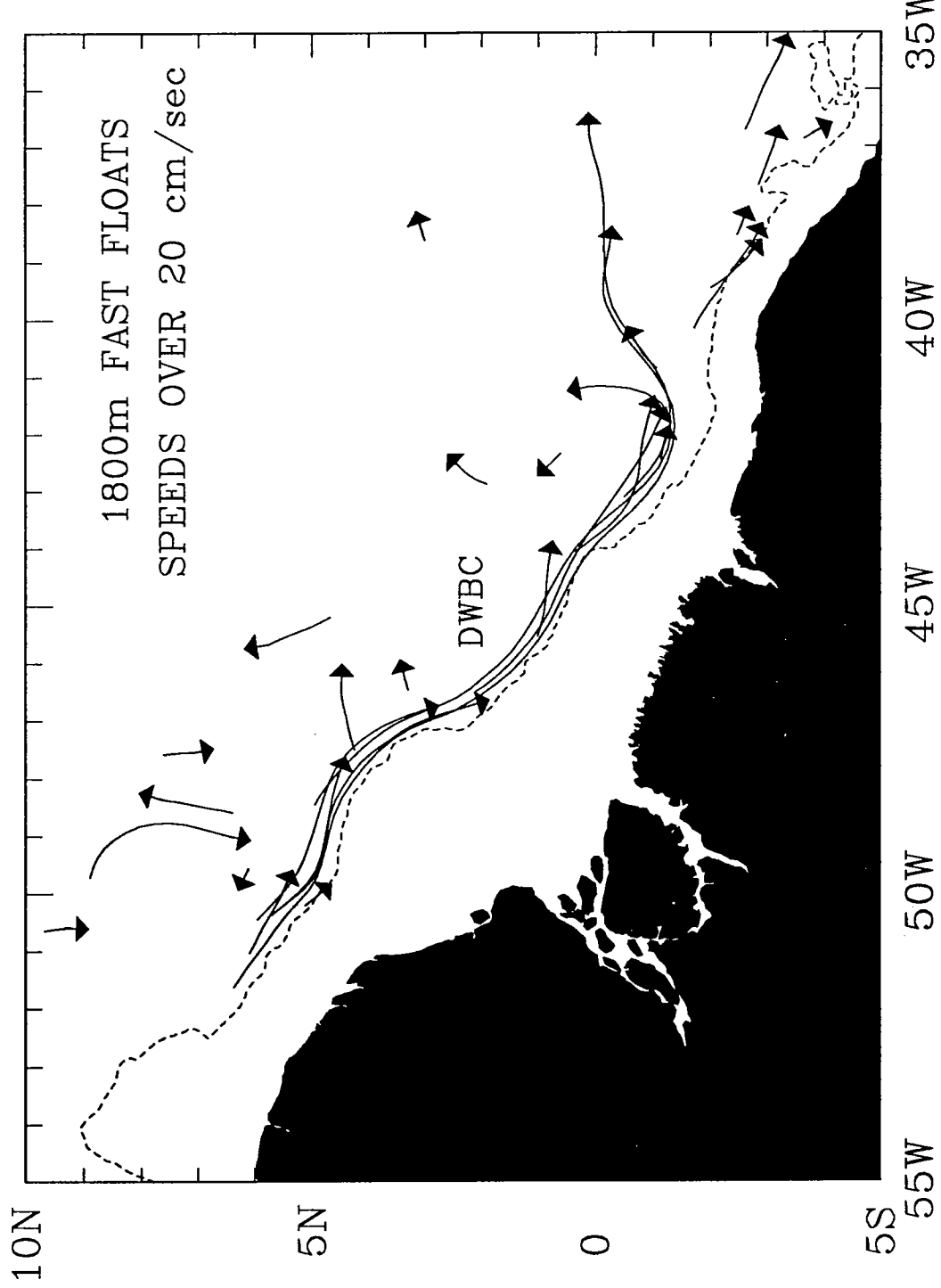


Figure 5: Segments of 1800 m trajectories of floats that drifted faster than 20 cm/sec. Fastest speeds, reaching 55 cm/sec, were along the western boundary near the equator (float 5). Dashed contour is 1800 m from the ETOPO5 data base (1989) obtained from the National Geophysical Data Center, Boulder, Colorado.

1800m DEEP WESTERN BOUNDARY CURRENT

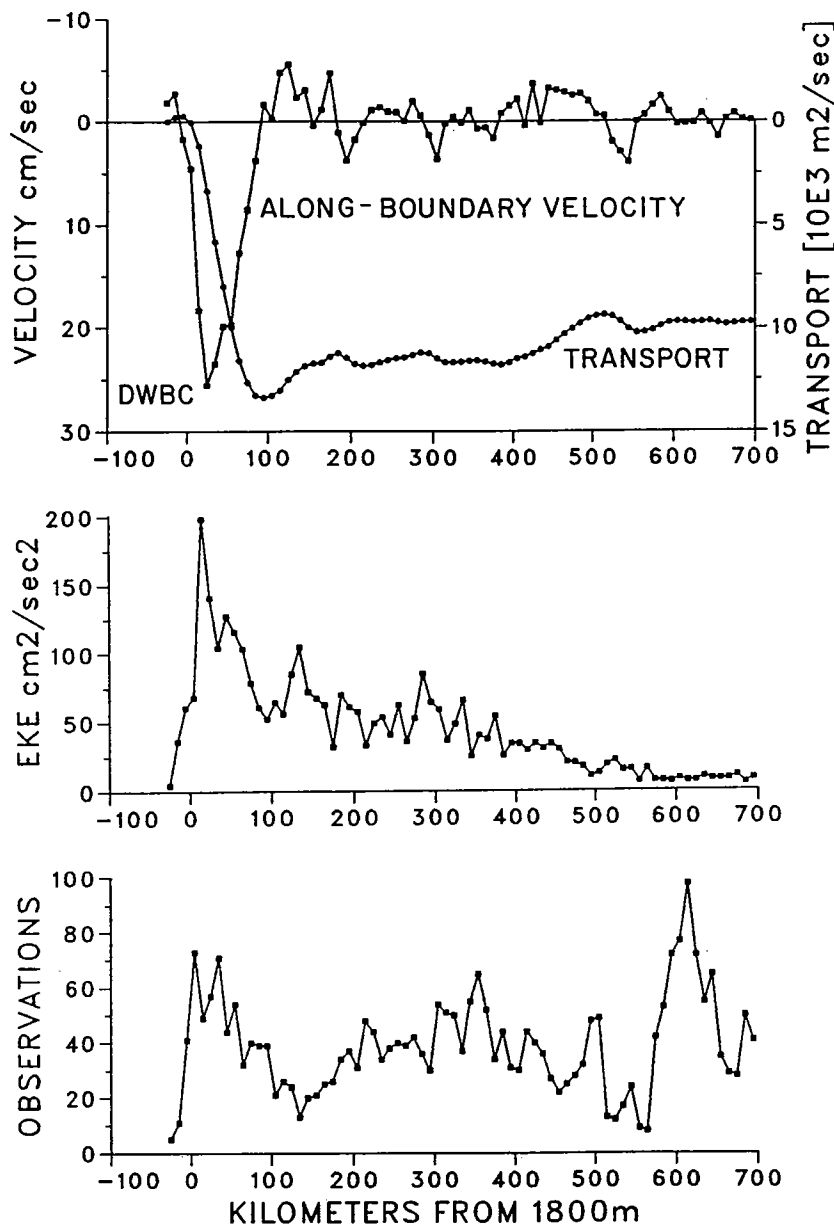


Figure 6: Average along-boundary velocity, transport, and eddy kinetic energy at 1800 m in the vicinity of the deep western boundary current (DWBC), west of 43W. All available individual daily velocities were grouped and averaged in 10-km-wide bins parallel to the 1800 m depth contour, which is from the ETOPO5 data base. Nine different floats were used to obtain this composite, which consists of roughly 3000 daily velocity observations. Eight floats drifted in the region of the mean DWBC jet and provided 500 daily observations. Transport per unit depth ($10^3 \text{ m}^3/\text{s}$) was obtained by summing, in the seaward direction, the product of bin width and the average velocity in each bin. Eddy kinetic energy (cm^2/sec^2) was calculated using $1/2(\bar{u}'^2 + \bar{v}'^2)$ where \bar{u}'^2 and \bar{v}'^2 are the variances of the velocity values parallel and normal to the 1800 m contour.

Table V: Summary of 1800 m Deep Western Boundary Current Observations, January 1989 to October 1990; 2S–12N west of 43W

Date	Number of floats in current	Number of observations in current	Peak Velocities (cm/sec)	Maximum Velocity (10 km average) and standard error (cm/sec)	Current Width (km)	Transport per unit depth (a) ($10^3 \text{ m}^2/\text{s}$)
Composite, Jan 89–Oct 90	8	500	50–60	26 ± 5 (b)	100	14 ± 3 (b)
1) Jan 89–Oct 89	4	124	50–60	39 ± 5	100+	23 ± 4 (c)
2) Nov 89–Apr 90	3	188	40–50	30 ± 4	100	16 ± 3
3) May 90–Oct 90	3	177	30–40	19 ± 6	100	8 ± 2

(a) The total transport of the upper core of the DWBC was estimated to be $14.7 \times 10^6 \text{ m}^3/\text{s}$ by combining the horizontal velocity profile from floats with the vertical profile from a current meter array (Colin et al., 1991) that was moored near the center of the DWBC jet as observed at 1800 m. The mooring was located at 6.2N, 51.0W from March 31, 1990 to November 18, 1990, a duration of 230 days. The depth of the meters and southward along-boundary mean velocities were 800 m, -1.6 cm/sec ; 1400 m, 11.4 cm/sec ; 2000 m, 18.9 cm/sec ; and 2700 m, 15.6 cm/sec . The velocity was assumed to be zero at the sea floor at 2800 m. The total transport was calculated from the width and thickness of the DWBC and by assuming it was elliptical in shape.

(b) The standard error of maximum velocity was estimated from individual observation in 10-km bins. The standard error of transport was estimated in two ways: first as listed from the average velocities in 10-km bins, second, from the three values of transport over the 21 months, which imply a standard error for the composite of around $4 \times 10^3 \text{ m}^2/\text{s}$.

(c) Floats sampled the DWBC in January–March 1989. A data gap occurred offshore of the DWBC between 90–130 km; the transport is up to the data gap. The width and transport could have been larger than given here.

c) DWBC recirculation

Floats offshore of the DWBC reveal (1) a northwestward recirculation between the DWBC and the Mid-Atlantic Ridge and (2) an inflow to the DWBC in the region 5–10N. Evidence consists of four floats (2, 4, 8, and 13) launched offshore of the DWBC in latitudes 6–10N. These floats gradually drifted westward and were entrained into the DWBC with a mean velocity of $u = -1.5 \pm 0.5$ cm/sec, $v = -0.2 \pm 0.2$ cm/sec. In addition, after floats 8 and 14 had reached the equator in the DWBC, they recirculated northwestward offshore of the DWBC. In contrast to these floats in the west, the easternmost floats (7 and 12) near 11N drifted very slowly, implying very weak or zero recirculation east of the Mid-Atlantic Ridge. The combined mean velocity of floats 7 and 12 was $u = -0.11 \pm 0.19$ cm/sec, $v = 0.02 \pm 0.21$ cm/sec, not significantly different from zero. Evidence for recirculation is also seen in Figure 6. Although bin-averaged velocity values fluctuate around zero as a function of distance offshore of the DWBC, the integrated alongshore transport gradually decreases in the offshore direction.

Recirculation velocity and transport were estimated two ways. First the average velocities in 10 km bins (Figure 6) were grouped and averaged which gives a mean recirculation speed of 0.61 ± 0.25 cm/sec. Second, all individual float velocities in the 90-km to 700-km band seaward of the DWBC (west of 43W) were grouped and averaged which gives a mean northwestward recirculation velocity parallel to the 1800 m contour of 0.47 ± 0.52 cm/sec and inflow velocity toward the DWBC of 0.73 ± 0.55 cm/sec. These two mean recirculation velocities suggest that around 39% of the 1800 m DWBC recirculated west of the Mid-Atlantic Ridge (which is located around 1100 km from the 1800 m contour). Assuming that this percentage is representative of volume transport implies that around 5.8×10^6 m³/s of the upper DWBC recirculated, leaving 8.9×10^6 m³/s to cross the equator; however, the estimated standard errors are only slightly smaller than the mean values, so the magnitude of the recirculation is still uncertain.

d) Equatorial currents

A vertical profile of velocity was measured with a freely falling velocity profiler near the equator when the floats were launched there (Figure 7). The profile revealed a well-developed pattern of alternating eastward and westward currents or jets over the upper 2200 m. The most prominent eastward jets were (1) the Equatorial Undercurrent, reaching 76 cm/sec at 70 m, (2) a 28 cm/sec jet at 1000 m, and (3) an 11 cm/sec jet at 2000 m. Four 1800 m floats appeared to be located in this third jet, which extended from around 1600 m to 2200 m. The trajectories imply

EQUATORIAL VELOCITY PROFILE (cm/sec)
0°N 30°W 17 JAN 1989

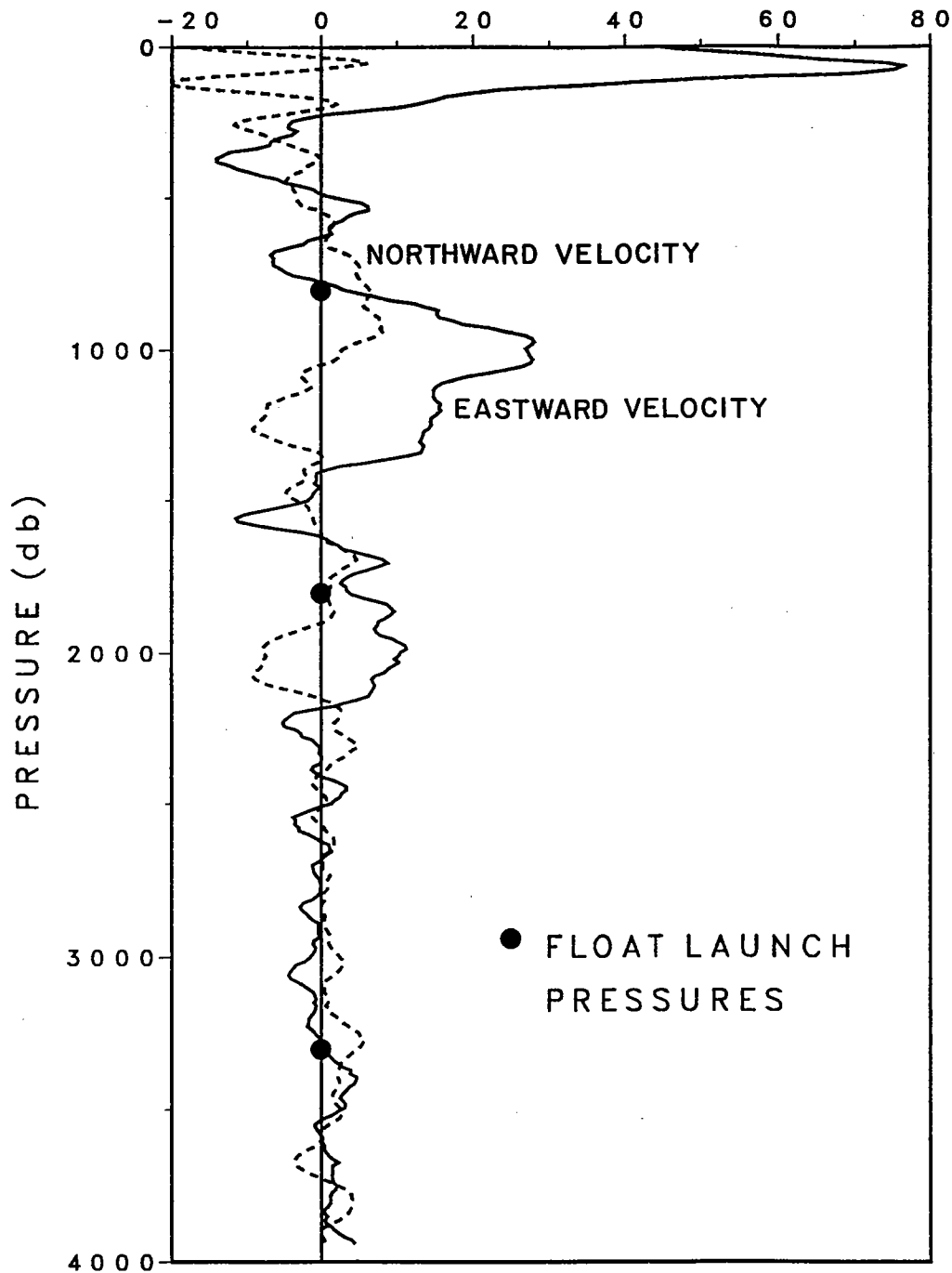


Figure 7: Profile of velocity (cm/sec) as a function of pressure measured on 17 January 1989 at 0N, 30W (from Ponte et al., 1990). The profile extended down to within 200 m of the sea floor. Solid line represents the eastward velocity component; dashed line is northward velocity; large dots show nominal float depths at launch.

that this equatorial jet extended at least 2° - 3° north and south of the equator (Figures 3, 8) and around 25° longitudinally.

Three floats launched near the equator (1, 6, and 9) plus another (5) that peeled off from the DWBC into the equatorial band drifted long distances in this 1800 m current. Float 1 drifted along 2S-3S from 39W to 14W, a distance of 2750 km over 310 days at a mean velocity of 10 cm/sec. Float 6 drifted eastward along 1N-3N from 42W to 27W and then back to 40W, where it turned and headed south in the DWBC.

Three of the floats (5, 6, and 9) that first drifted eastward along the equator turned and then drifted back westward along the equator. Grouping all available velocities into a large equatorial box, 2.5S-2.5N, 20W-40W, and calculating monthly mean velocity values (Figure 9) shows the mean flow near 1800 m was 4.1 cm/sec eastward from February 1989 to February 1990, and then 4.6 cm/sec westward from March 1990 to October 1990. These values include float 15, which differed by slowly drifting westward over the 21 months. A confirmation of the time variation of the equatorial current system is seen in a second velocity profile near 0N, 30W in June 1991 that showed a westward current from 1600 m to 2000 m where the profile stopped (Böning and Schott, 1992).

In summary, of the floats that were launched on the equator (1, 6, 9, and 15) or that drifted there in the DWBC (2, 5, 8, and 14), one (14) recirculated, two (2 and 8) crossed the equator in the DWBC, and one (6) entered the DWBC from the equator, leaving four near the equator at the end of tracking in November 1990.

e) DWBC-equatorial current connection

The 1800 m trajectories show that when the equatorial current was going eastward, some of the DWBC water turned and flowed eastward along the equator (floats 5, 9). Eventually, after about a year, the equatorial current reversed and flowed westward (floats 5, 6, and 9). When the westward equatorial current reached the western boundary, some of the equatorial current turned southward and entered the DWBC south of the equator (float 6). At this time two of the DWBC floats (2 and 8) crossed the equator. Thus the pattern of cross-equatorial flow in the DWBC seems to be coupled with the direction of equatorial currents. An implication is that the equatorial currents act as a temporary reservoir for DWBC water, storing it in eastward flow and releasing it in westward flow. Virtually all net cross-equatorial flow occurred in the west near the boundary, except for temporary crossings by floats farther east trapped in higher frequency motion within a few degrees of the equator. A schematic diagram of the inferred general circulation of upper North Atlantic Deep Water is given in Figure 10.

1800m TRAJECTORIES ALONG THE EQUATOR

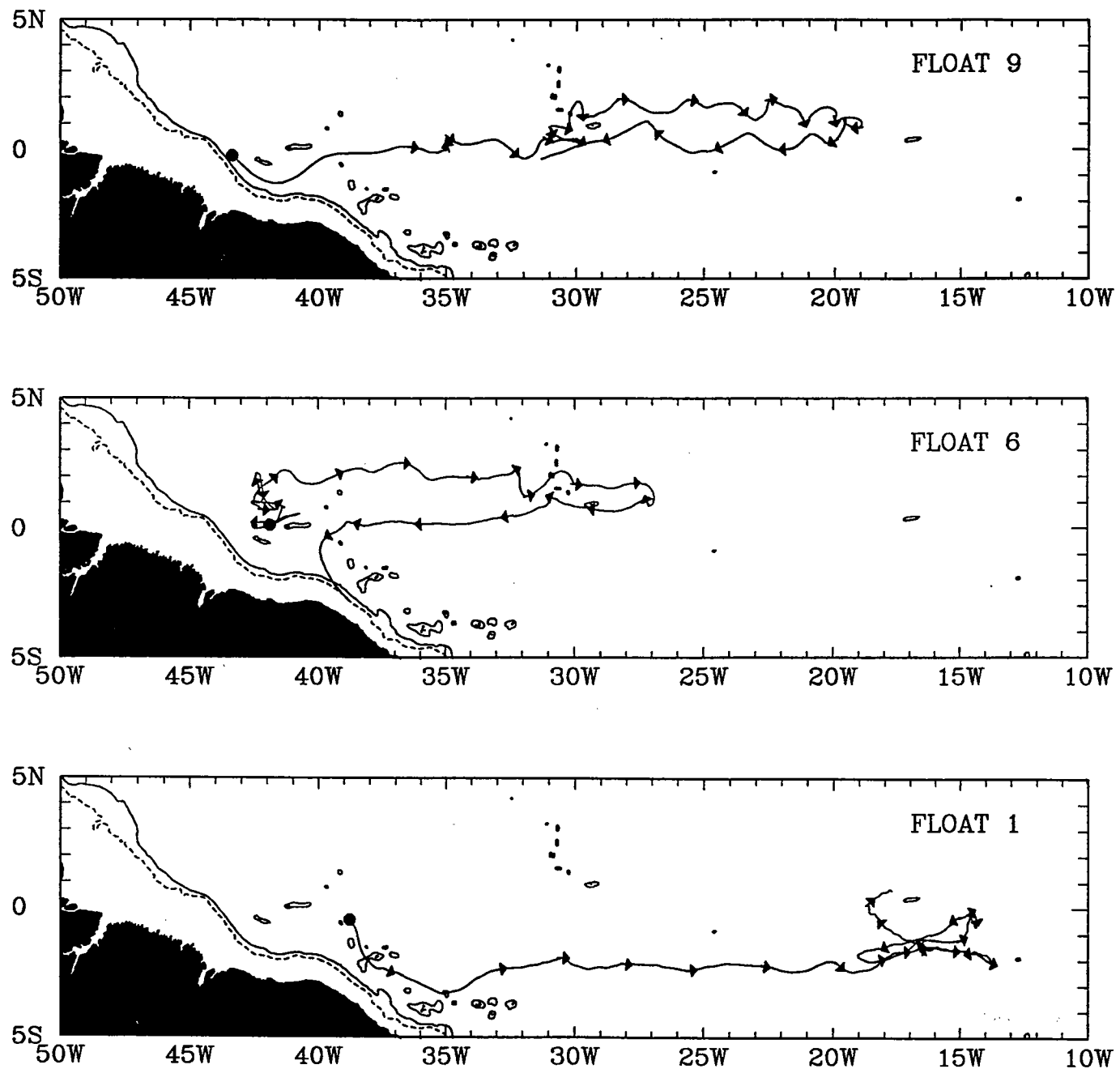


Figure 8: Individual 1800 m float trajectories along the equator from January 1989 to November 1990. Arrowheads are spaced at 30-day intervals.

1800m EQUATORIAL FLOATS

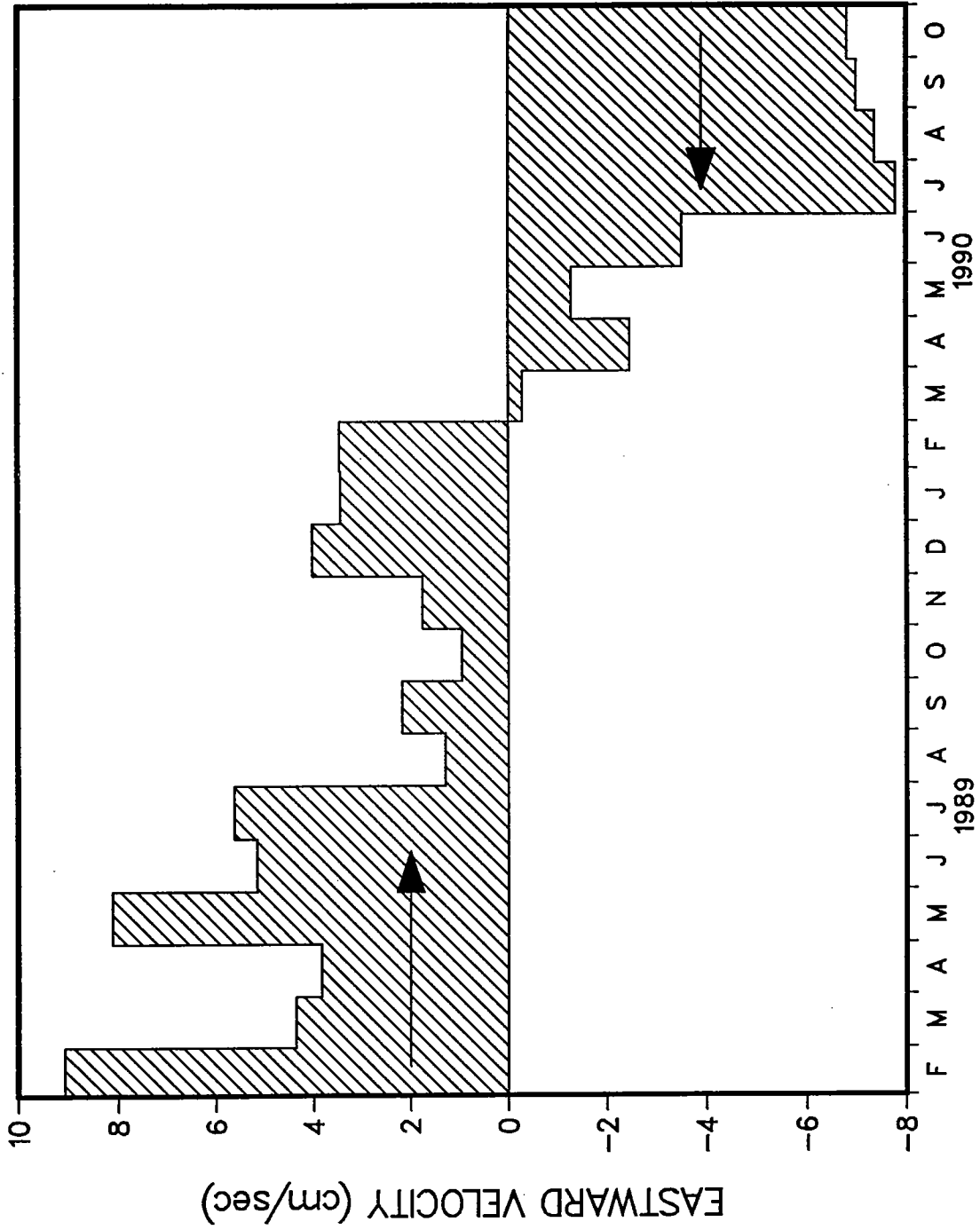


Figure 9: Time series of 1800 m eastward velocity along the equator, calculated by grouping individual velocity values in a box whose limits are 20°–40°W, 2.5°S–2.5°N. Plotted values are monthly averages. On average there were approximately four floats and 120 daily observations per month in the box.

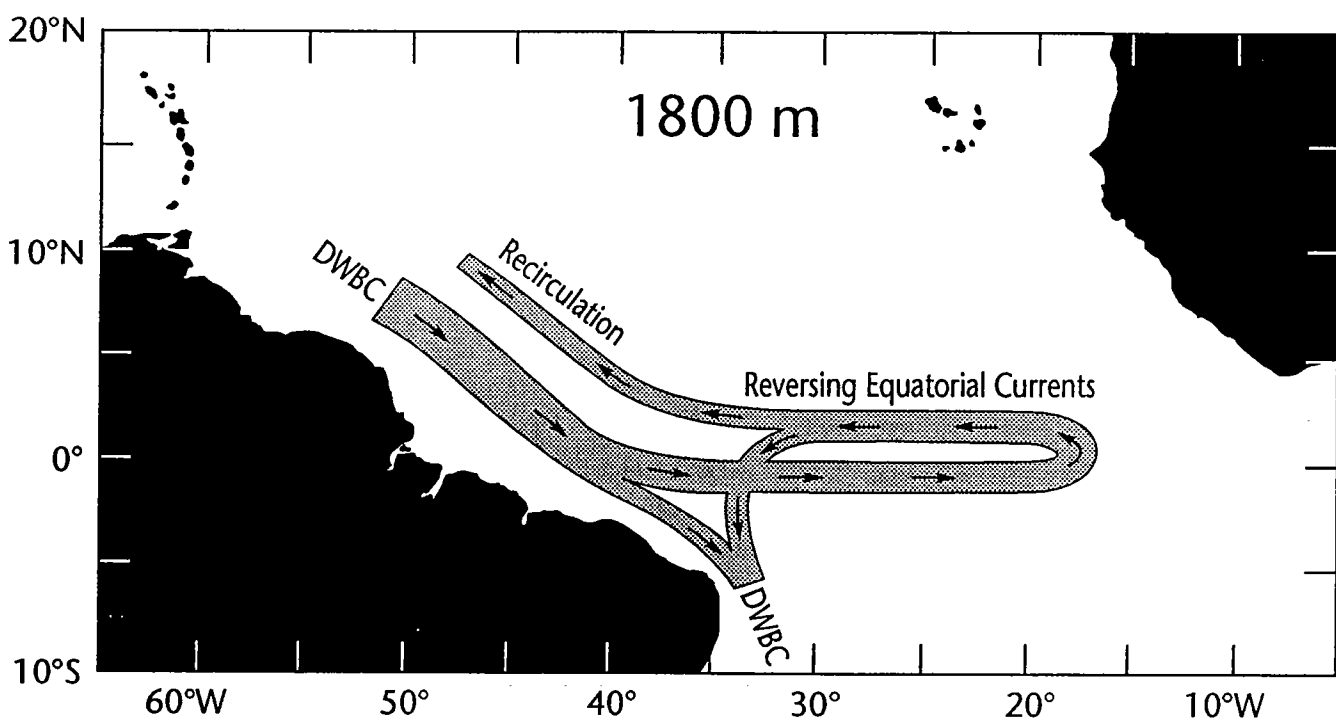
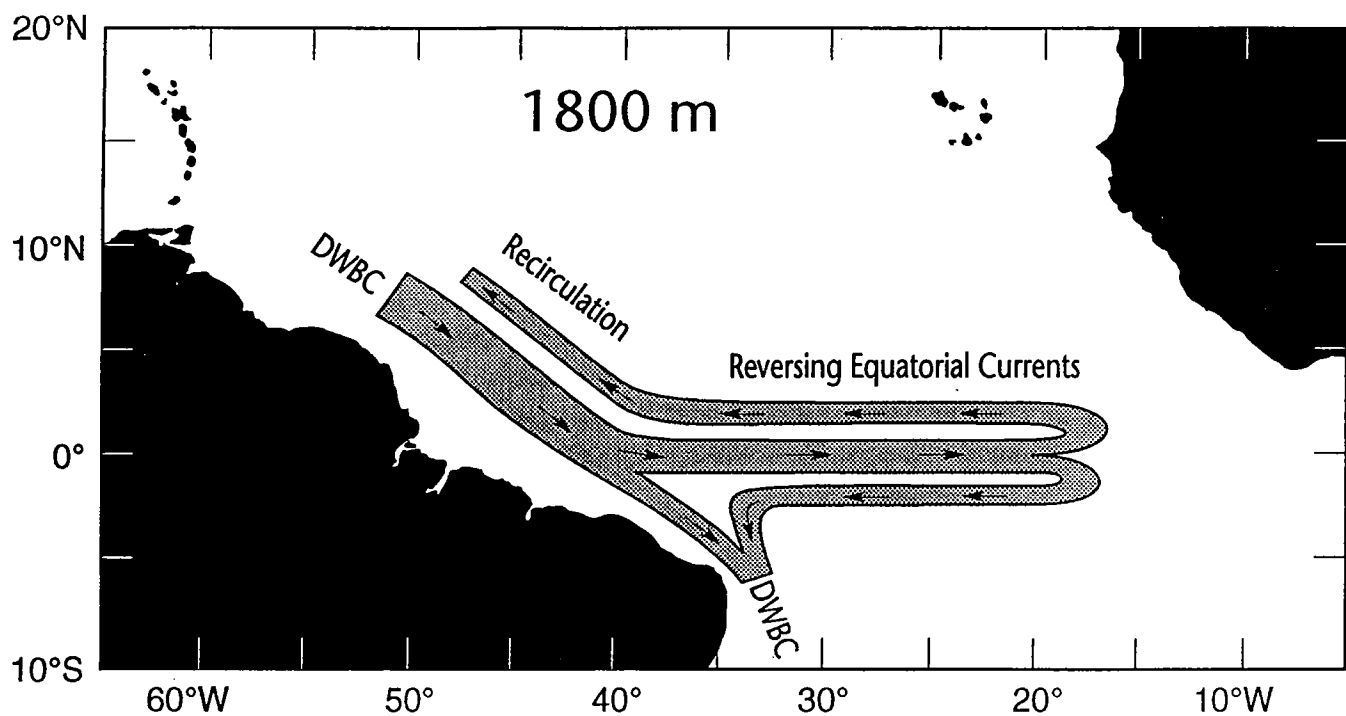


Figure 10: Schematic diagrams summarizing the 21 months of 1800 m float data. The width of currents is roughly proportional to estimated transport: $15 \times 10^6 \text{ m}^3/\text{s}$ in the DWBC north of the equator, $6 \times 10^6 \text{ m}^3/\text{s}$ in the recirculation there, and $9 \times 10^6 \text{ m}^3/\text{s}$ in the DWBC south of the equator.

4 3300 m Trajectories

The 3300 m float trajectories look very different from the 1800 m ones (Figure 11). No obvious DWBC is seen, which was surprising because the 3300 m floats were launched near the western boundary in the lower North Atlantic Deep Water. Four trajectories (floats 36, 39, 40, and 42) were obtained near 7N, 50W from February 1989 to February 1990, but none of these looks like those in the DWBC at 1800 m. Thus the evidence from the 3300 m floats suggests that there was either no DWBC or a very weak one at this depth, with the core of lower deep water located significantly below 3300 m.

Three of the four equatorial floats also drifted rather erratically without any indication of being in the DWBC. Their mean velocity was $u = -0.04 \pm 0.39$ cm/sec, $v = 0.30 \pm 0.42$ cm/sec. The one exception, float 30, drifted southeastward at 1.4 cm/sec over topography shallower than 3000 m. In addition, it was tracked longer than the others, implying it was probably shallower than they were. For these reasons, we think this float was in the upper part of the North Atlantic Deep Water and therefore unrepresentative of velocity at 3300 m. We conclude that there is no evidence of a prominent DWBC at 3300 m.

The 3300 m floats near the equator did not drift far eastward, as the 1800 m floats did. This lack of significant flow along the equator at 3300 m agrees with the equatorial velocity profile (Figure 7) that showed weak flow below 2200 m.

5 800 m Trajectories

a) Intermediate Western Boundary Current (IWBC)

Two 800 m floats launched near 6N (22, 23) and a third near the equator (28) clearly translated in a mean northwestward direction along the boundary (Figures 12, 13 and Table VI) in the inferred direction taken by Antarctic Intermediate Water. One of these (28) probably entered the Caribbean through the Grenada Passage in April 1990. In addition, a 650 m bobber float (B63) launched near the equator translated up the boundary. The mean velocity of these four floats was 3.5 ± 0.8 cm/sec toward 307° , where the standard error was calculated from the four velocity values. Several other 800 m floats (20, 21, 25, and 26) translated eastward and southeastward in counterflows. Floats 19 and 26 drifted southward and then eastward long distances in equatorial currents. These floats suggest that some of the water in a countercurrent offshore of the IWBC fed into the equatorial current.

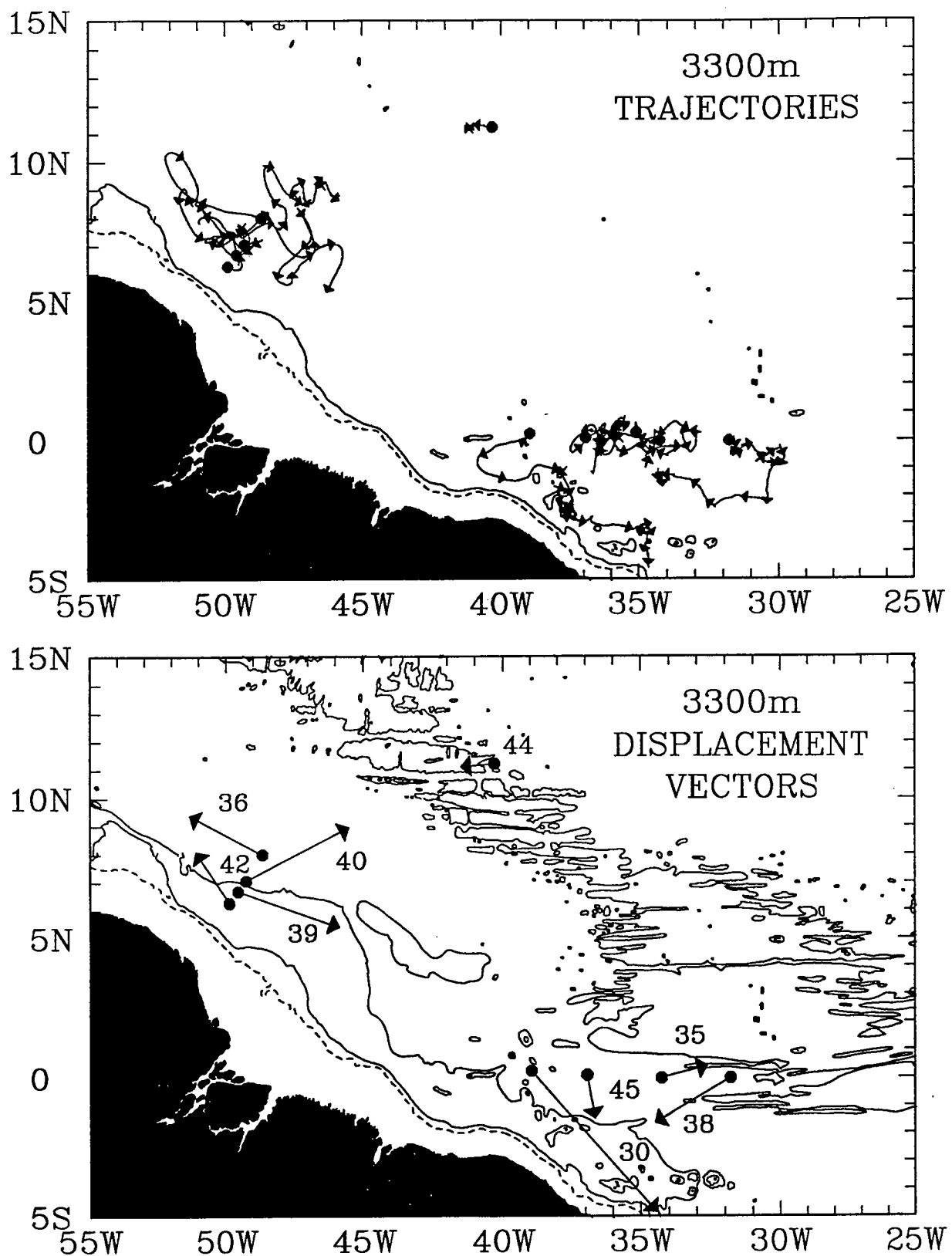


Figure 11: Summary of 3300 m float trajectories and displacement vectors from January 1989 to October 1990. Arrowheads are spaced at 30-day intervals.

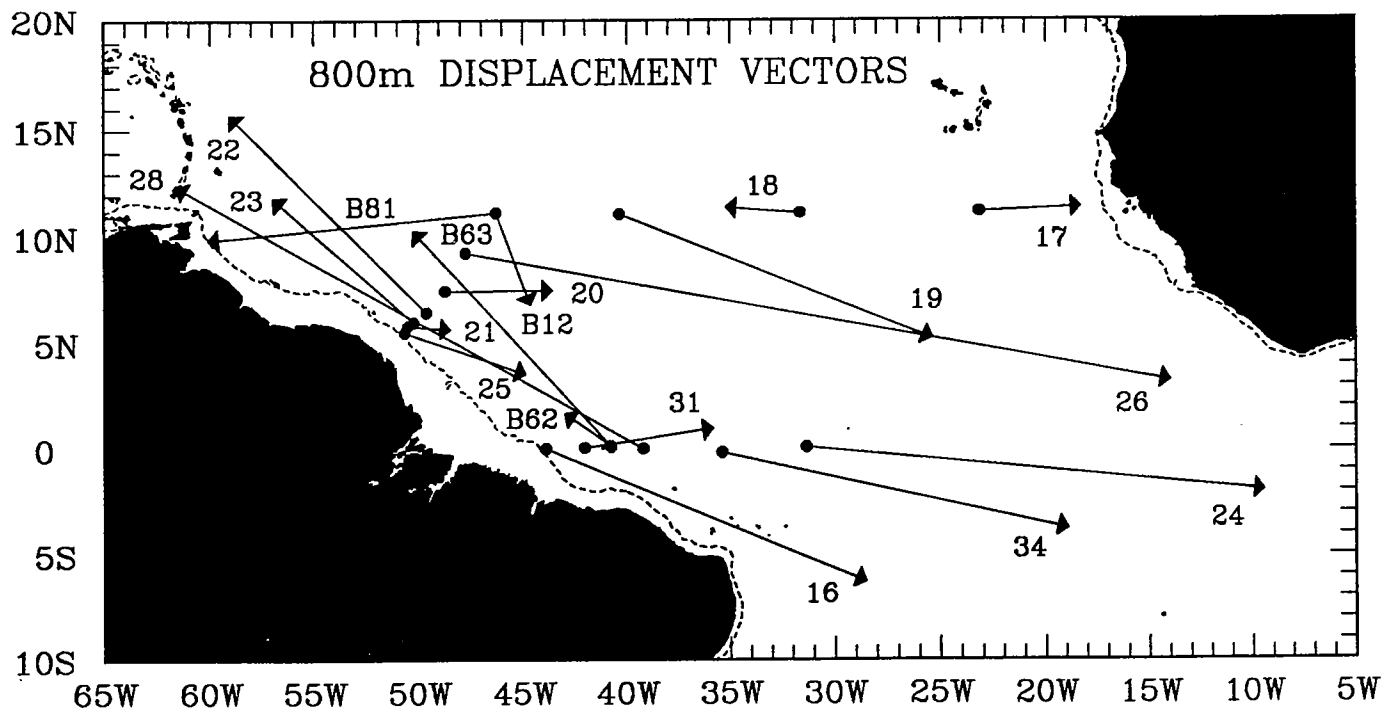
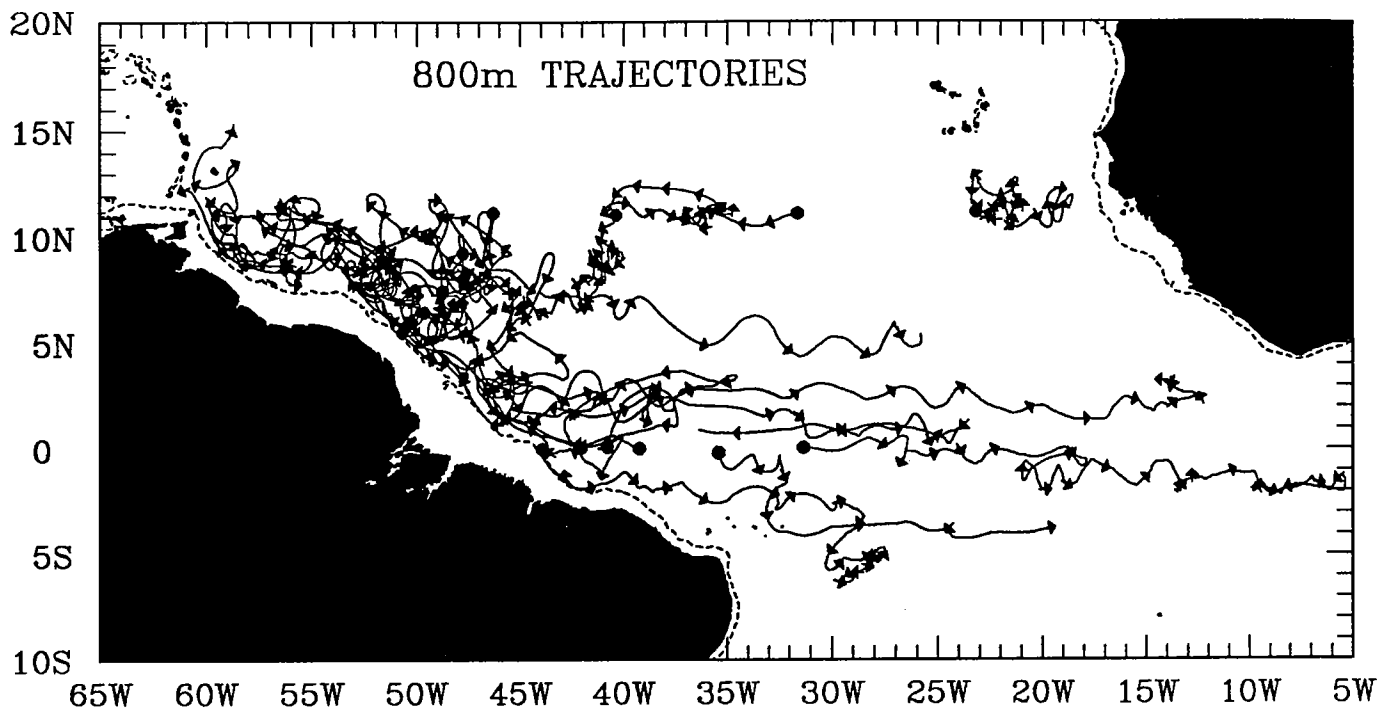


Figure 12: Summary of 800 m trajectories and displacement vectors from January 1989 to November 1990. Float 34 was tracked up to July 25, 1989 when it stopped being heard, and float 28 was tracked up to April 22 when it is inferred to have entered the Caribbean. Four Bobber (B) floats at shallower depths were included; three of these were short records. Arrowheads are spaced at 30-day intervals.

800m WESTERN BOUNDARY CURRENT TRAJECTORIES

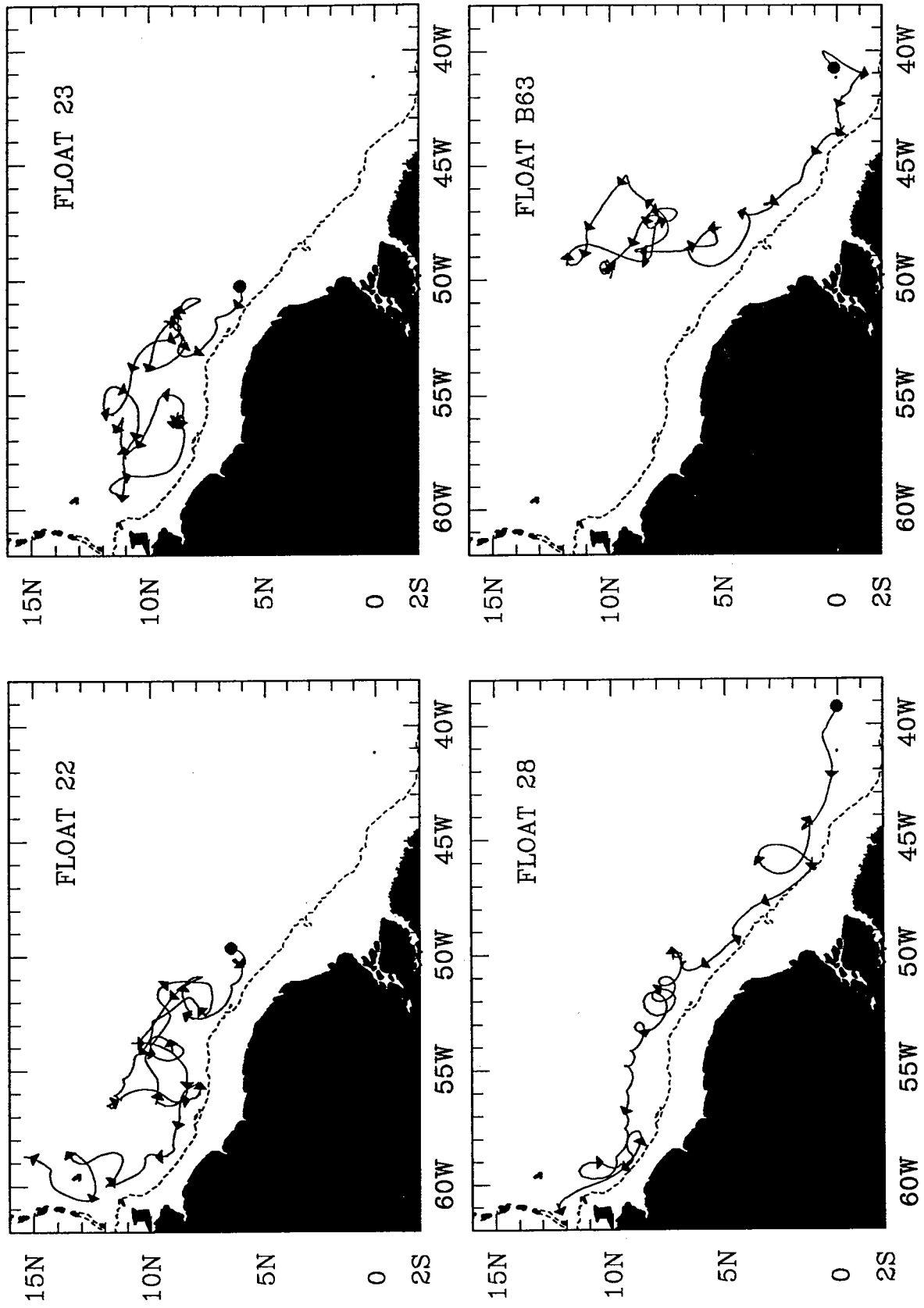


Figure 13: Trajectories of four 800 m floats that drifted, on average, northwestward along the western boundary. Floats 22, 28, and B63 (at 650 m) looped in anticyclones that translated northwestward.

Table VI: Northwestward Intermediate Western Boundary Current (IWBC) at 800 m

	Number of observations in IWBC	Maximum Velocity (20 km average) and standard error (cm/sec)	Width (km)	Transport per unit depth ($10^3 \text{ m}^2/\text{s}$)
I All Floats including Bobbers	1833	7.1 ± 3.8	300	5.8 ± 1.8 (a)
II No Loopers (b)	1606	4.5 ± 3.6	300	2.7 ± 1.6
III No Bobbers (c)	1091	6.8 ± 3.8	180	4.2 ± 1.6
IV No Bobbers or Loopers	782	4.5 ± 3.6	160	2.2 ± 1.6

(a) Float velocity values were grouped in 20-km bins as a function of distance seaward of the 800 m depth contour. Only floats within the rectangle extending from 4N–13N, 43W–55W were included in order to screen out floats in equatorial currents. The northwestward transport in the IWBC was estimated by integrating the mean velocity in 20-km bins seaward from the western boundary to the point of maximum transport, near a distance of 200–300 km from the 800 m contour. The standard error of IWBC transport was estimated from the different 20-km mean velocity values within the region of the IWBC. Total transport did not vary much when the size of the rectangle 4N–13N, 43W–55W was varied, except for increasing somewhat as the western edge was shifted farther to the west to include more of the northwestward going trajectories.

(b) Loopers are floats looping in anticyclonic eddies (see Table VII).

(c) Two Bobber floats located near 650 m were included in I and II.

b) Anticyclonic eddies

Three of the four floats (22, 28, and B63) that drifted northwestward the farthest looped for various amounts of time in three different anticyclonic eddies as the eddies translated up the western boundary (Figure 14, Table VII). The mean velocity of the eddies, which was northwestward at 8.1 ± 1.0 cm/sec, contributed significantly to the mean velocity and transport in the IWBC (Table VI). Approximately 50% of the total northward transport in the IWBC was accounted for by the measurements of these floats looping in anticyclones.

c) Equatorial currents at 800 m

Most visually striking of the 800 m trajectories (Figures 12, 15) is the long eastward drift of floats in a band from around 5S to 6N. These floats equilibrated at a depth near the top of an eastward equatorial jet that had a peak speed of 28 cm/sec and thickness of 500–600 m (Figure 7). The floats apparently descended into the jet and were carried eastward by it. Most remarkable is the broad width, $\sim 11^\circ$ in latitude, of the dominantly eastward equatorial currents. Peak speed along eastward trajectories was ~ 30 cm/sec, and the average eastward velocity calculated by grouping all eastbound floats in the box 5S–6N, 5W–40W was 10.6 ± 0.9 cm/sec. Coupling this value with the 11° width and 500 m thickness gives an eastward transport per unit width of 128×10^3 m²/s and a volume transport of 64×10^6 m³/s. Of course, regions of westward flow could be embedded in the eastward current, which would reduce the mean velocity, and a few are seen. Still, the trajectories imply that very large amounts of water can flow in equatorial currents at this depth.

Six different floats drifted eastward in the equatorial currents; two of these drifted southward into the equatorial band and then eastward. Float 24, launched on the equator at 30W, went 26° east along 0–2S to 5W, the farthest east of any float. This float was ballasted to equilibrate near 1125 m, near the center of the jet (Figure 7). Assuming that the eastward jet began near the western boundary implies that the current extended coherently eastward about 38° of longitude, to at least 5W.

d) Reversal

Three of the four floats (24, 26, and 31) that were still in the 5S–6N band at the end of the 21 months reversed direction shortly before the end. The fourth float (19) looked as if it had just stopped near 5N, 26W, and was perhaps about to reverse direction. This reversal of the equatorial current is inferred to be primarily a tempo-

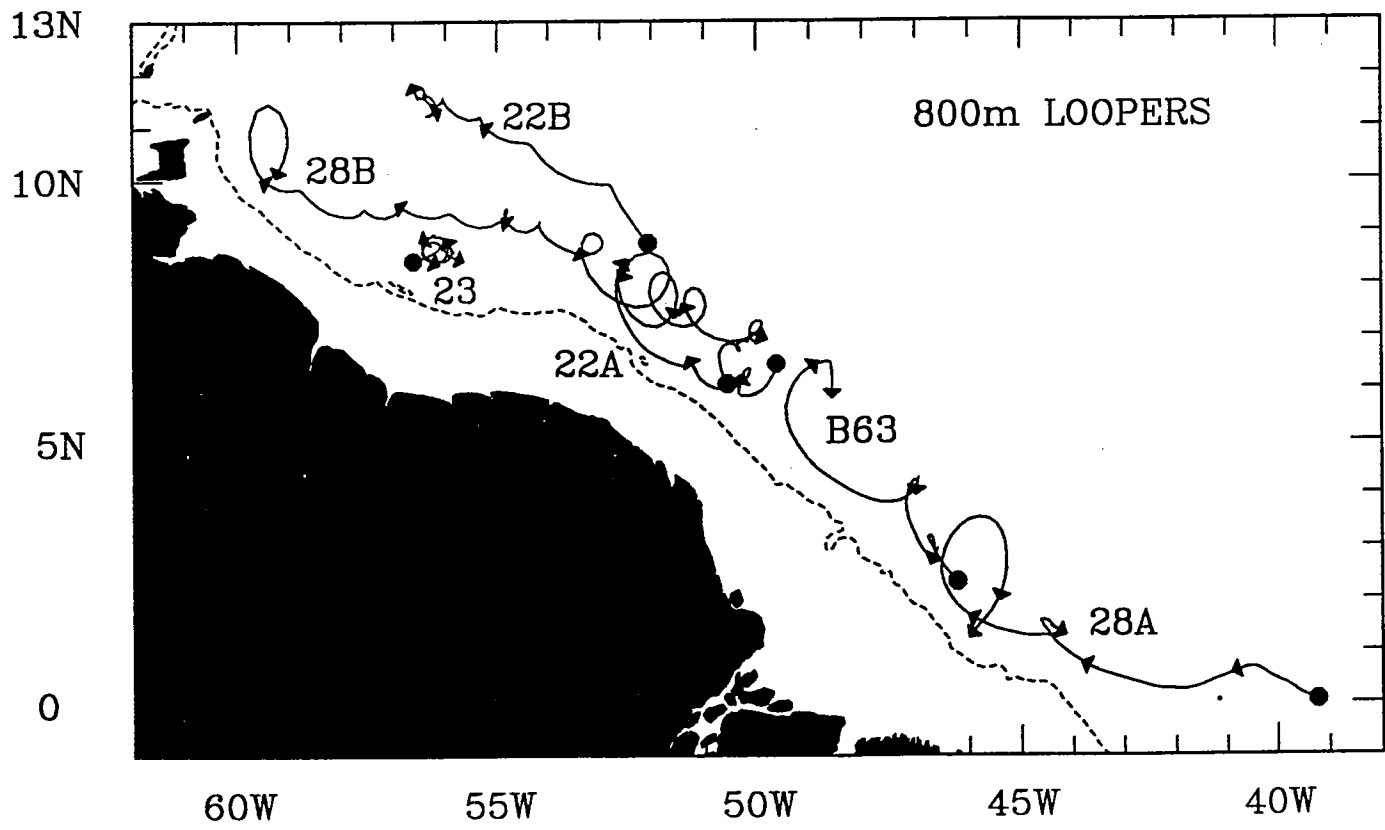


Figure 14: A) Trajectories of 800 m floats trapped in eddies as inferred from looping trajectories (see Table VII). In each case shown, a float made at least two consecutive loops in the same direction, implying it was trapped in an eddy. Anticyclone A was tracked by floats 28 and B63 almost continuously from January 25, 1989 to January 22, 1990. An early meander in the trajectory of 28 was found to be a loop when the mean translation of this float was subtracted from the trajectory.

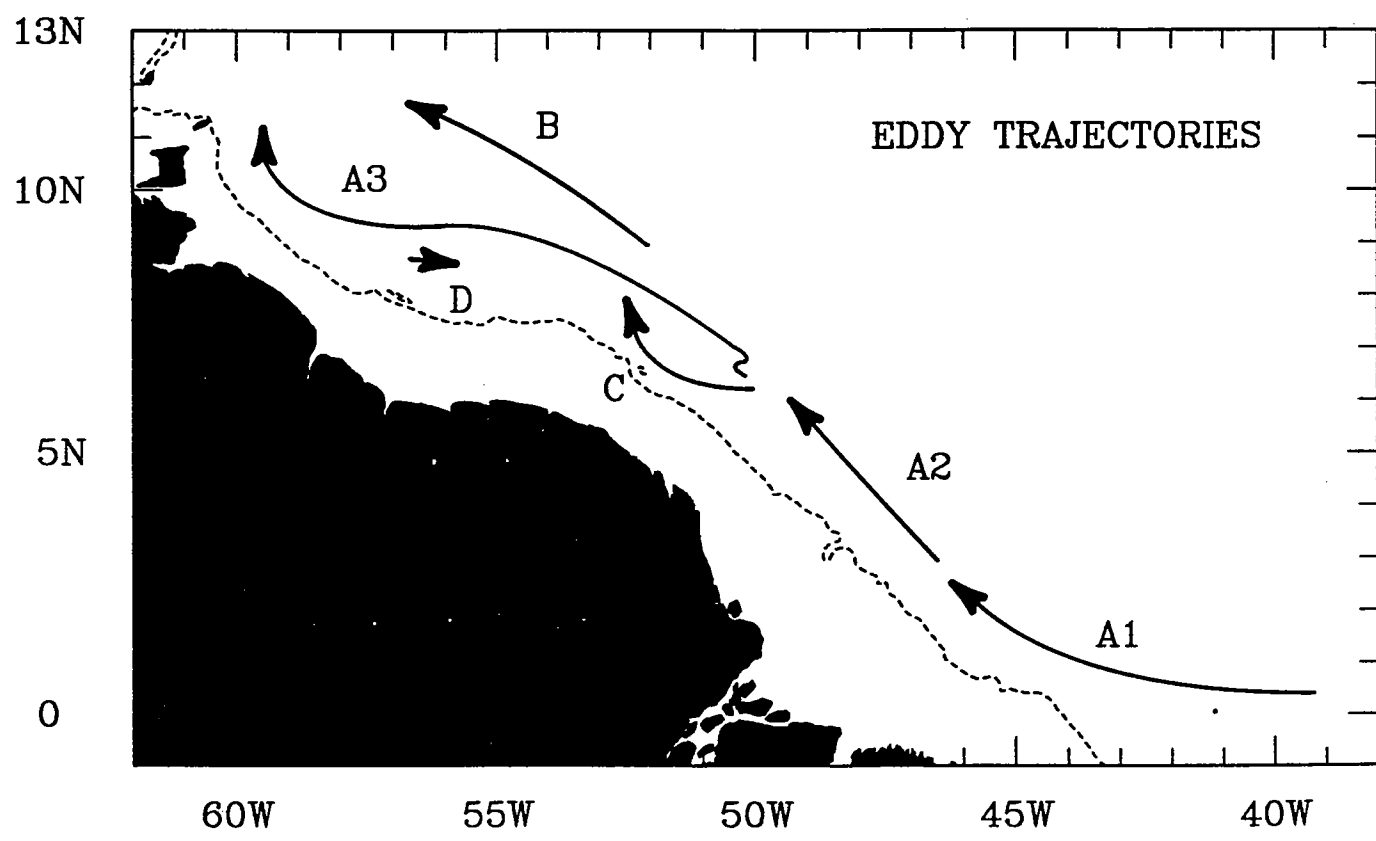


Figure 14: B) Trajectories of the eddies, estimated from the looping float trajectories.

Table VII: Summary of Eddy Characteristics Estimated from Looping Float Trajectories at 800 m

Float	Dates	Duration (days)	Number of Loops	Period of Rotation (days)	Swirl Velocity (cm/sec)	Diameter (km)	Mean Velocity (cm/sec)	EKE (cm ² /sec ²)
<i>Anticyclones</i>								
A1	28A	89 01 25 - 89 05 16	111	2.8	40	-15.8	173	-7.8 1.5 125
A2	B63	89 06 21 - 89 08 27	67	2.6	26	-17.7	125	-4.6 6.8 158
A3	28B	89 08 25 - 90 01 22	150	13.7	11	-24.0	72	-7.4 3.5 288
B	22B	90 01 21 - 90 03 14	52	7.5	7	-16.9	32	-9.9 6.1 144
C	22A	89 02 08 - 89 04 23	74	3.0	25	-11.7	79	-5.0 2.8 68
<i>Cyclone</i>								
D	23B	90 04 30 - 90 07 15	76	2.9	26	7.6	55	1.5 0.1 29

The mean translation velocity of the anticyclones from the 5 individual estimates is $u = -6.9 \pm 1.0 \text{ cm/sec}$, $v = 4.2 \pm 1.0 \text{ cm/sec}$ or 8.1 cm/sec toward 301° .

The number of loops was estimated visually and used to calculate the period of rotation. Swirl velocity was estimated as being equal to the root mean square (RMS) velocity of a float about its mean velocity. Diameter (D) of the loops was estimated from the mean period of rotation (T) and mean swirl velocity (V_θ) with the relation $D = (V_\theta T)/\pi$. The mean translation velocity of each eddy was estimated by calculating the mean velocity of each float. Eddy Kinetic Energy (EKE) was estimated from the average of the u and v velocity variances about their respective mean velocity values.

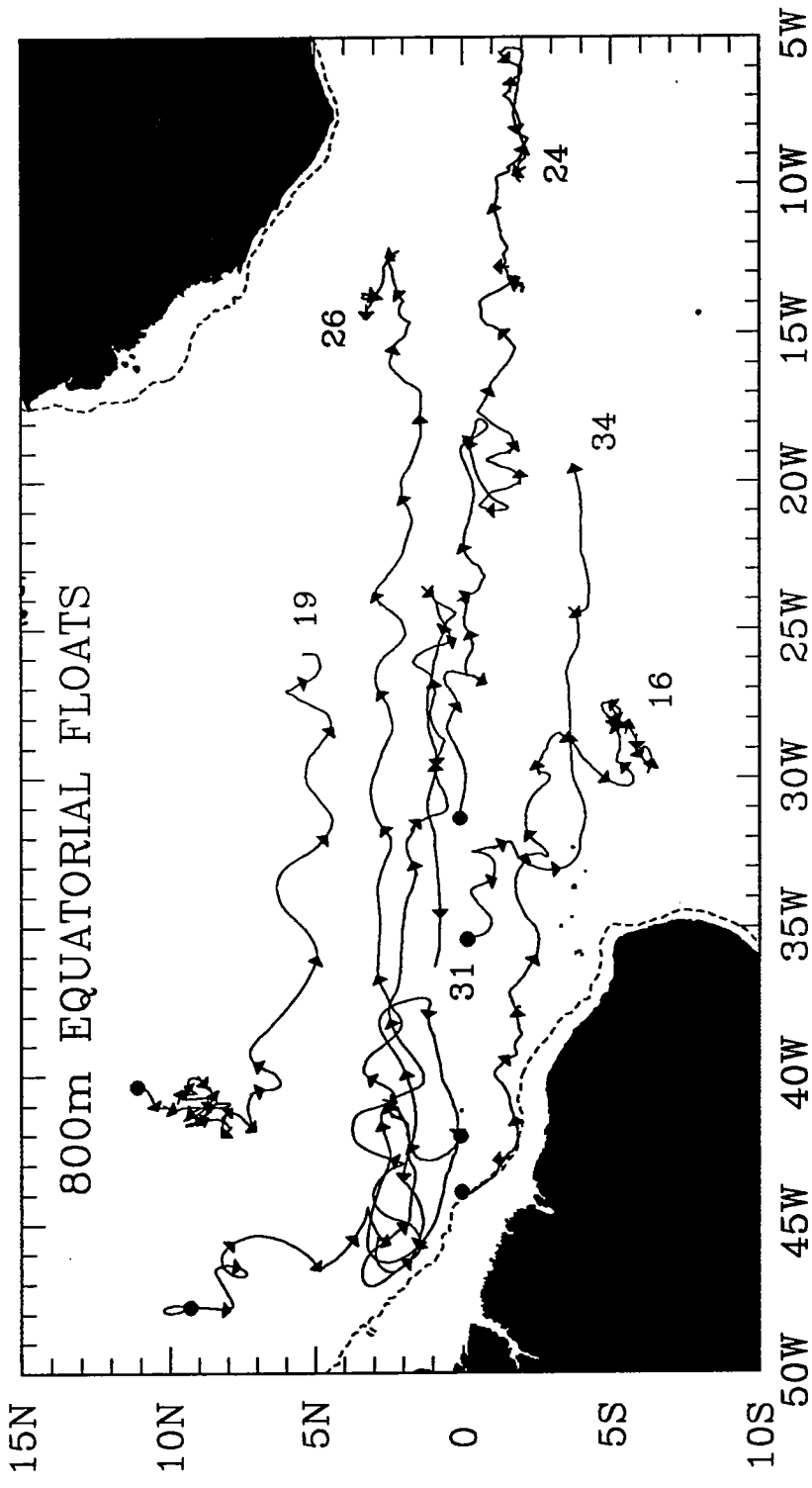


Figure 15: Trajectories of six 800 m floats that drifted eastward in equatorial currents. Float 24, which was ballasted to lie near the center of the eastward jet (Figure 7), equilibrated near 1125 m.

ral change because the 800 m floats would have still been well within the equatorial jet seen on Figure 7. The one deeper float (24) would have been near 1350 m when it reversed, close to the lower limit of the jet. The mean westward velocity of the westbound trajectories in the box 5W–40W, 5S–6N was 7.8 ± 1.4 cm/sec, roughly equal to the eastbound velocities.

e) Southward velocity

Three of the five 800 m floats launched near the equator (16, 24, and 34) plus two others launched near 9N (26) and 11N (19) drifted on average southward between Brazil and Africa. This can be seen in the southward tilt of their trajectories and displacement vectors (Figure 12). The mean southward velocity of these five floats was 1.3 ± 0.3 cm/sec, with the standard error estimated from the five individual mean velocity values. Although the mean southward velocity of all observations in the box 5W–40W, 5S–6N was 0.8 ± 1.0 cm/sec, not significantly different from zero, the southward trend of the trajectories and displacement vectors suggests that the southward velocity might be of importance.

f) IWBC-equatorial current connection at 800 m

A schematic diagram of the inferred mean circulation at 800 m is shown in Figure 16. The IWBC is interpreted to be continuous along the boundary with part feeding into the equatorial current. Since the eastward equatorial current only reversed near the end of the 21 months, the mean circulation shown here does not include a westward equatorial current. If the westward flow persists for the same duration as the eastward flow, then a schematic of the longer term circulation at 800 m might look like Figure 10 with its arrows reversed in direction.

6 Summary and Conclusions

SOFAR floats have given a first Lagrangian view of flow in the upper core of the DWBC, its connection to equatorial currents, and its cross-equatorial flow. The DWBC at 1800 m was found to be a narrow, 100 km wide jet, flowing with peak speeds of 55 cm/sec and peak average (10 km bin) speeds of 26 cm/sec. Roughly 39% of its 14.7×10^6 m³/s transport recirculated between the current and the Mid-Atlantic Ridge, leaving around 9×10^6 m³/s to cross the equator. At times DWBC water flowed eastward along the equator long distances. At other times, when the equatorial current was westward, the DWBC crossed the equator, joined

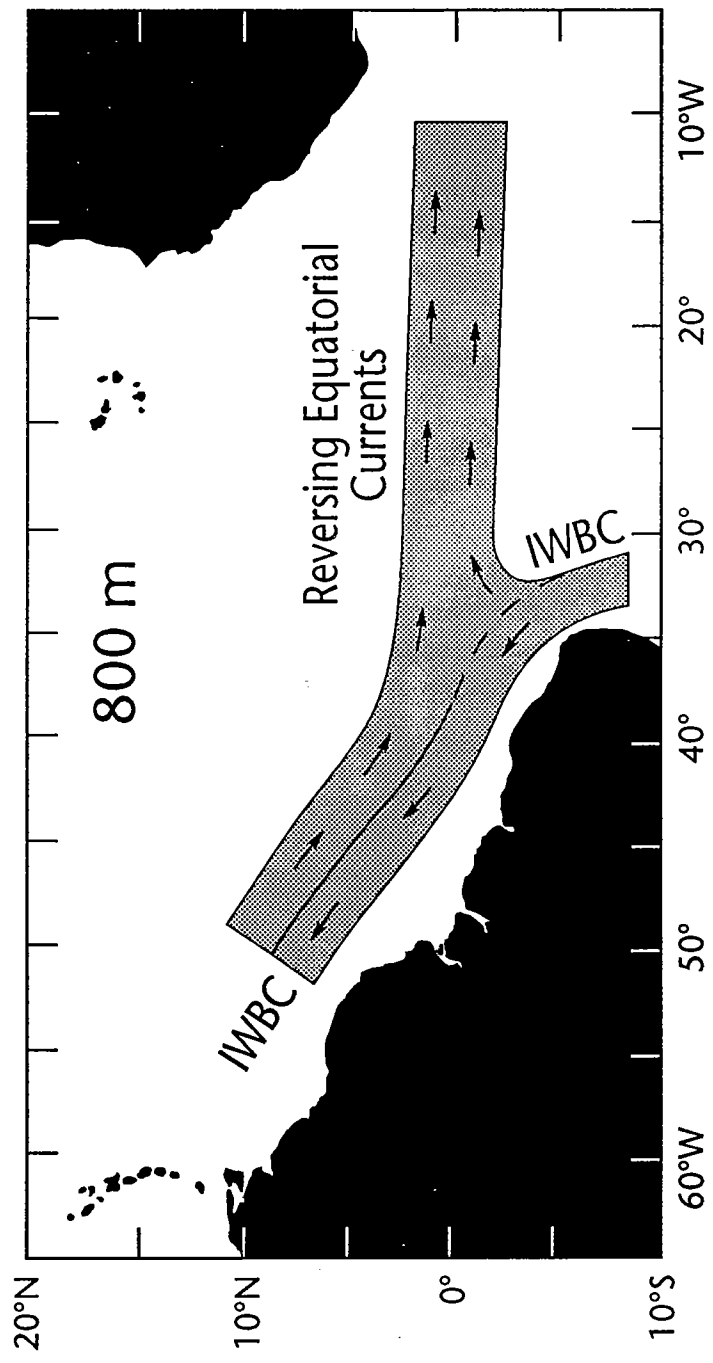


Figure 16: Schematic diagram summarizing the 21 months of 800 m float data. The direct connection between the IWBC and the equatorial current was not obvious from the trajectories because the IWBC floats went northwestward and the equatorial floats went eastward. The schematic shown here is thus based partially on a consideration of continuity.

by flow turning south from the equator. Thus the equatorial current seems to serve as a temporary reservoir for DWBC water. Variations in the DWBC and its cross-equatorial flow seem to be linked to low-frequency variations of the equatorial current. The inferred period of the variations is around three years based on the 21 months of data. The longer term drift of the floats over an additional two years should provide a better picture of the variations of these currents and the longer-term fate of DWBC water.

The 3300 m float trajectories look very different from the 1800 m ones; no indication of a DWBC was observed and the mean velocity was slow. We conclude that these floats were located in a low velocity layer separating the upper and lower cores of both freon and velocity in the DWBC. Thus the DWBC is very different off Northeast Brazil than off Abaco, where a single southward flowing jet extended from around 1000 m to the sea floor near 4700 m.

Most visually striking of the 800 m trajectories is the long eastward drift of floats between 5S–6N, which suggests large transports. The reversal in direction of several floats near the end of the 21 months implies that the flow varied with a period of around three years. Large southward transport in the equatorial band is suggested by the southward tilt of five trajectories there. If the equatorial currents are tilted on average, their reversal could also cause a reversal of transport, which implies that the cross-equatorial flow could have large low-frequency variations at this depth.

At 800 m, a northwestward-flowing IWBC was observed north of the equator, bounded in the offshore direction by counterflow which fed into the equatorial current from as far north as 11N. Around half of the transport per unit depth in the IWBC consisted of a series of three anticyclonic eddies that translated up the boundary. One was tracked all the way from the equator to 11N. North of 7N the anticyclones are inferred to be subsurface manifestations of North Brazil Current retroflection eddies.

Acknowledgments

Funds were provided by National Science Foundation grants OCE-8521082, OCE-8517375, and OCE-9114656. J. R. Valdes, R. Tavares, B. Guest and G. Tupper were in charge of the SOFAR floats and listening stations which were launched from the RV *Oceanus* and RV *Iselin*. M. Zemanovic and C. Wooding tracked the floats, generated figures, and calculated statistics. R. Goldsmith created the routine to calculate distance and direction of a float from topographic contours. G. Hufford

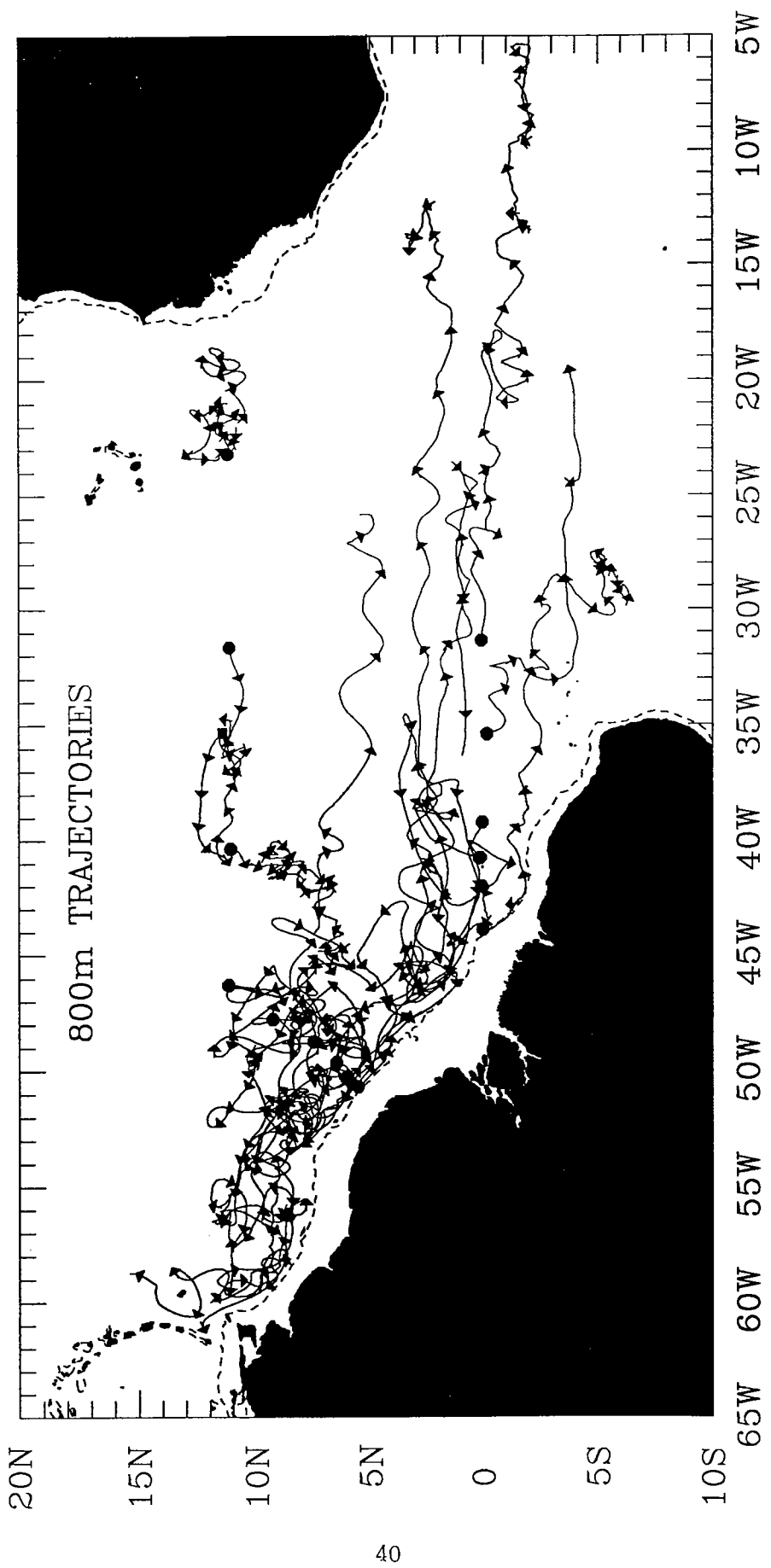
helped with the graphics and made a video of the trajectories which helped us to interpret them. B. Gaffron typed the manuscript.

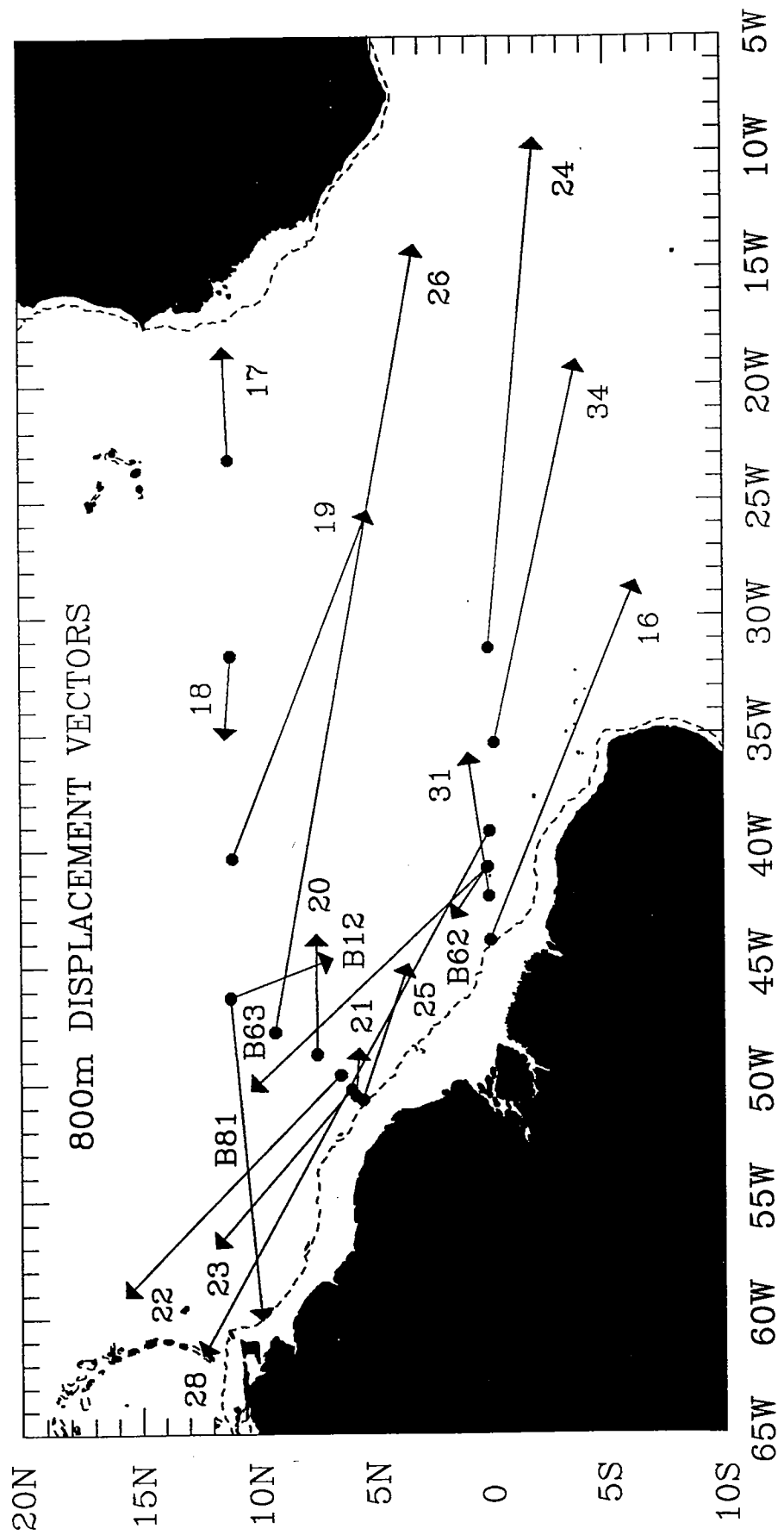
References

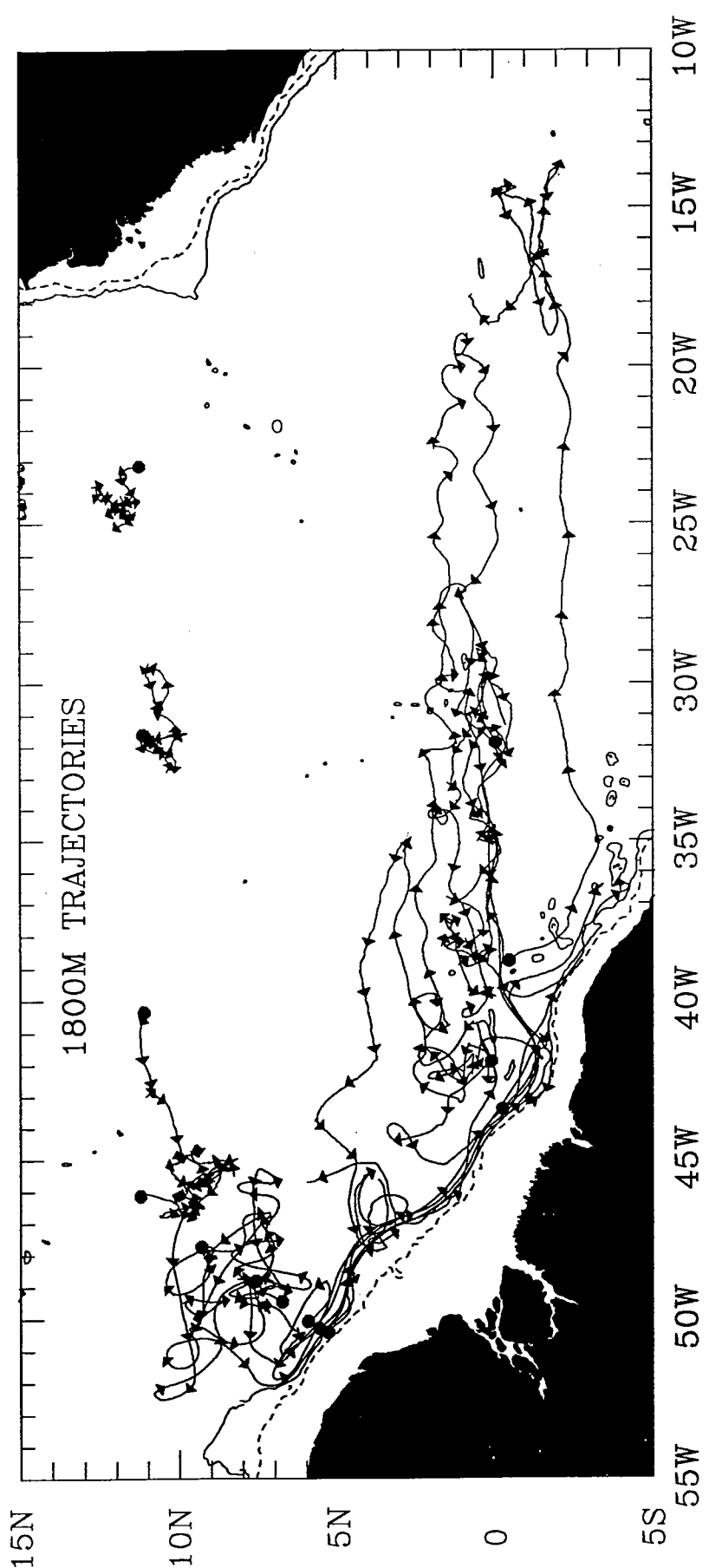
- Böning, C. W., and F. A. Schott, 1992. The WOCE model in the equatorial Atlantic: deep currents and the equatorial salinity tongue. Unpublished manuscript.
- Colin, C., J. M. Bore, R. Chuchla, and D. Corre, 1991. Programme Noe, Resultats de courantometrie. Centre ORSTOM de Cayenne: Documents Scientifiques No. O.P.IV 1991, 54 pp.
- Ponte, R. M., J. Luyten, and P. L. Richardson, 1990. Equatorial deep jets in the Atlantic Ocean. *Deep-Sea Res.*, **37**, 711-713.
- Schmitz, W. J., Jr., and P. L. Richardson, 1991. On the sources of the Florida Current. *Deep-Sea Res.*, **38**, Suppl. 1, S379-S409.
- Uchupi, E., 1971. Bathymetric atlas of the Atlantic, Caribbean, and Gulf of Mexico. Woods Hole Oceanog. Inst. Tech. Rept., WHOI-71-72, 10 pp.

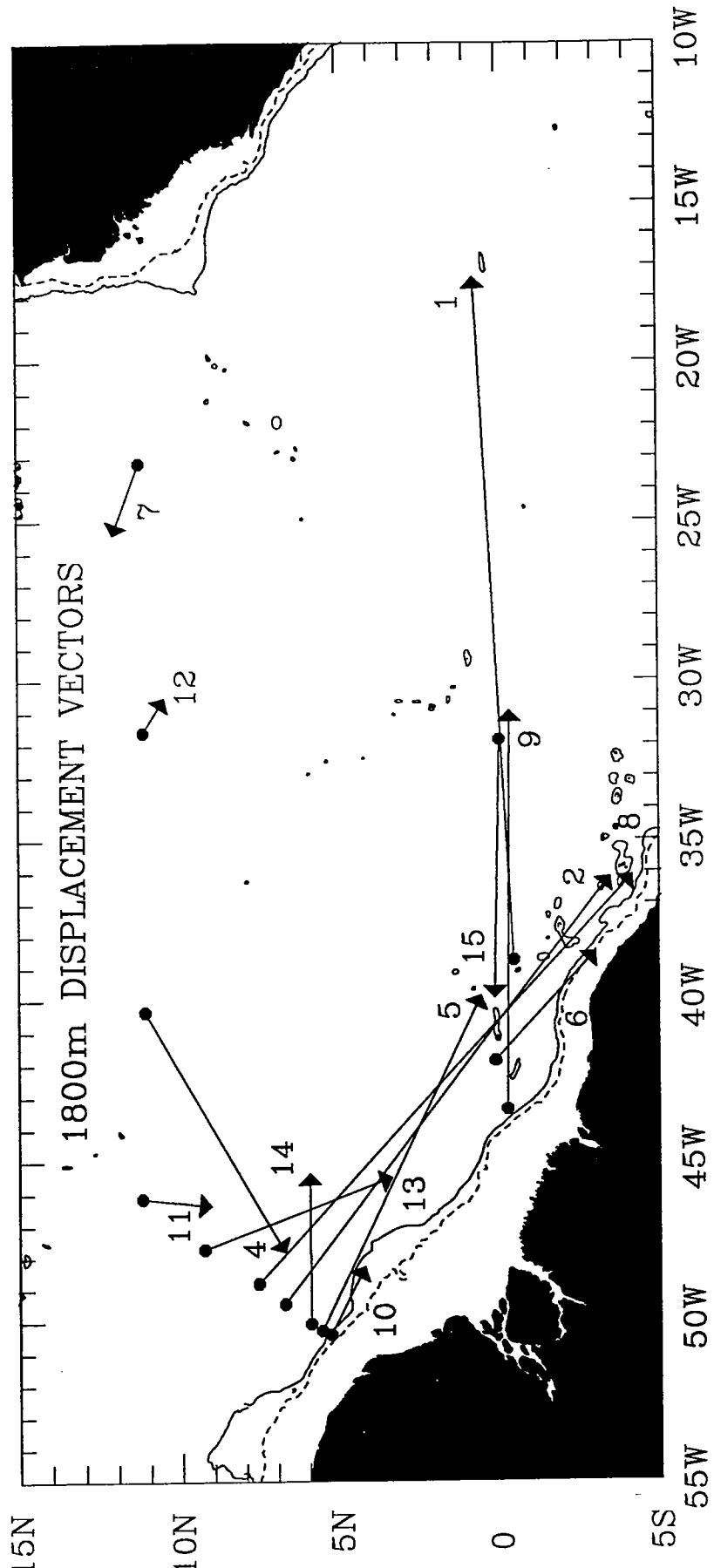
Appendix A: Summary Composites of Trajectories

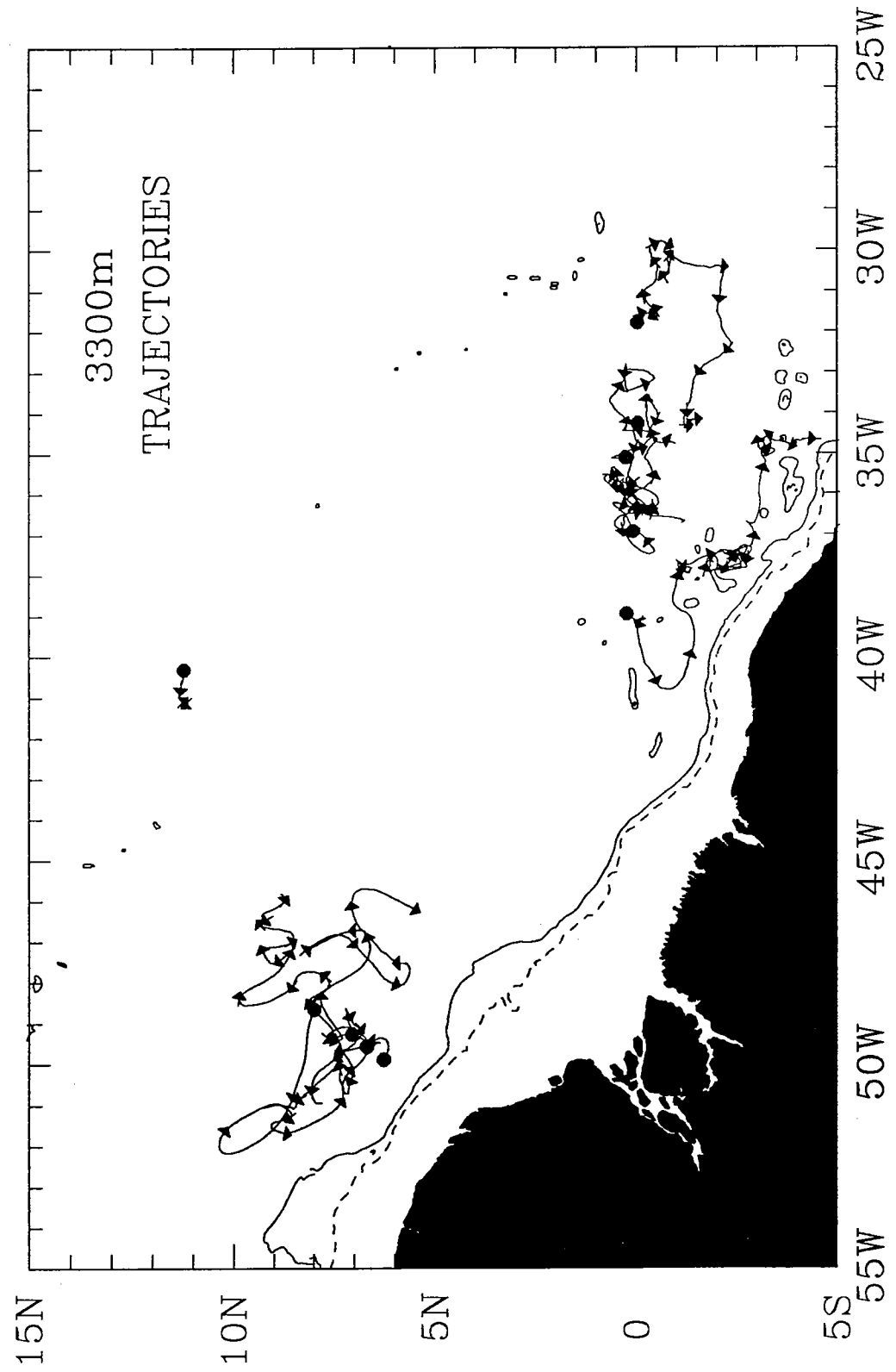
The following figures include: (1) summaries of all trajectories and displacement vectors at each depth (6 figures), (2) summaries of eastbound and westbound floats near the equator at 800 m (floats 16, 19, 24, 26, 31, 34) and 1800 m (floats 1, 5, 6, 9) (4 figures), and (3) three-month composites of all floats at each depth (12 figures).

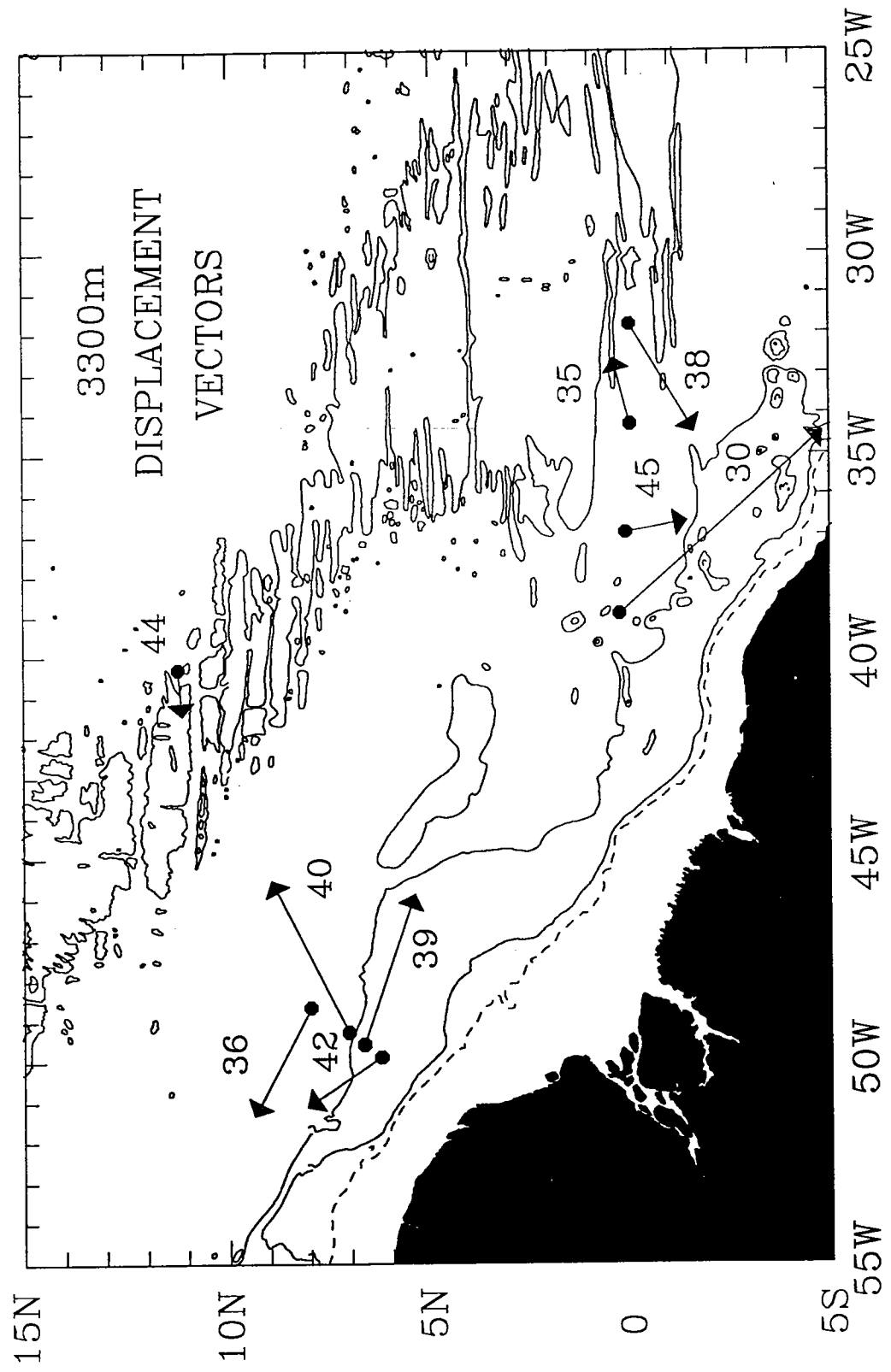


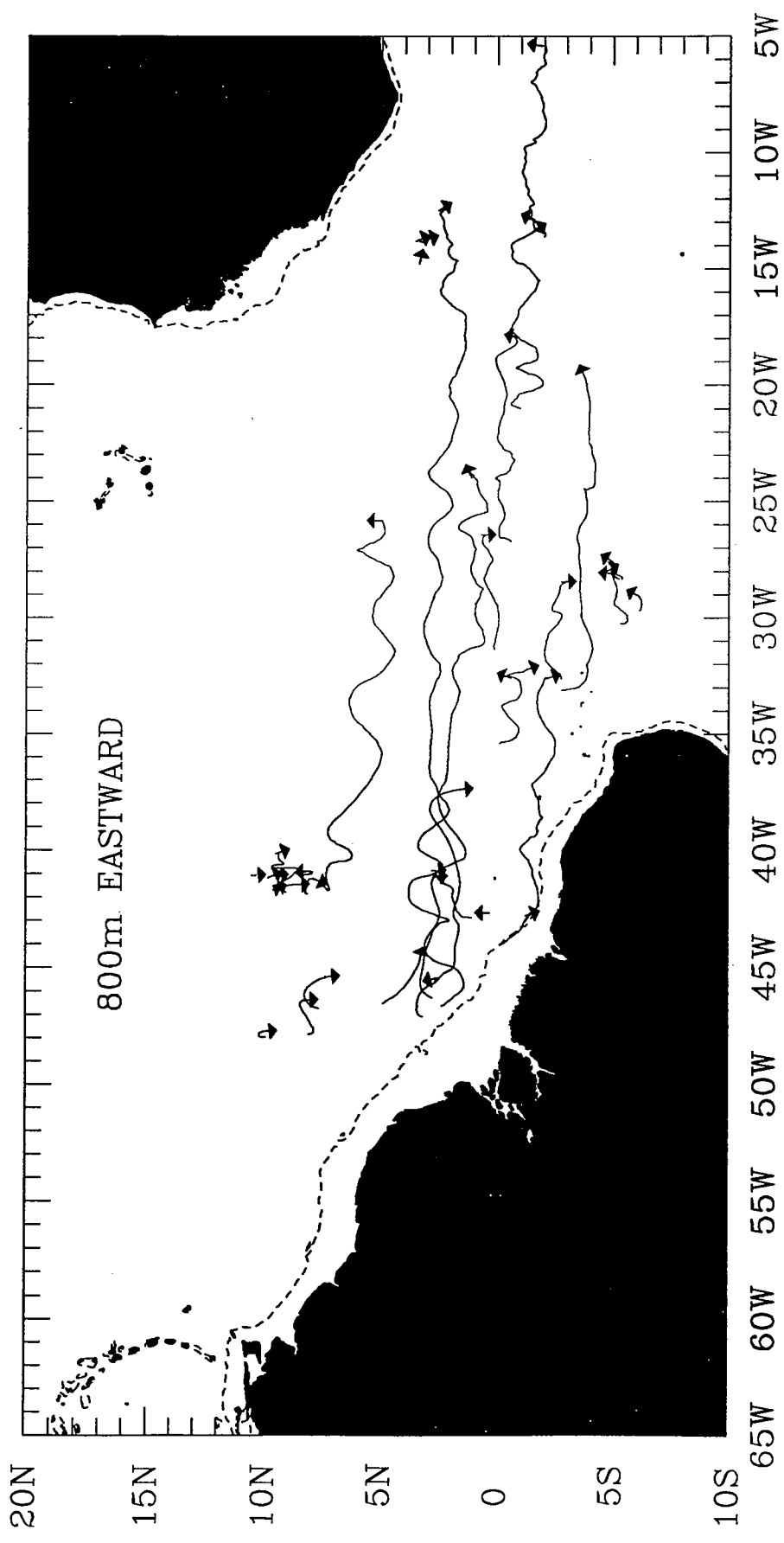


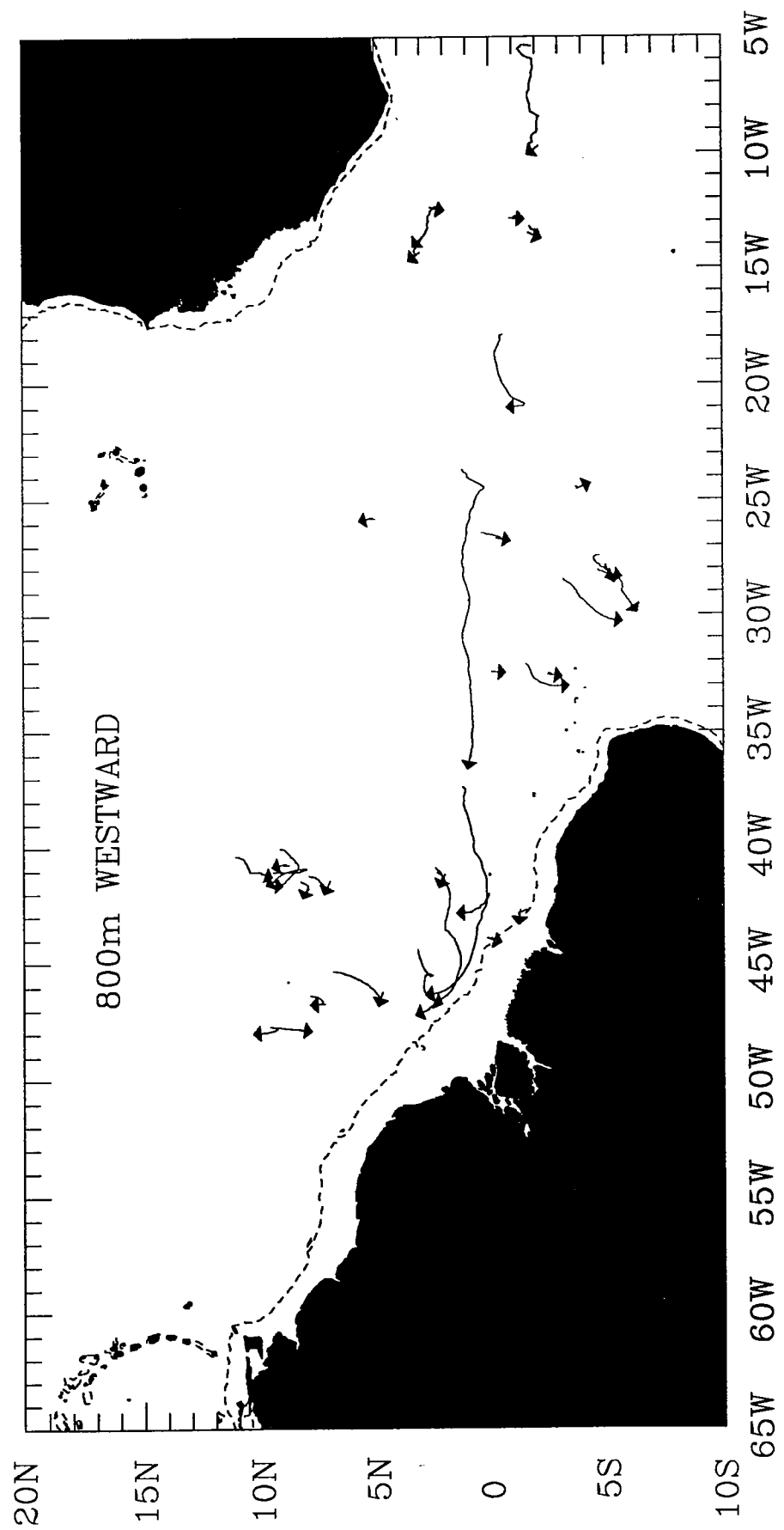


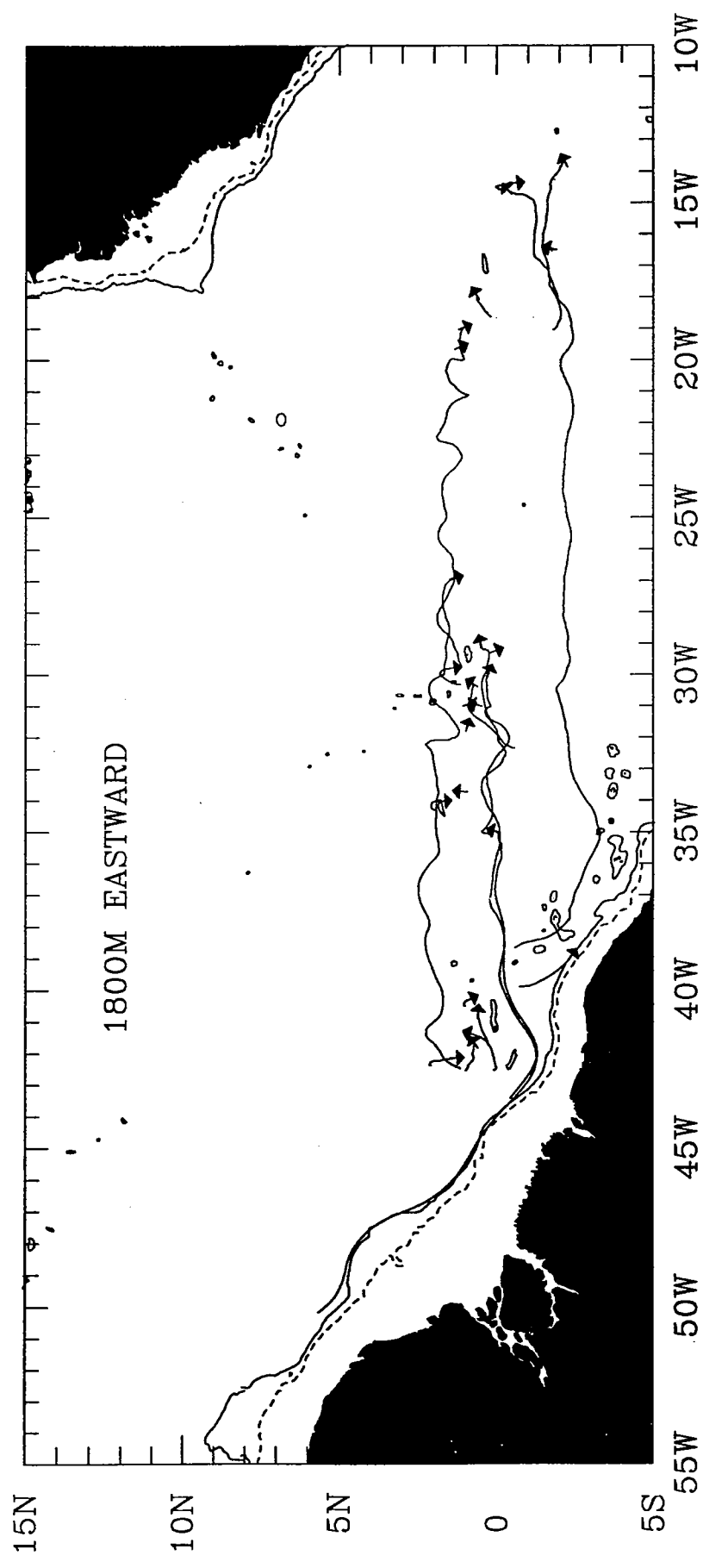






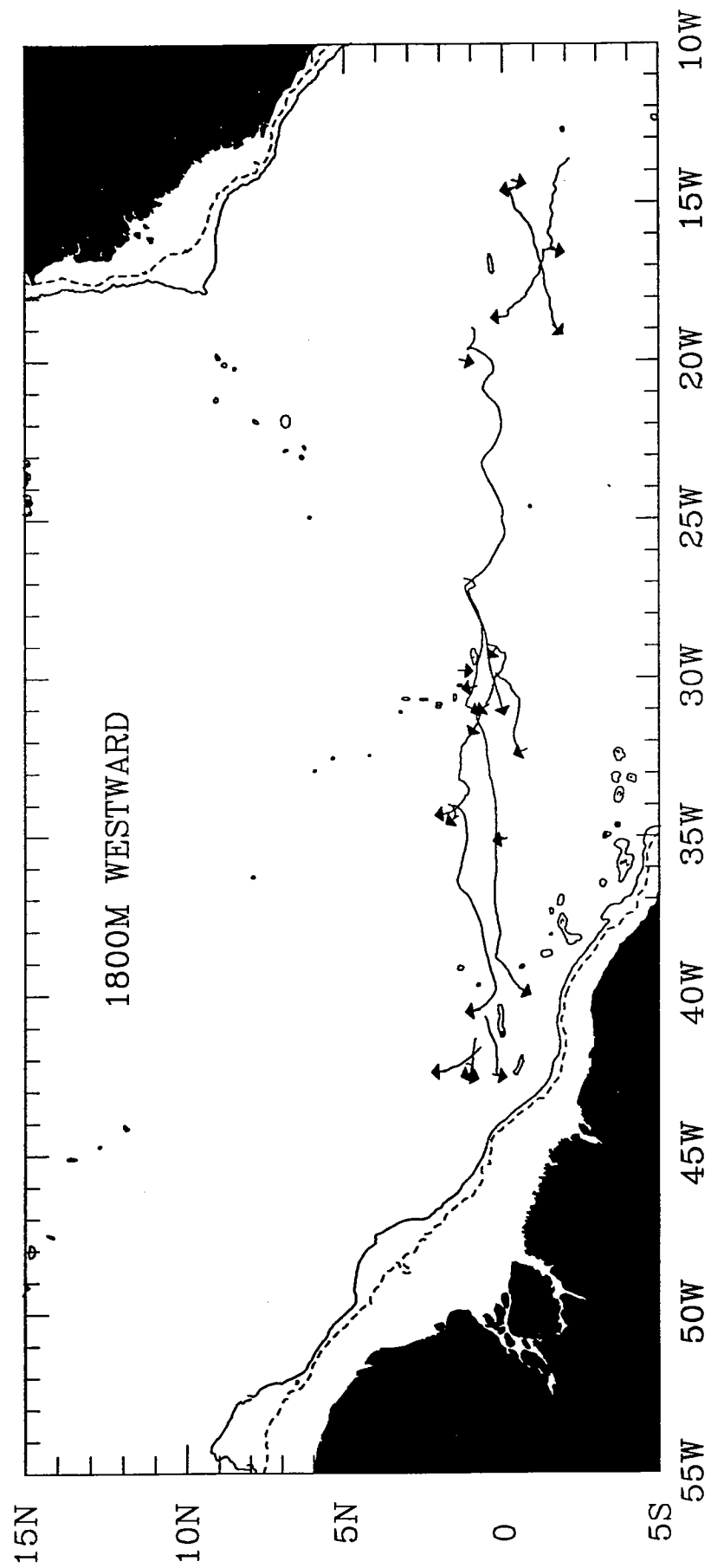




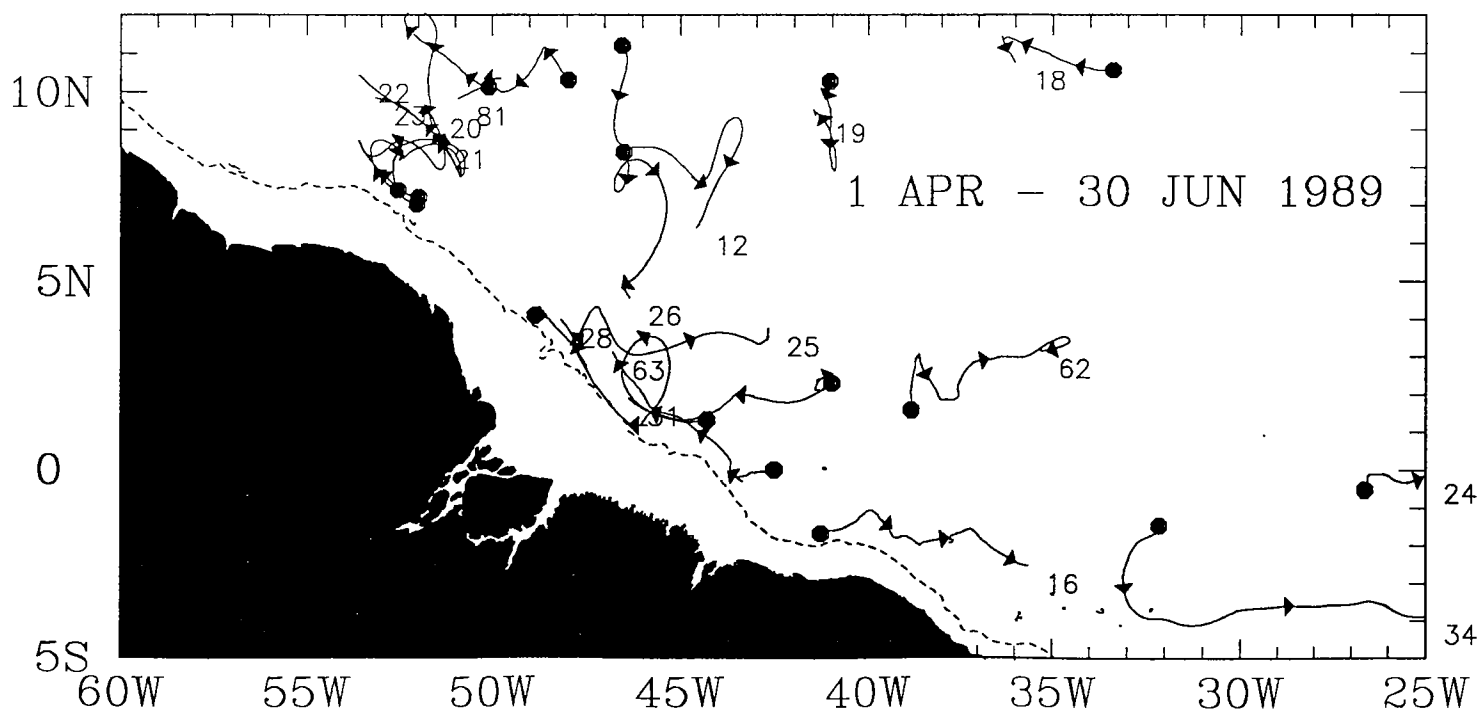
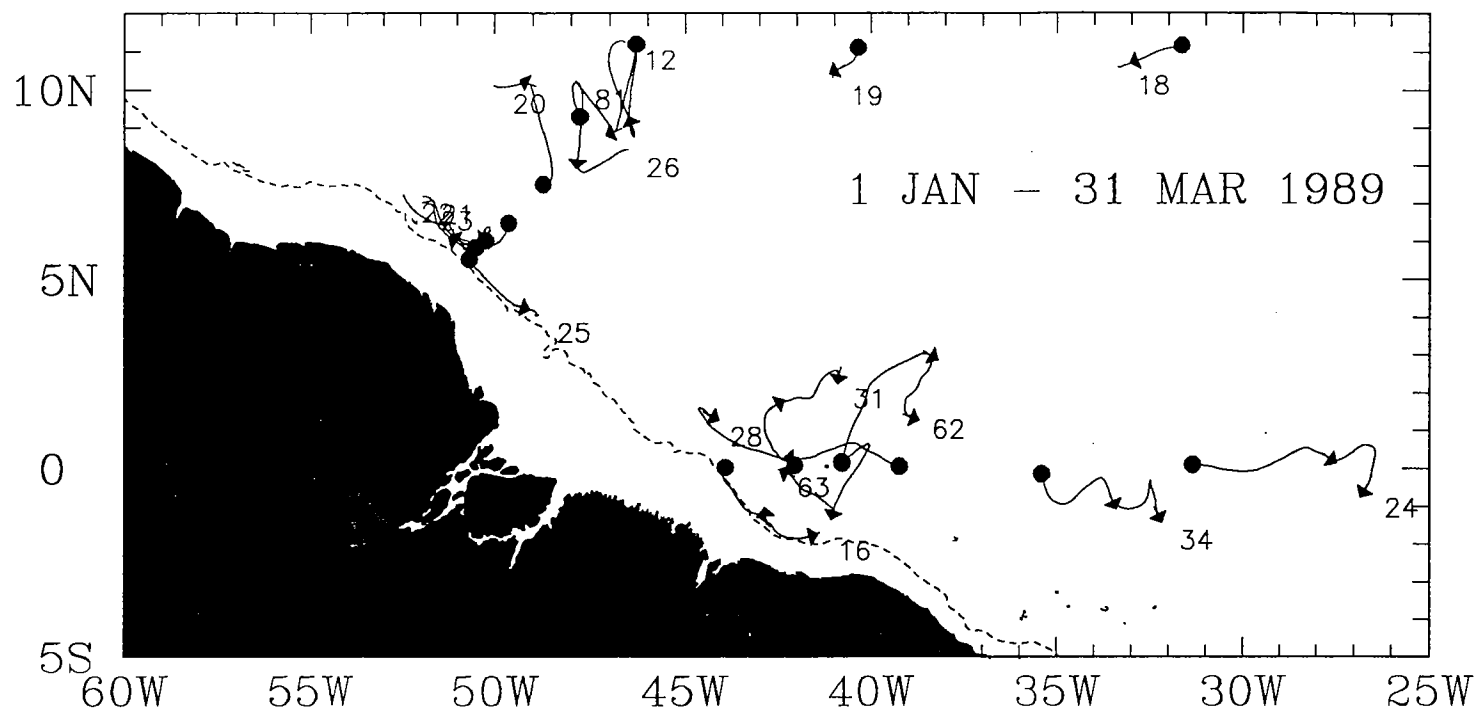


15N
10N
5N
0
5S

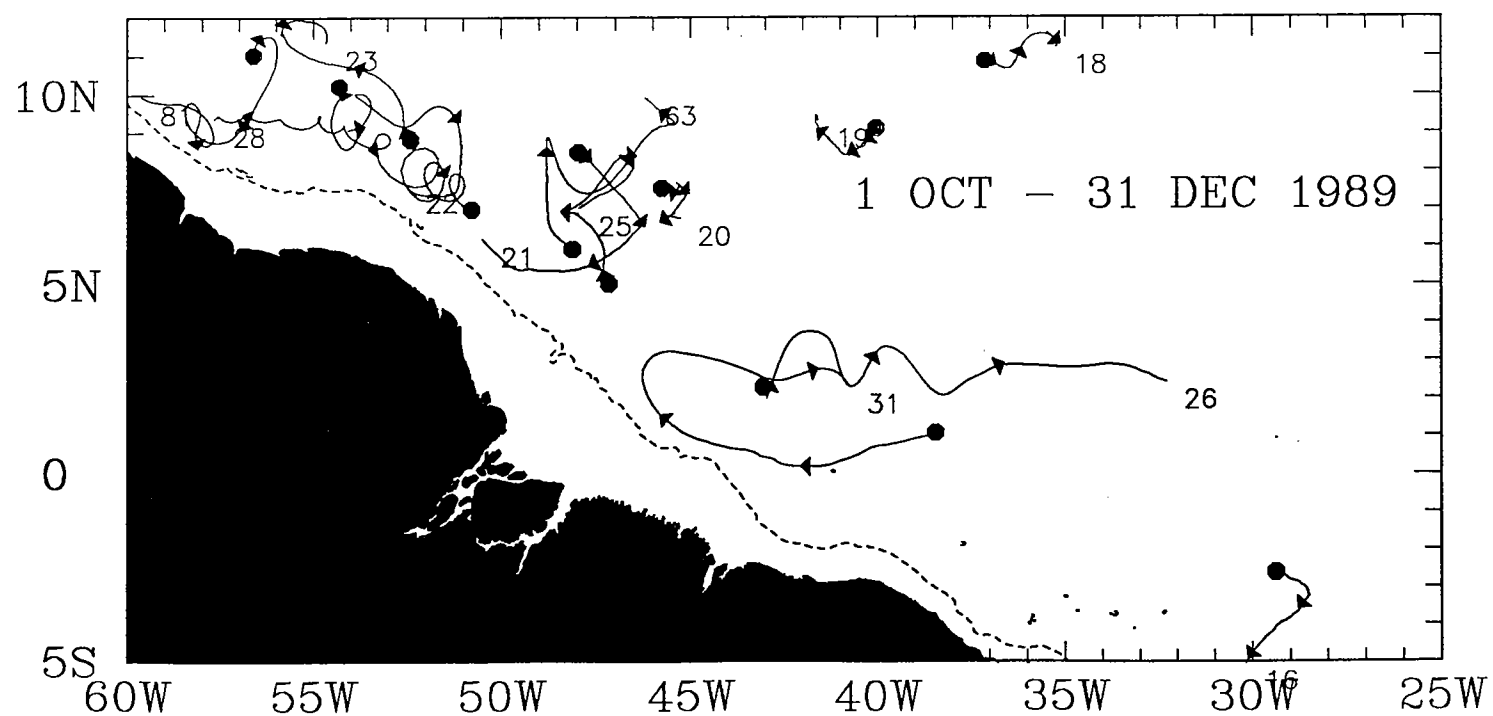
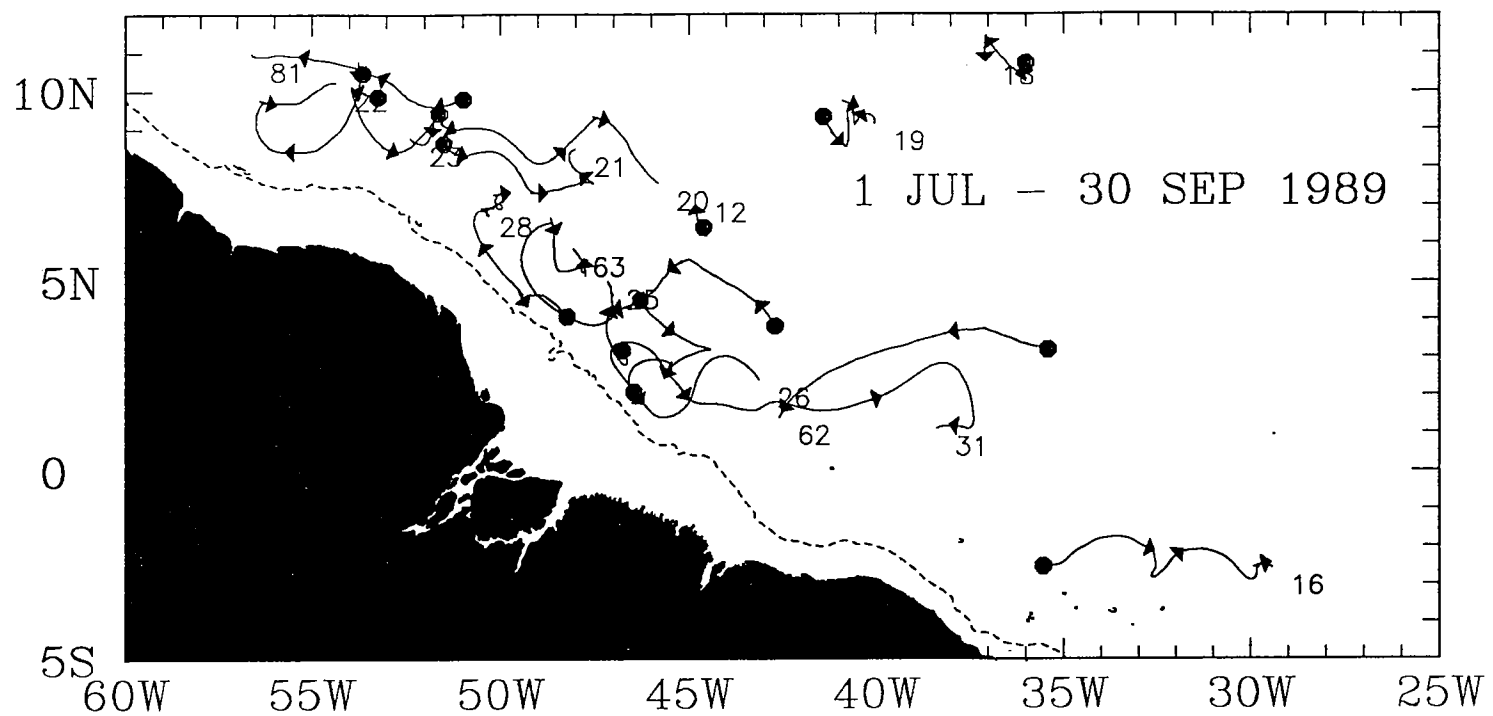
1800M EASTWARD



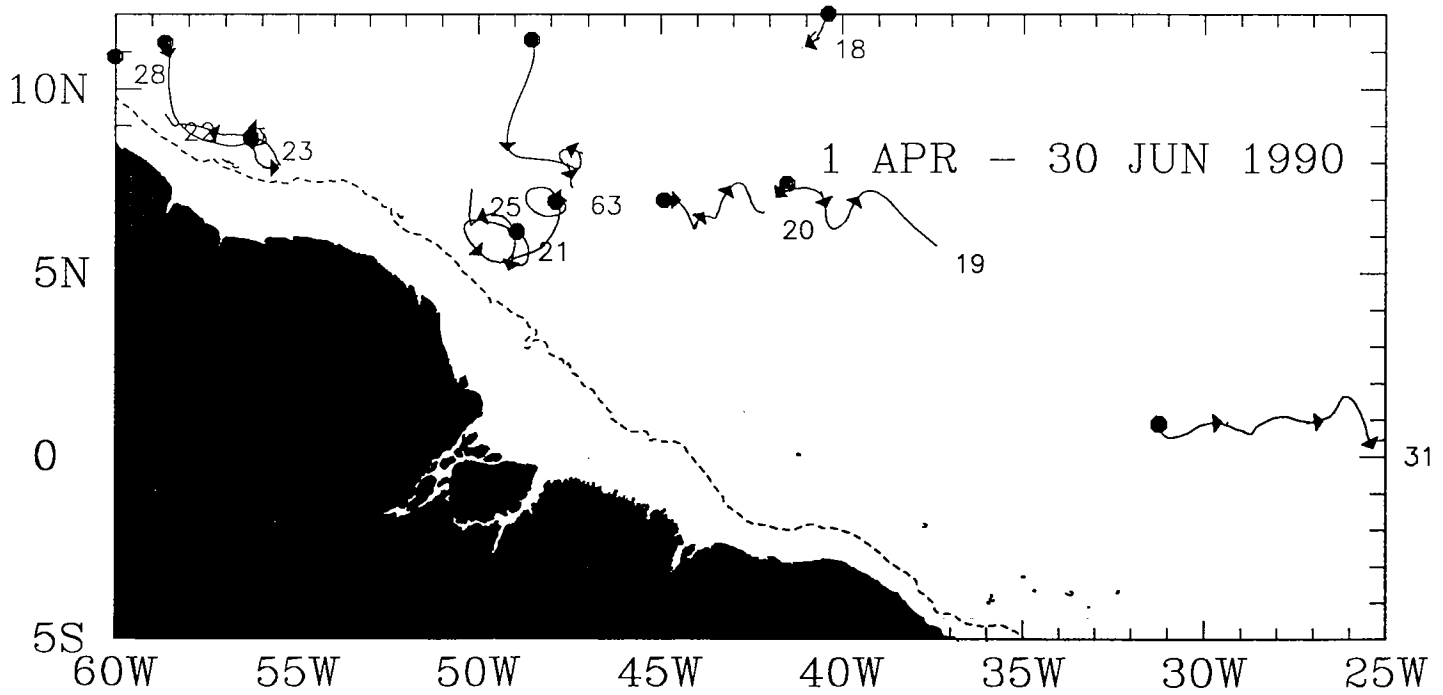
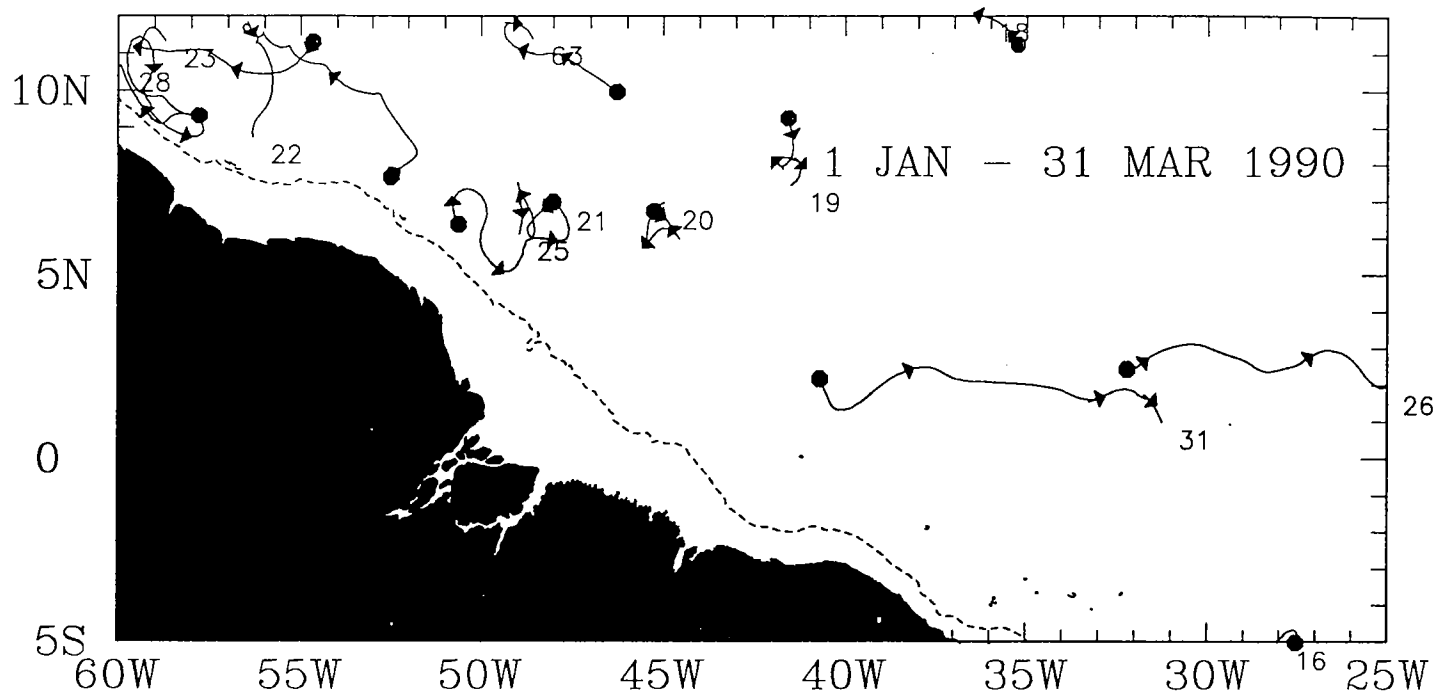
800m



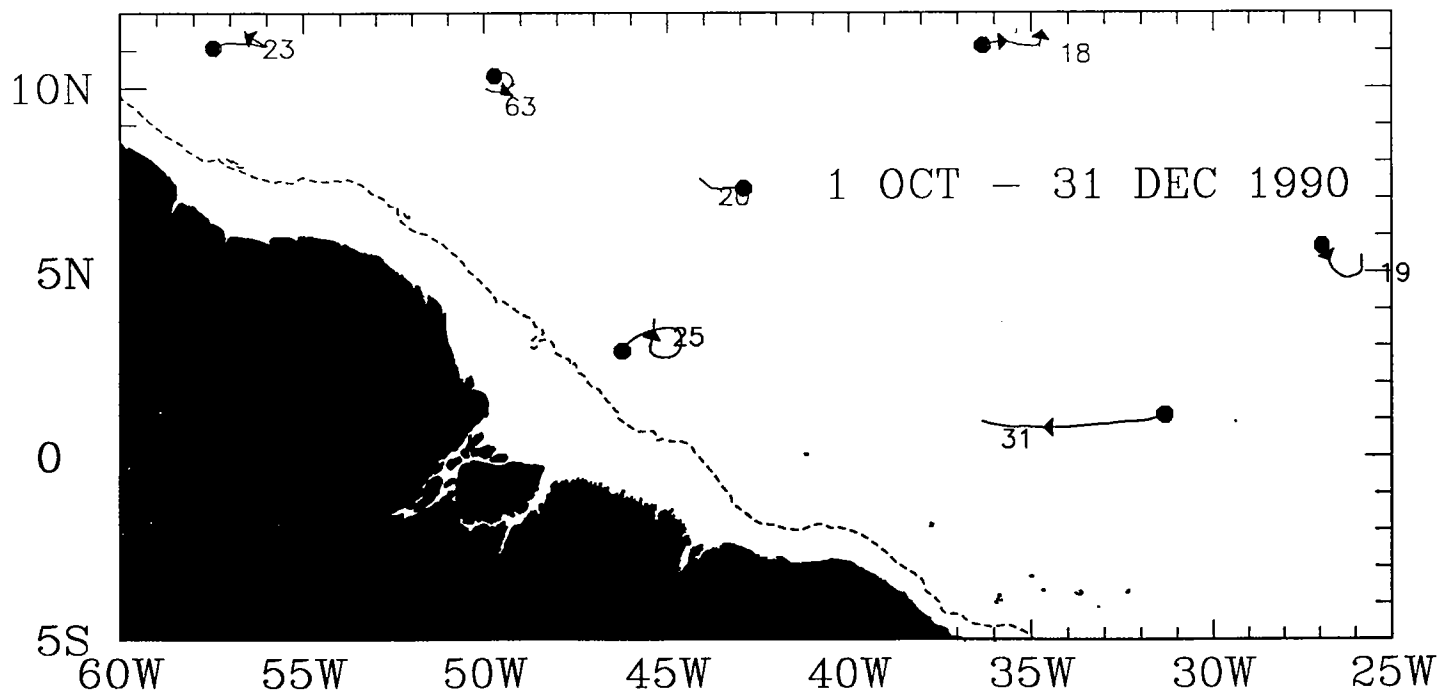
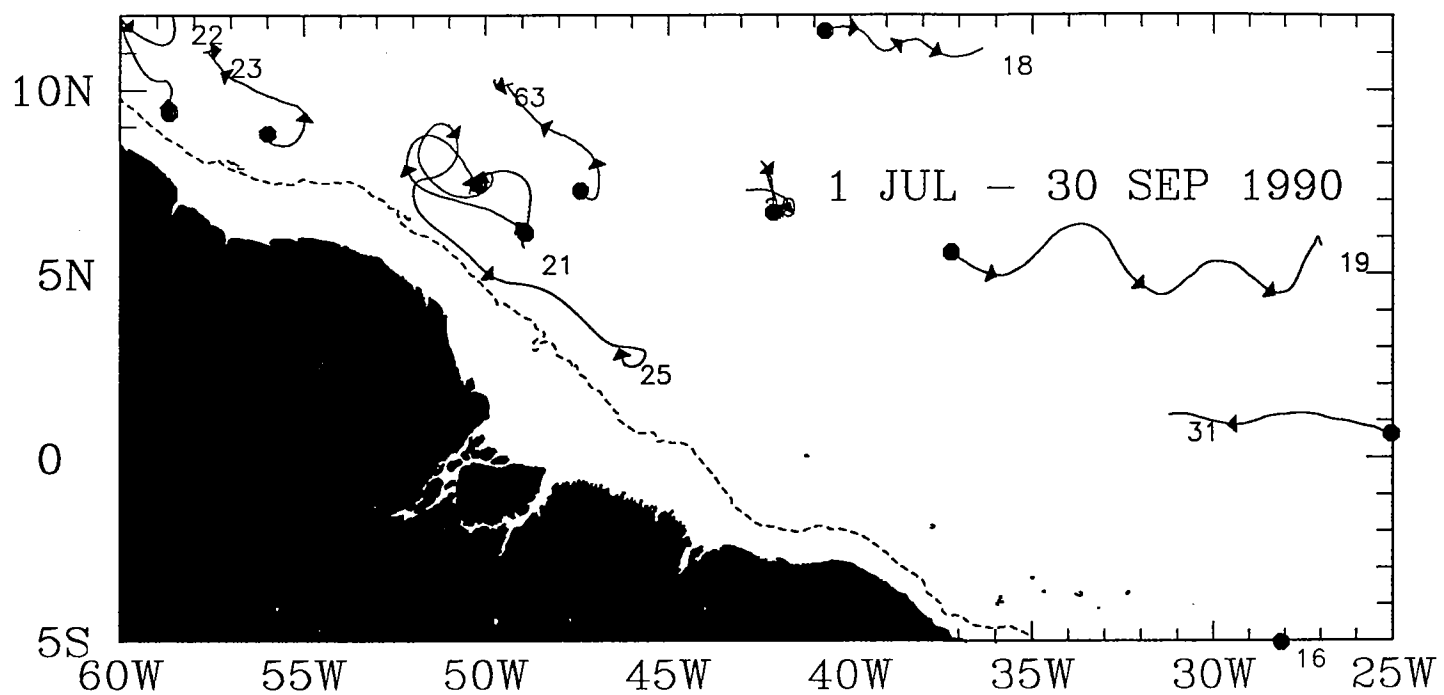
800m



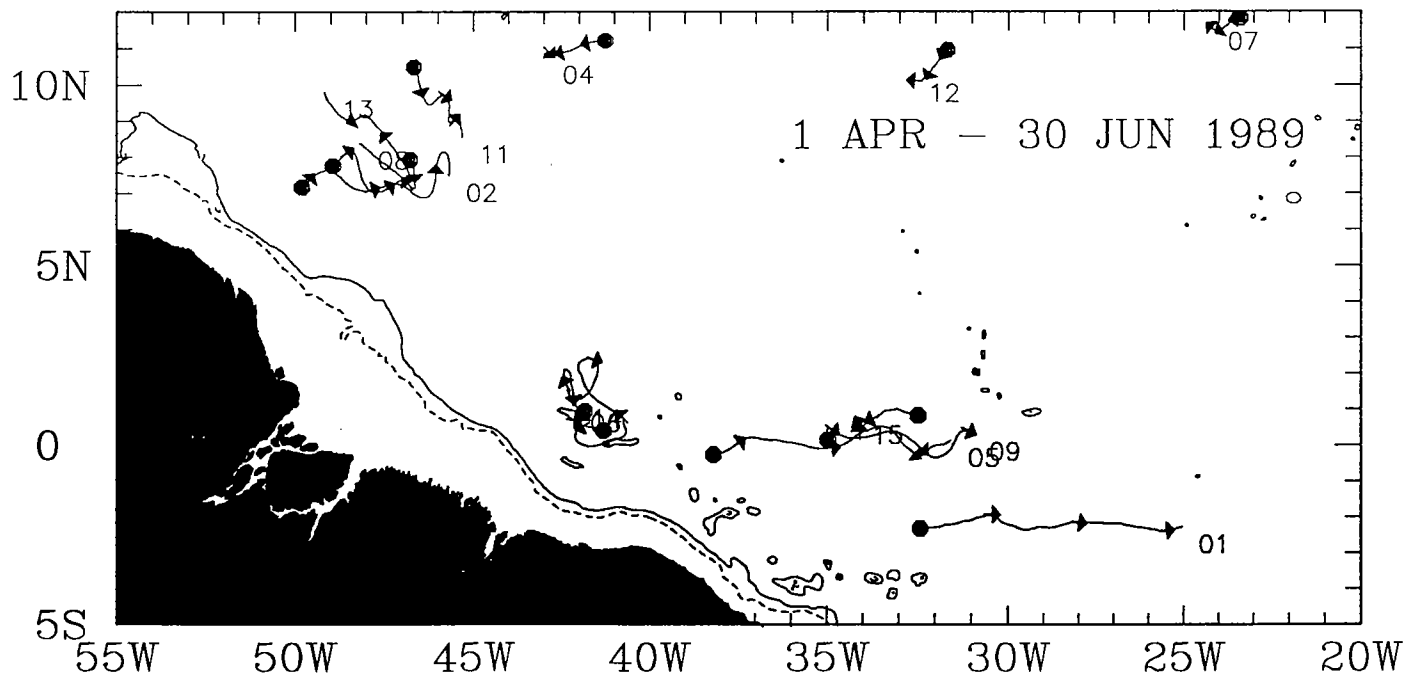
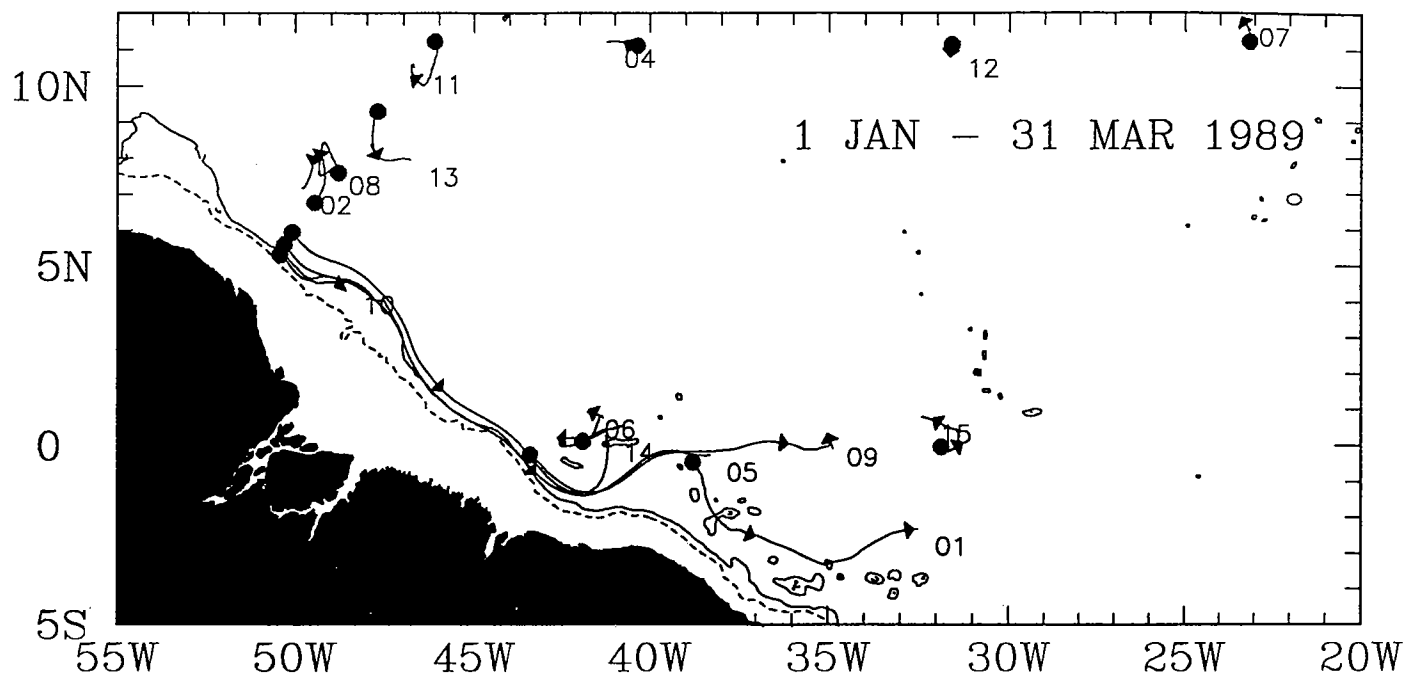
800m



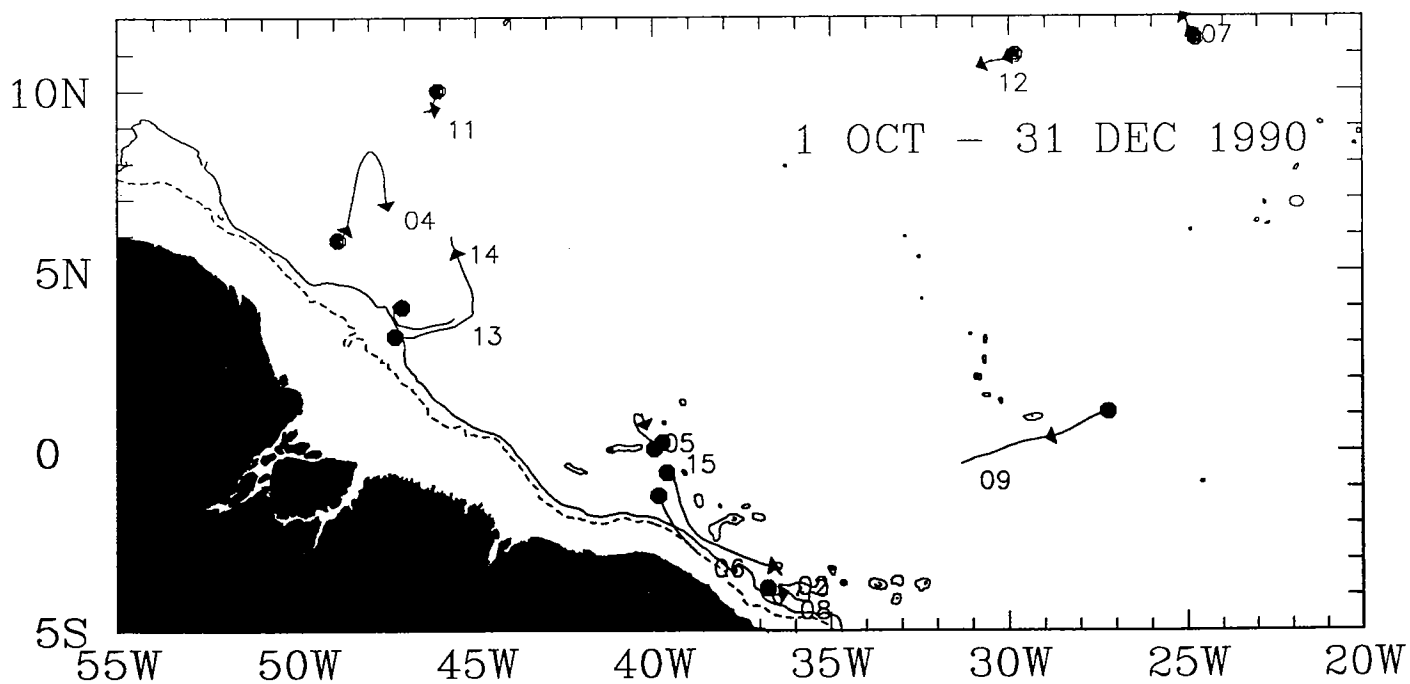
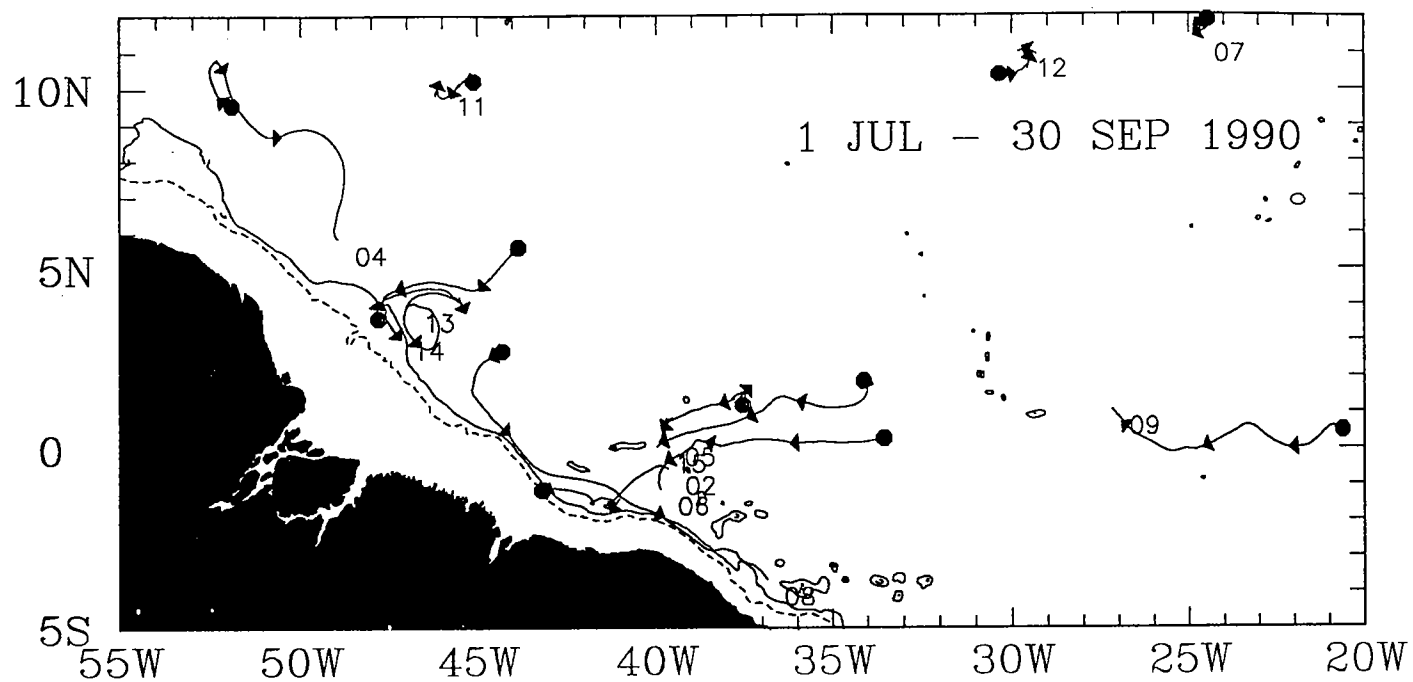
800m



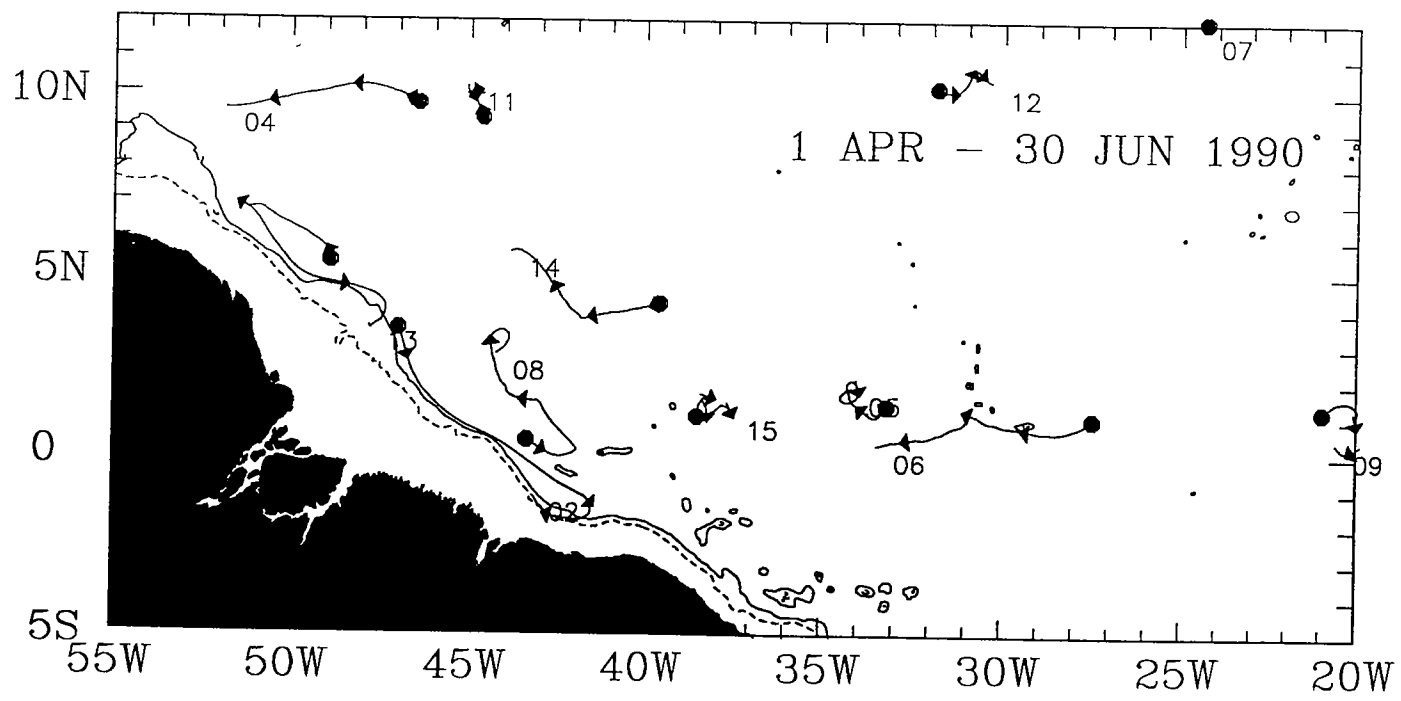
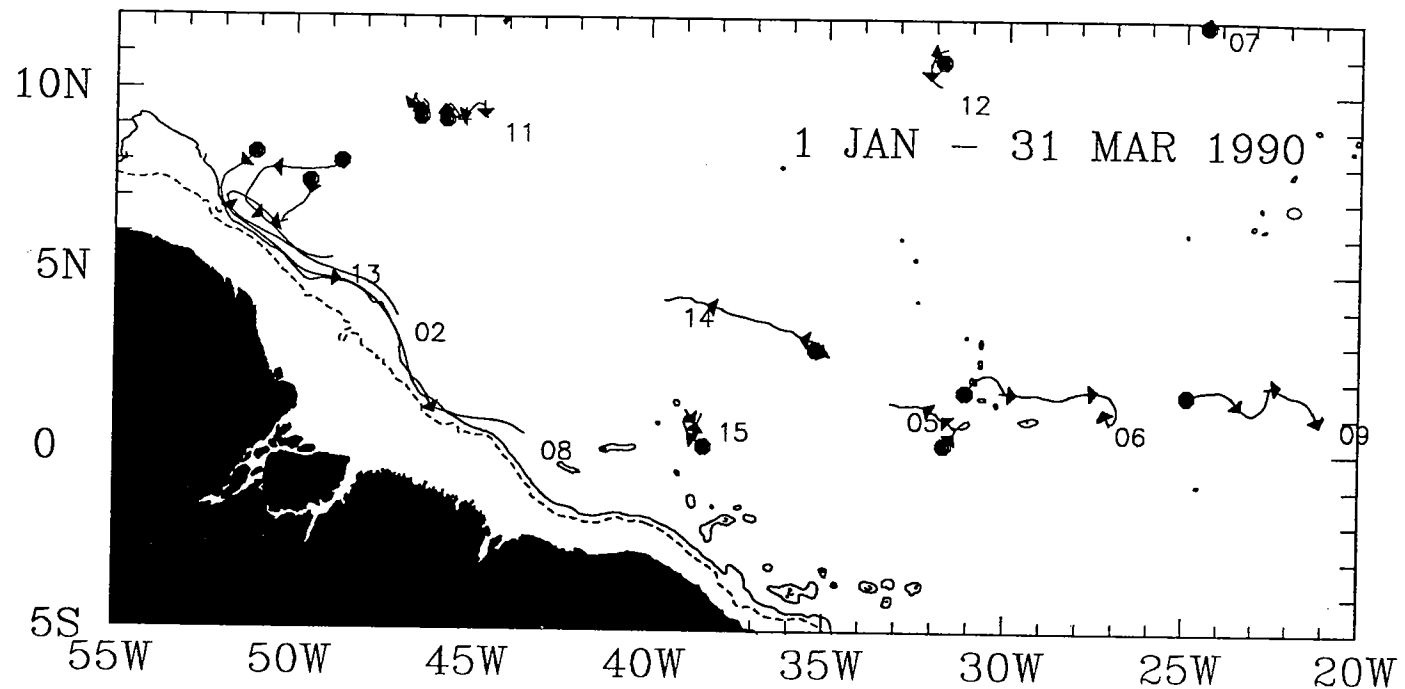
1800m



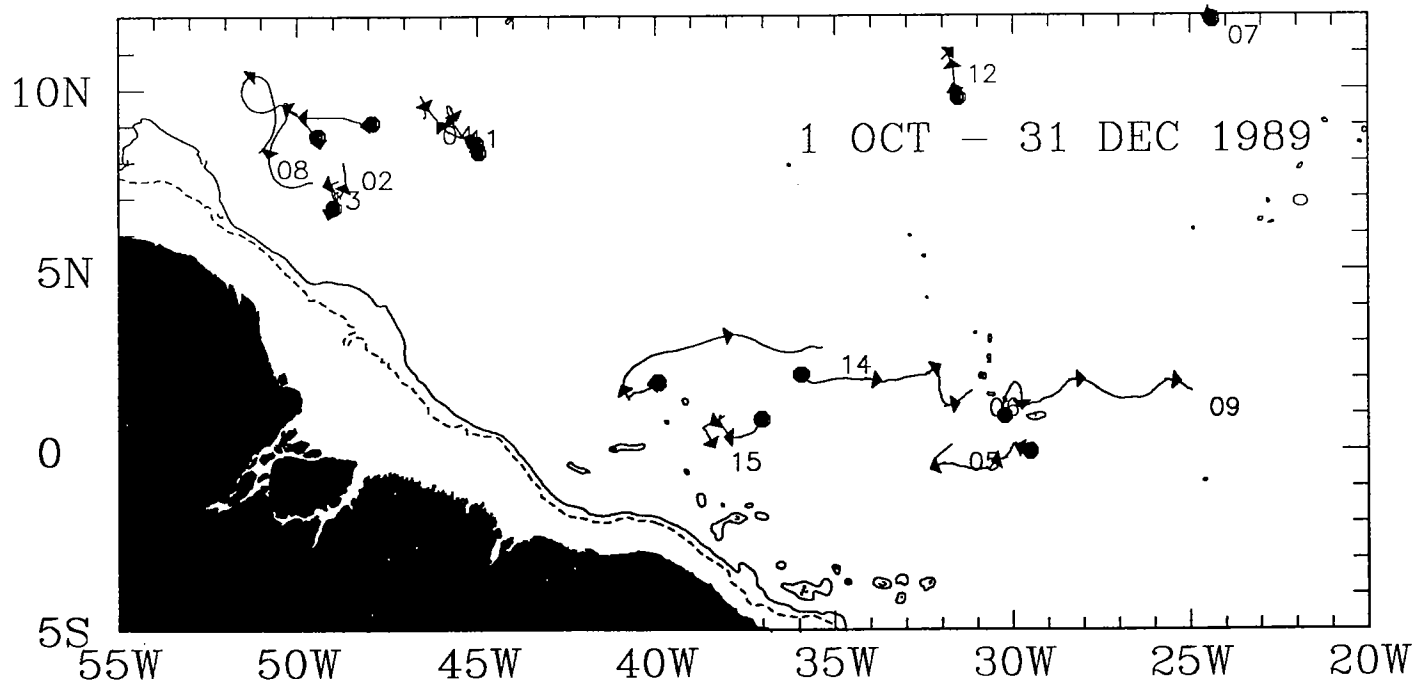
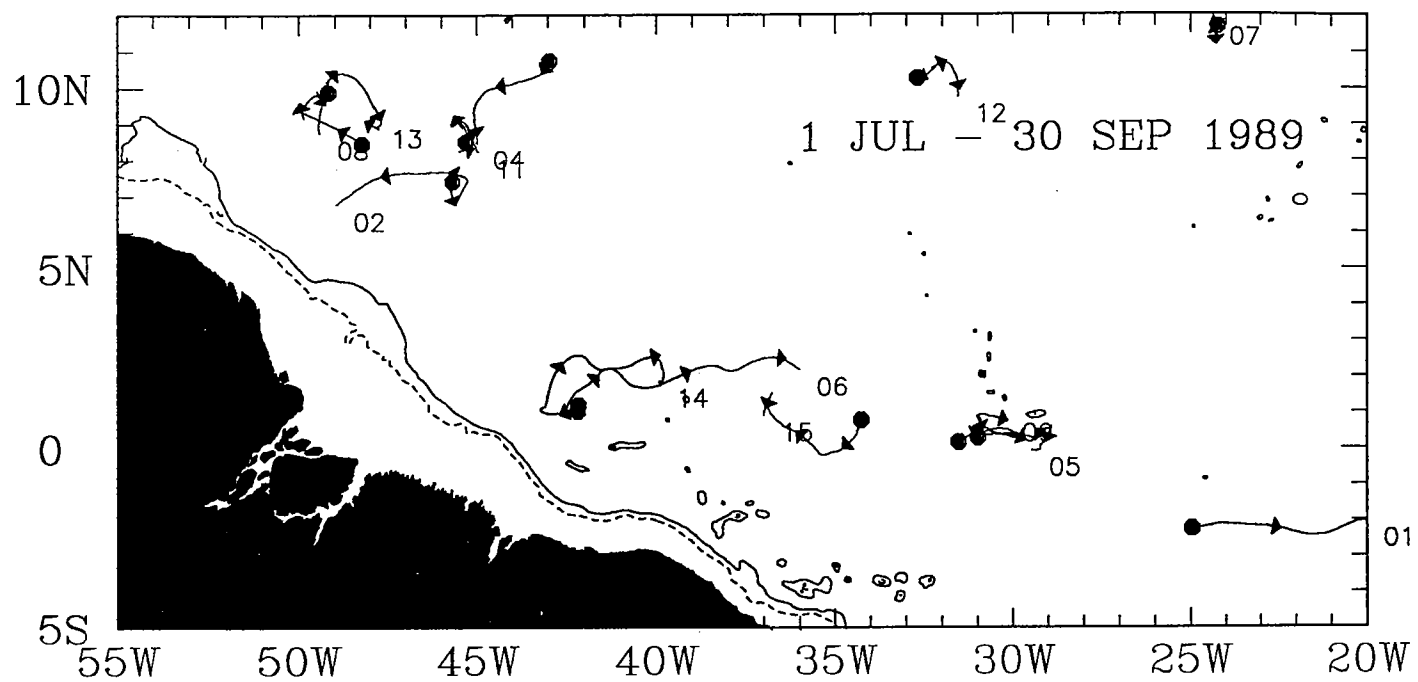
1800m



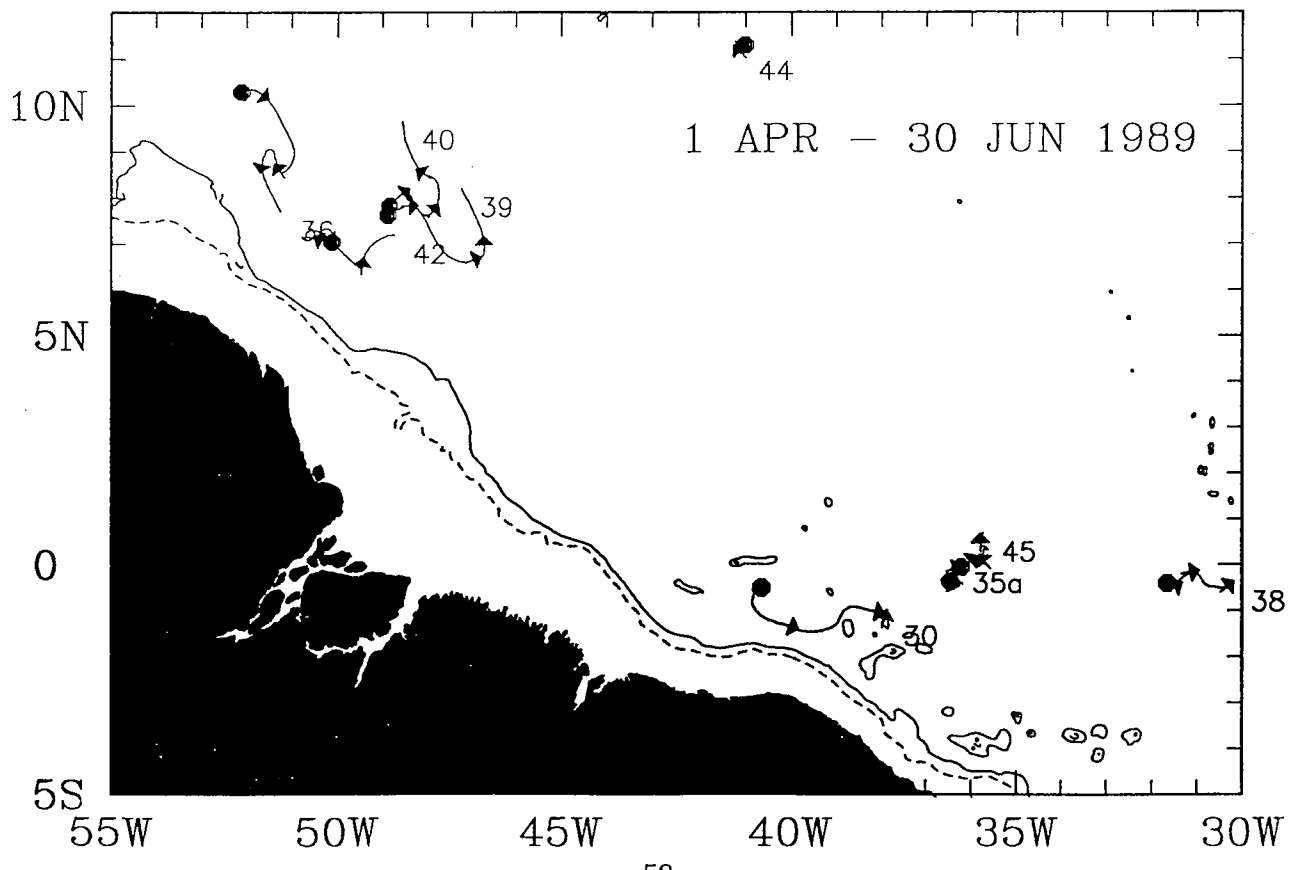
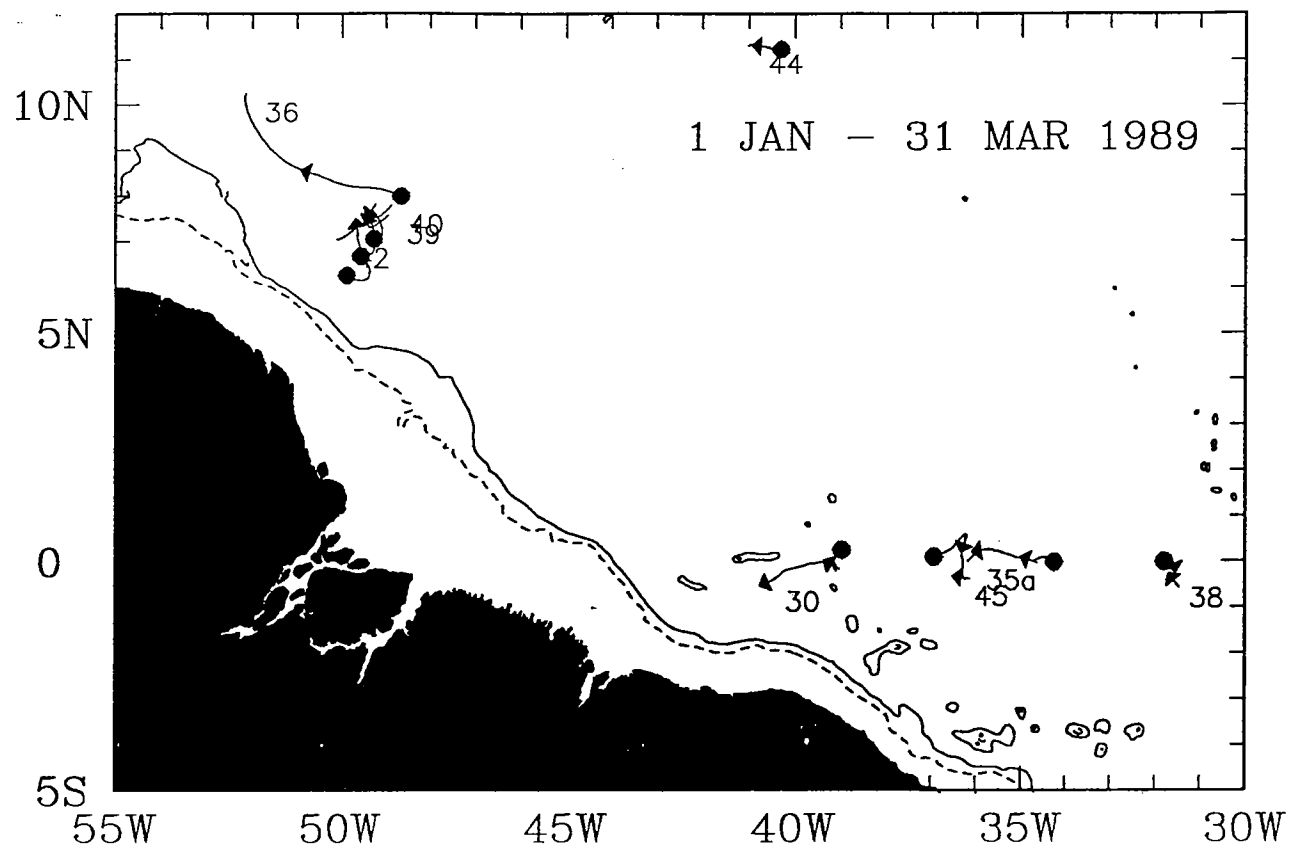
1800m



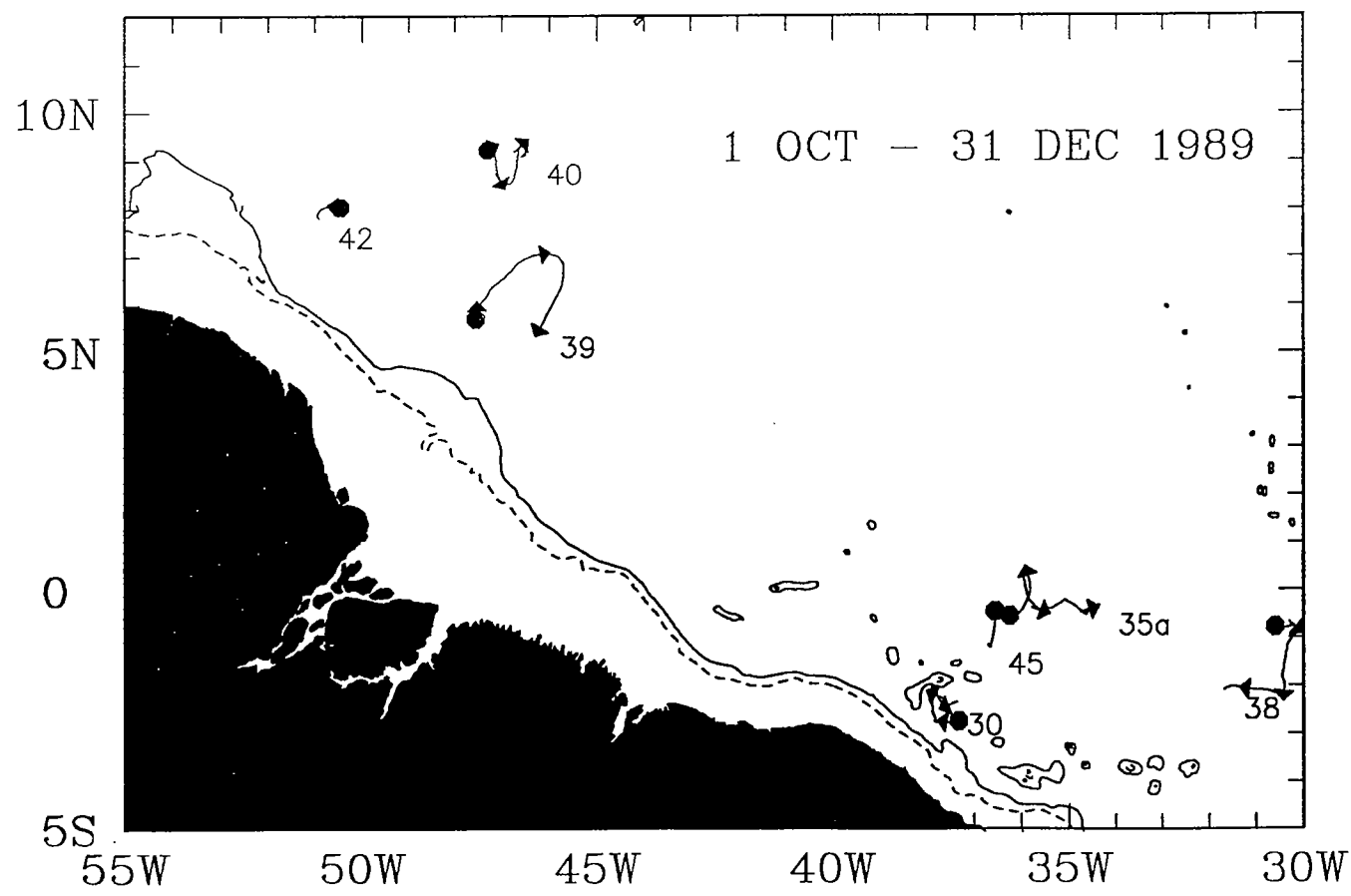
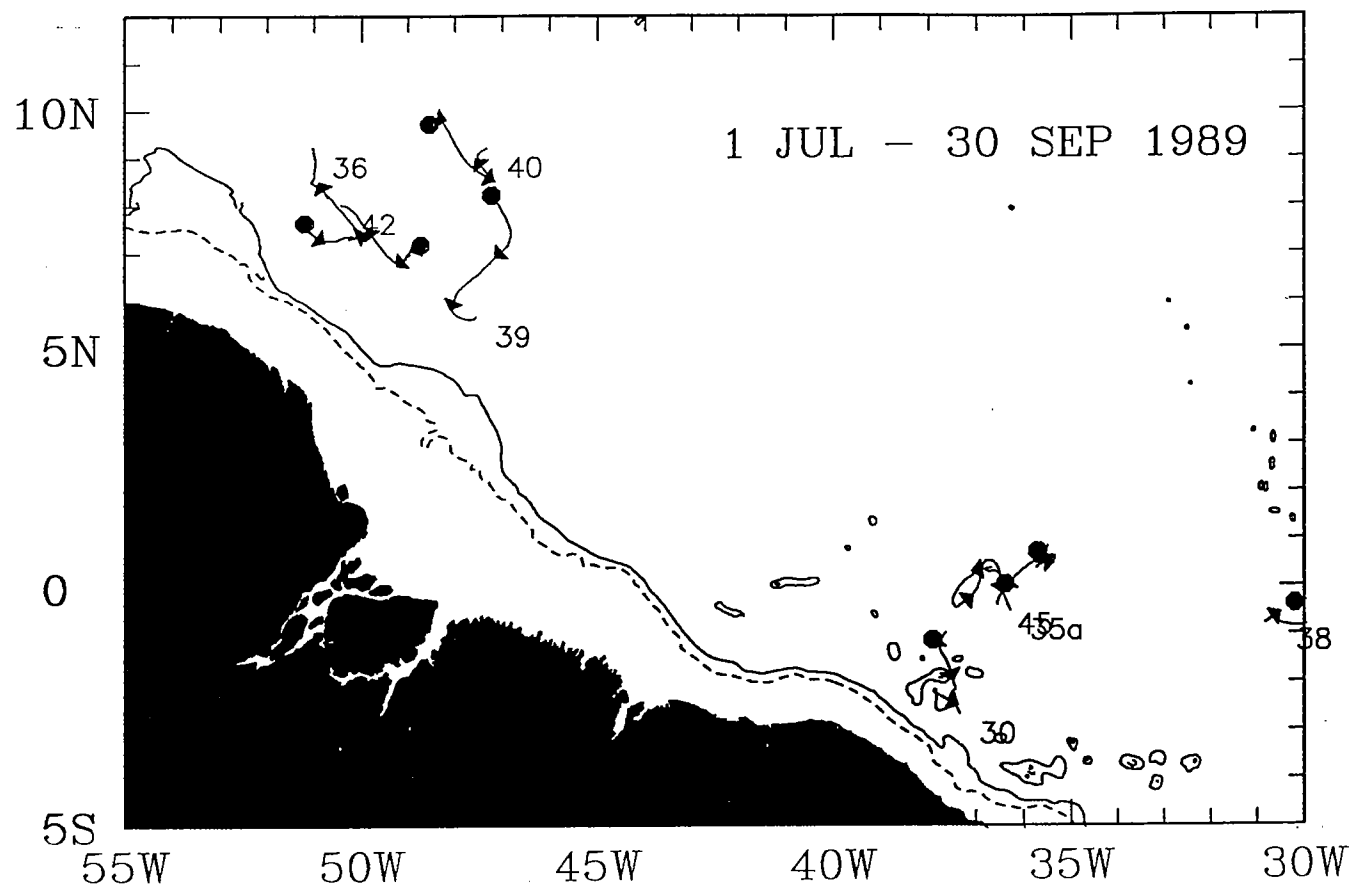
1800m



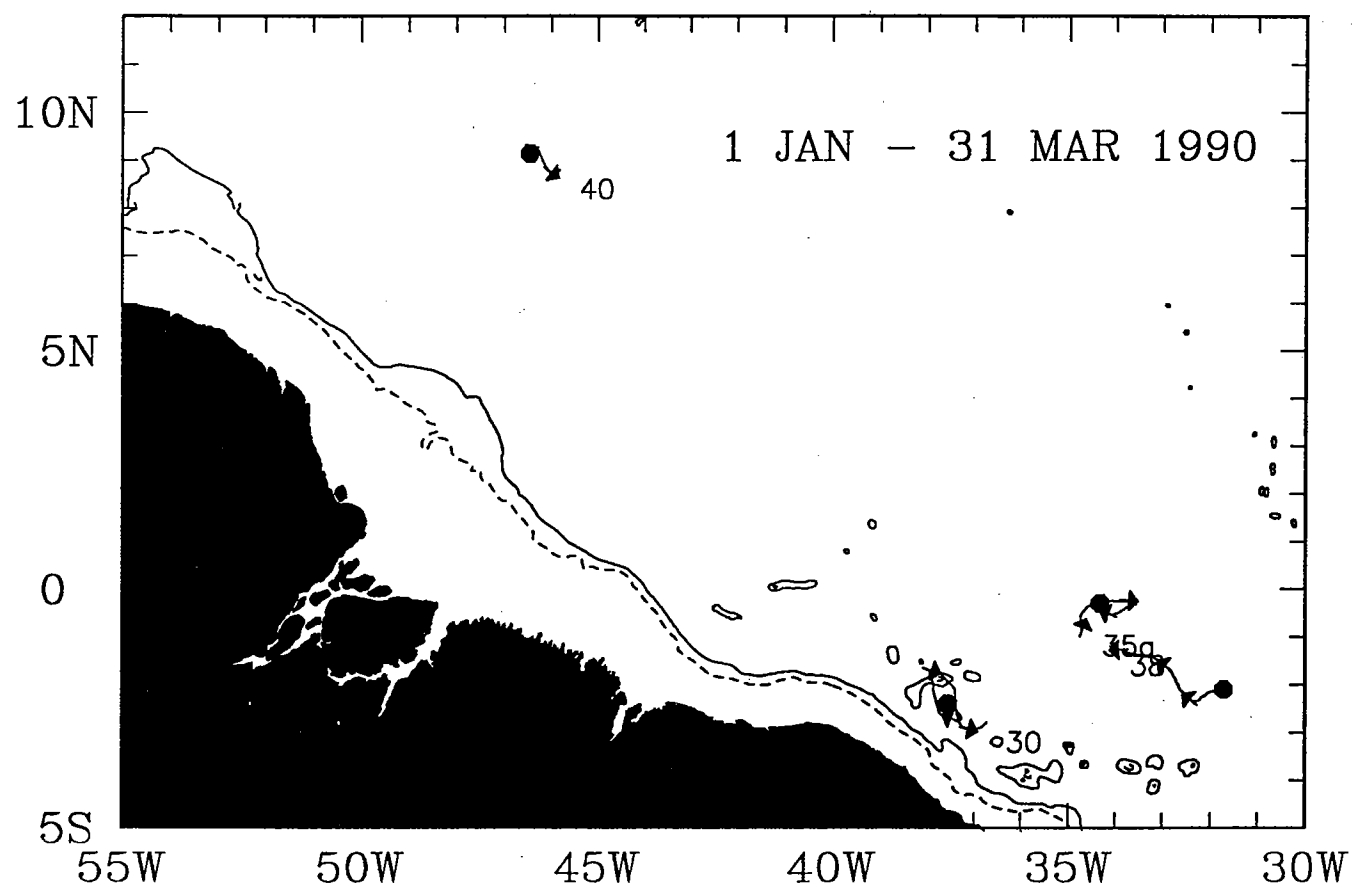
3300m



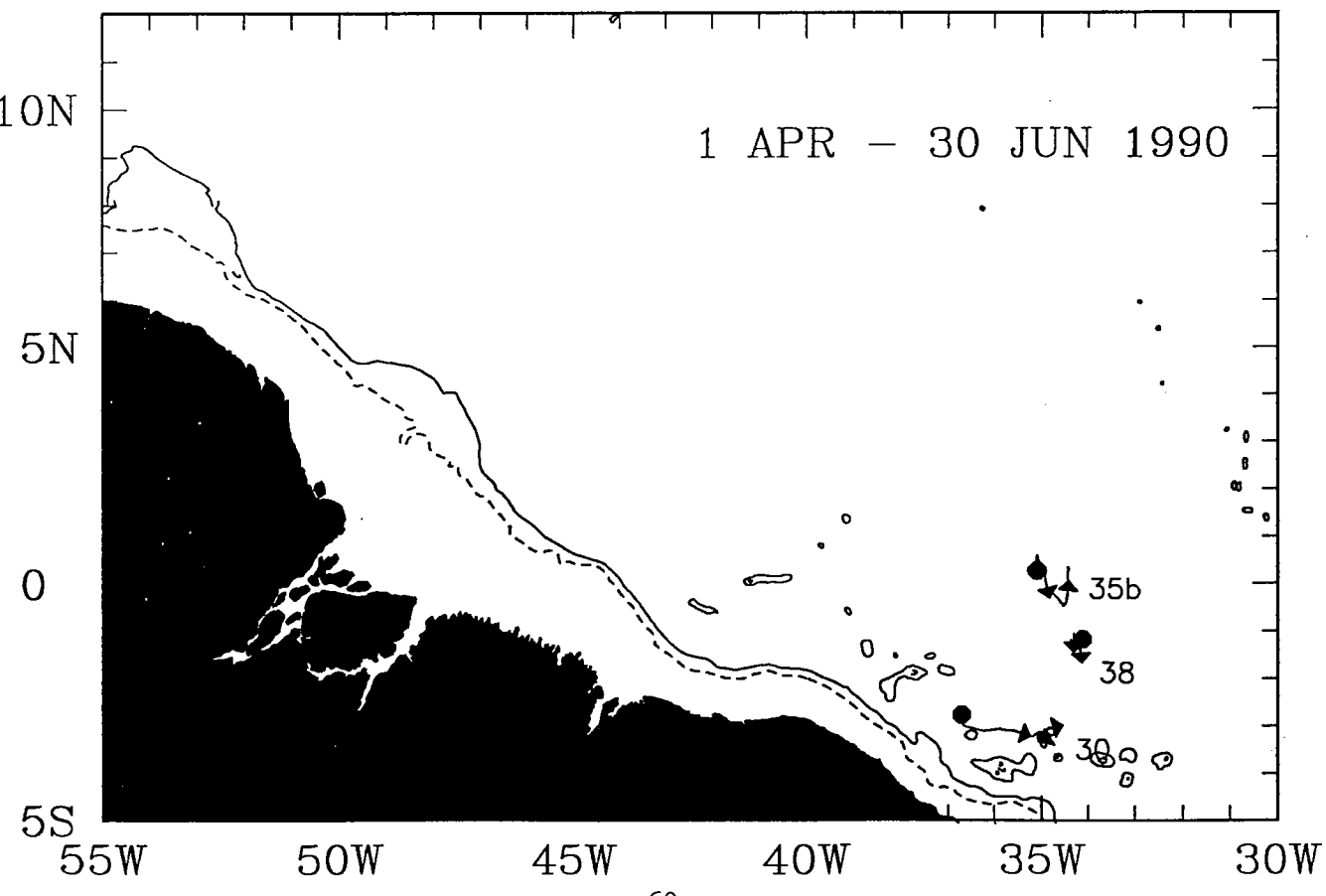
3300m



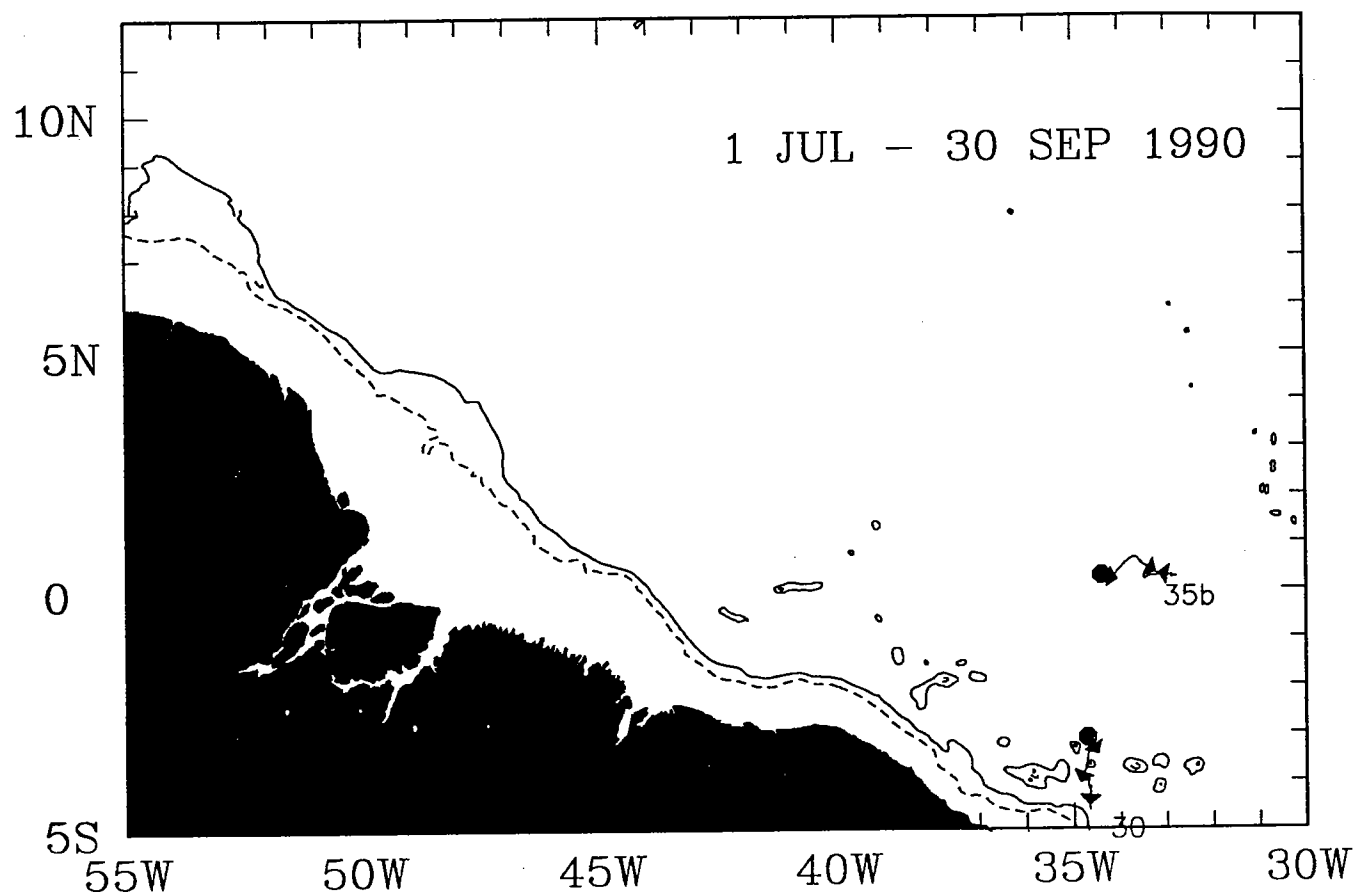
3300m



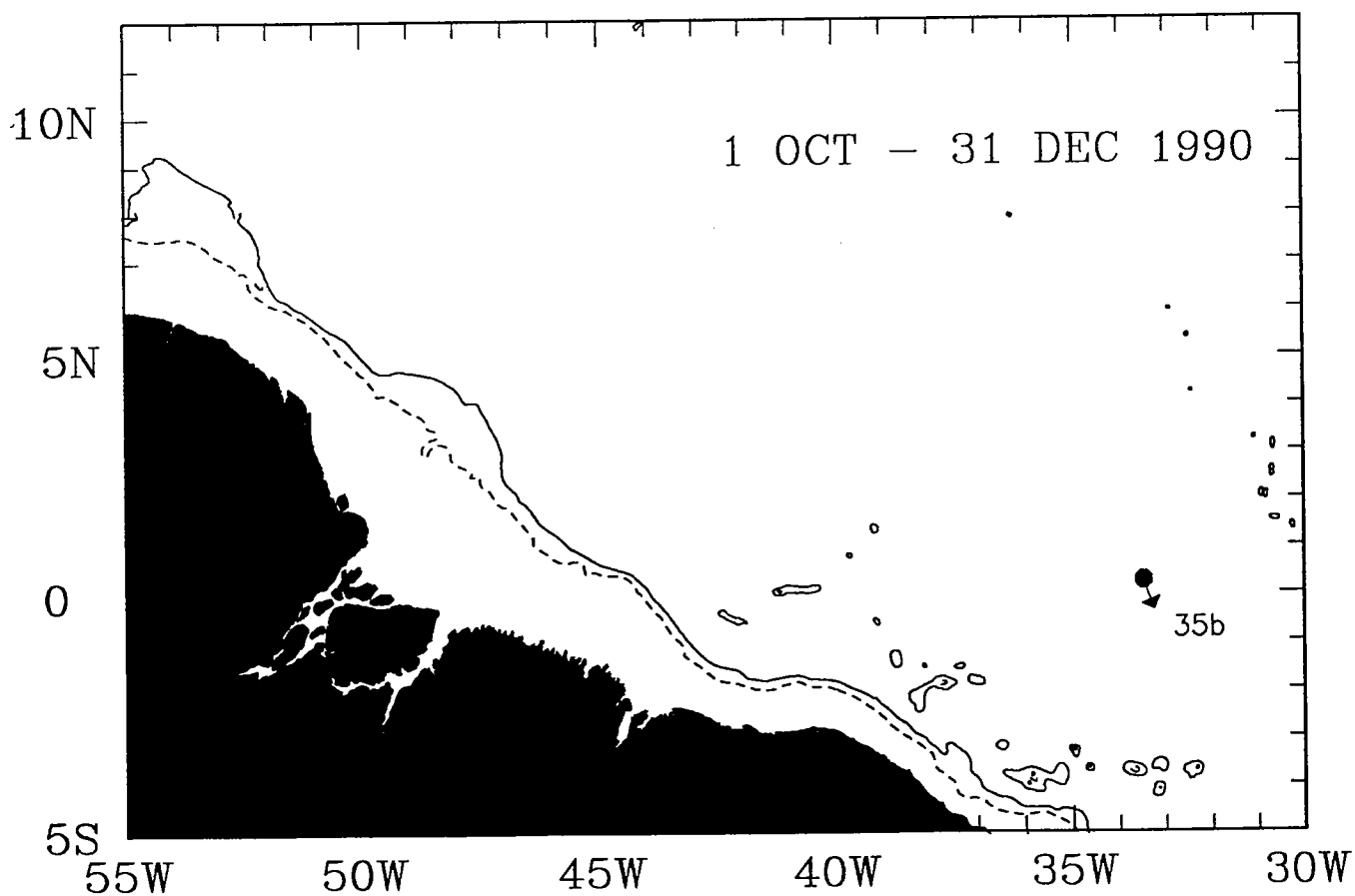
1 APR - 30 JUN 1990



3300m

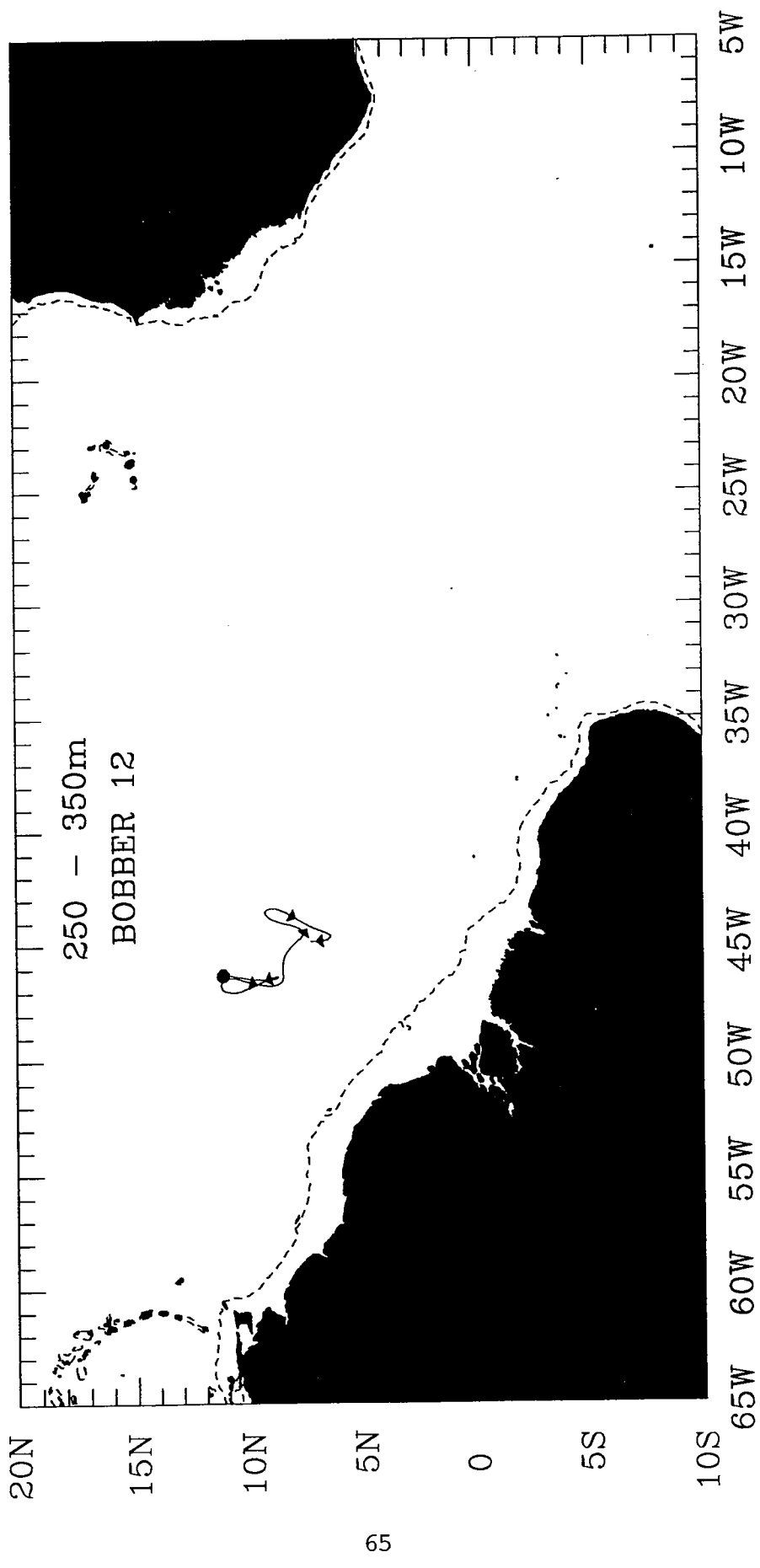


1 OCT - 31 DEC 1990

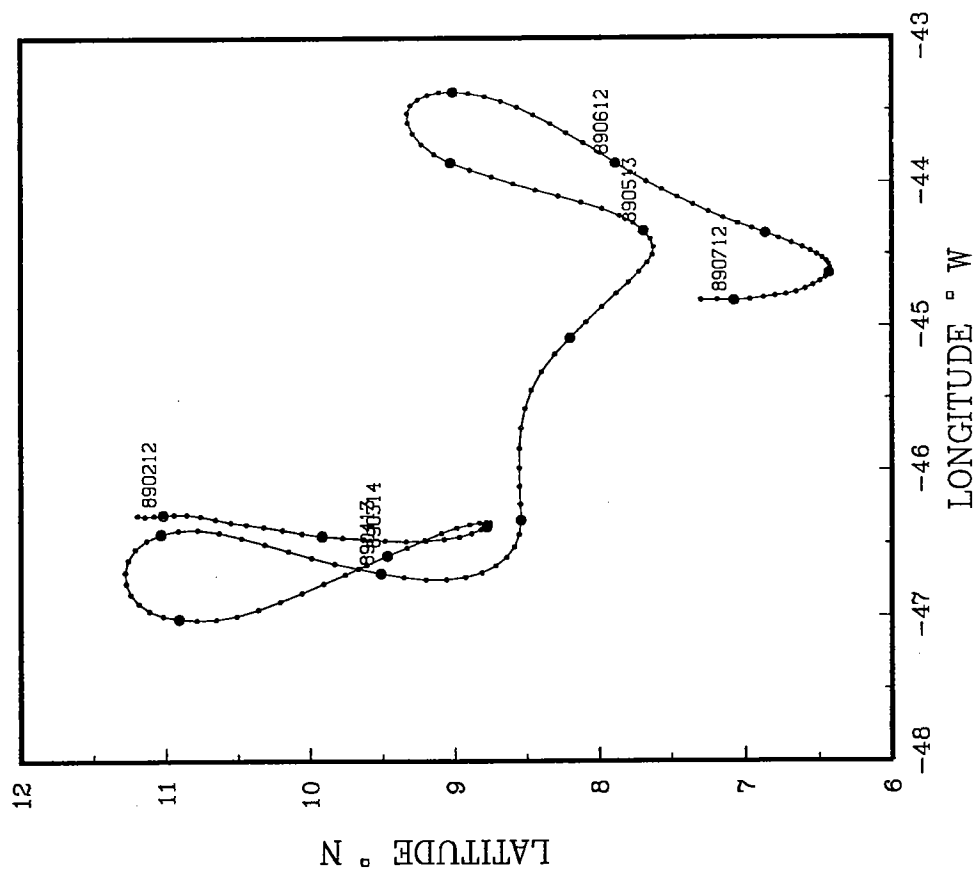


Appendix B: Plots of Individual Floats

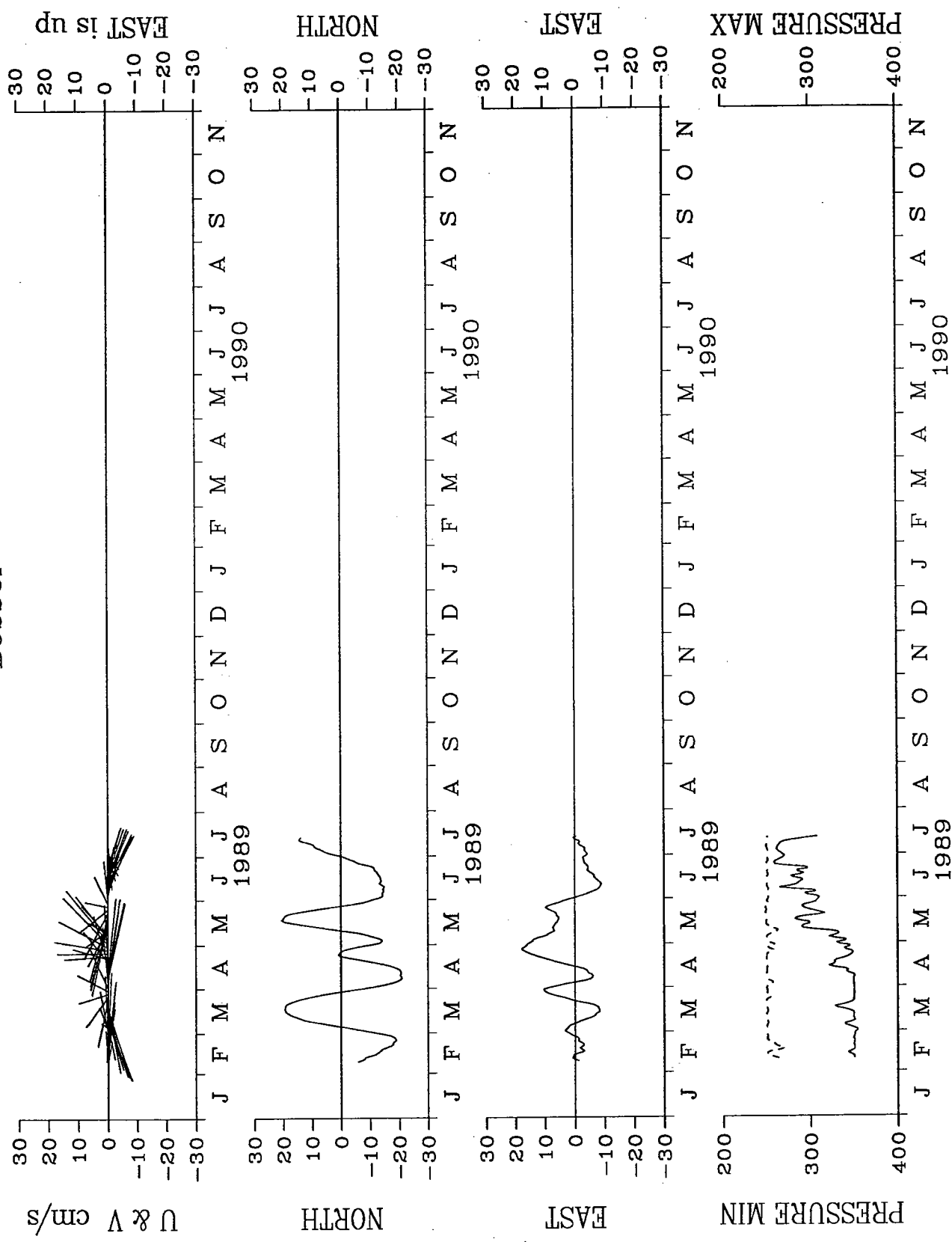
The following figures are ordered by increasing depth into four groups: (1) Bobbers, (2) 800 m floats, (3) 1800 m floats, and (4) 3300 m floats. Three plots are included for each float: a common-area trajectory plot with arrowheads spaced at intervals of 30 days, a trajectory enlargement showing daily positions and dates every 30 days, and velocity vectors and eastward and northward velocity components. Maximum and minimum pressures are added for Bobber floats.

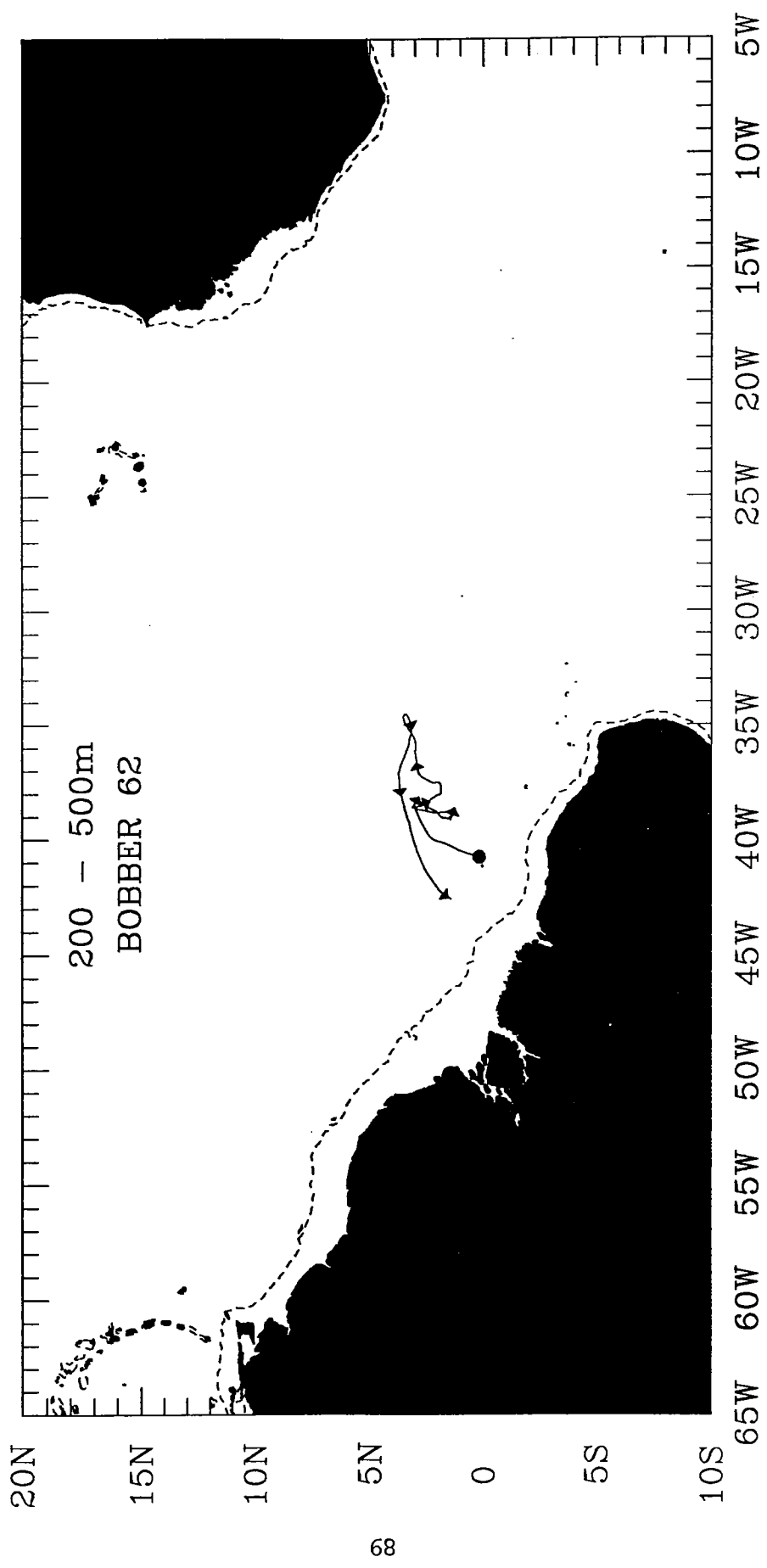


TROPICAL ATLANTIC B 12

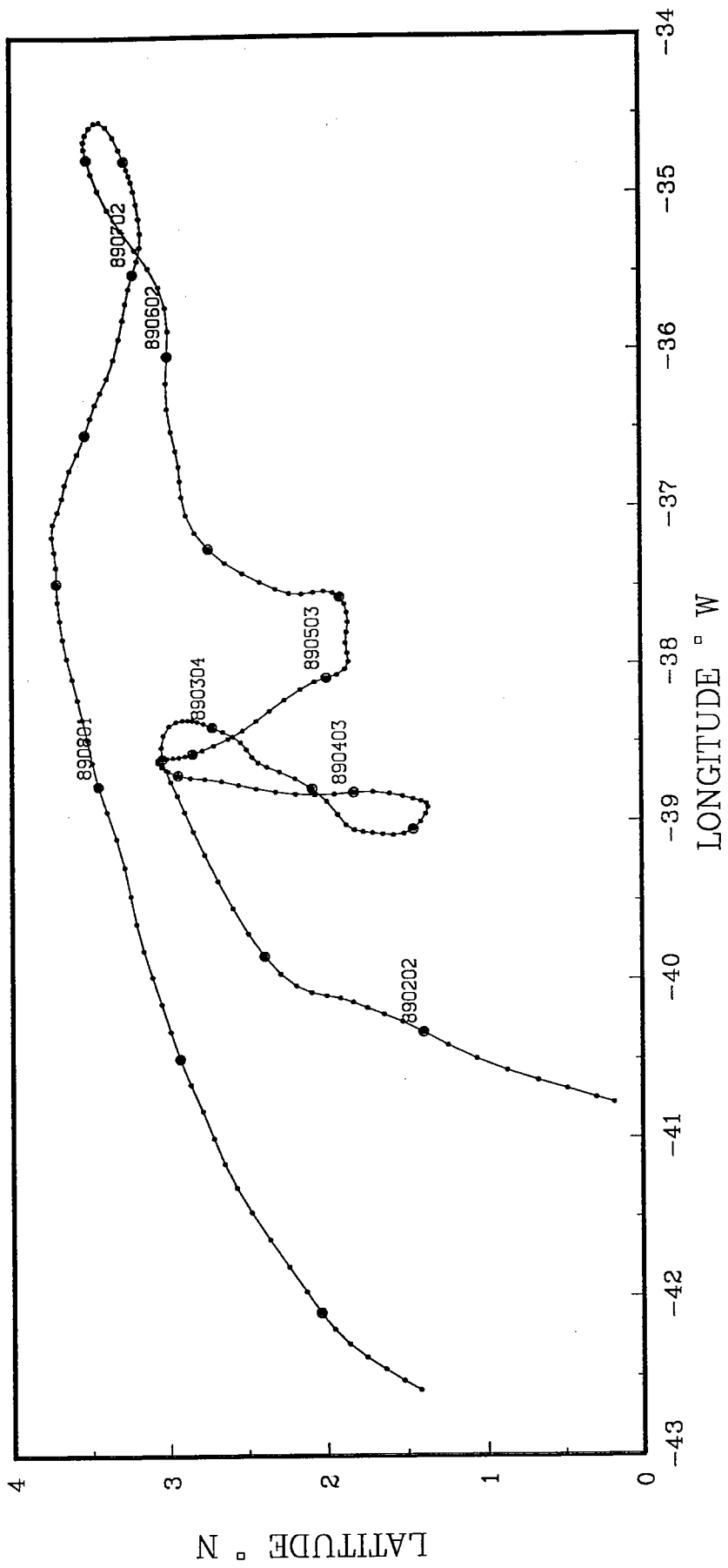


TROPICAL ATLANTIC B 12
Bobber

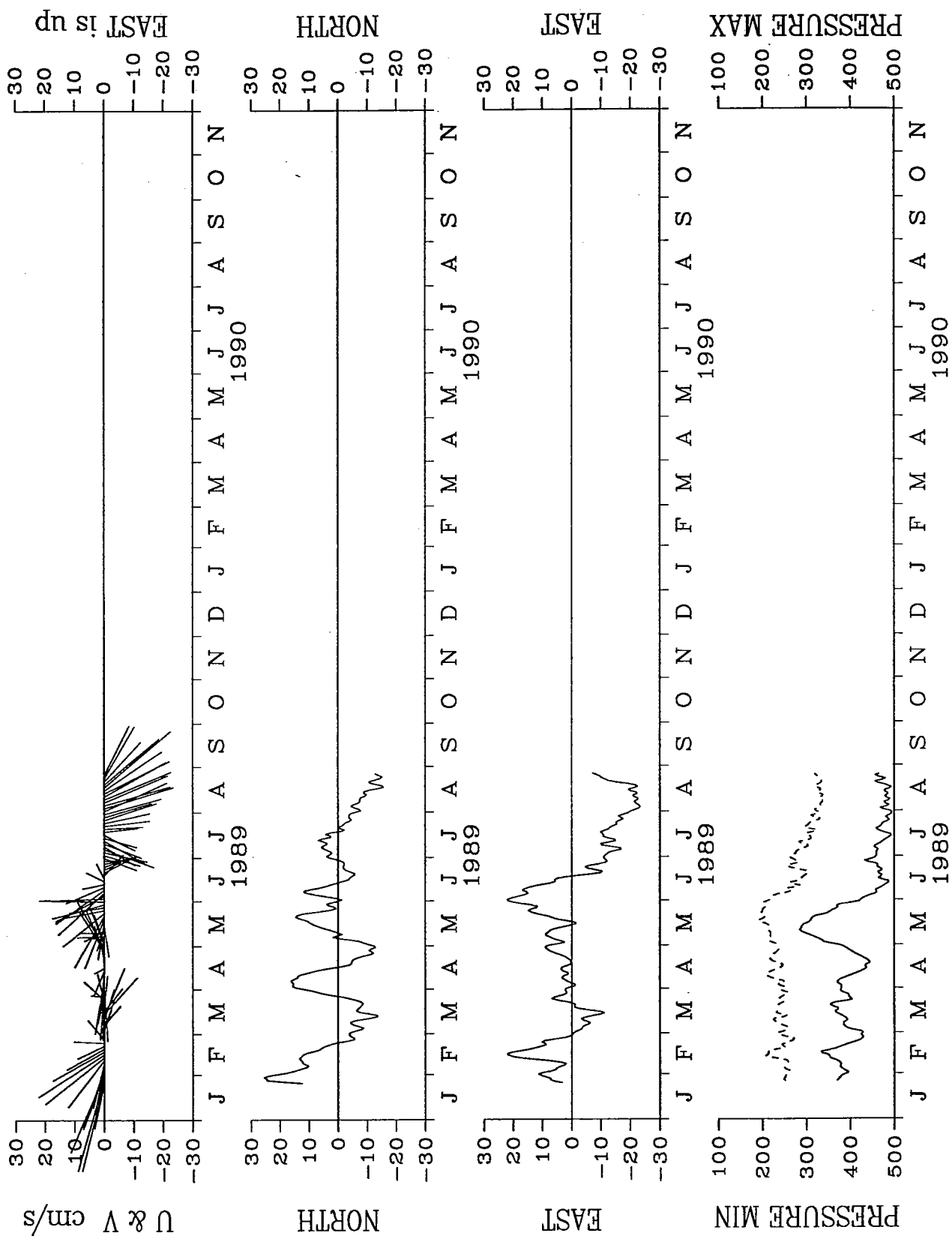


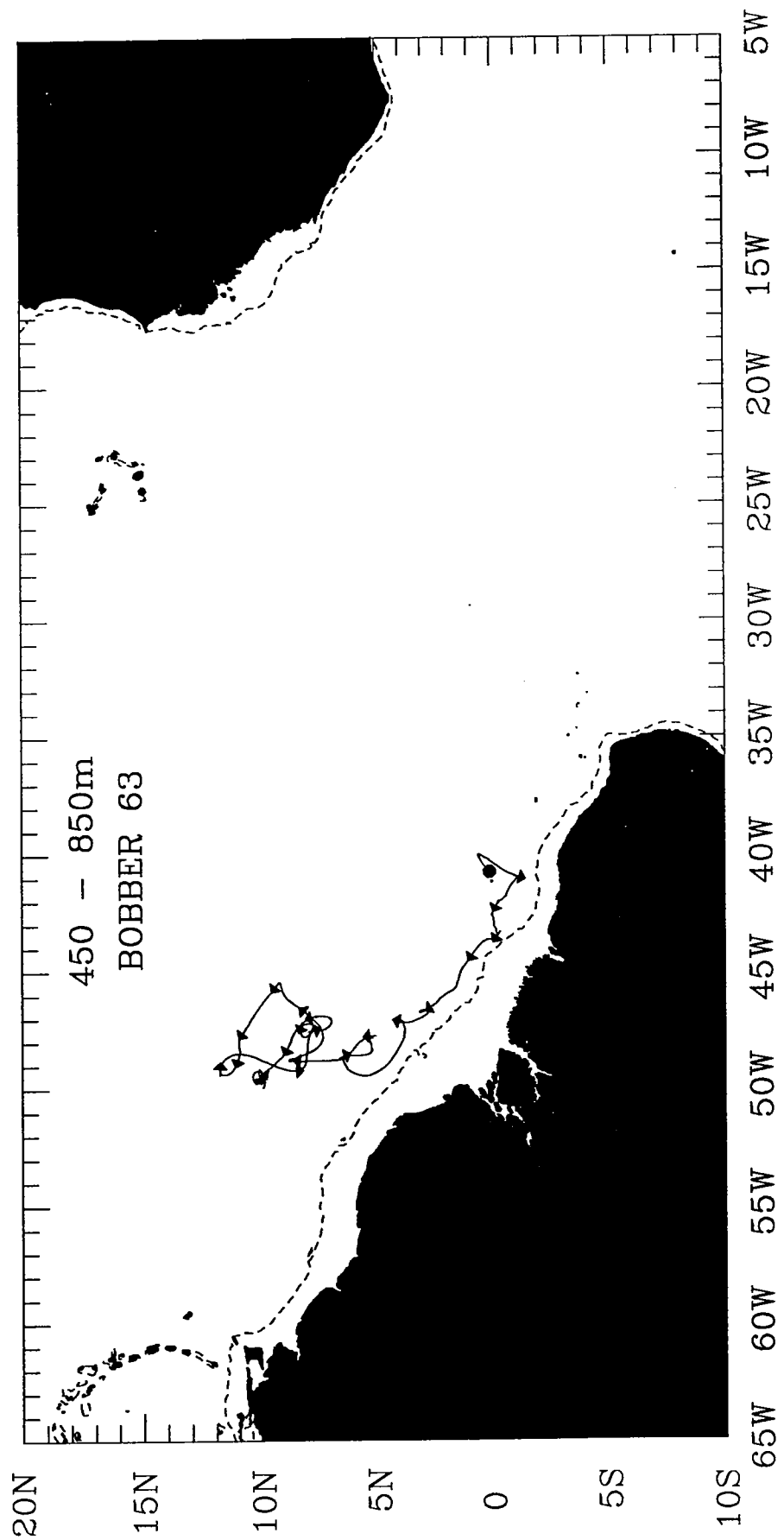


TROPICAL ATLANTIC B 62

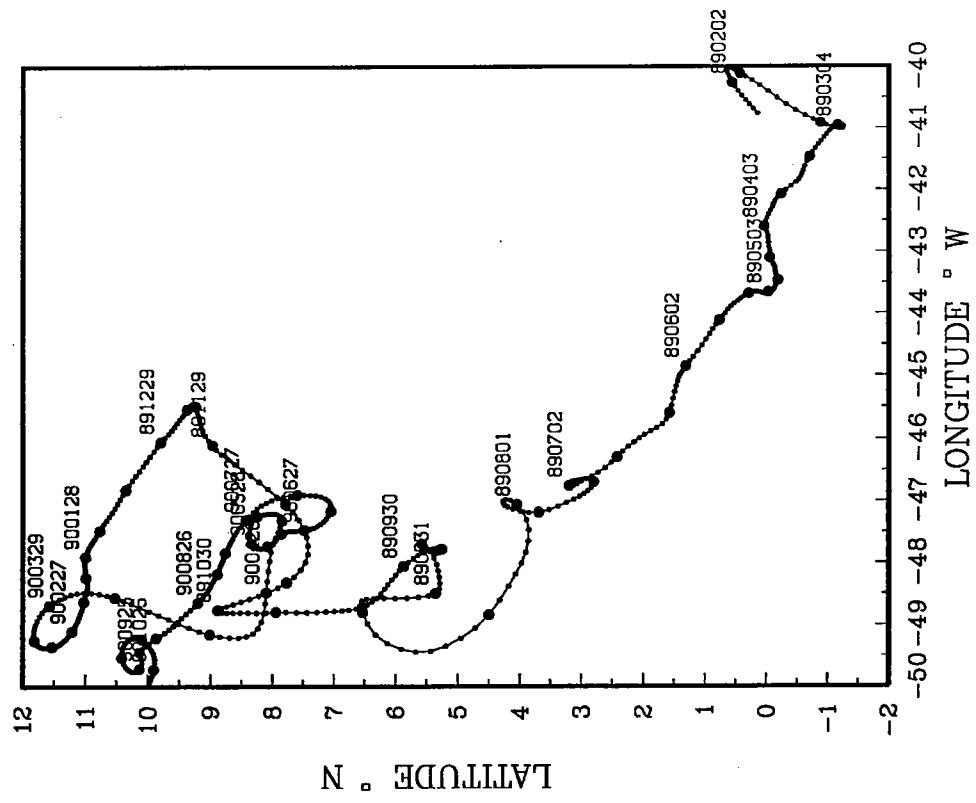


TROPICAL ATLANTIC B 62
Bobber

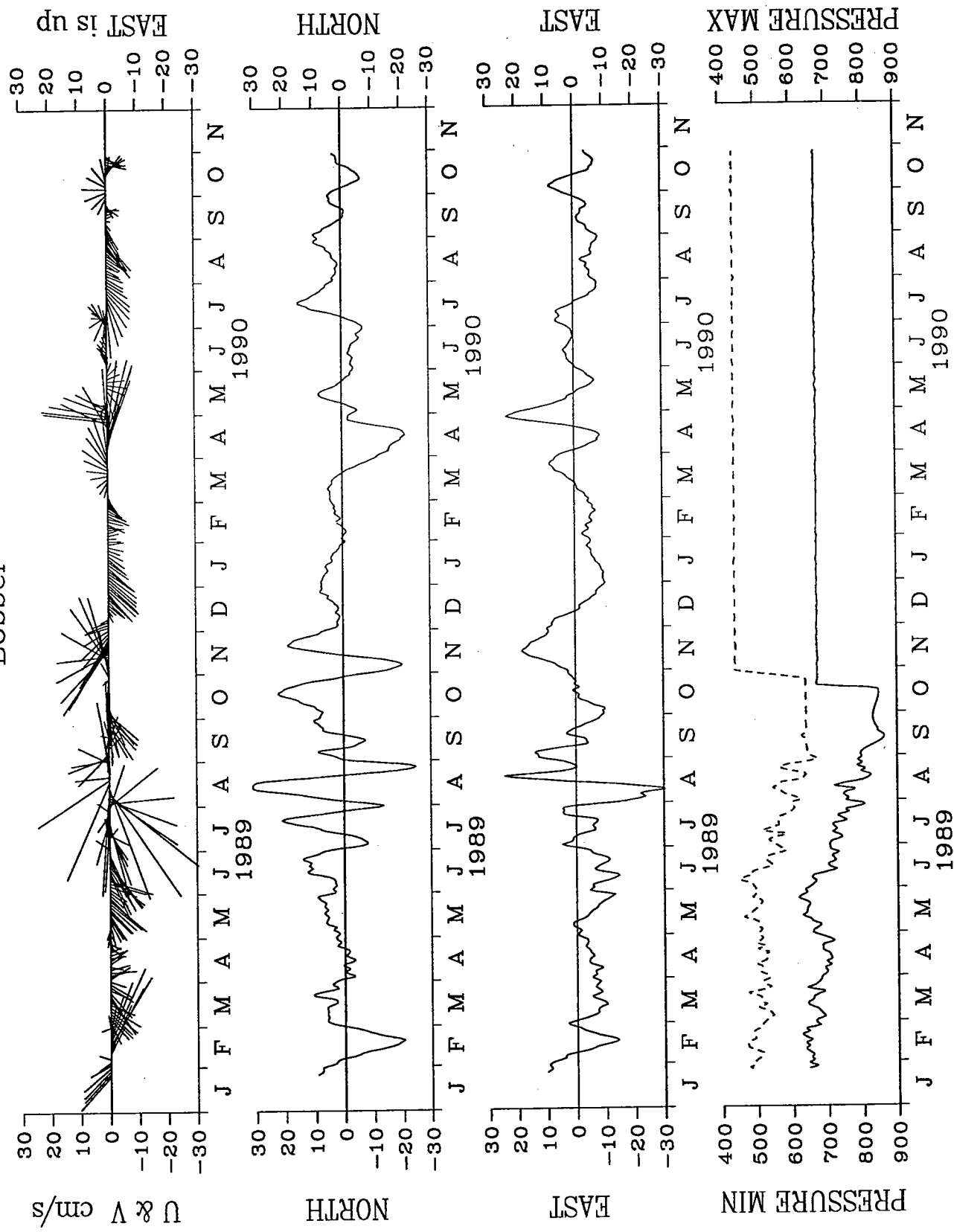


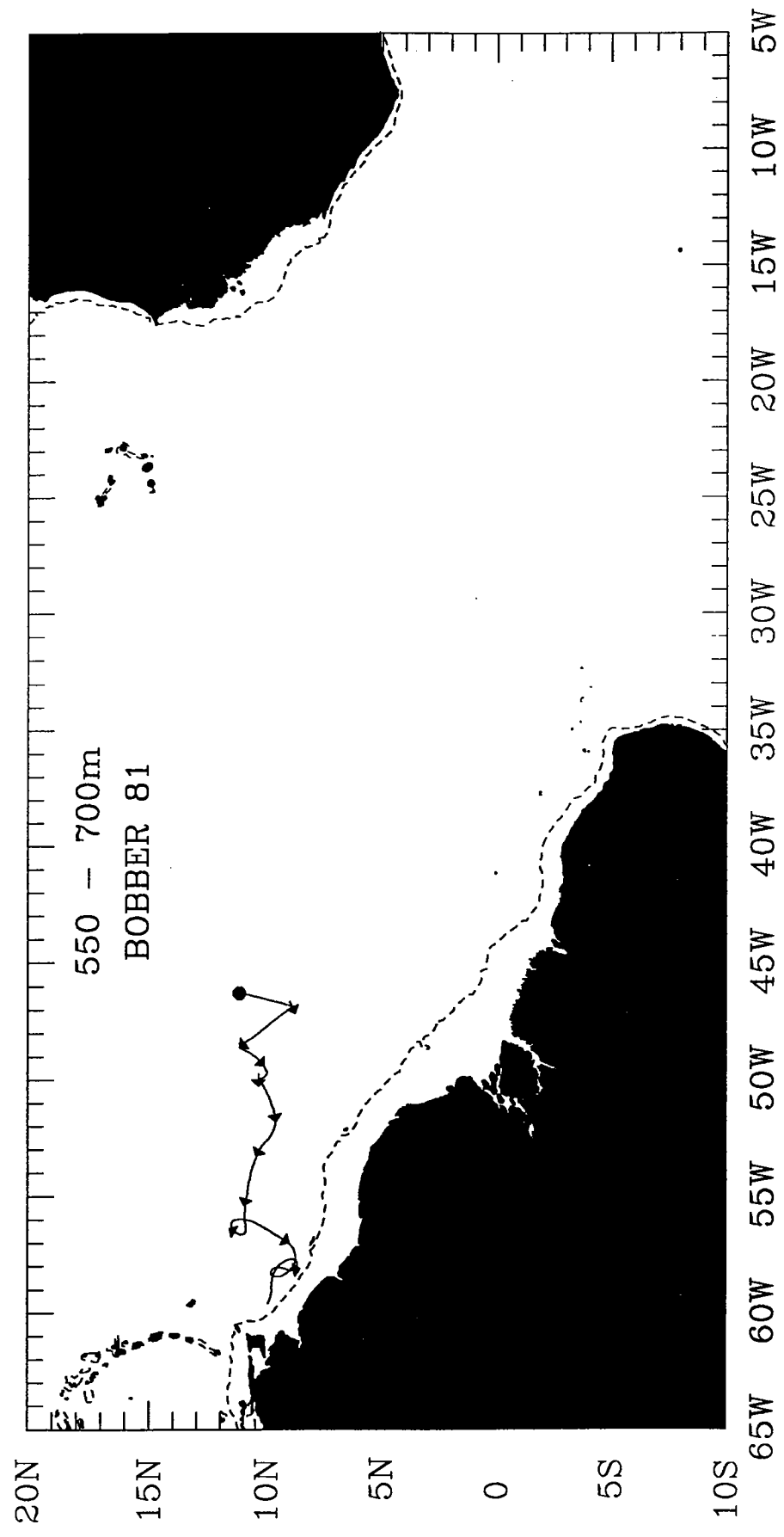


TROPICAL ATLANTIC B 63

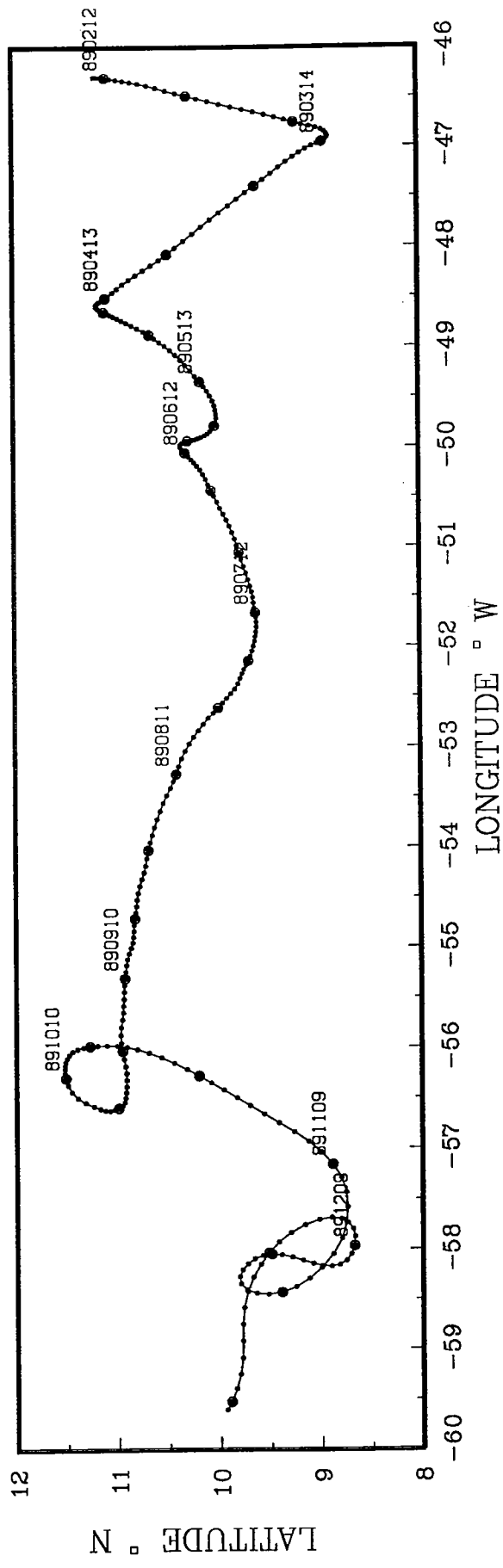


TROPICAL ATLANTIC B 63
Bobber

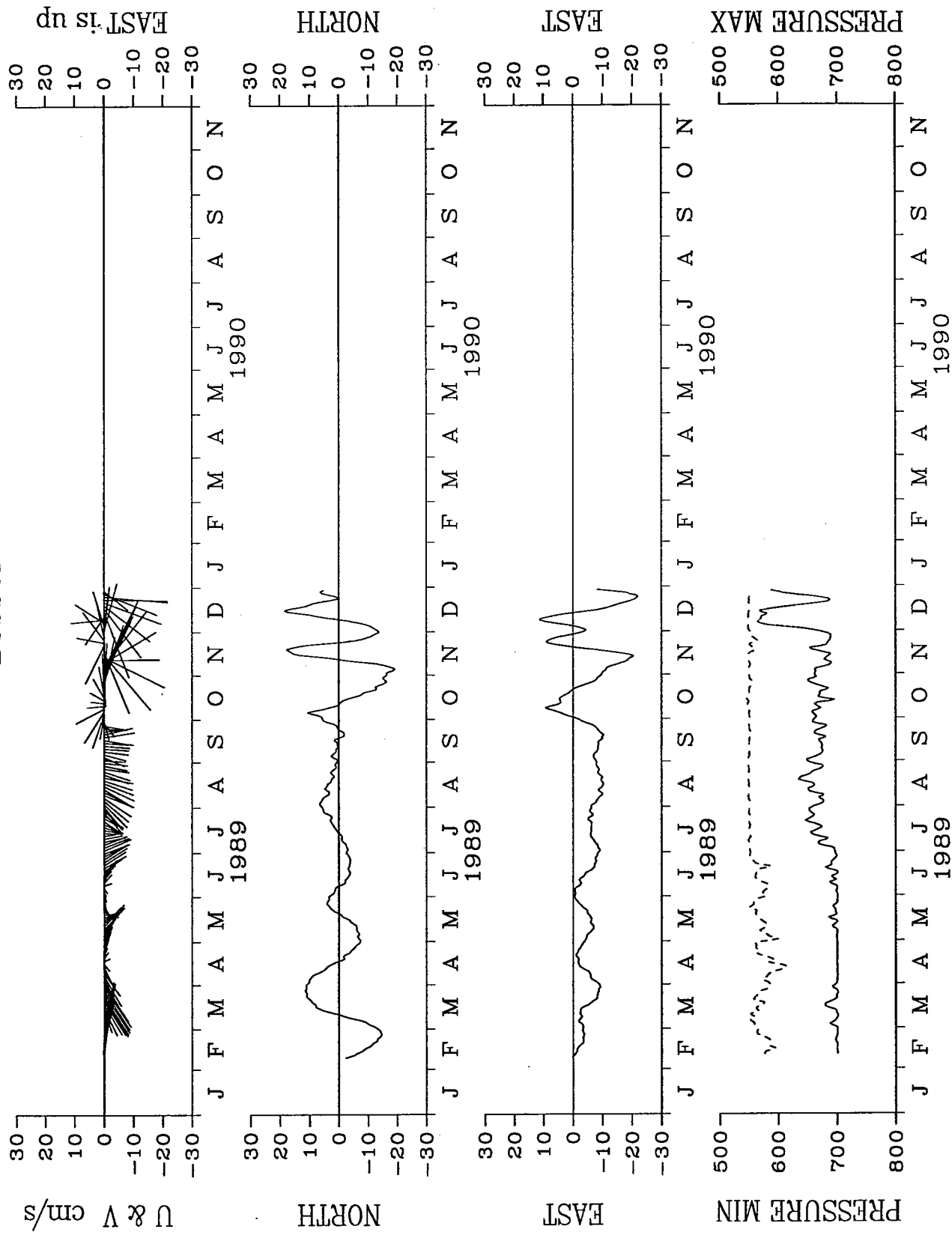


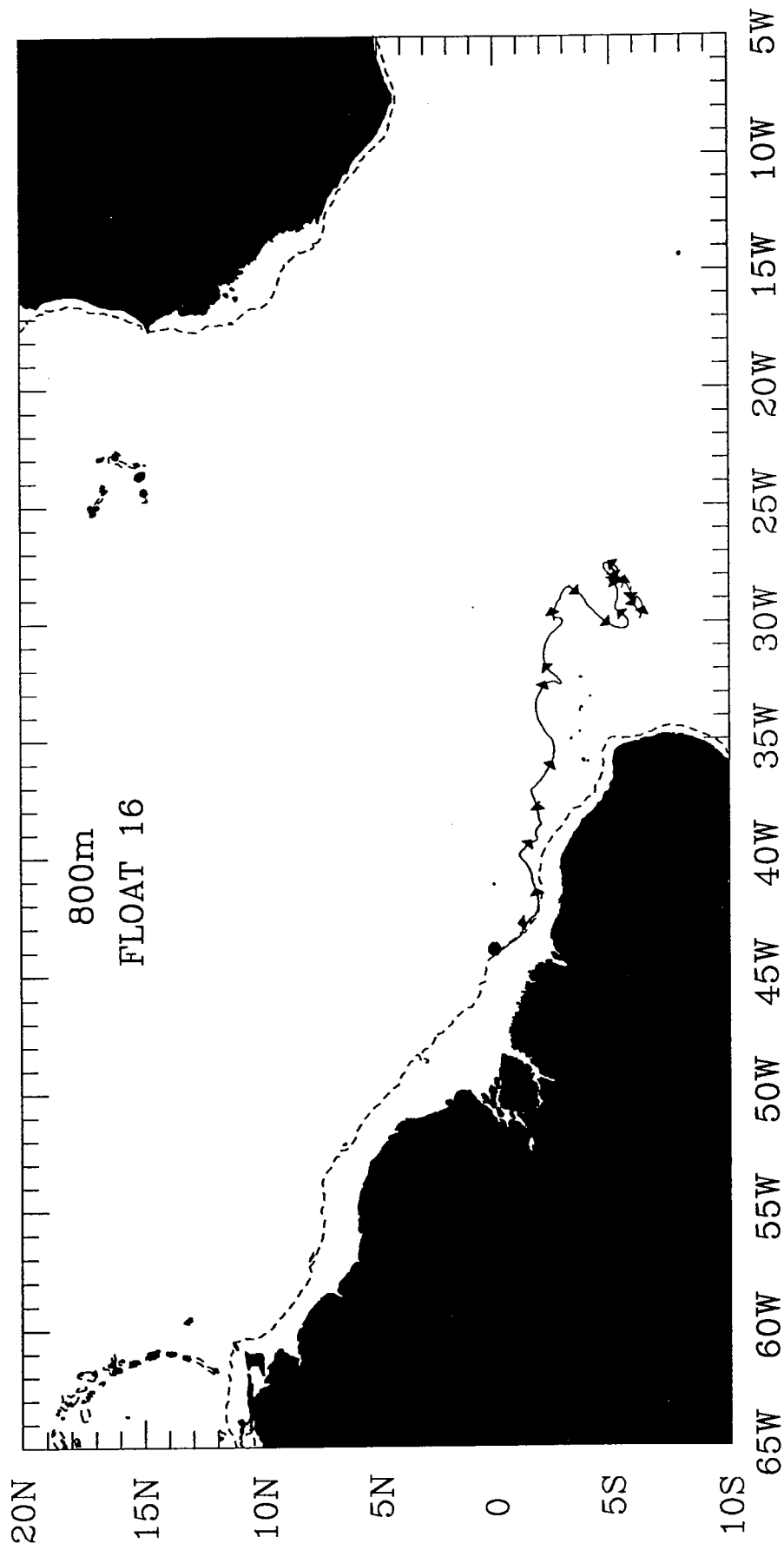


TROPICAL ATLANTIC B 81

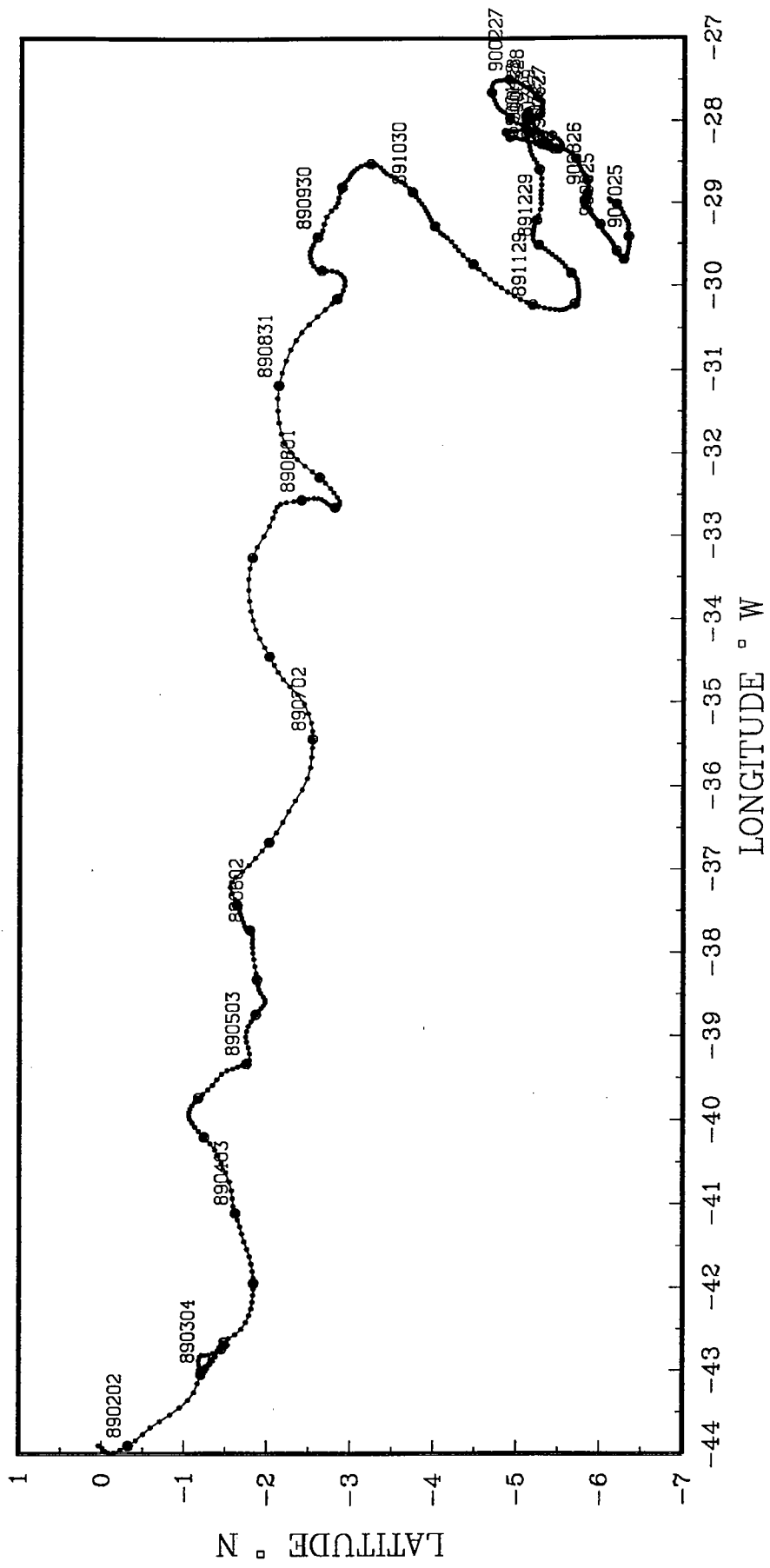


TROPICAL ATLANTIC B 81
Bobber

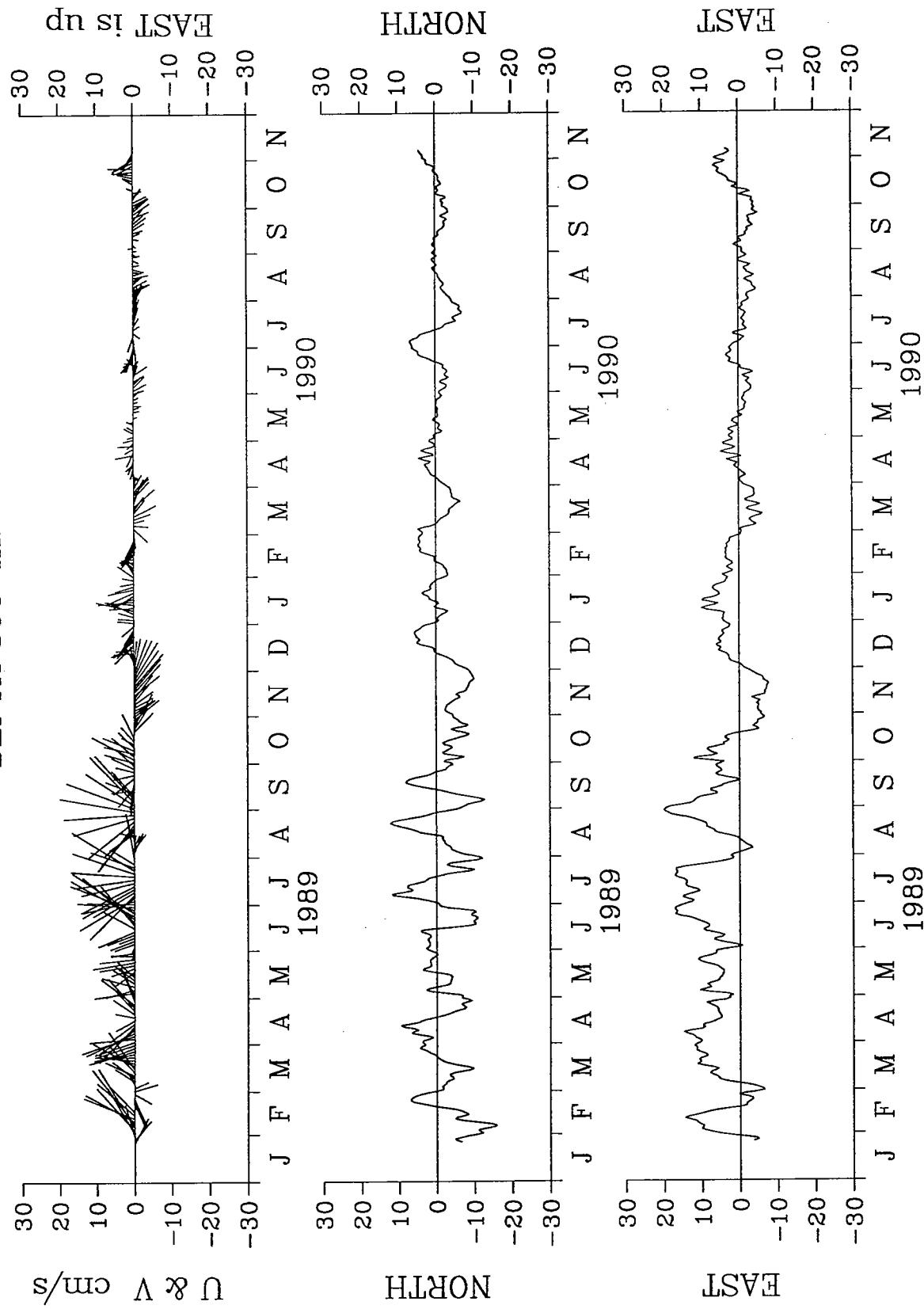


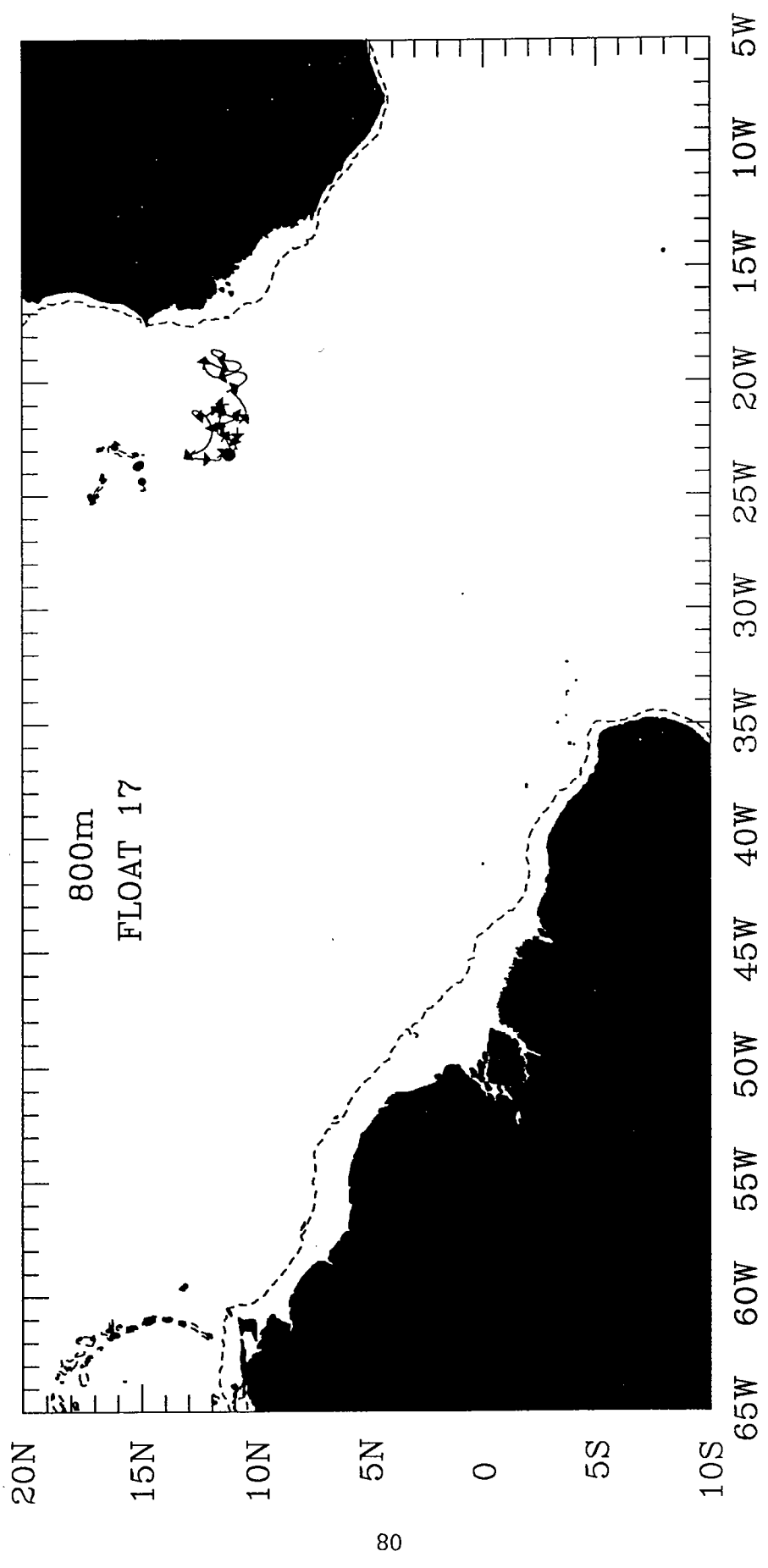


TROPICAL ATLANTIC 16

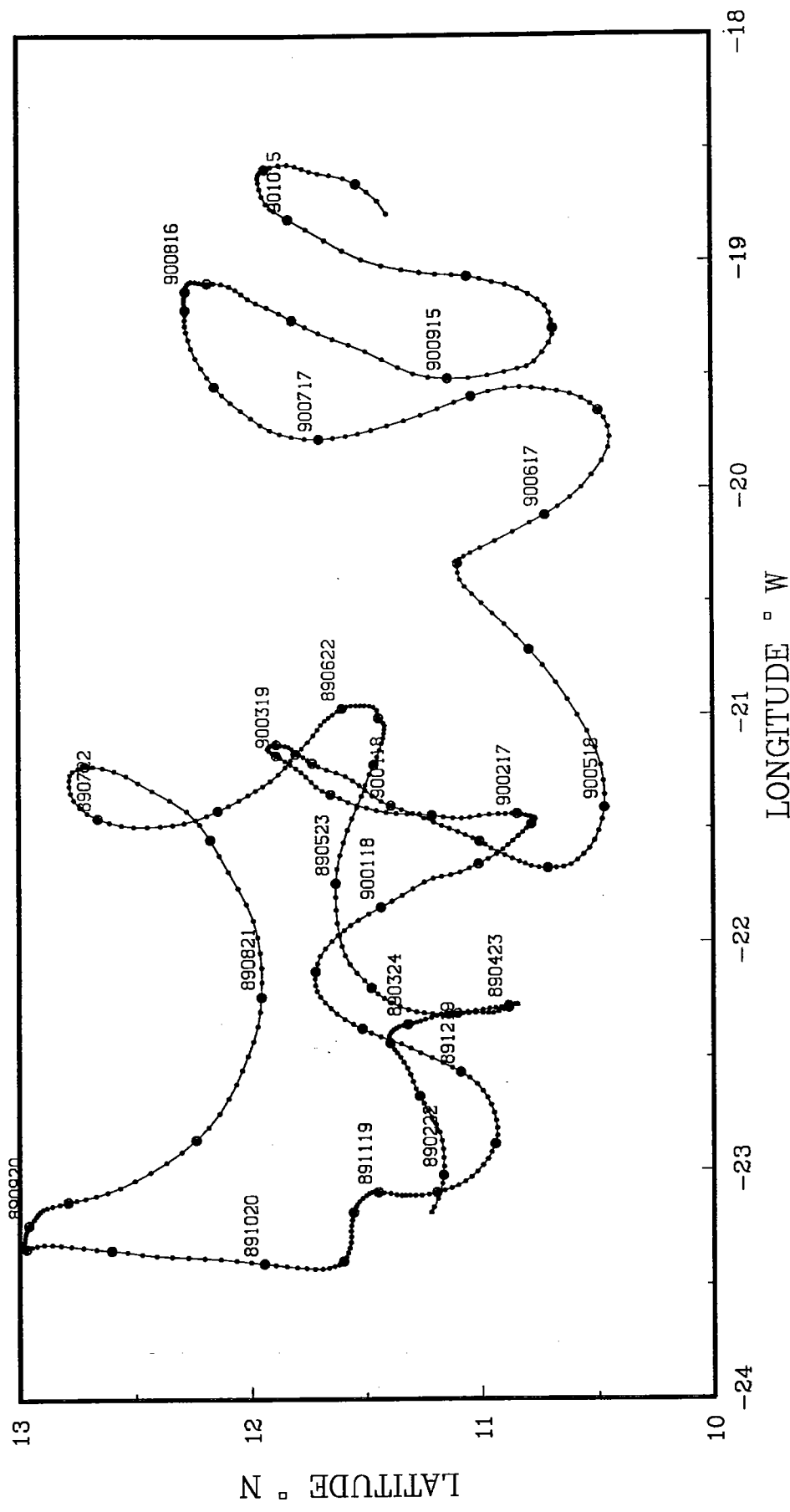


TROPICAL ATLANTIC 16
DEPTH 800 m.



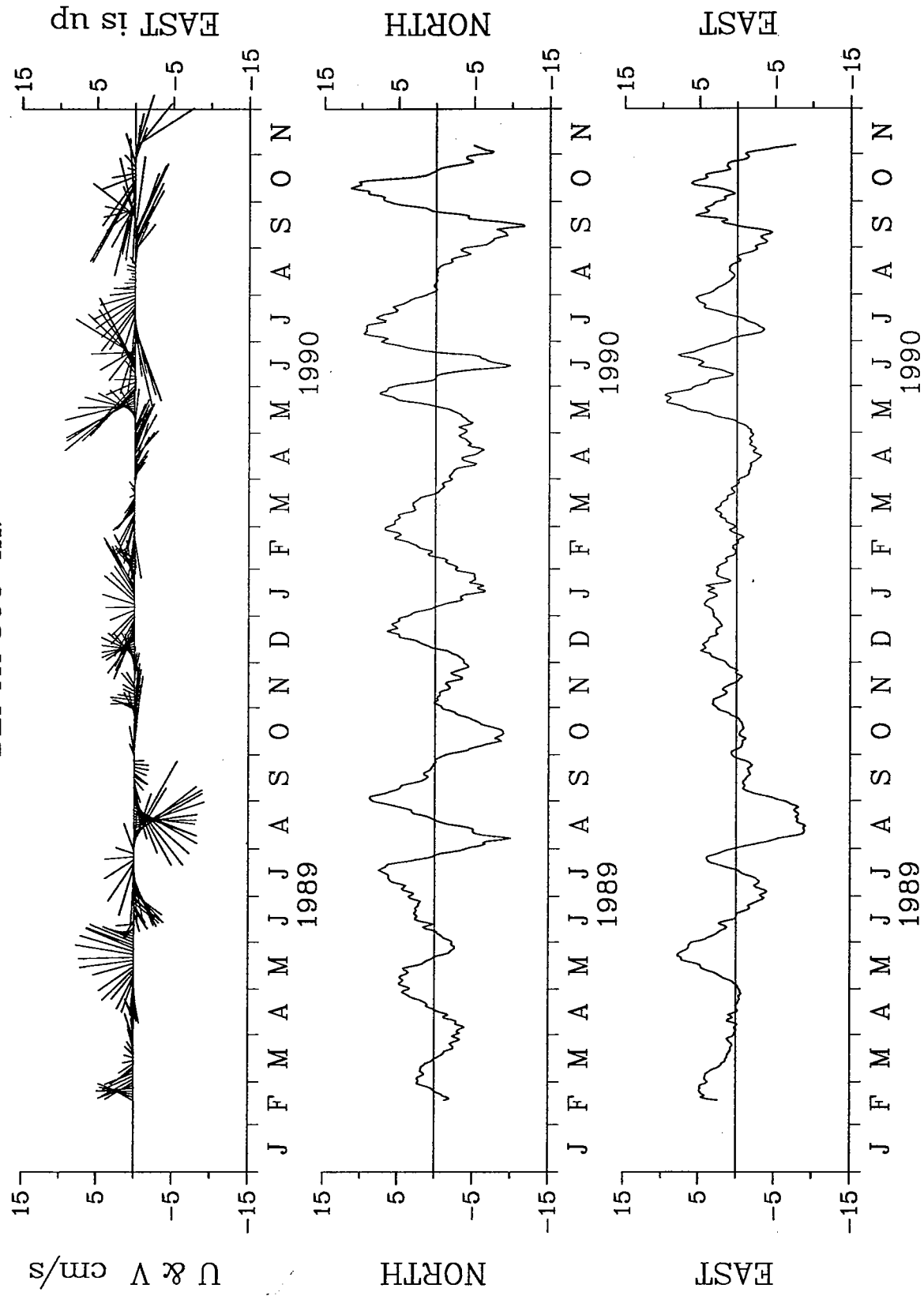


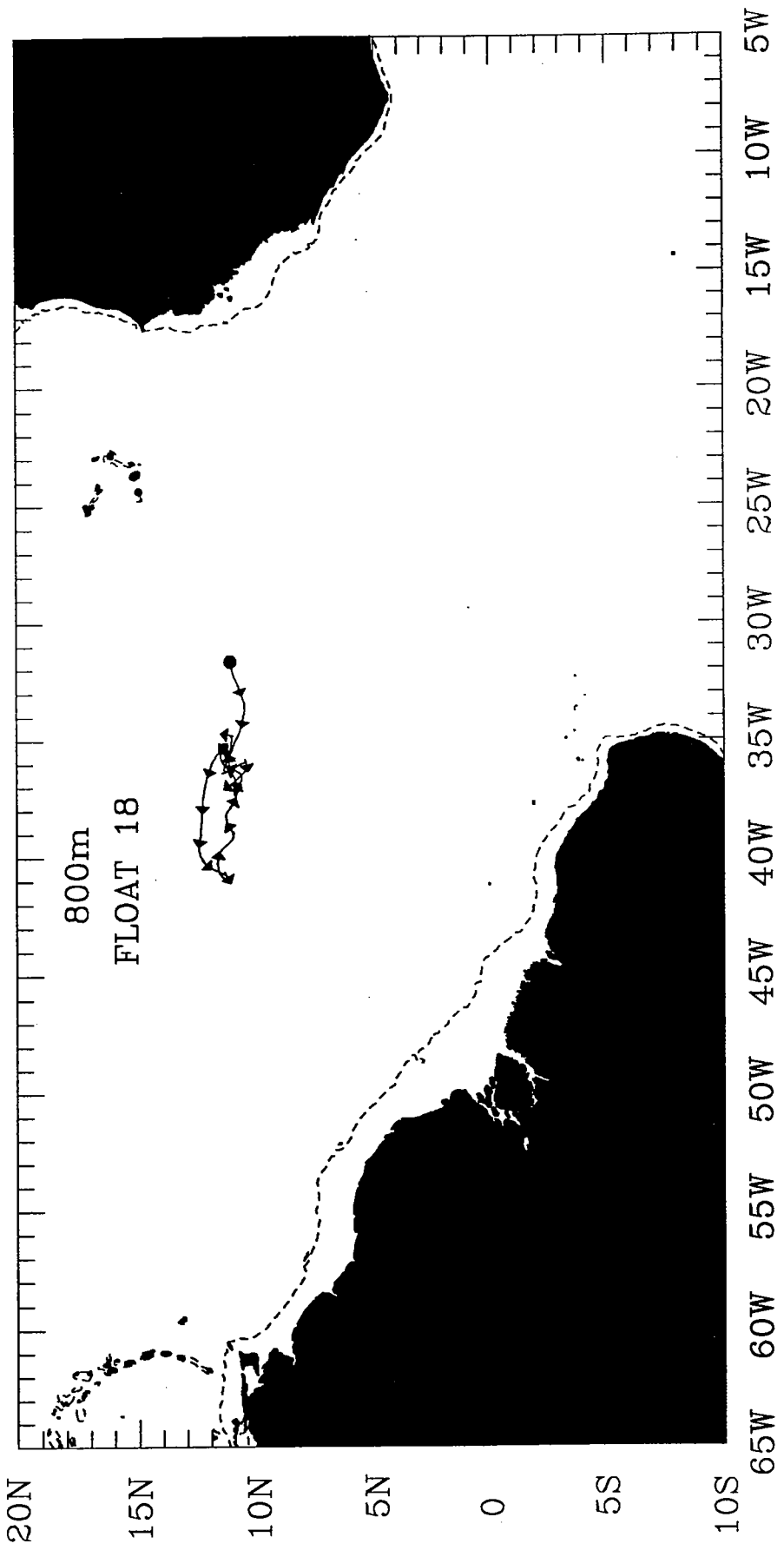
TROPICAL ATLANTIC 17



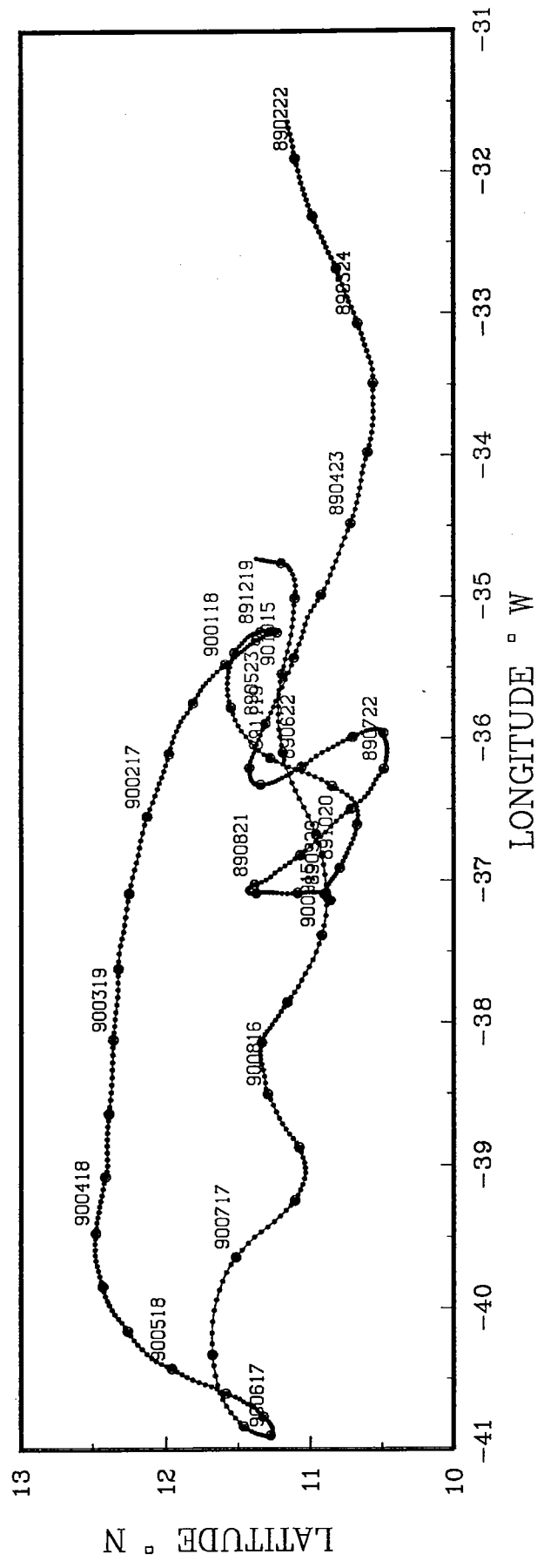
LATITUDE ° N

TROPICAL ATLANTIC 17
DEPTH 800 m.

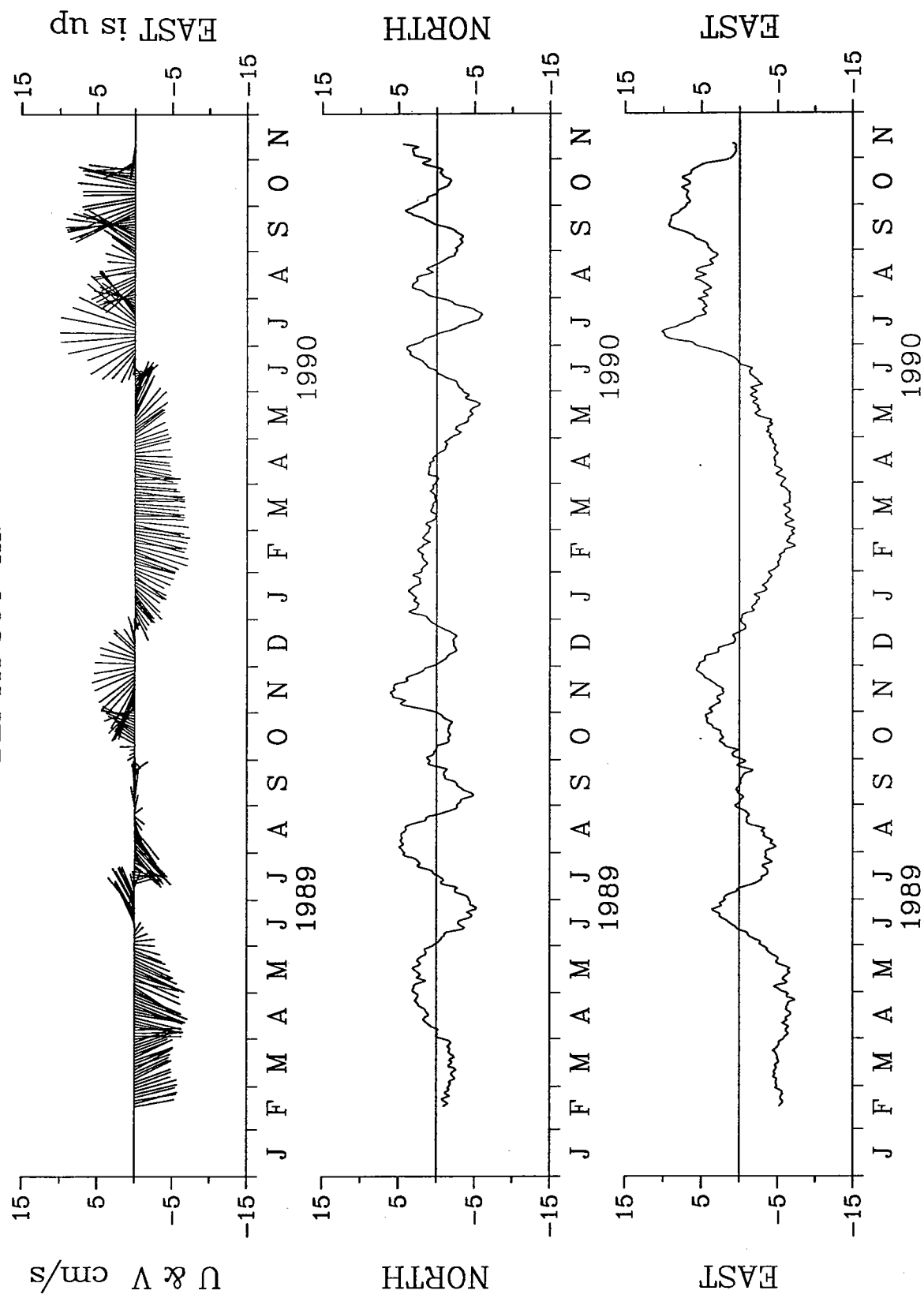


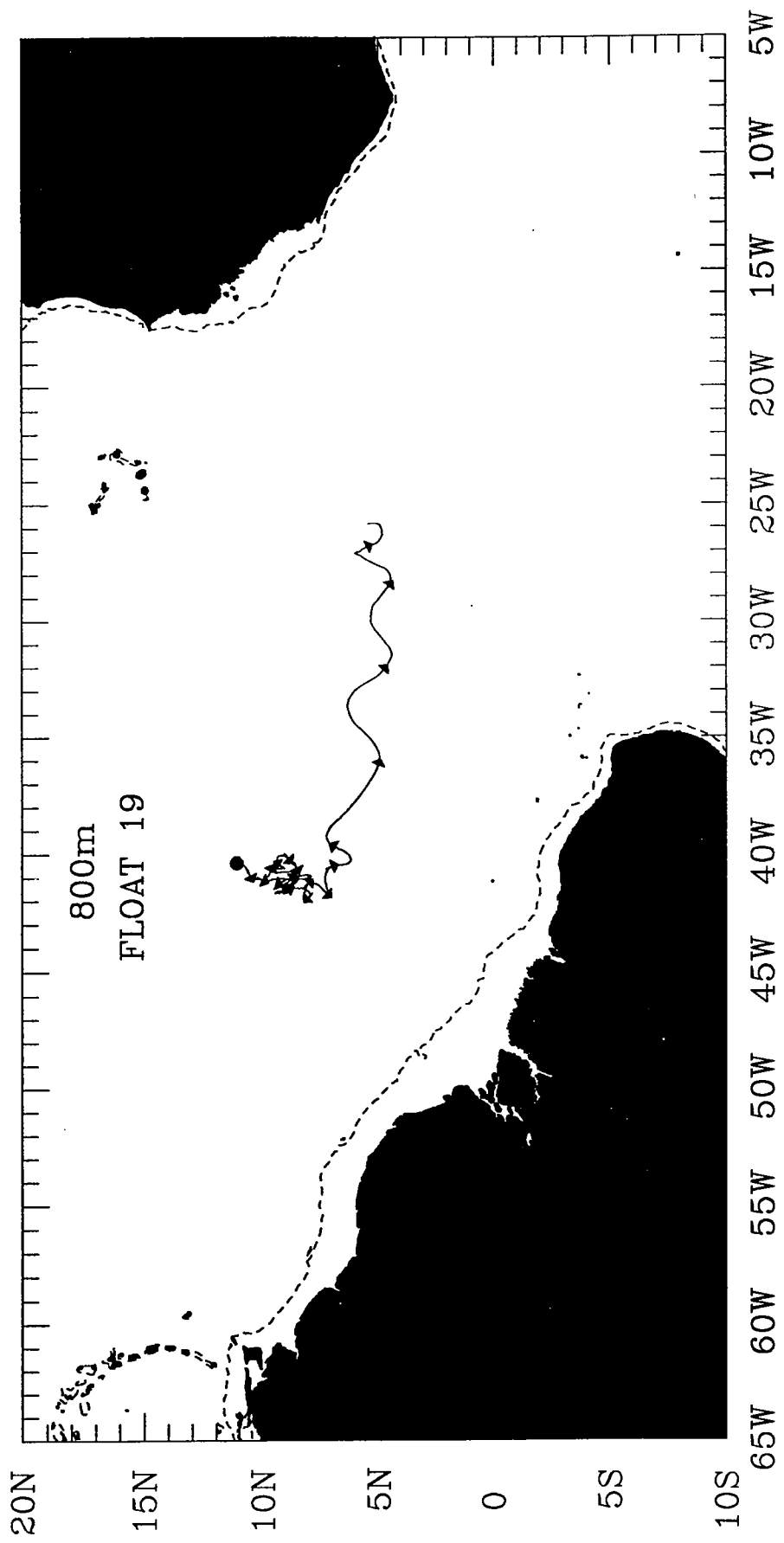


TROPICAL ATLANTIC 18

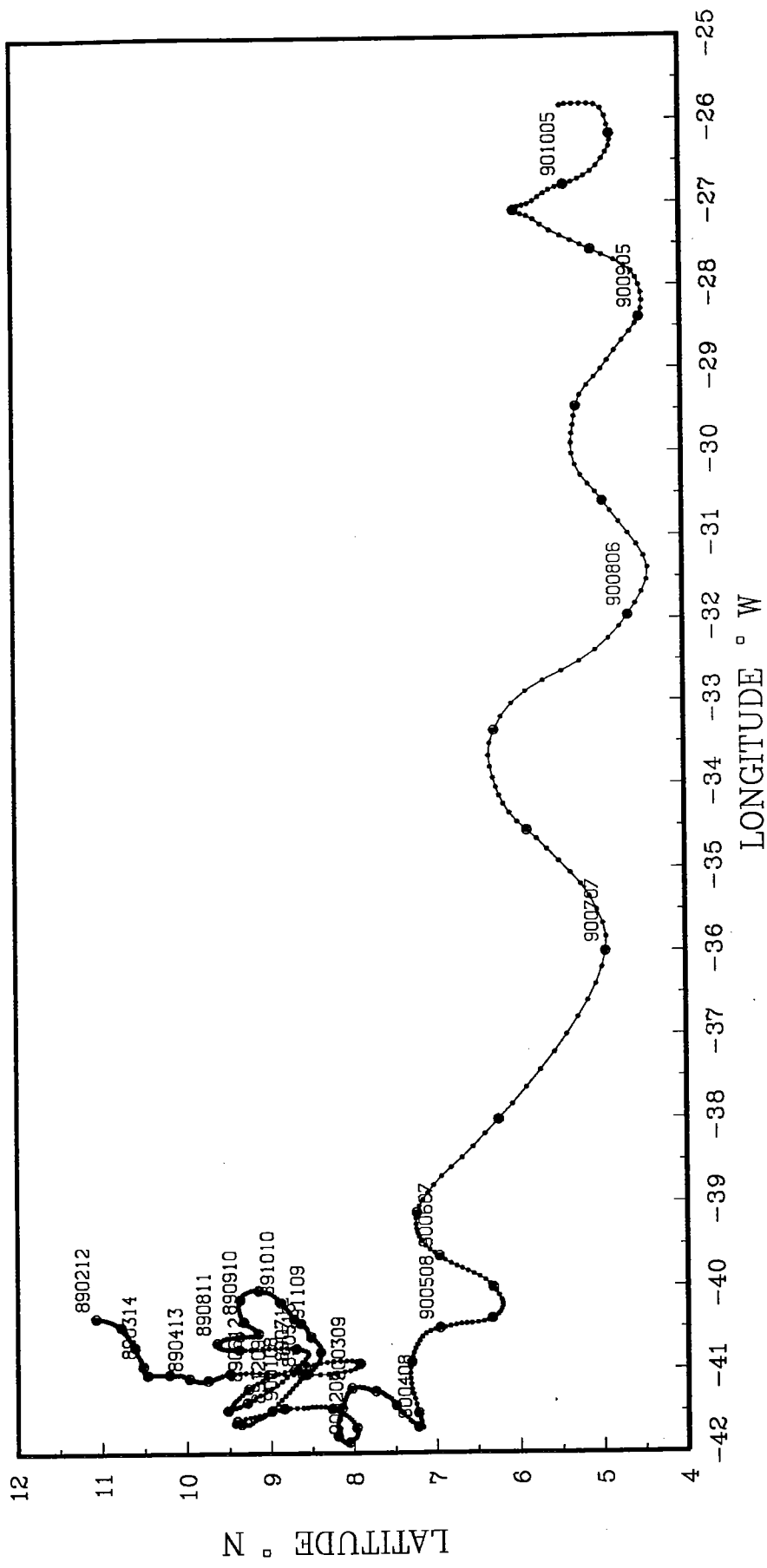


TROPICAL ATLANTIC 18
DEPTH 800 m.

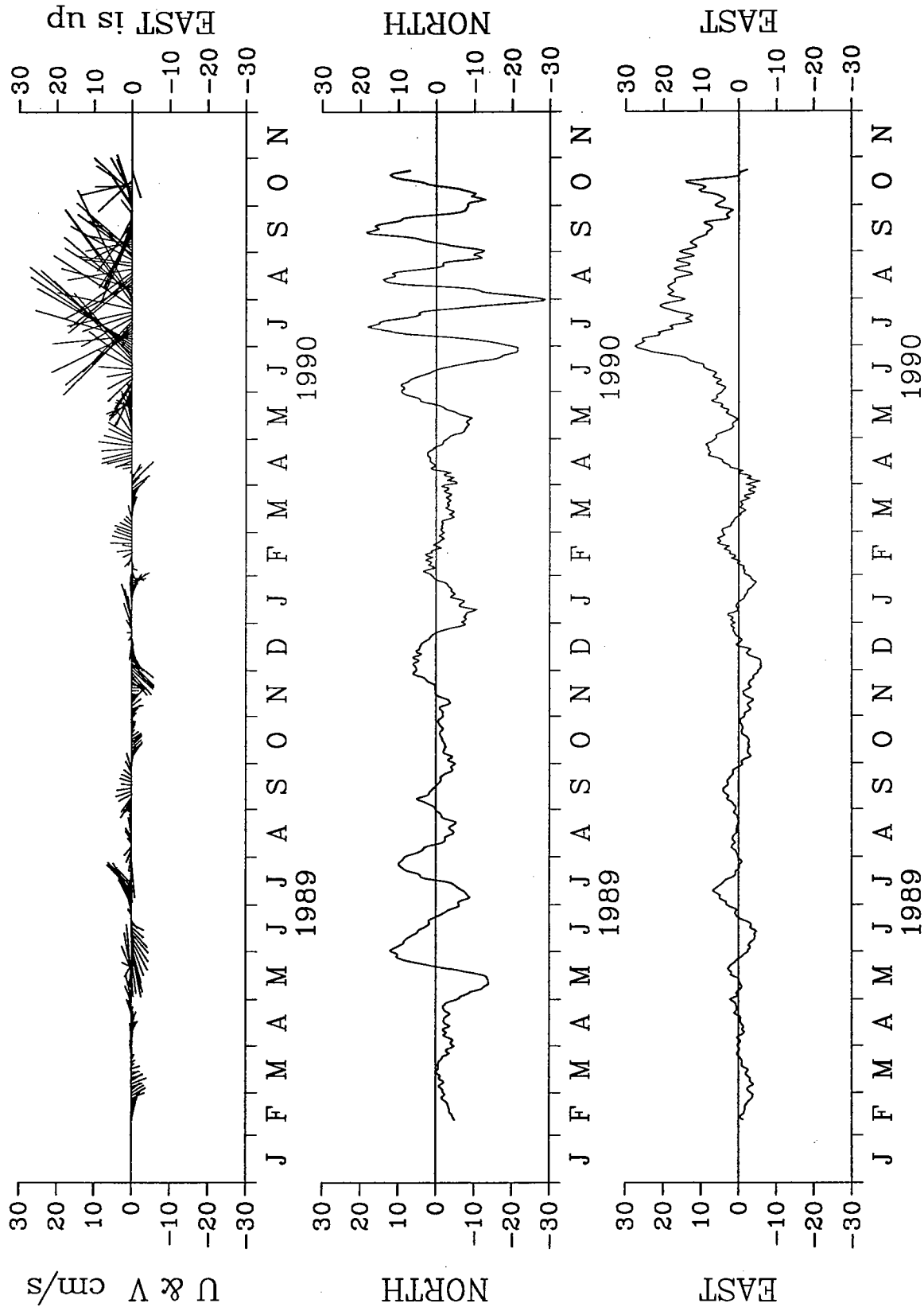


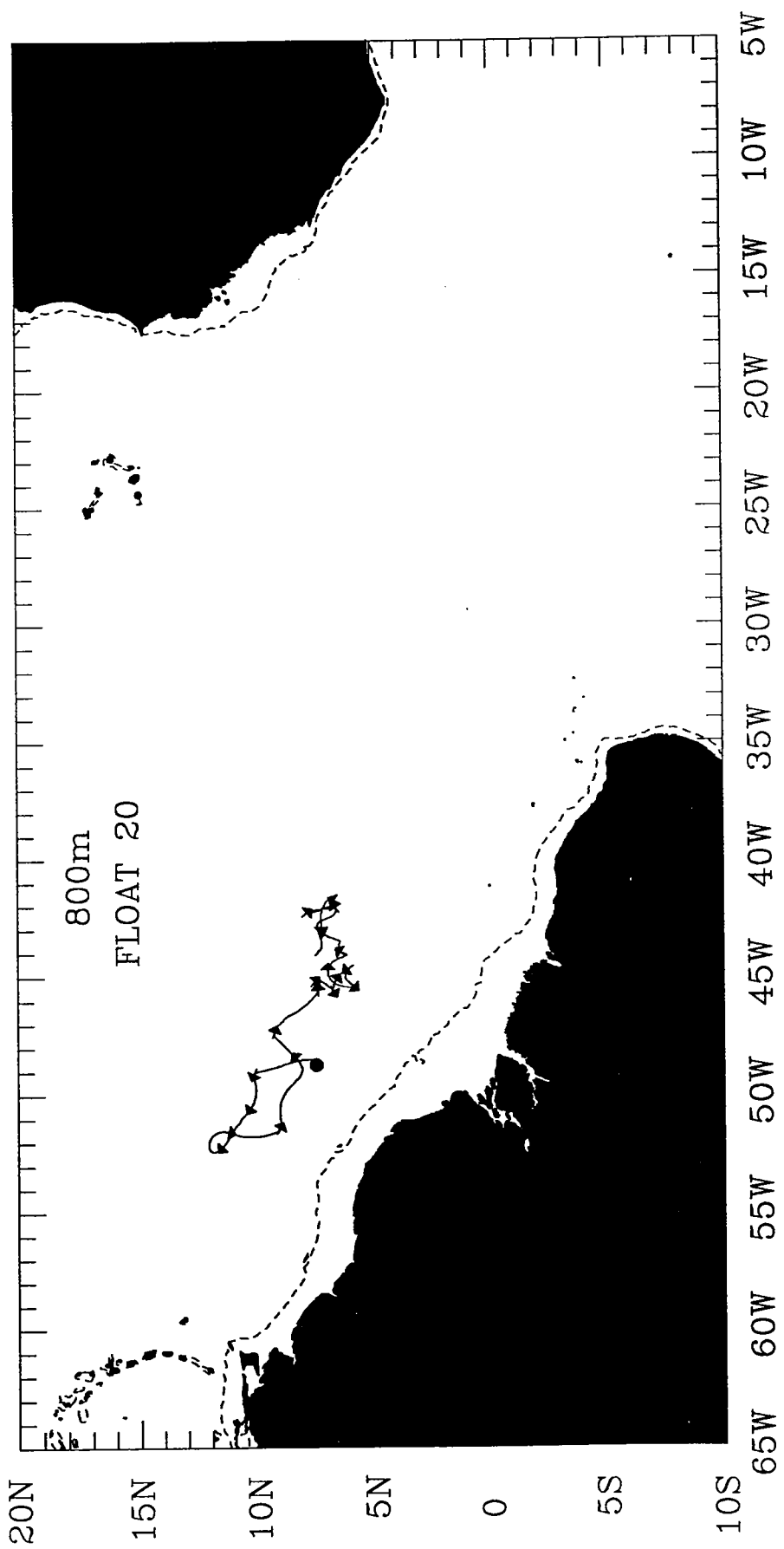


TROPICAL ATLANTIC 19

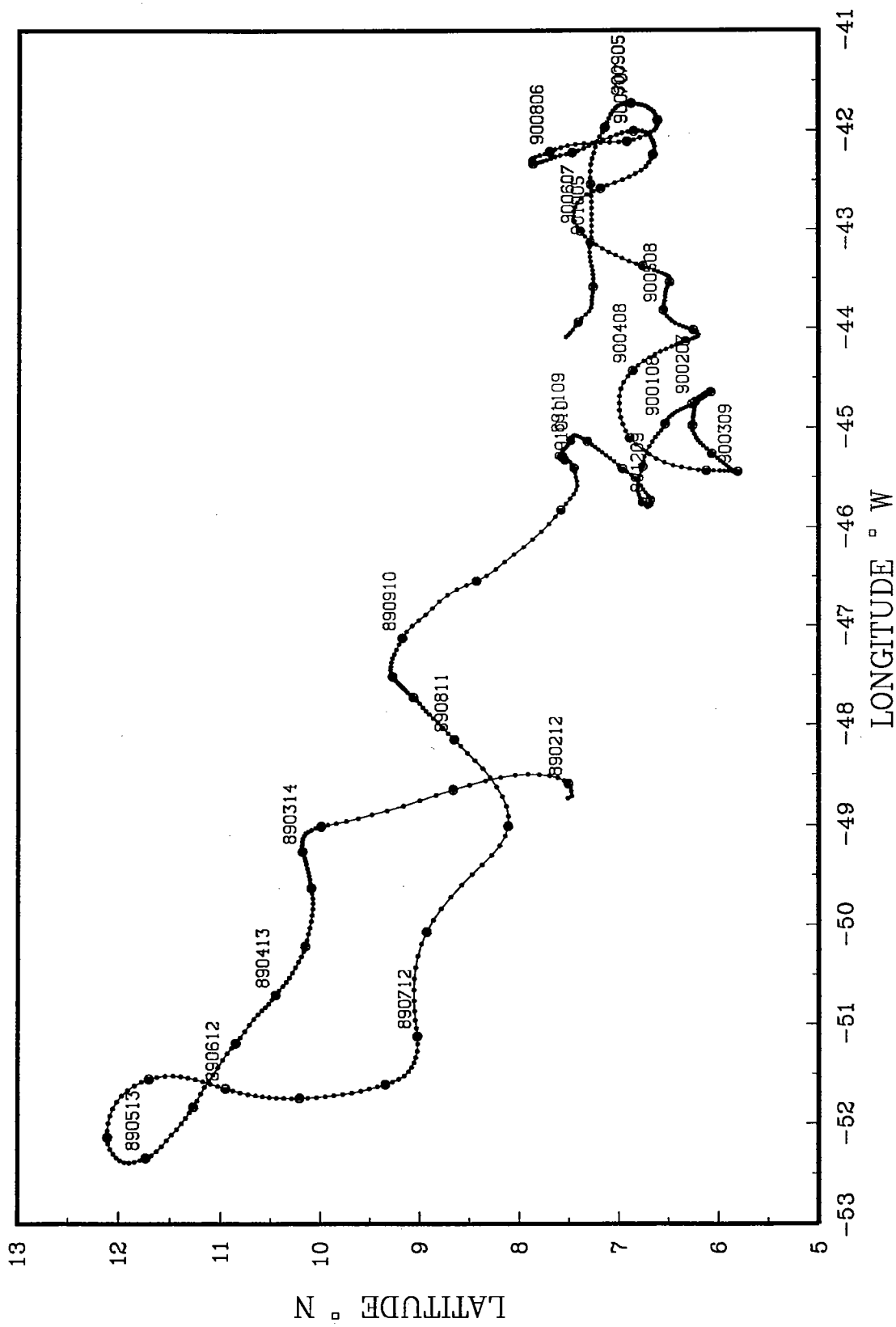


TROPICAL ATLANTIC 19
DEPTH 800 m.

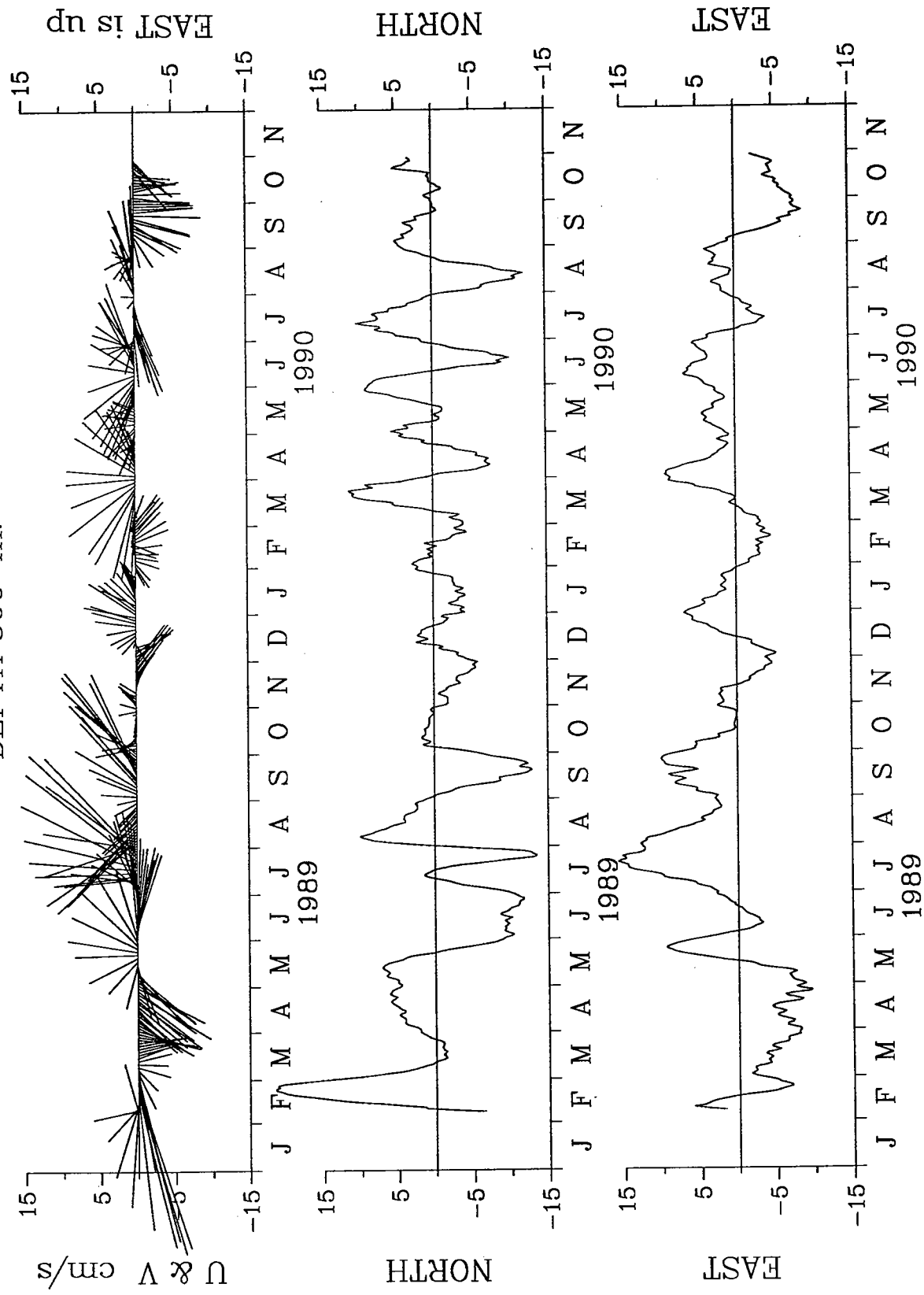


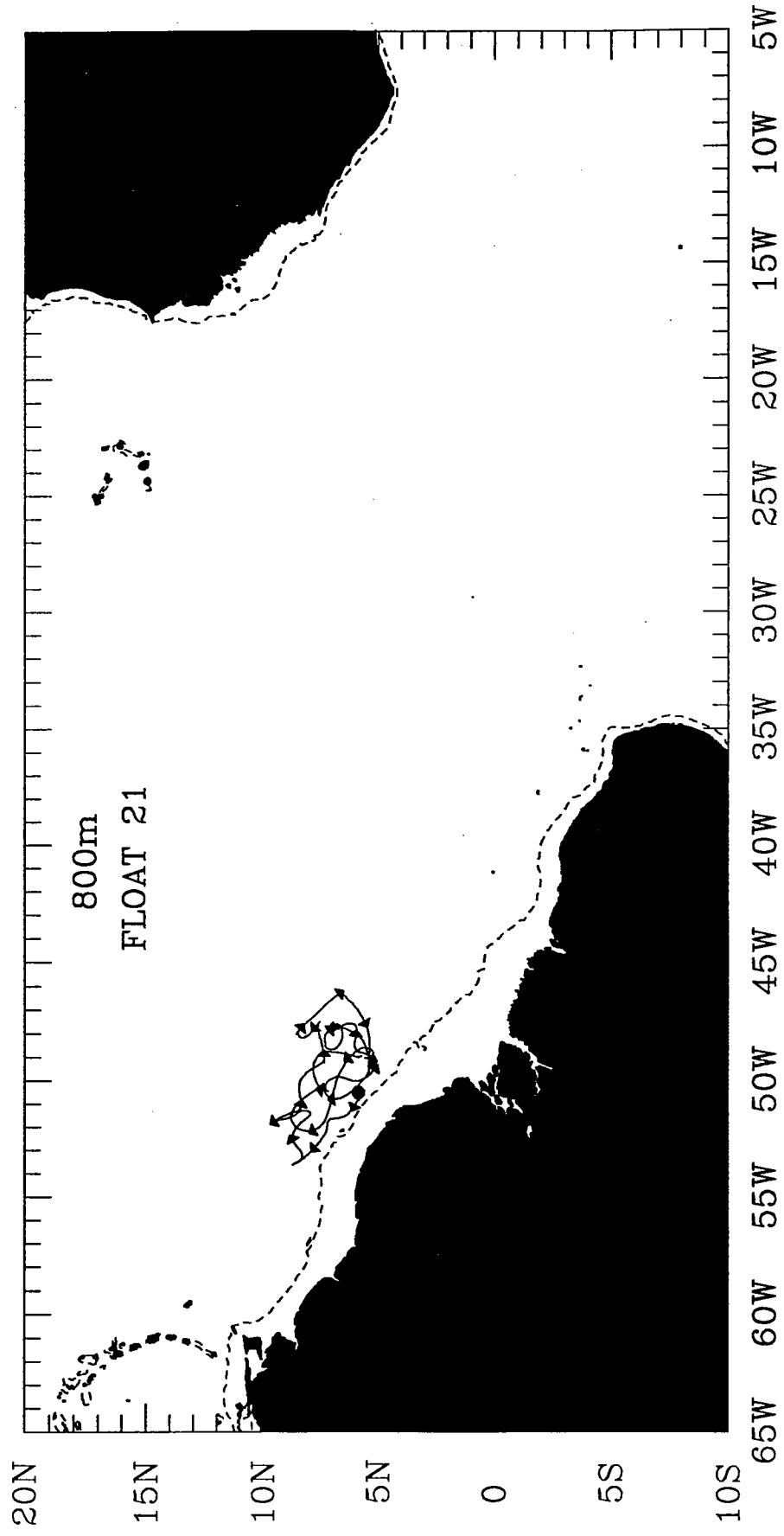


TROPICAL ATLANTIC 20

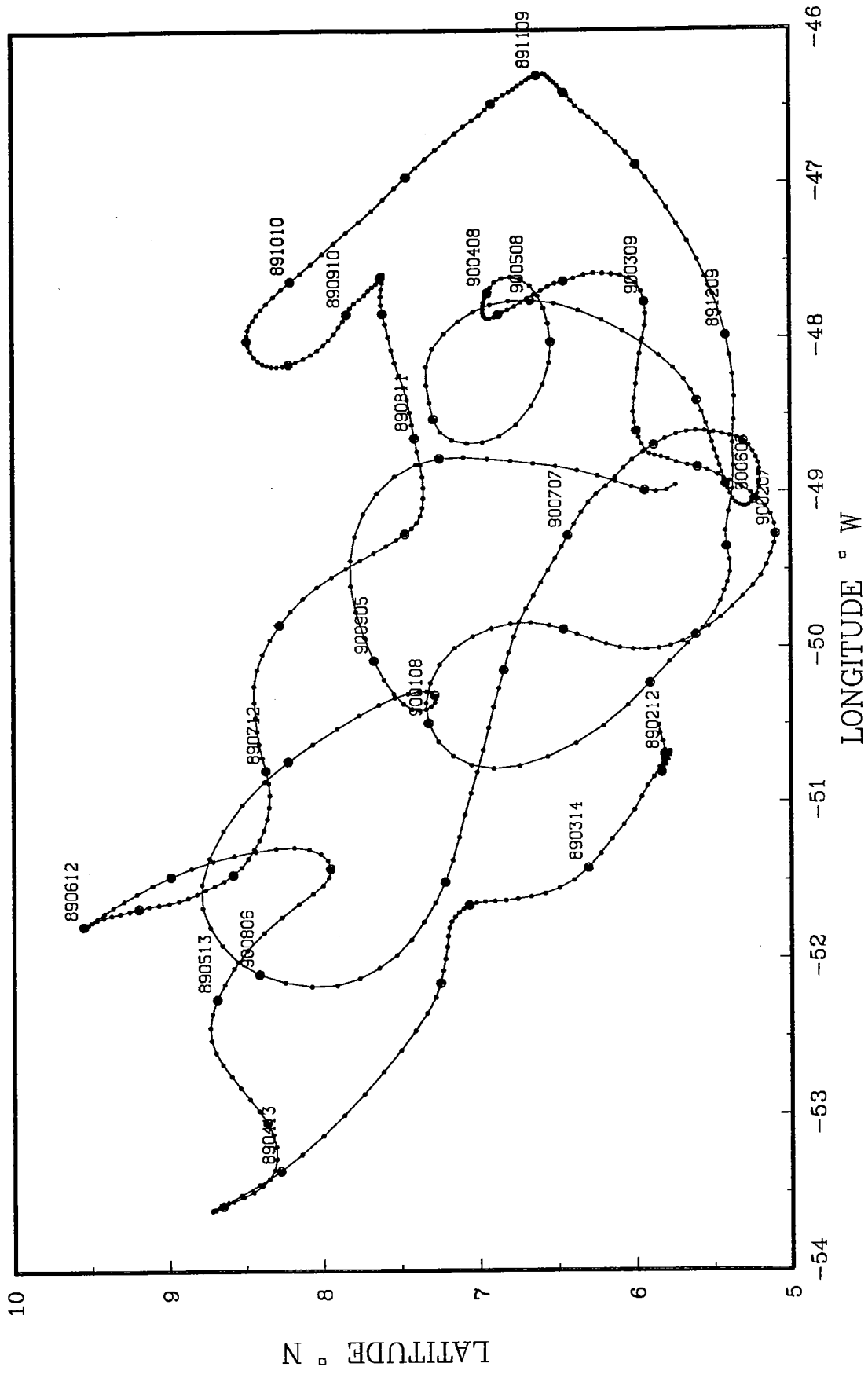


TROPICAL ATLANTIC 20
DEPTH 800 m.

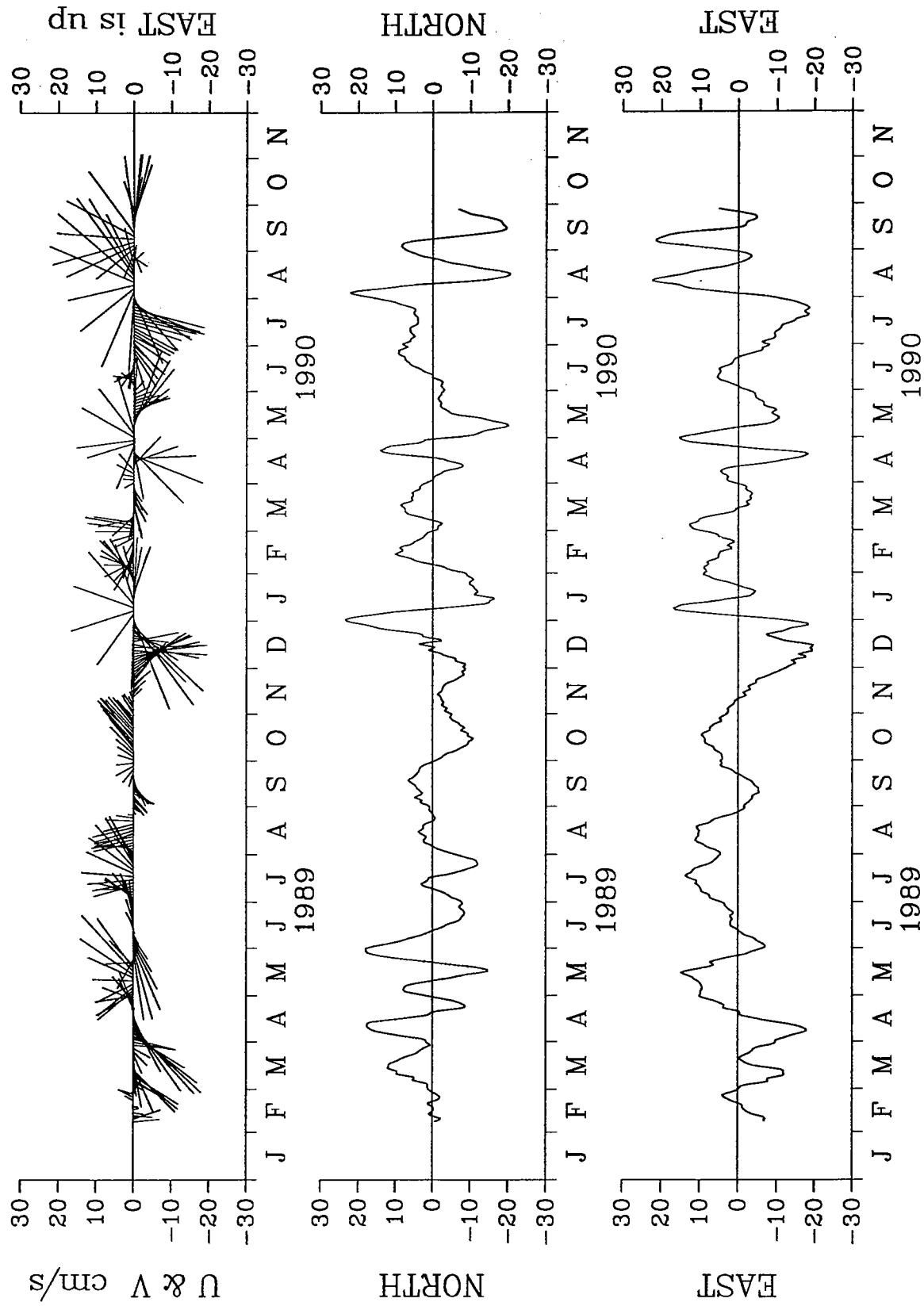


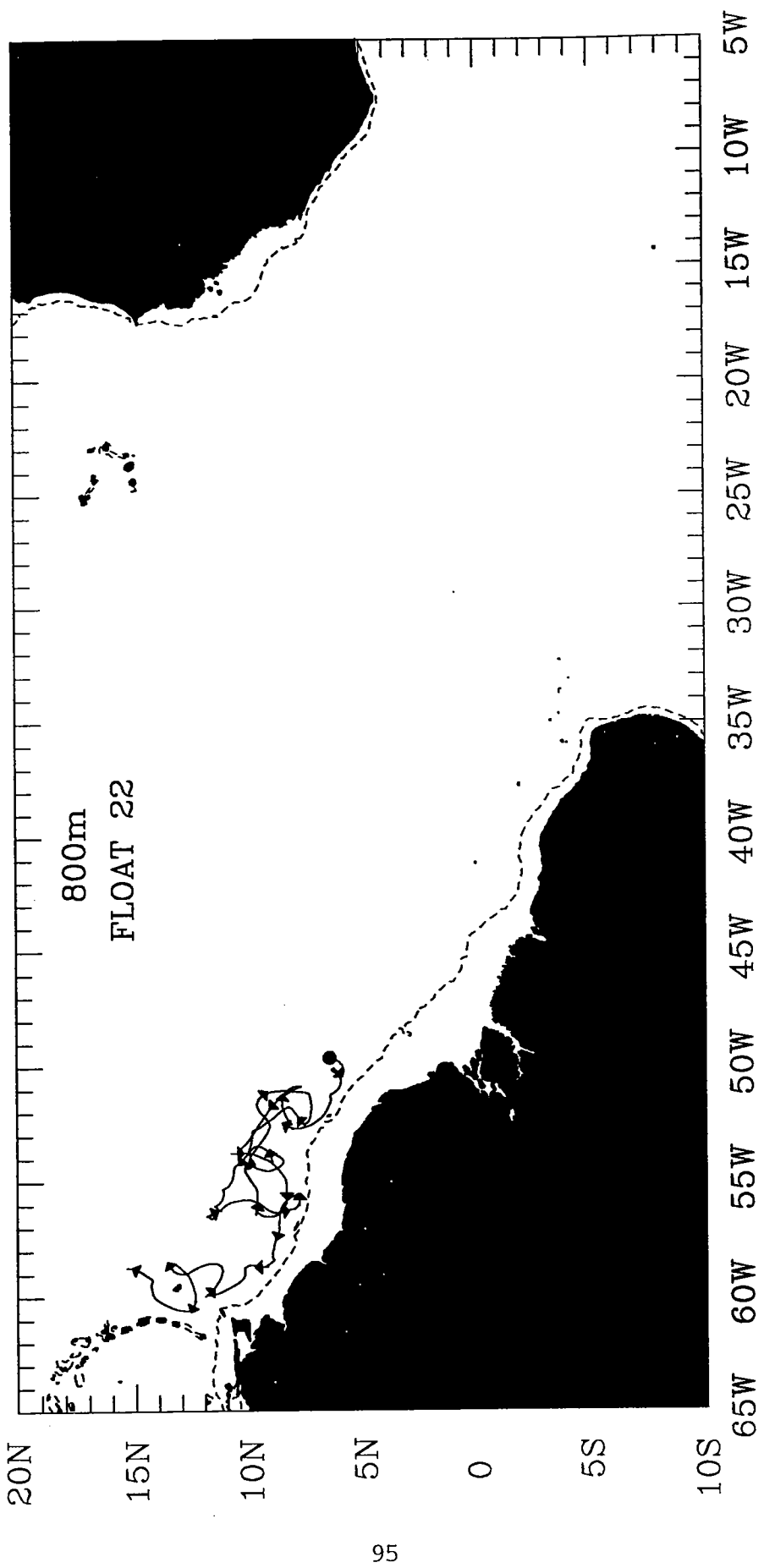


TROPICAL ATLANTIC 21

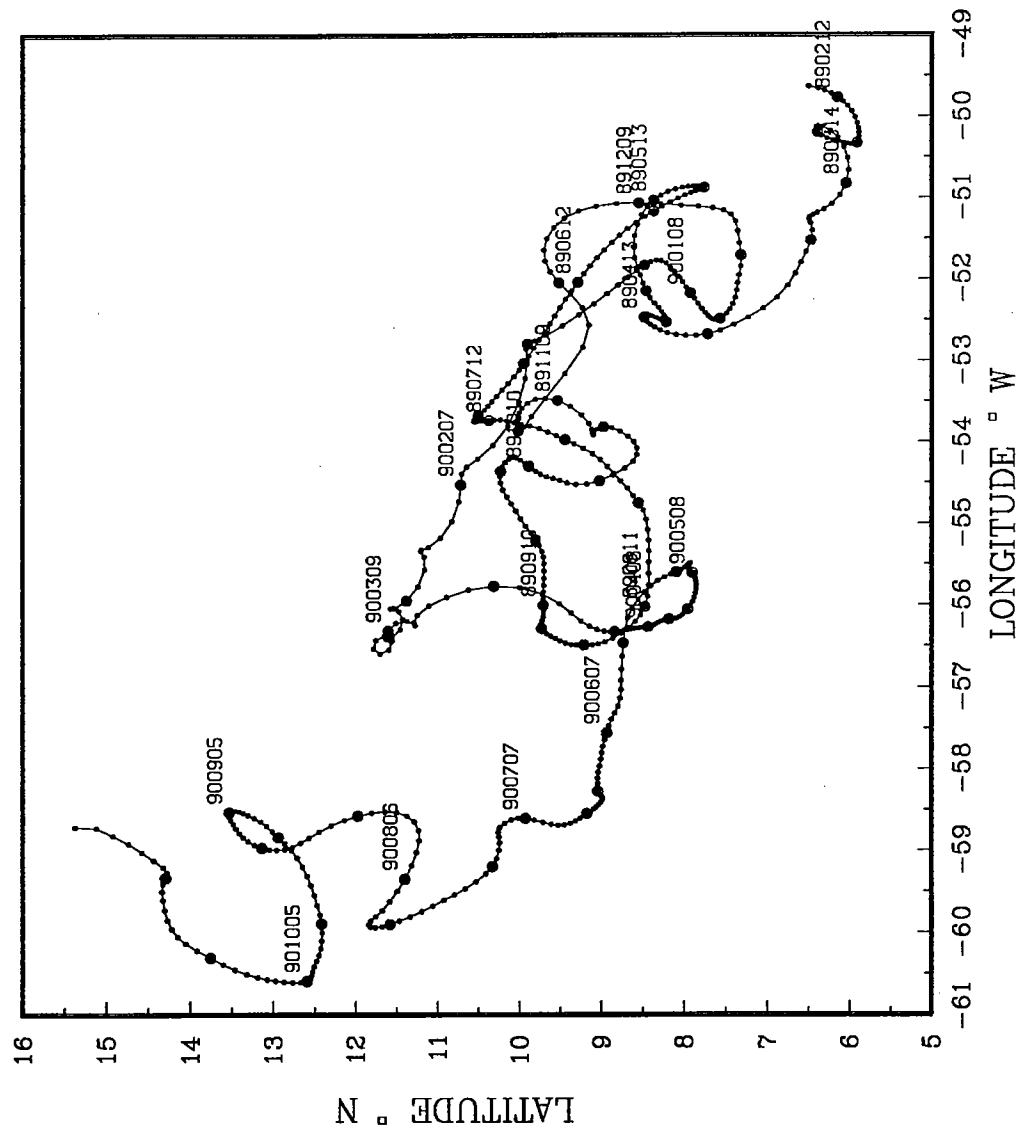


TROPICAL ATLANTIC 21
DEPTH 800 m.

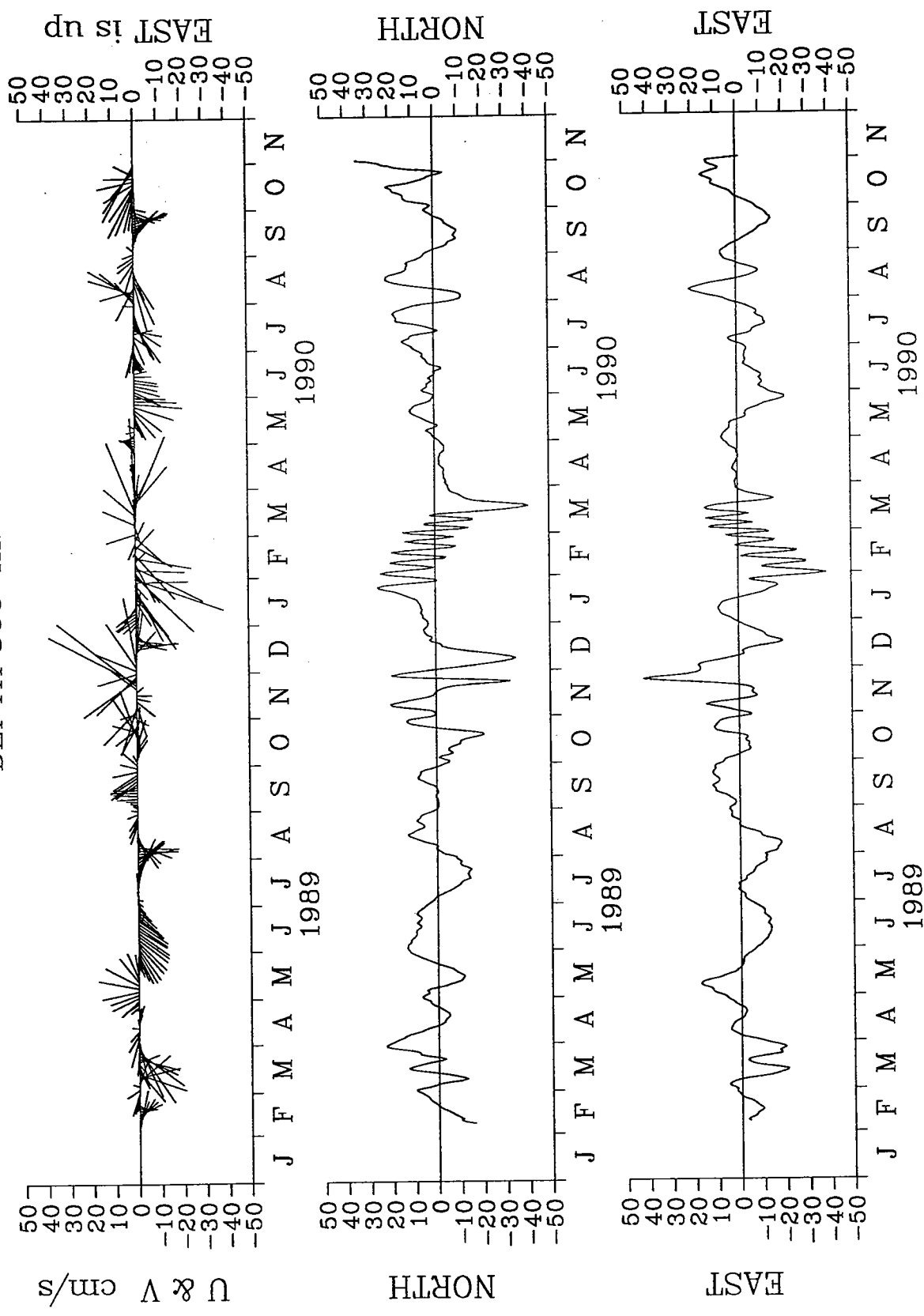


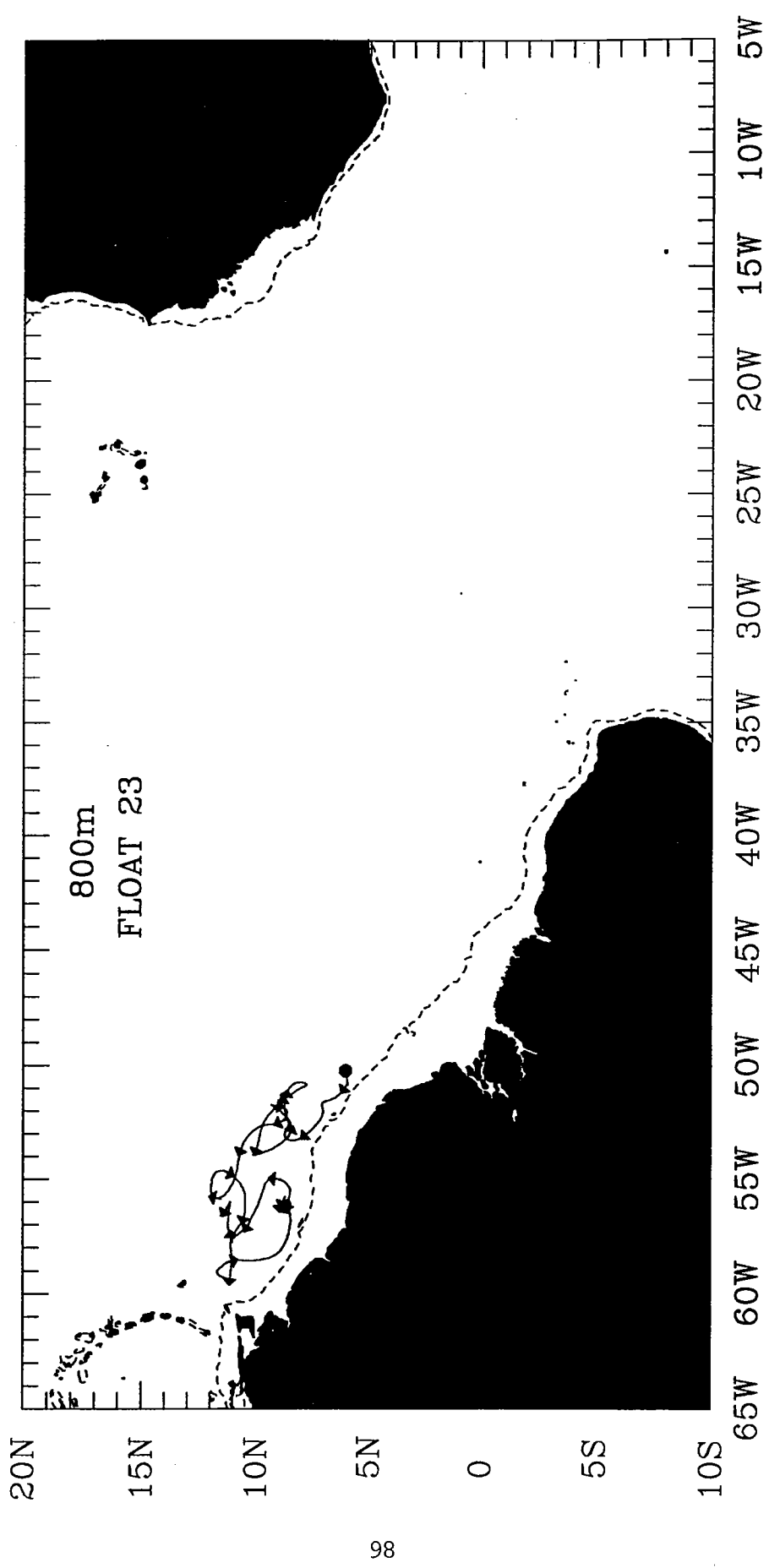


TROPICAL ATLANTIC 22

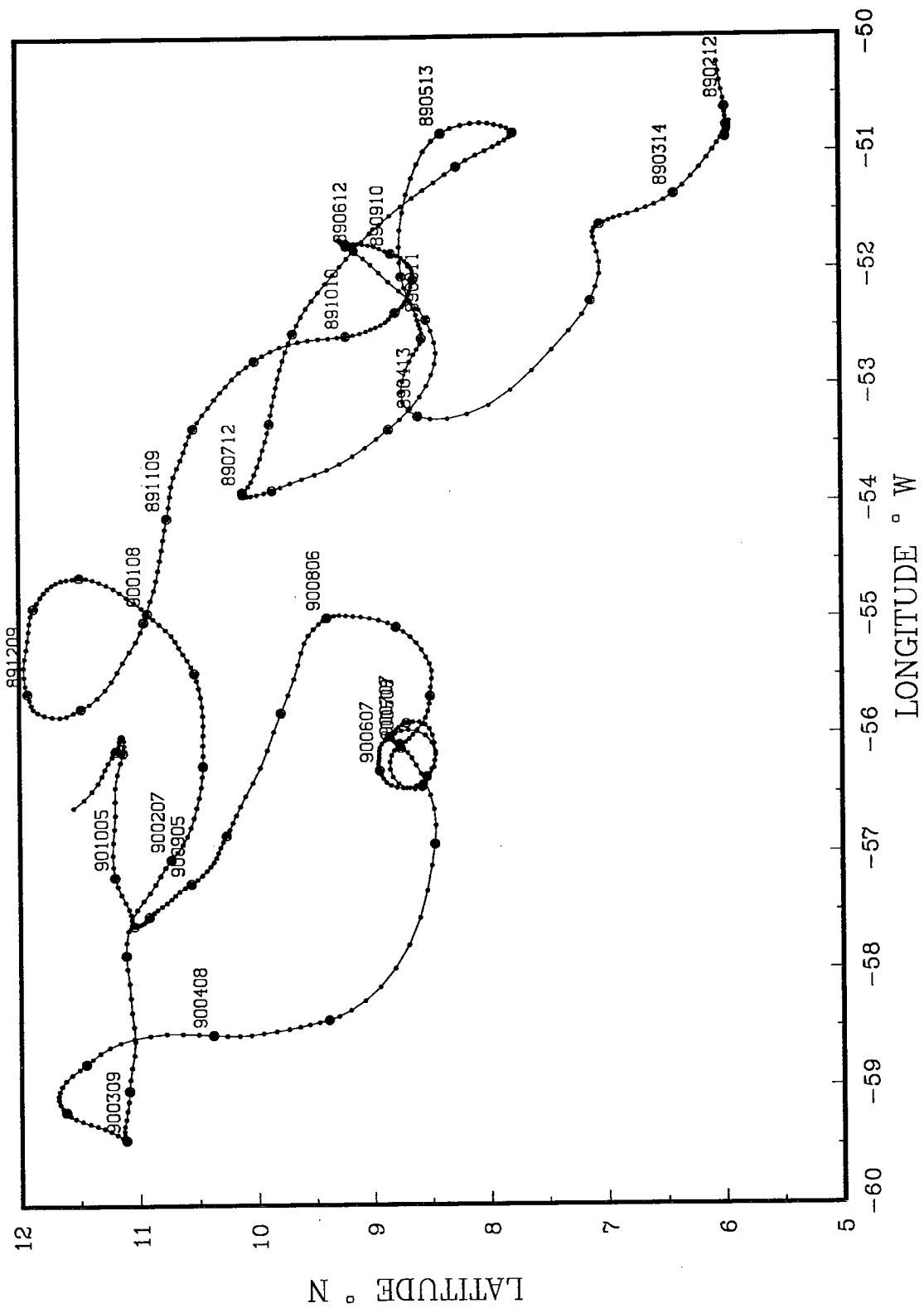


TROPICAL ATLANTIC 22
DEPTH 800 m.

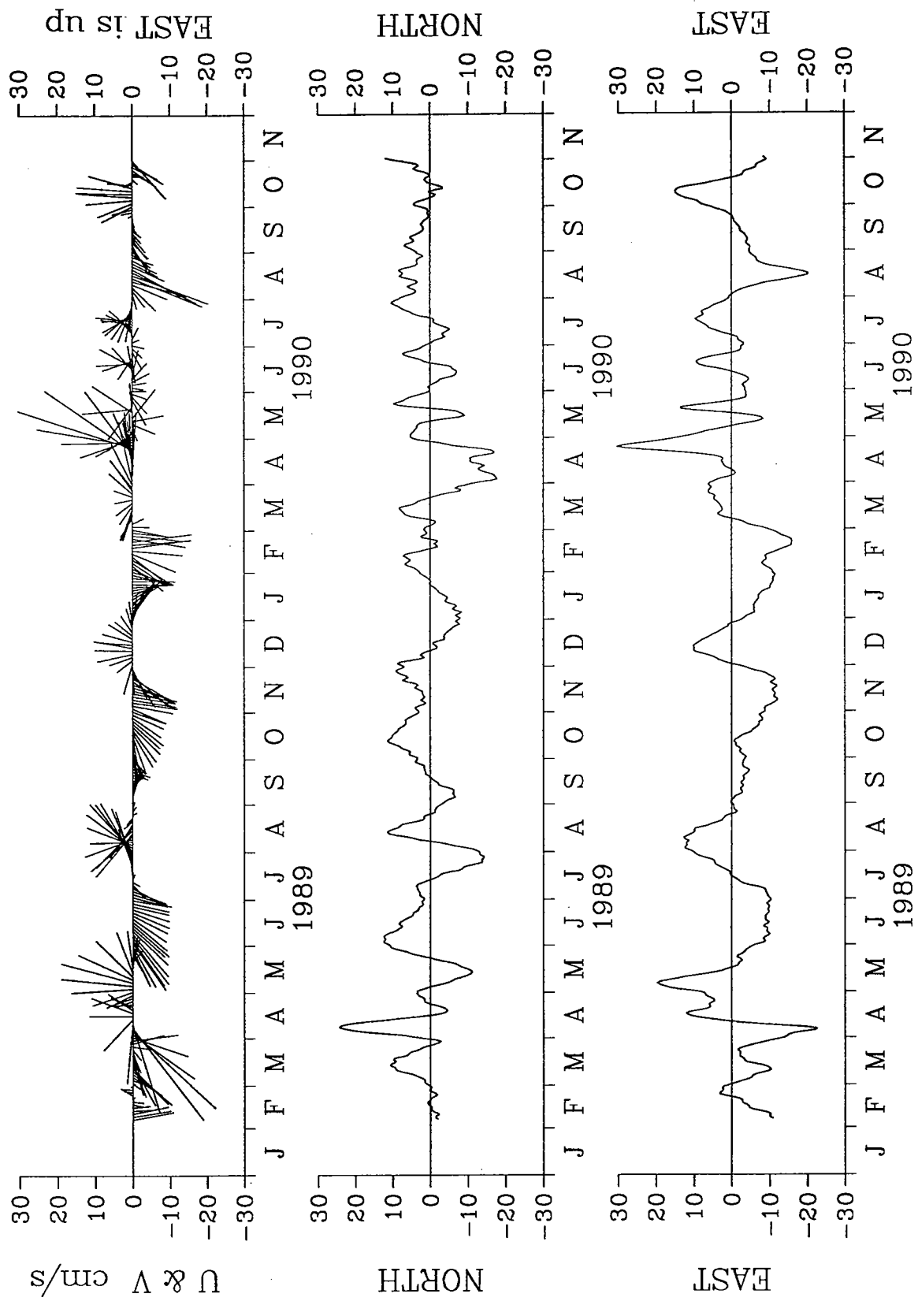




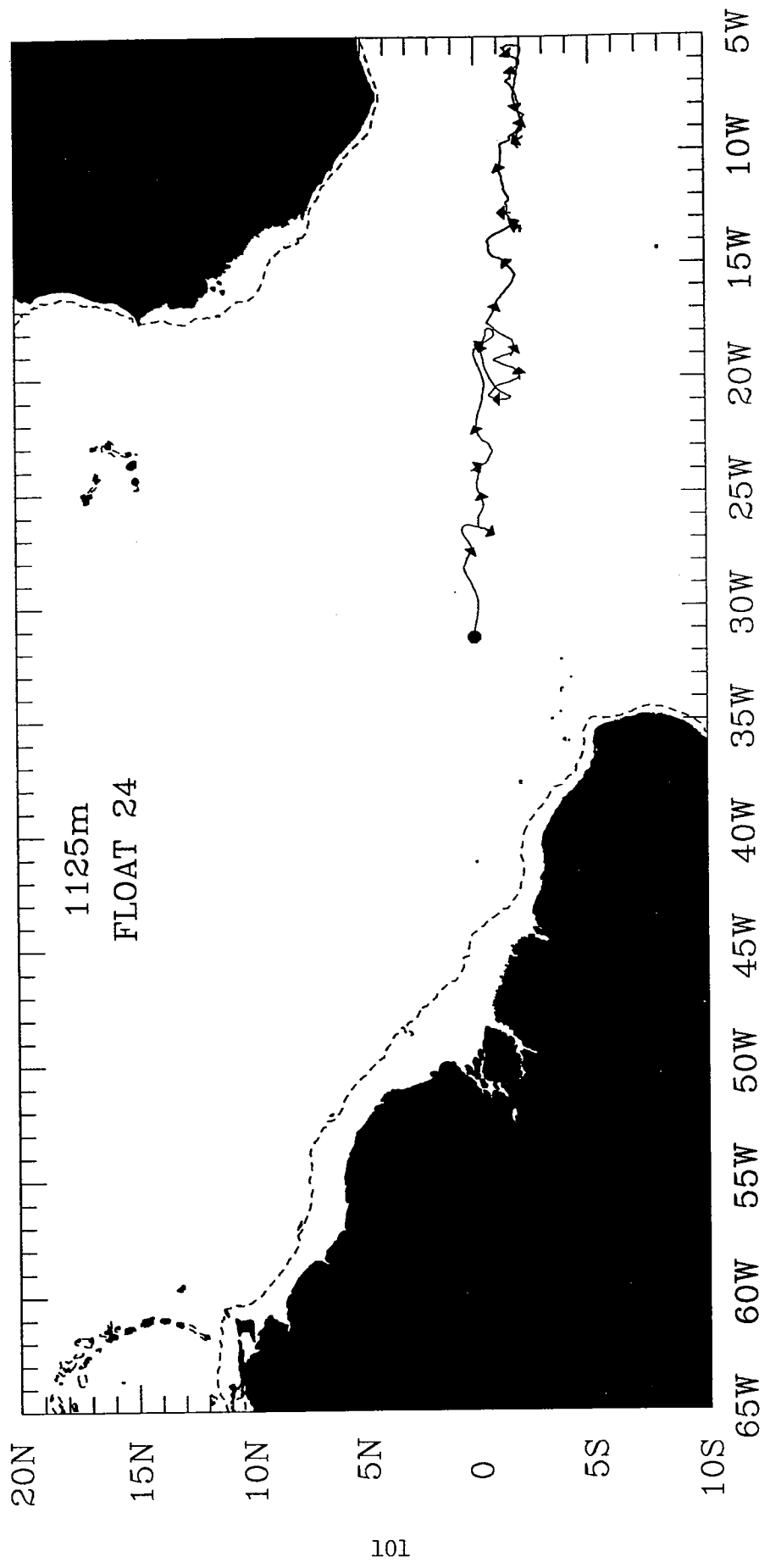
TROPICAL ATLANTIC 23



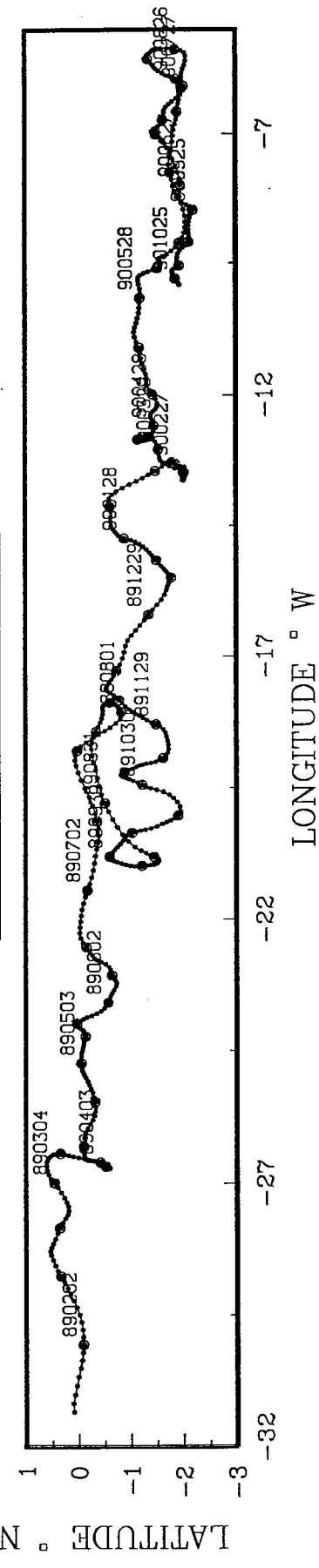
TROPICAL ATLANTIC 23
DEPTH 800 m.



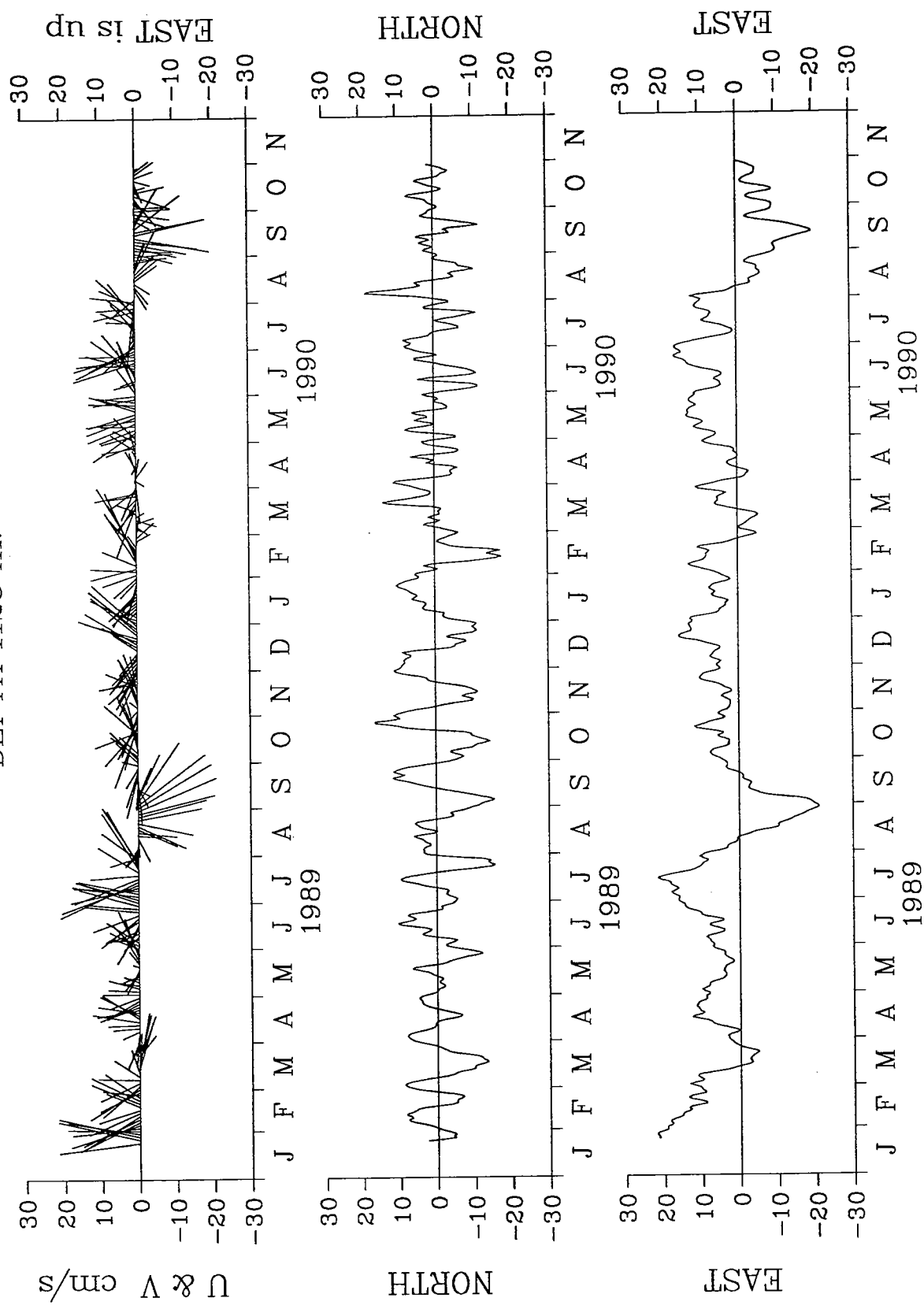
100

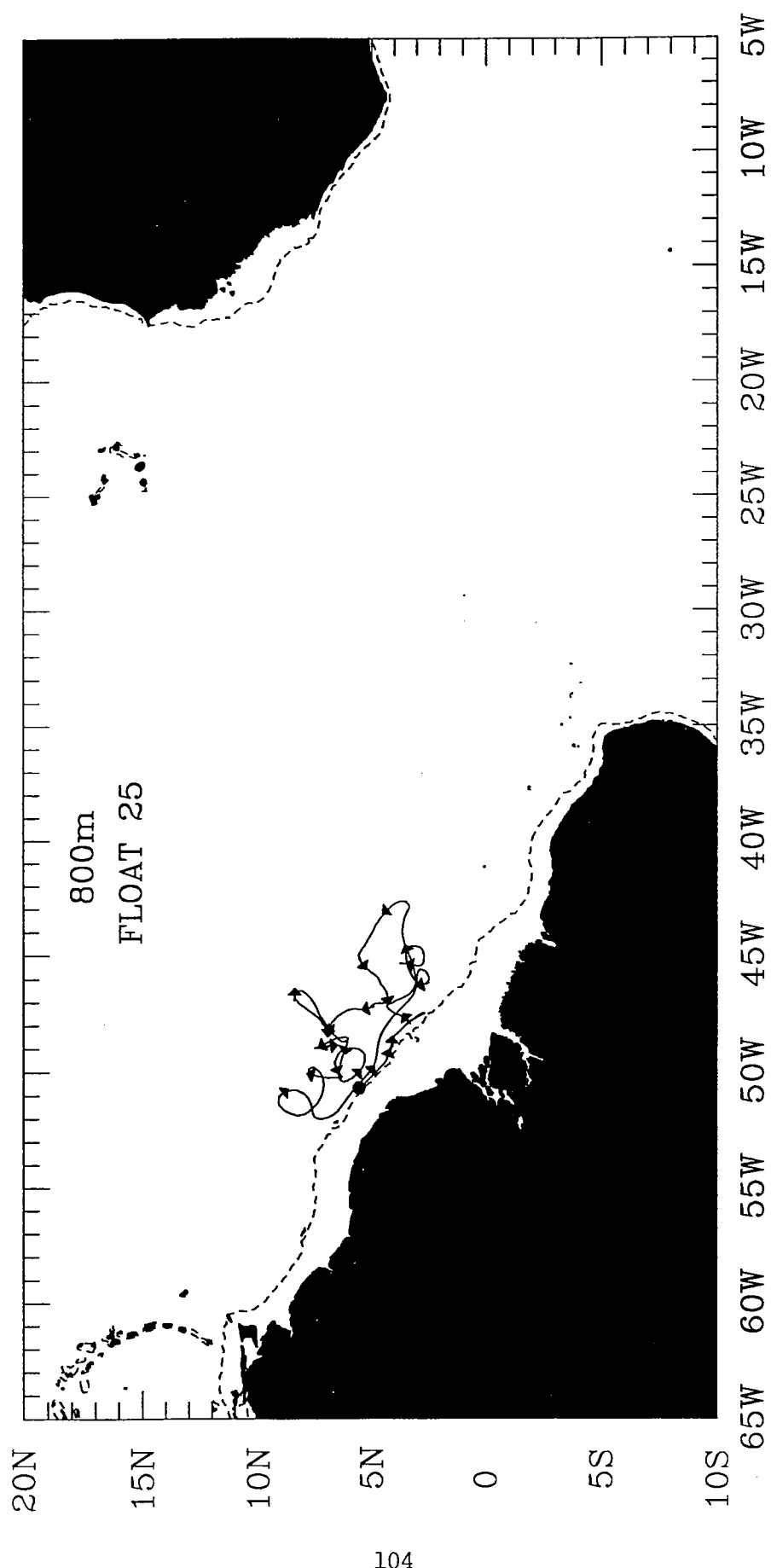


TROPICAL ATLANTIC 24

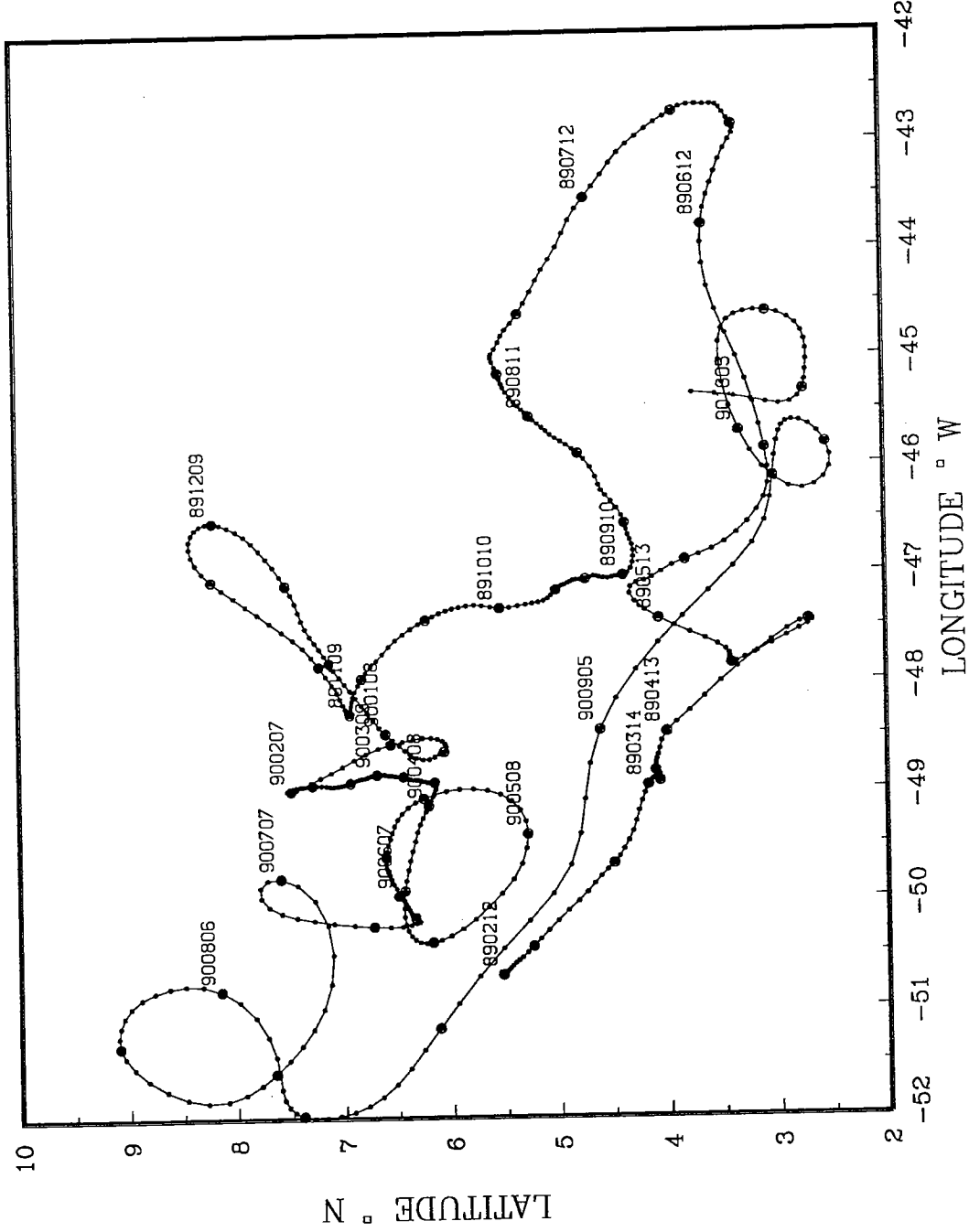


TROPICAL ATLANTIC 24
DEPTH 1125 m.

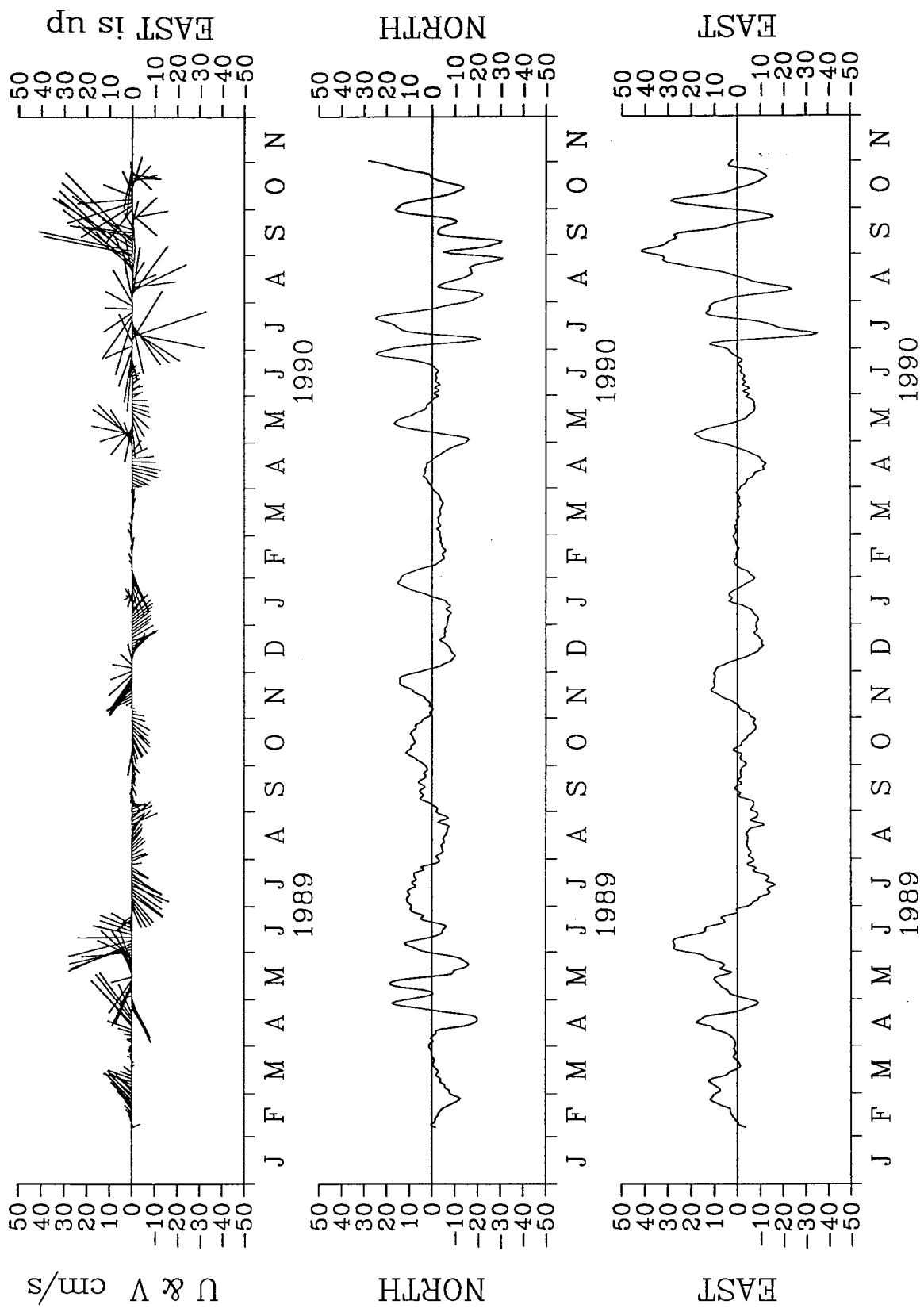


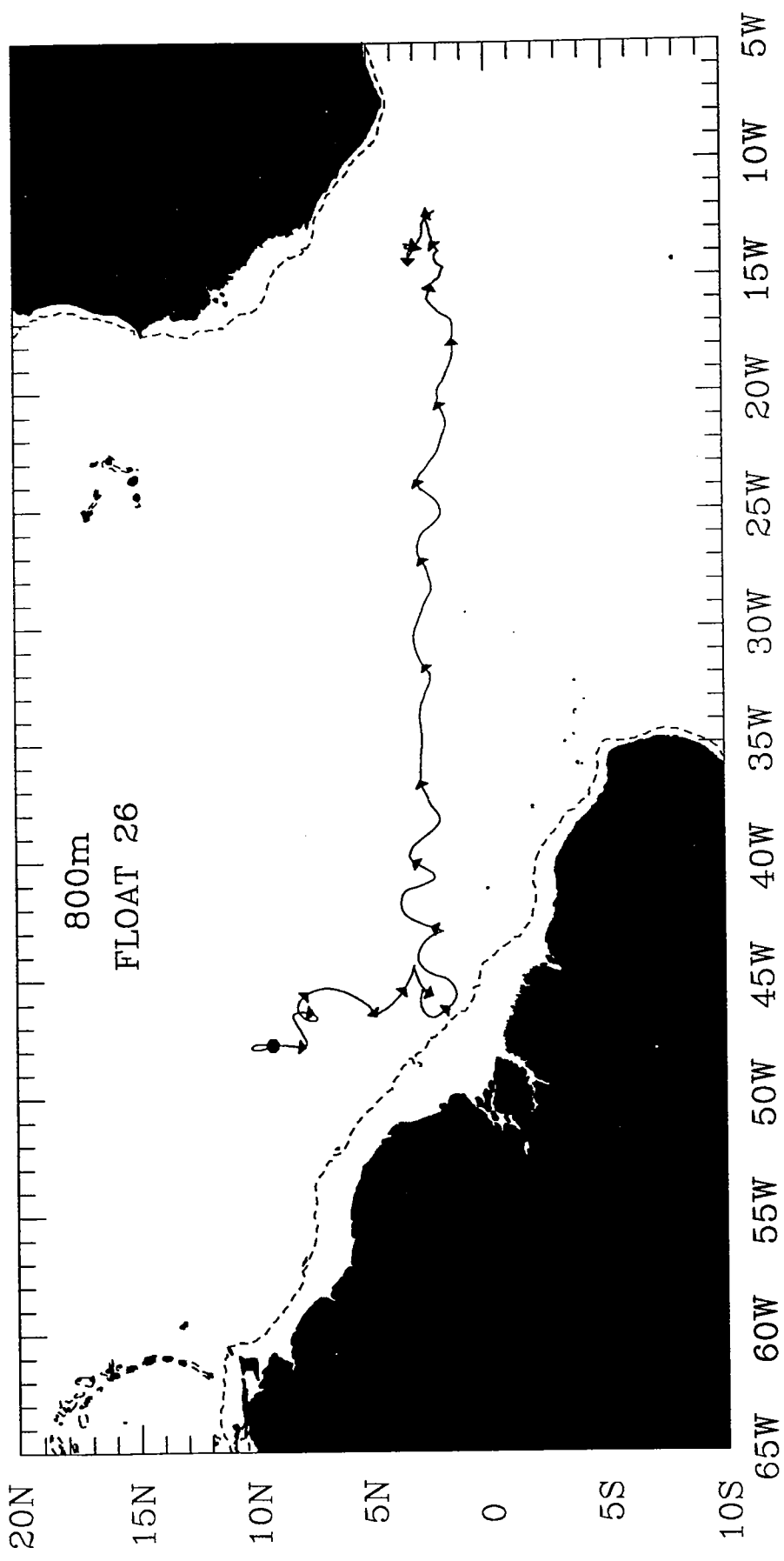


TROPICAL ATLANTIC 25

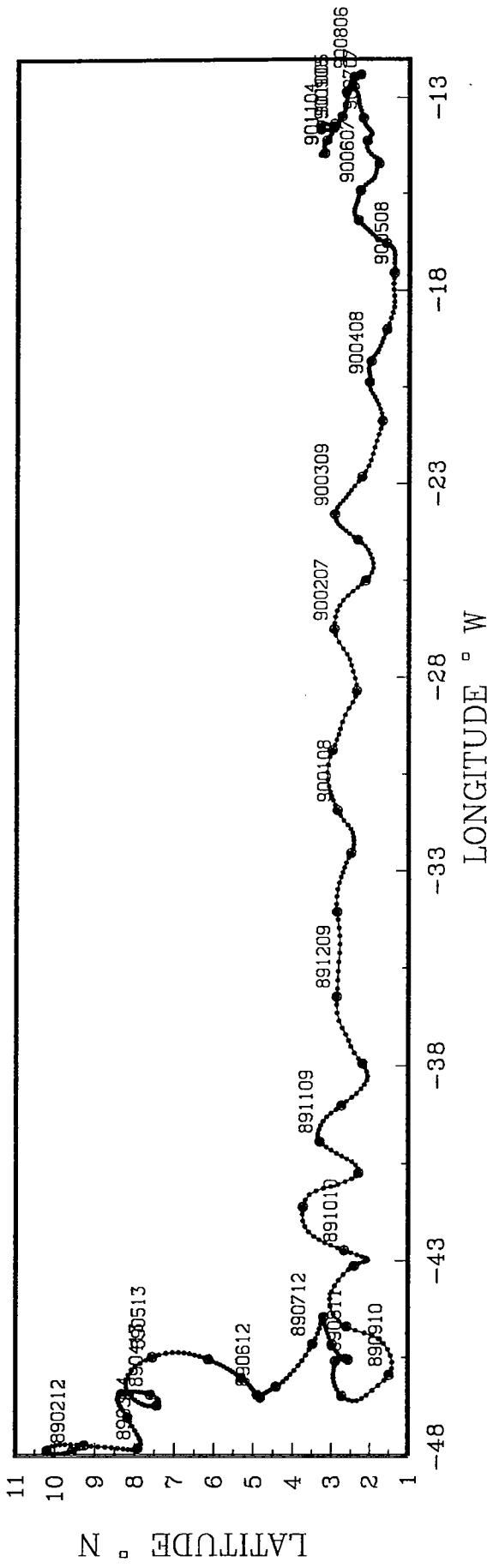


TROPICAL ATLANTIC 25
DEPTH 800 m.

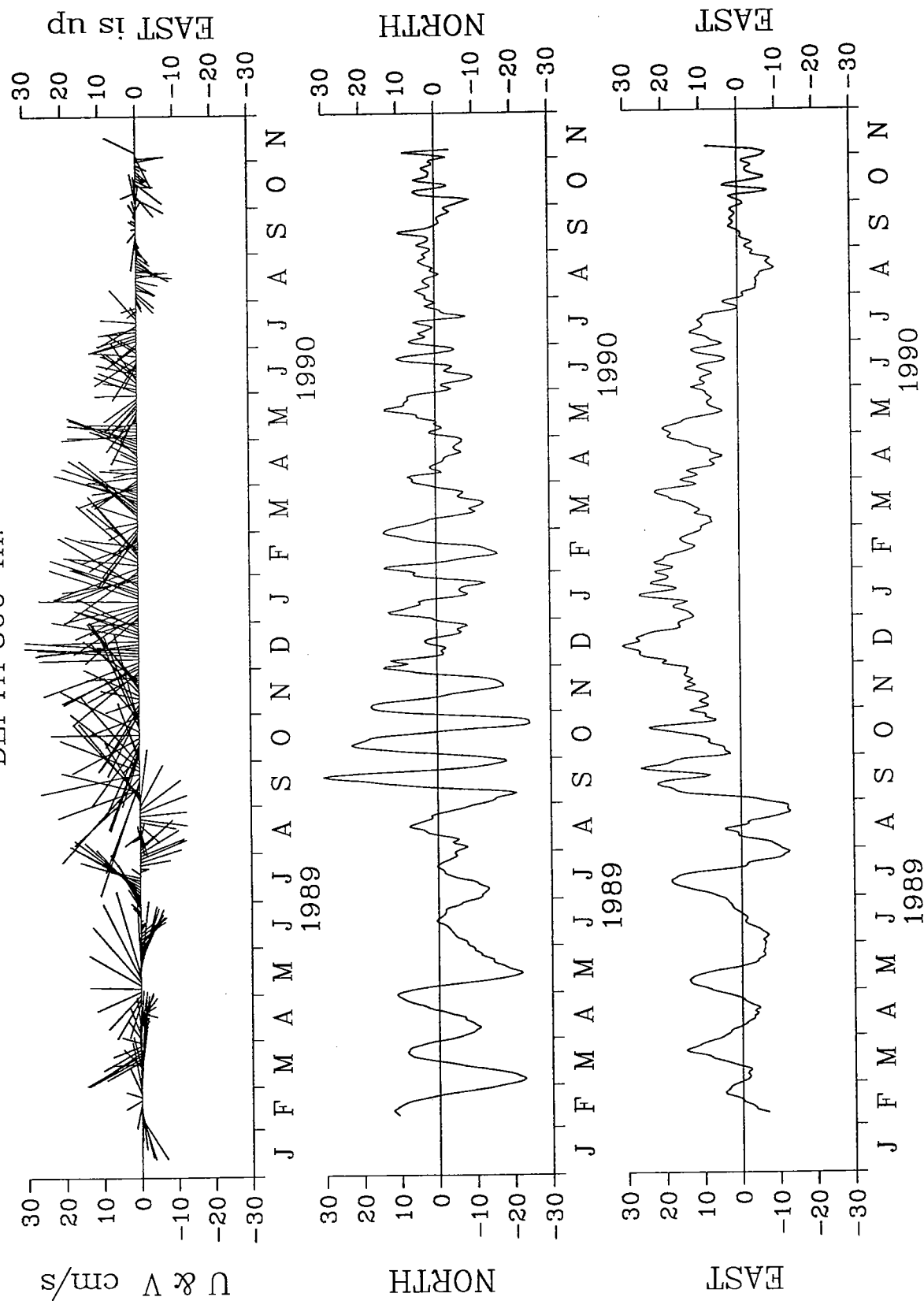


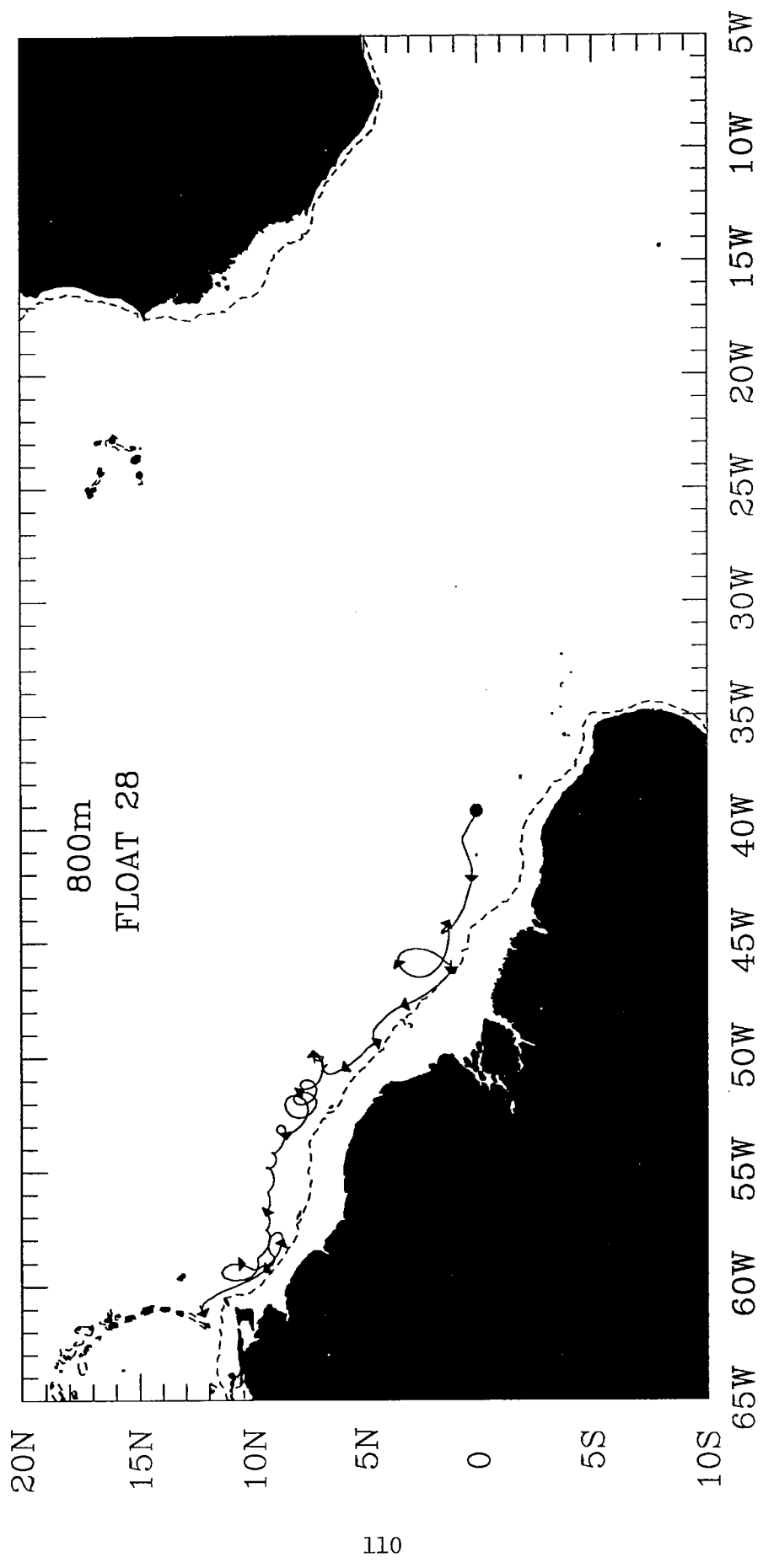


TROPICAL ATLANTIC 26

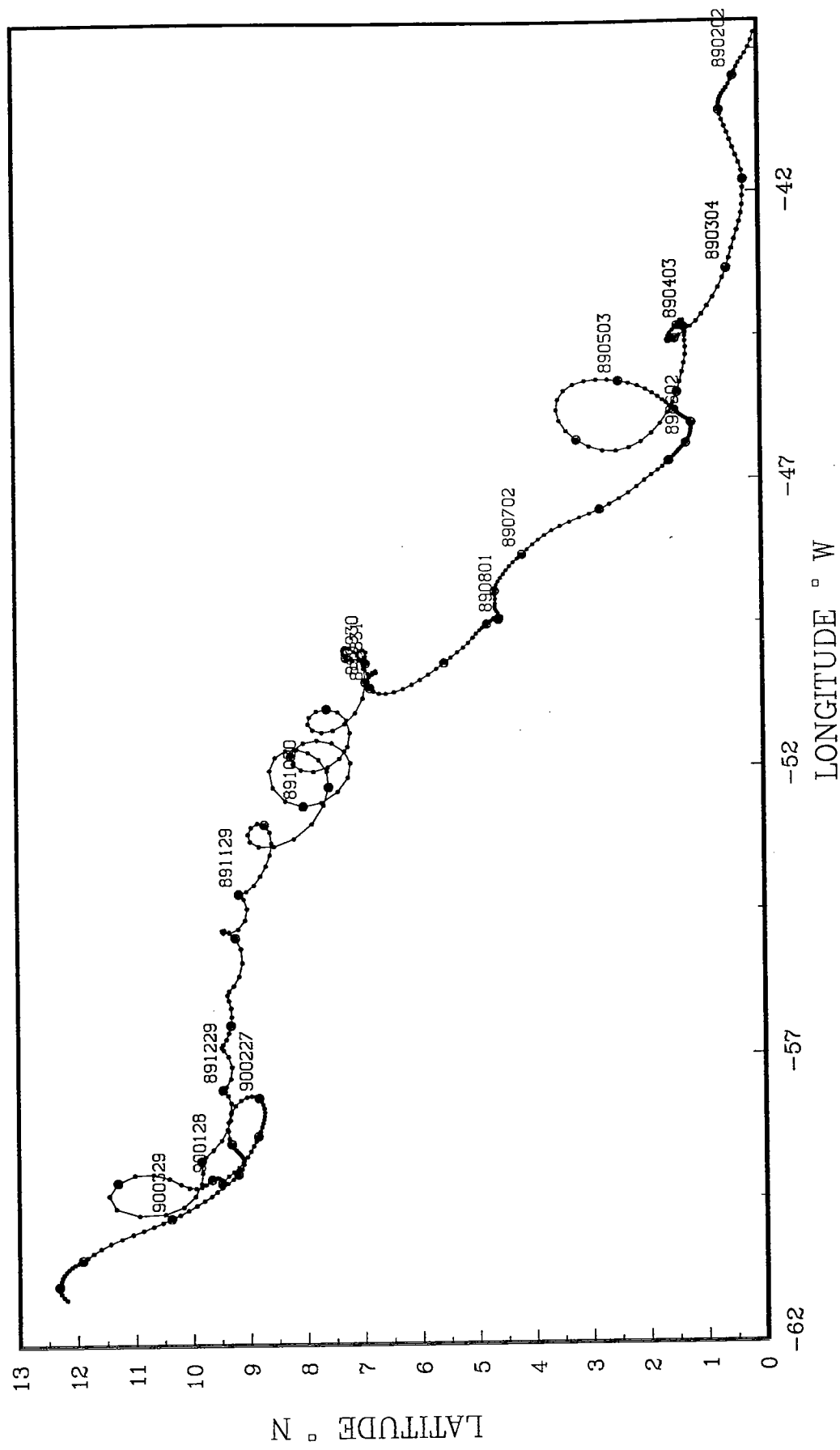


TROPICAL ATLANTIC 26
DEPTH 800 m.

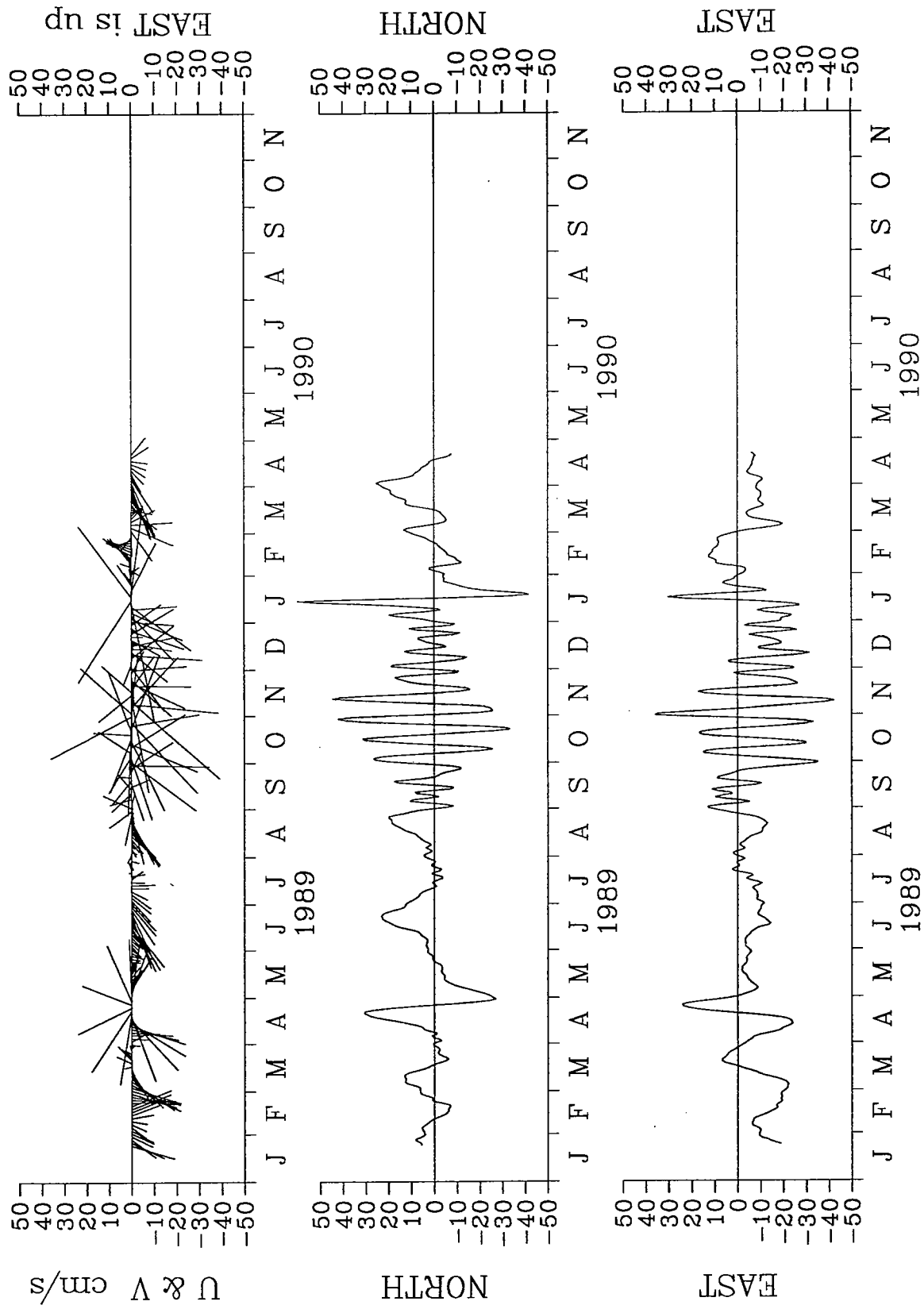


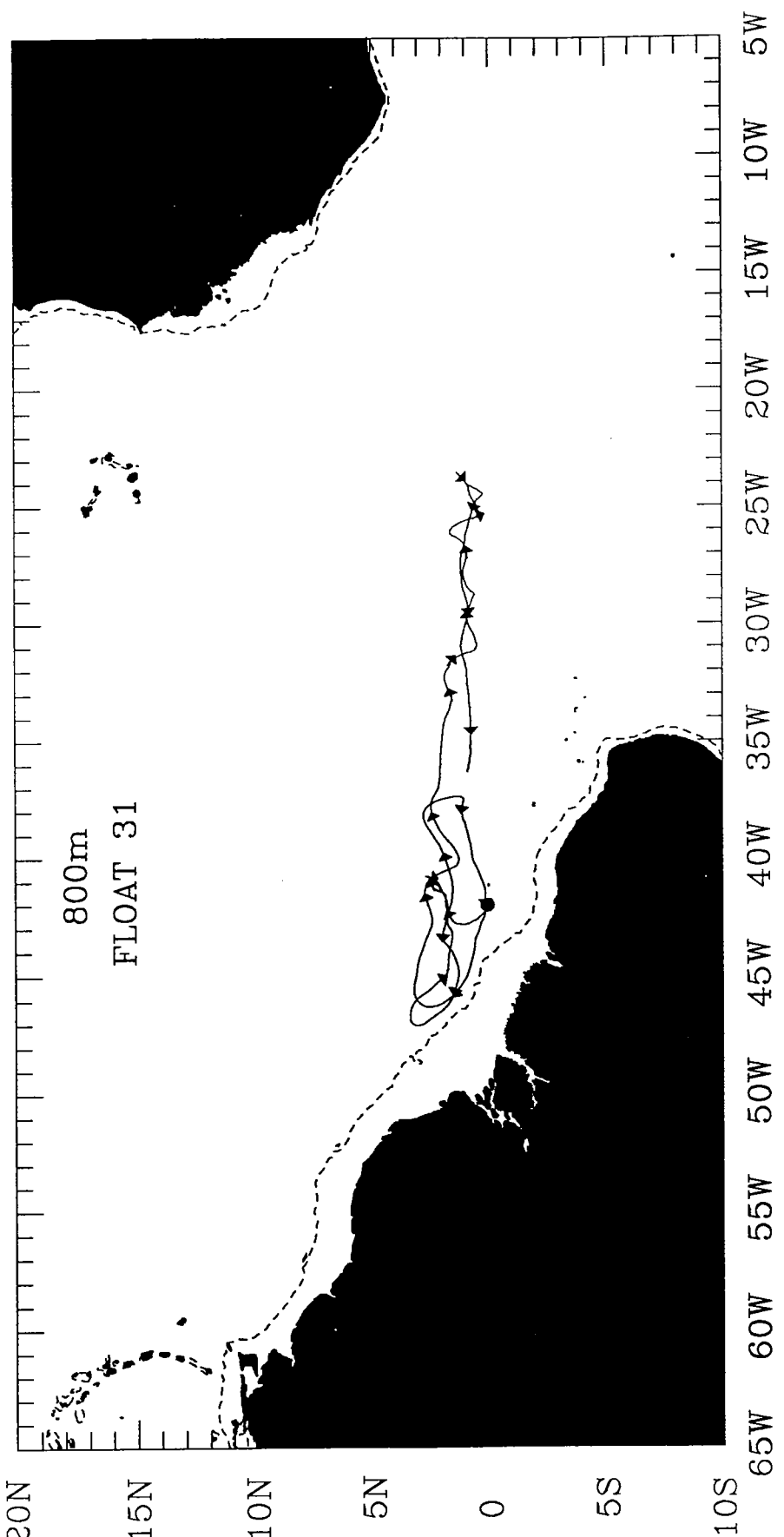


TROPICAL ATLANTIC 28

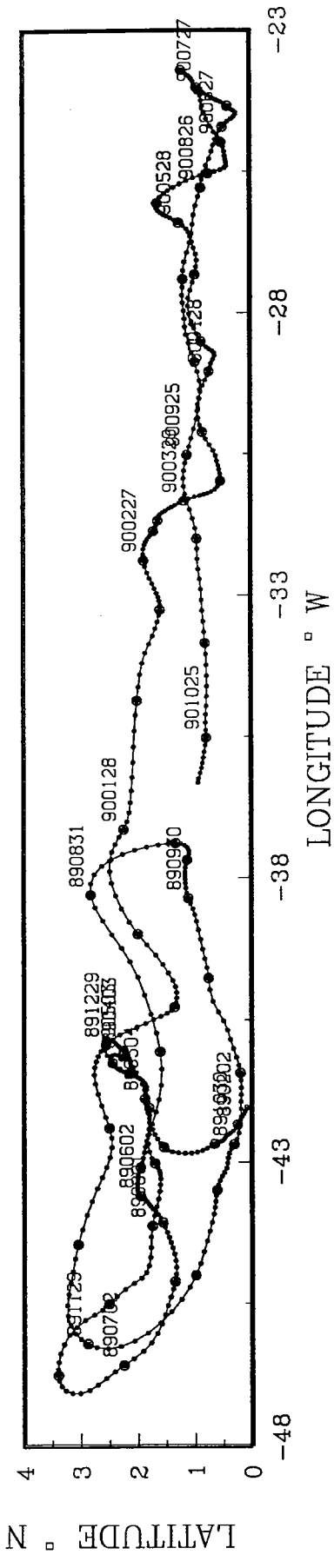


TROPICAL ATLANTIC 28
DEPTH 800 m.

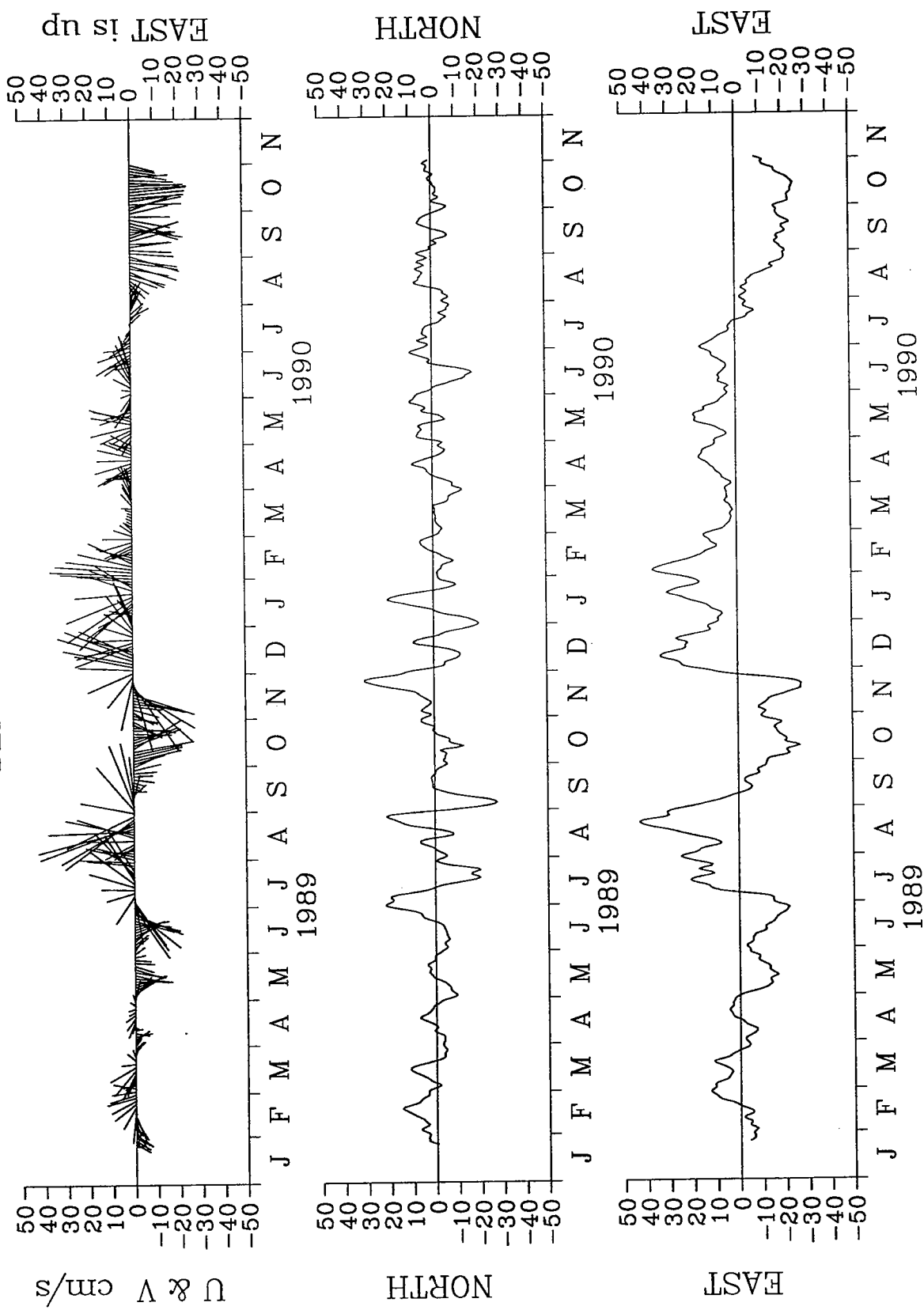


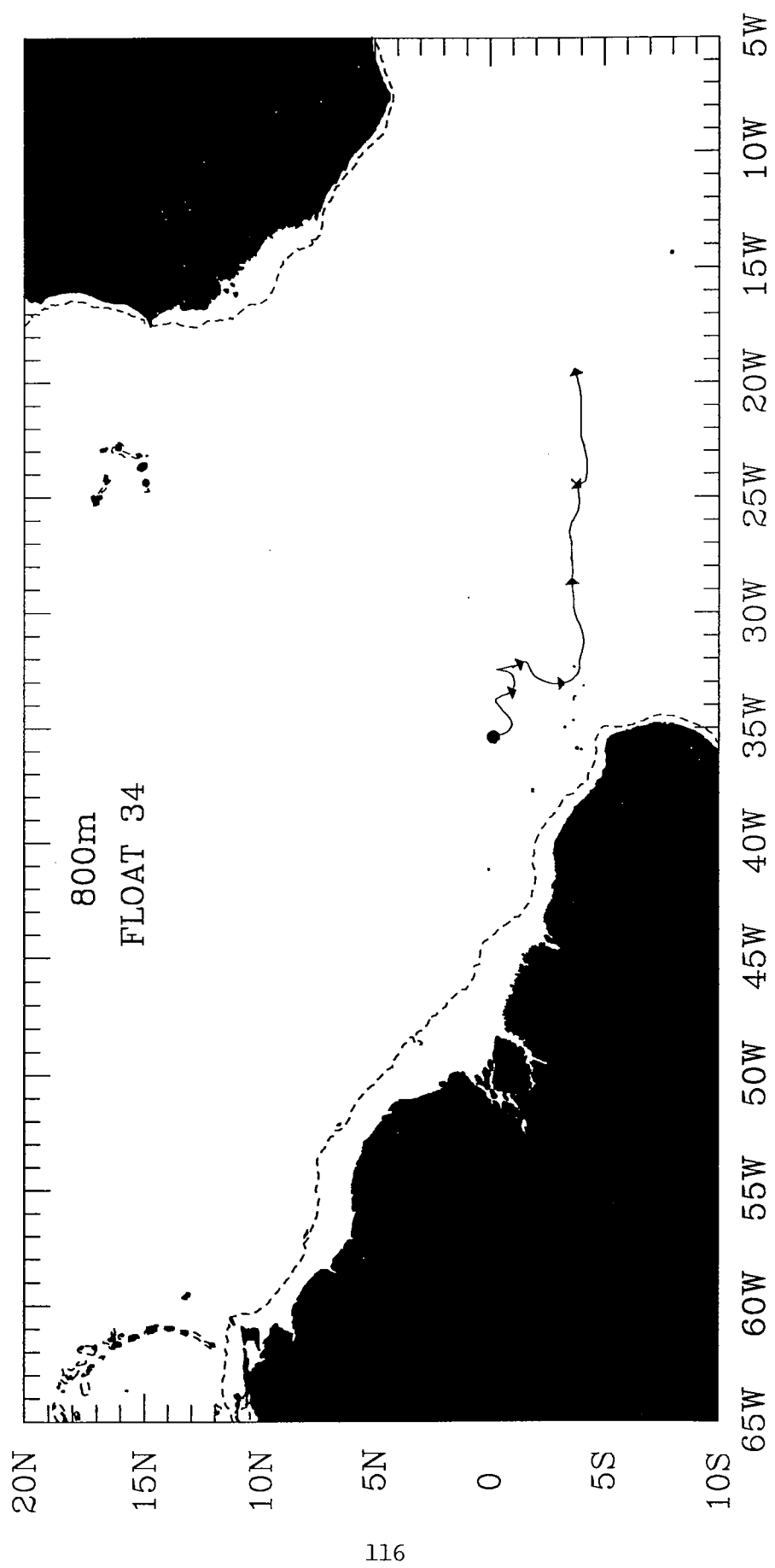


TROPICAL ATLANTIC 31

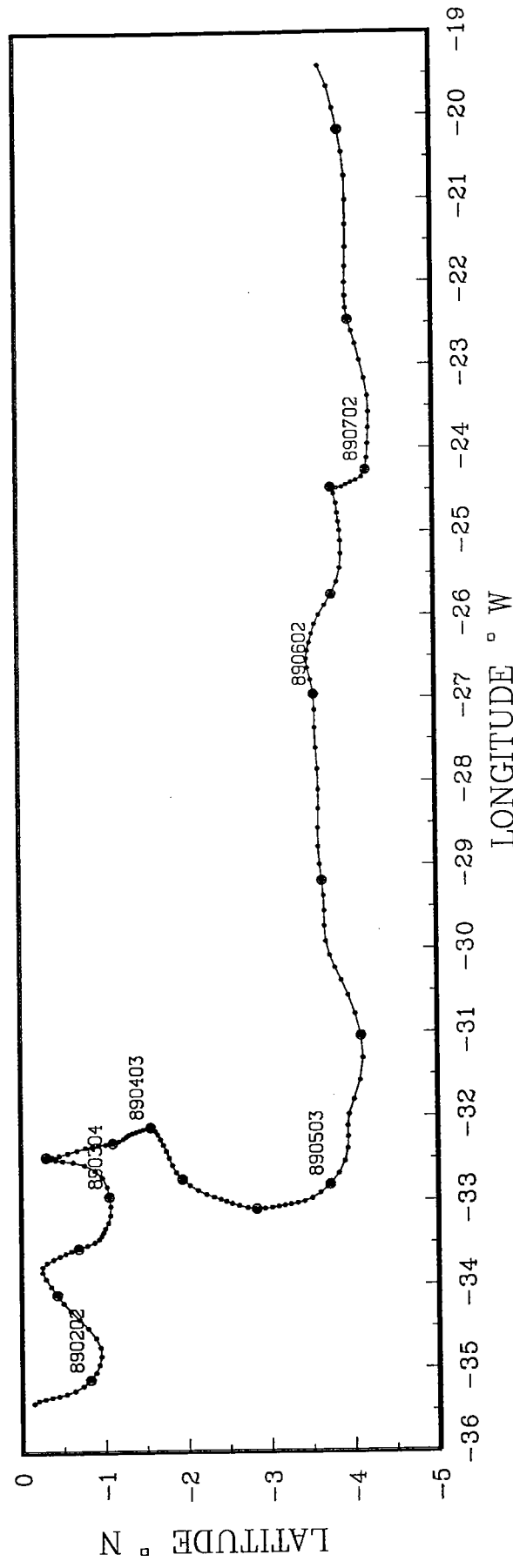


TROPICAL ATLANTIC 31
DEPTH 800 m.

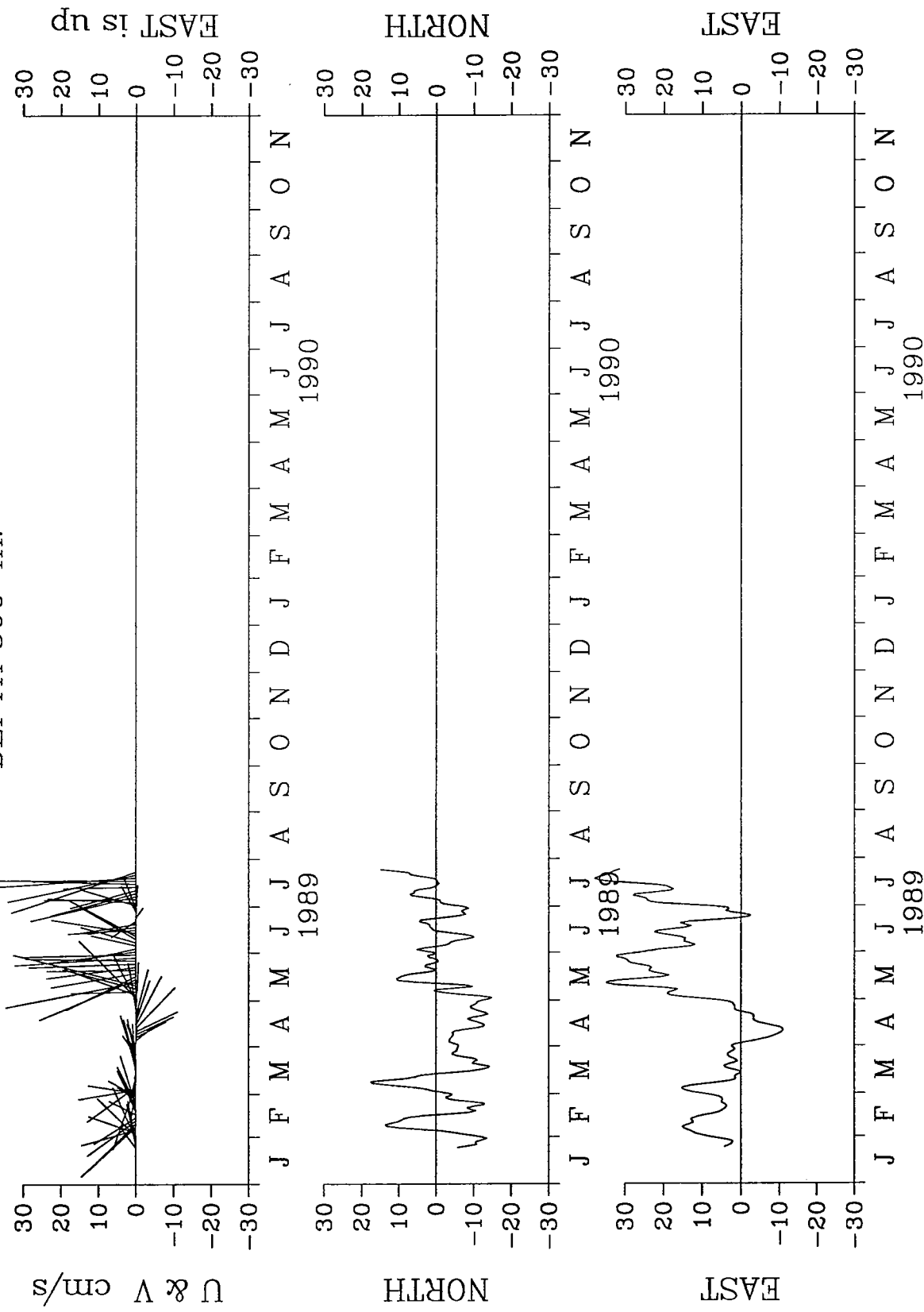


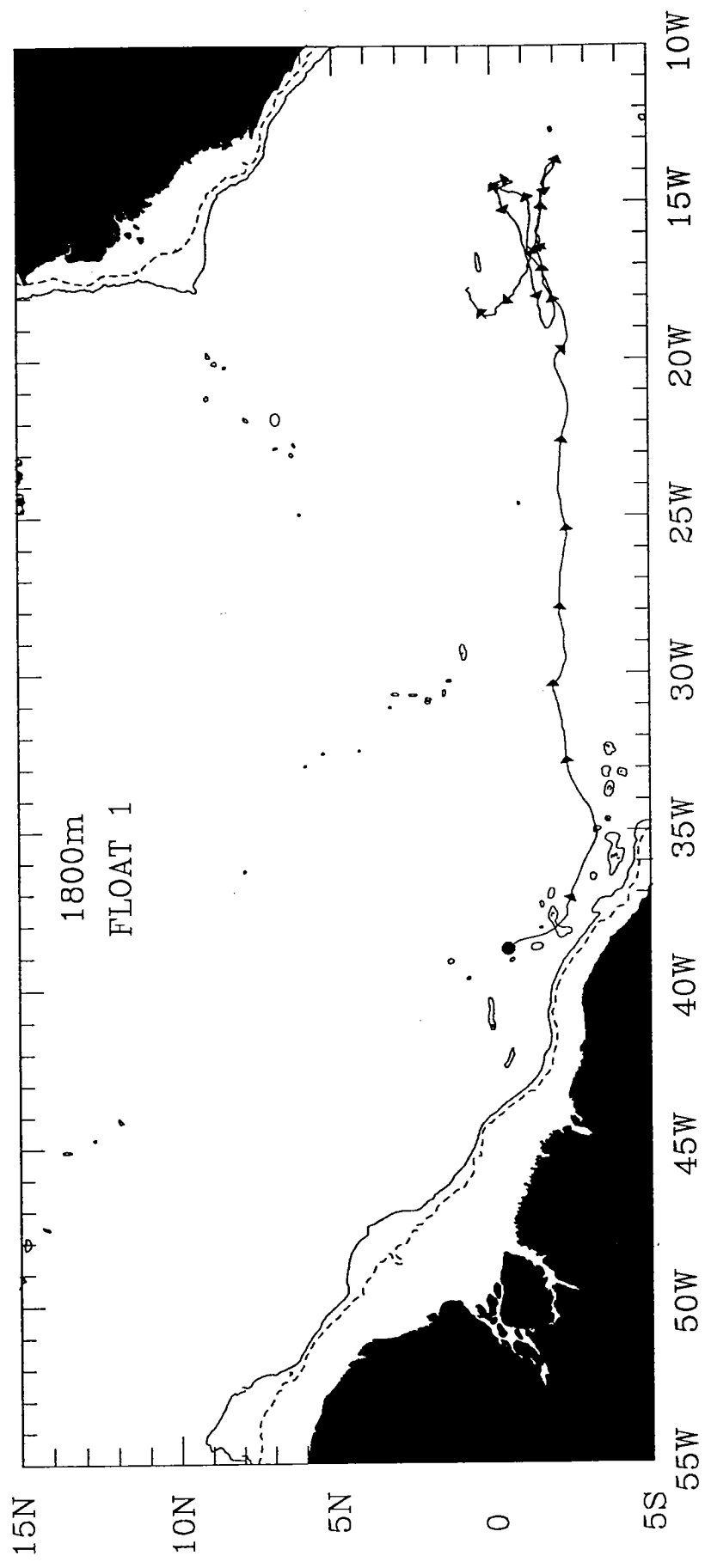


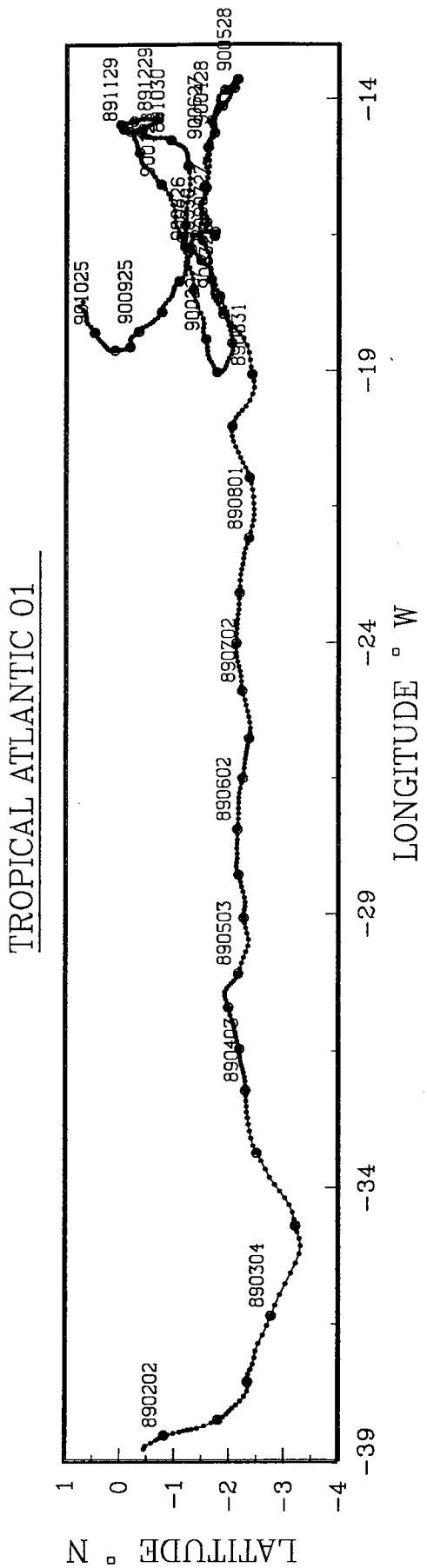
TROPICAL ATLANTIC 34



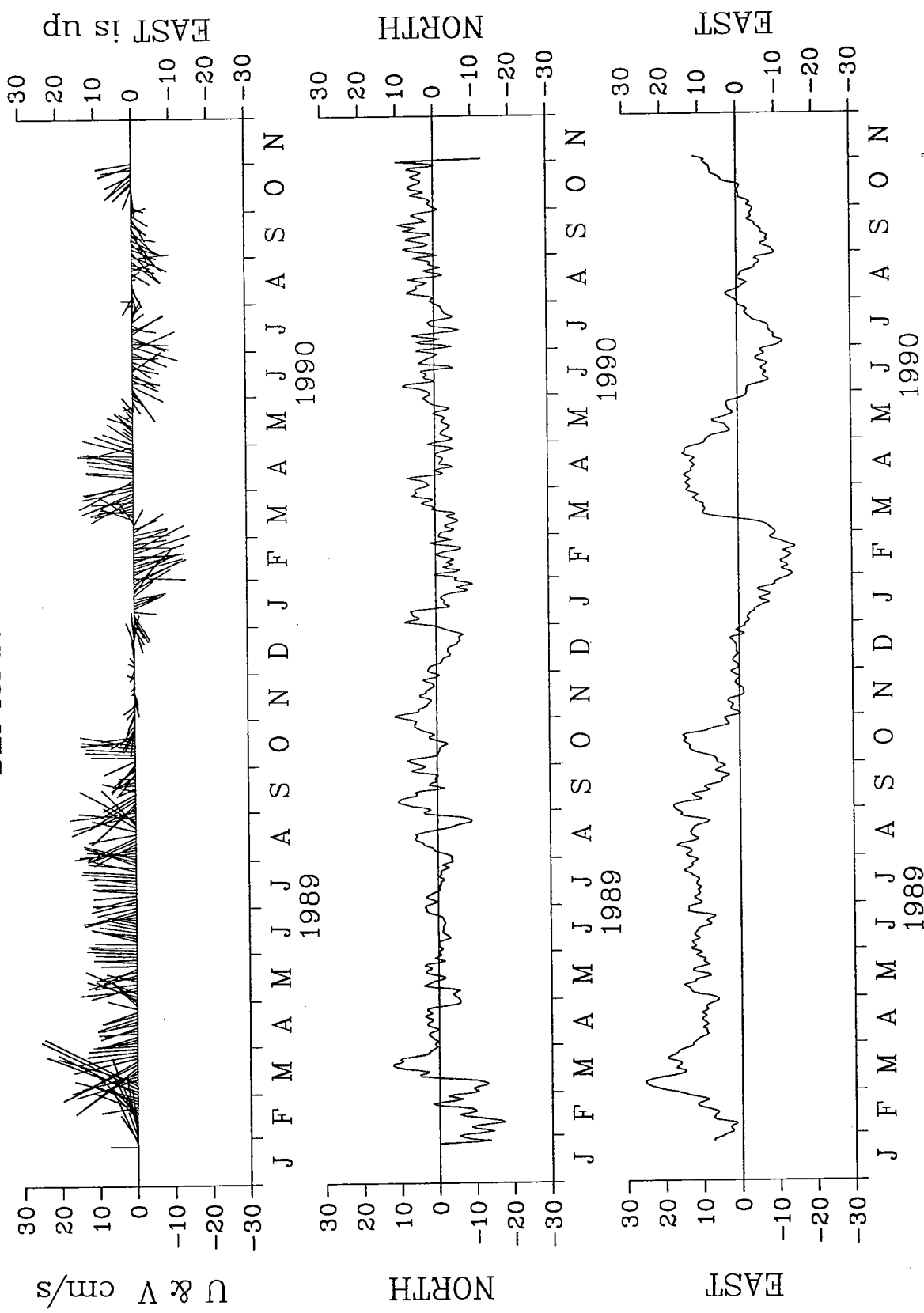
TROPICAL ATLANTIC 34
DEPTH 800 m.

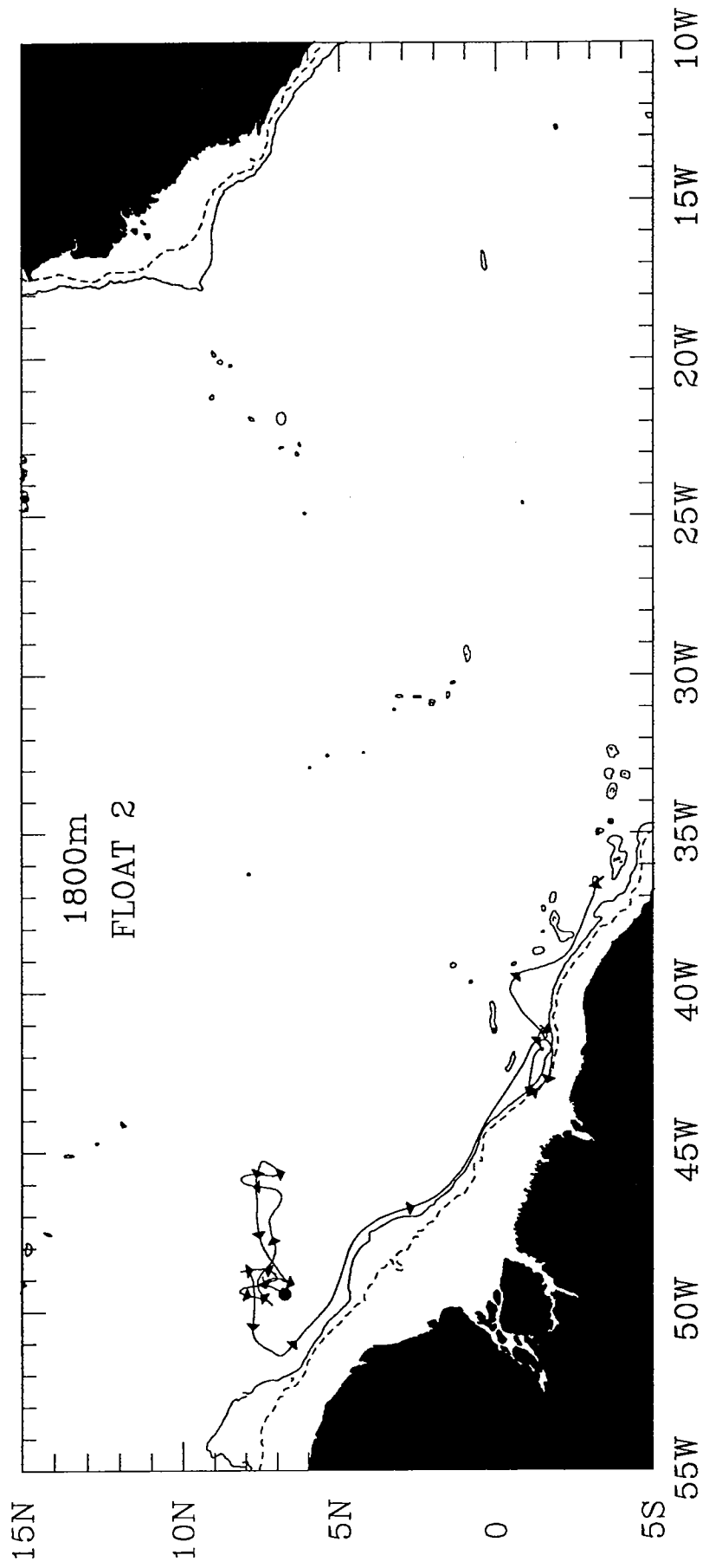




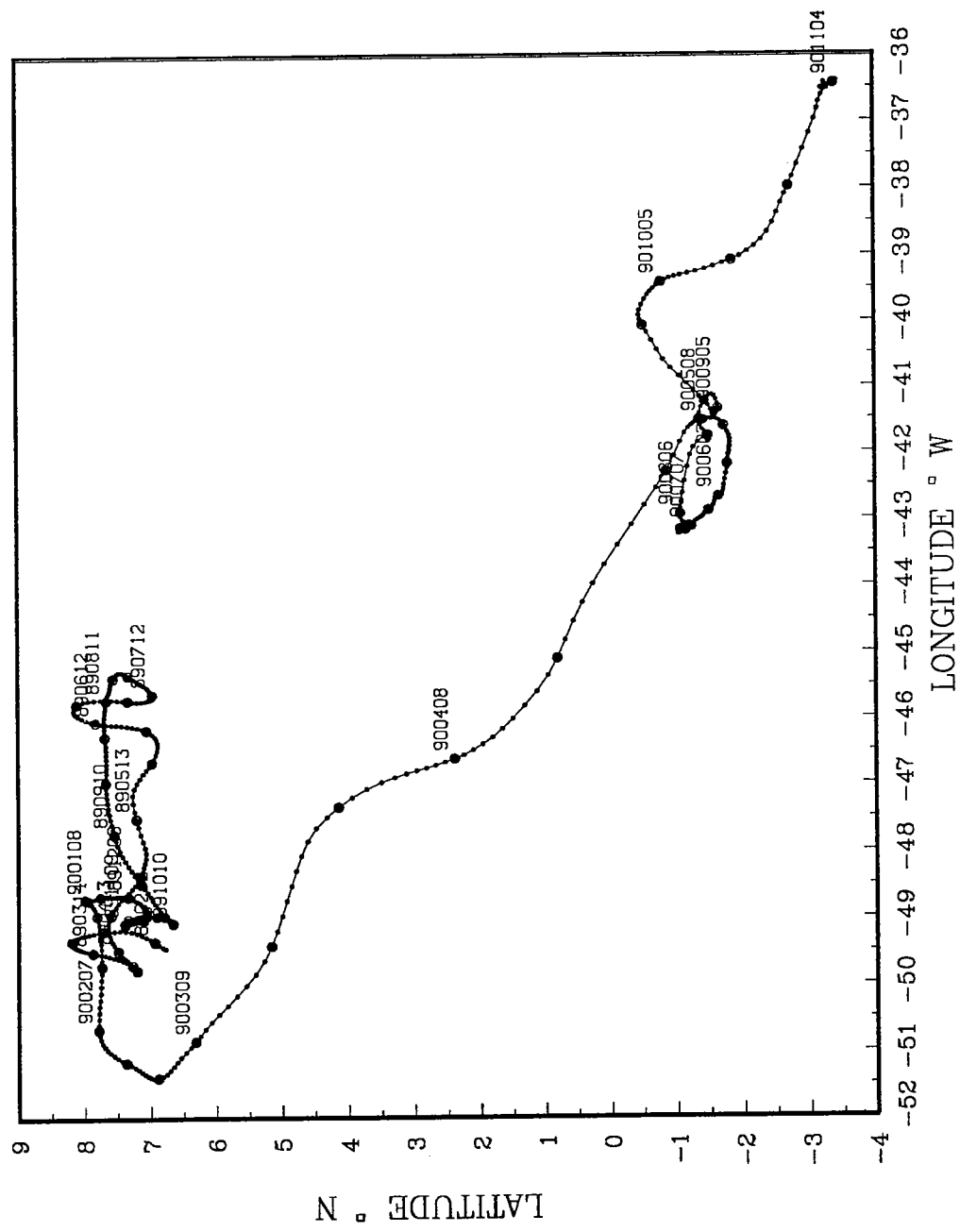


TROPICAL ATLANTIC 01
DEPTH 1800 m.

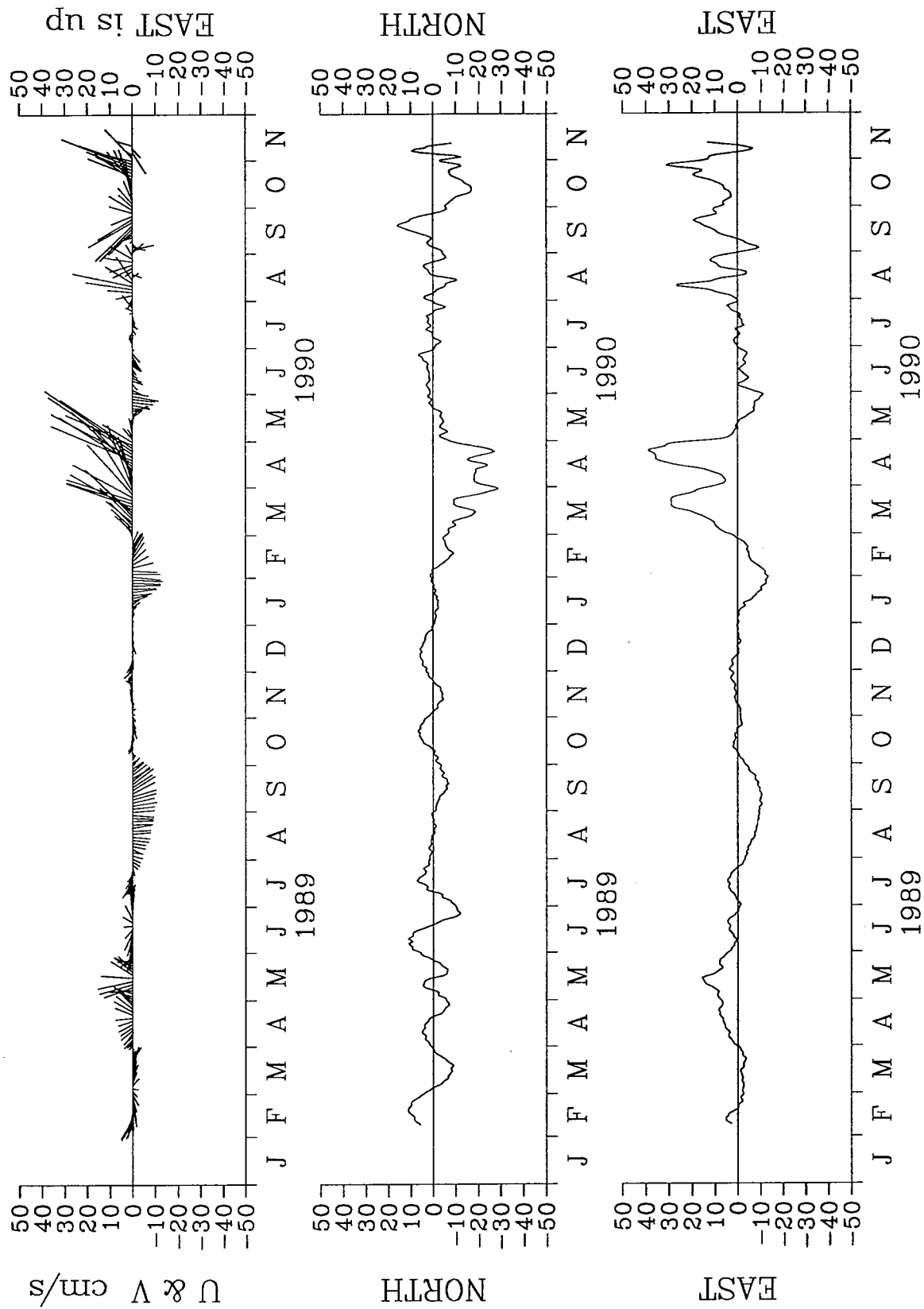


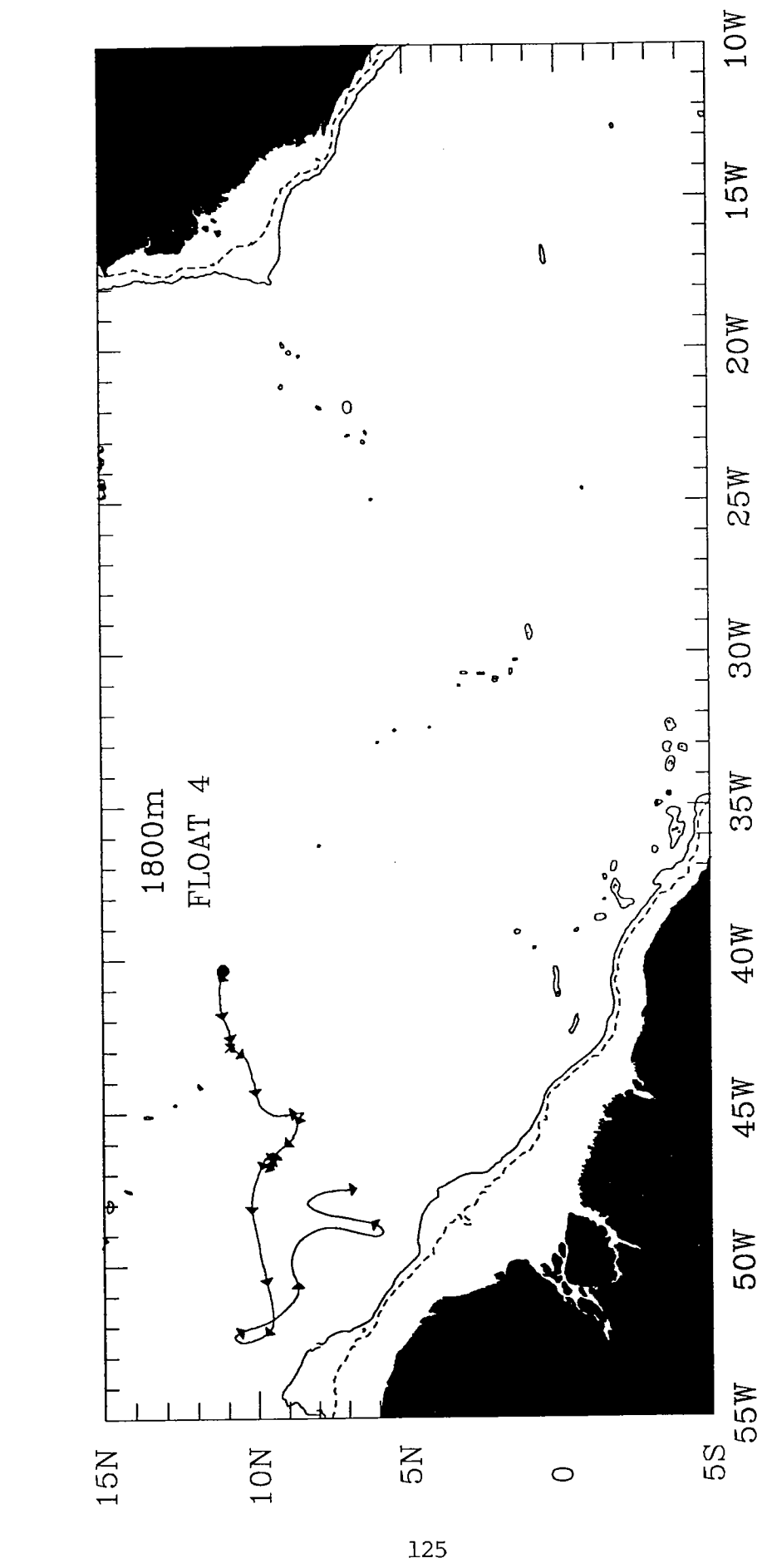


TROPICAL ATLANTIC 02

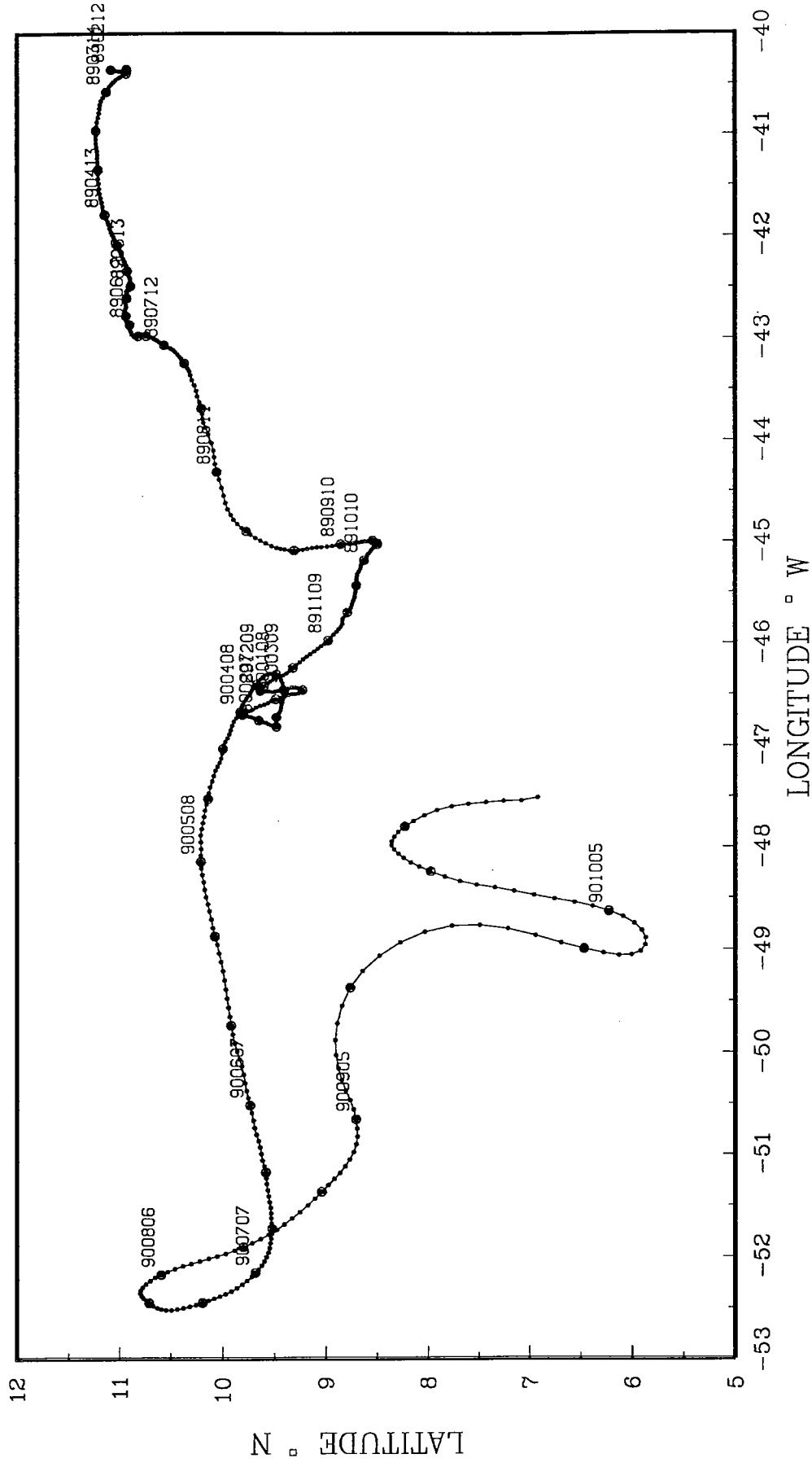


TROPICAL ATLANTIC 02
DEPTH 1800 m.

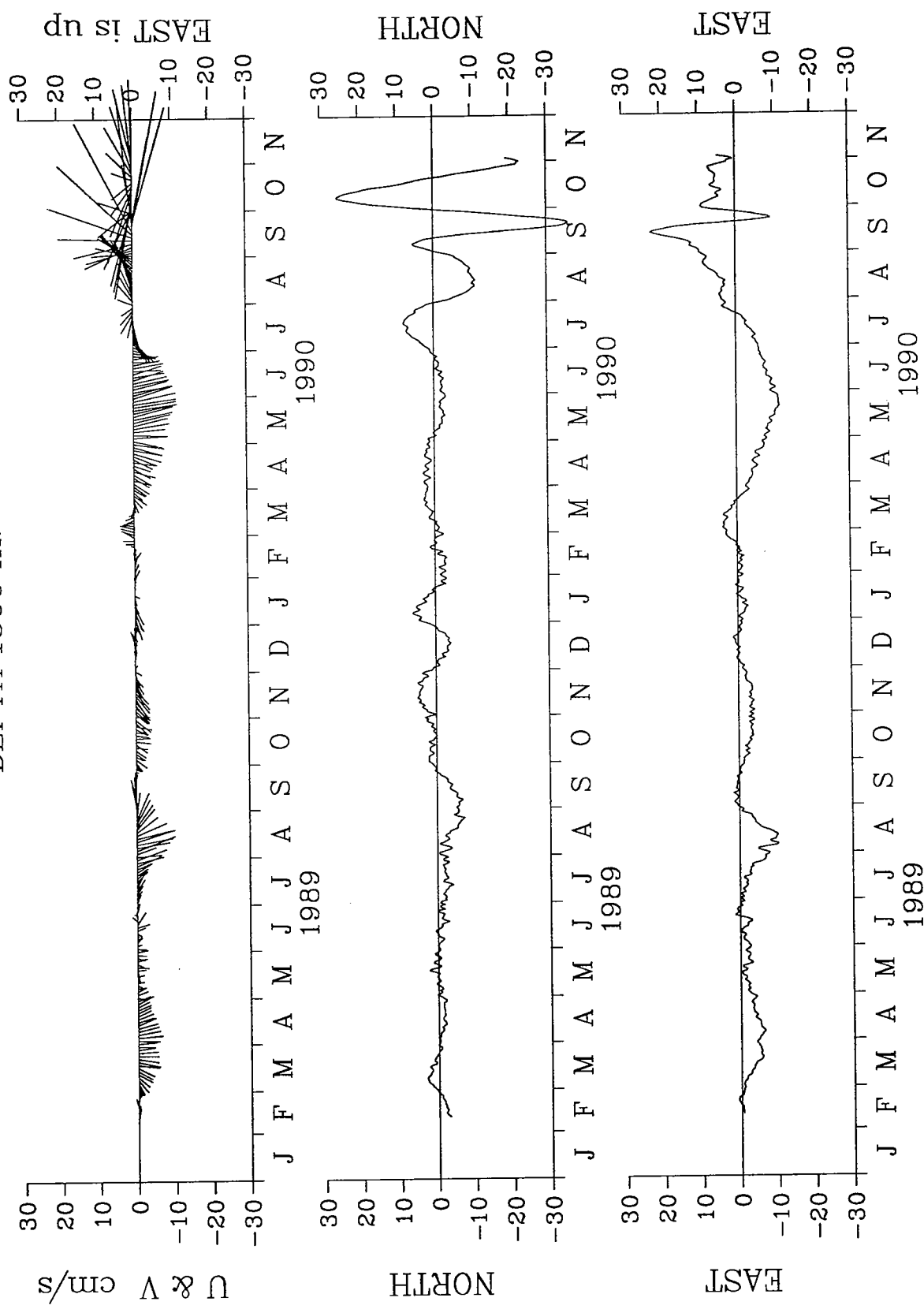


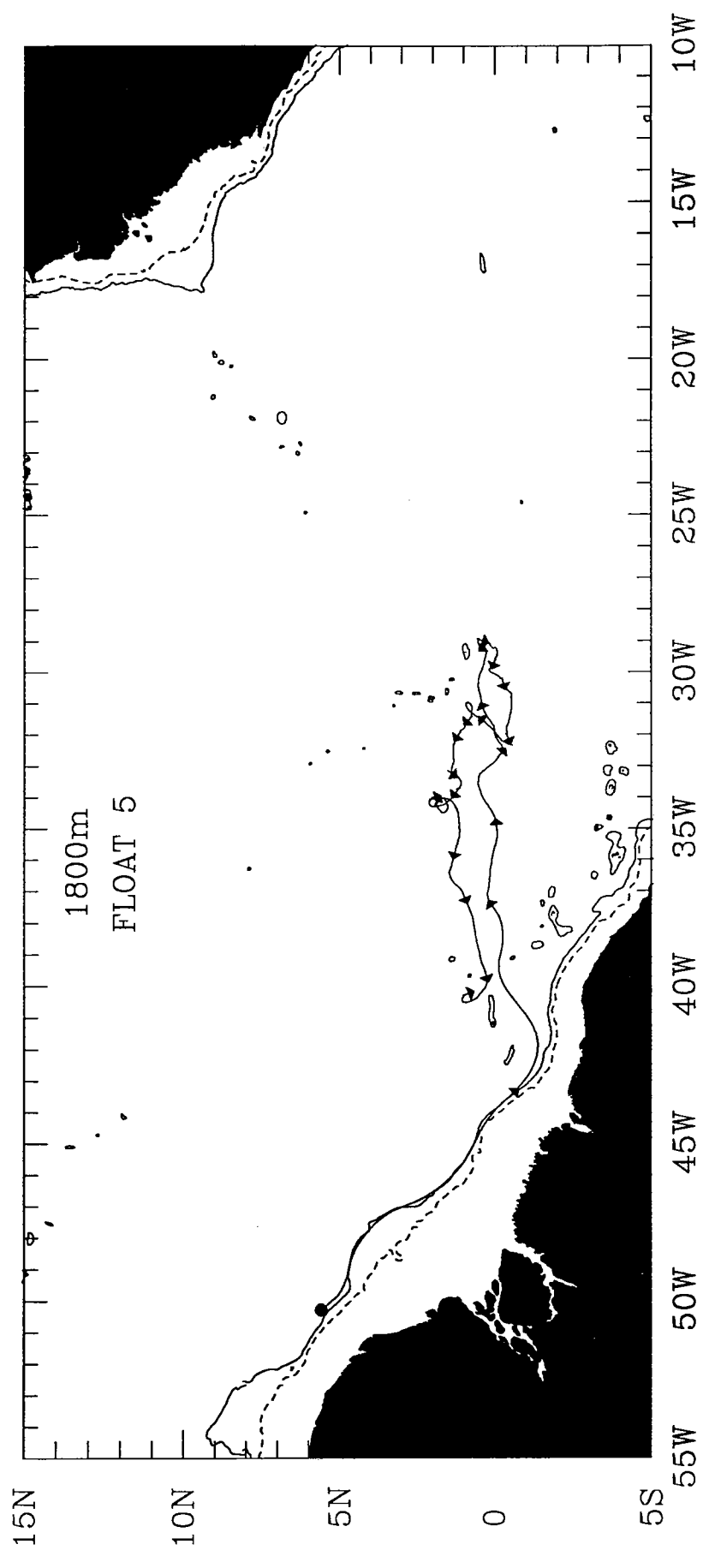


TROPICAL ATLANTIC 04

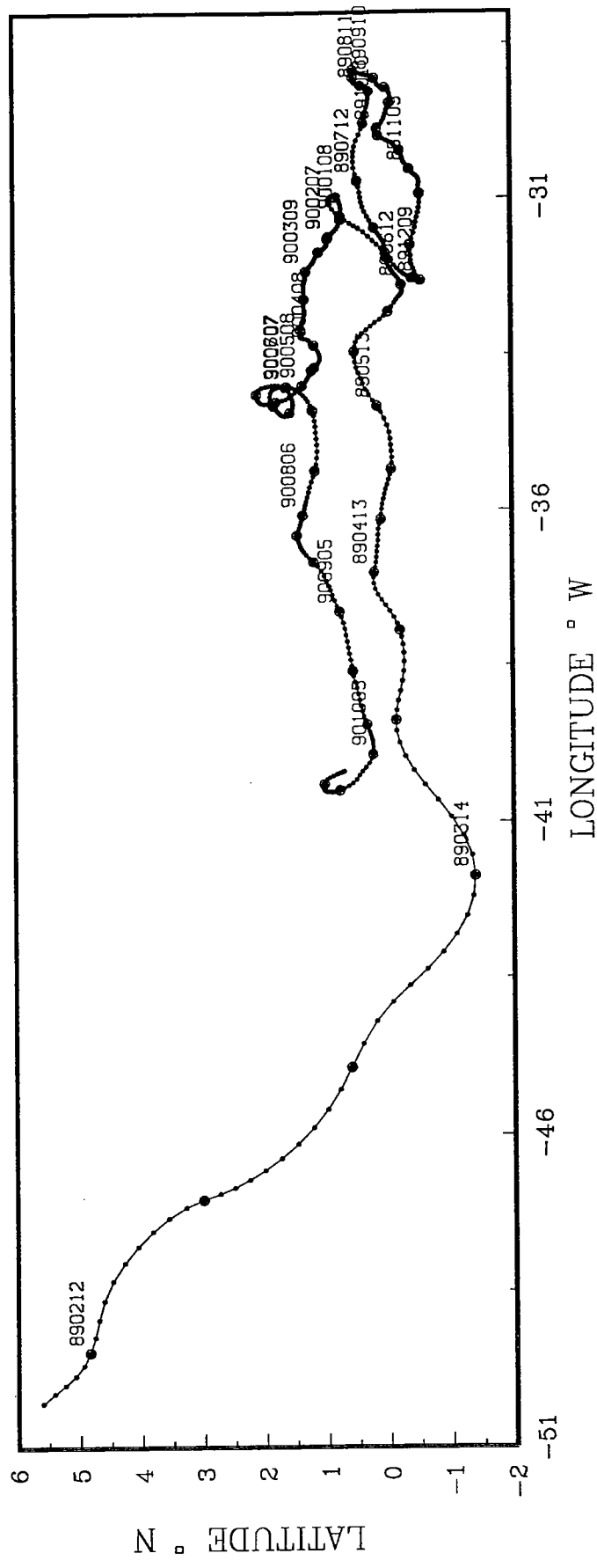


TROPICAL ATLANTIC 04
DEPTH 1800 m.

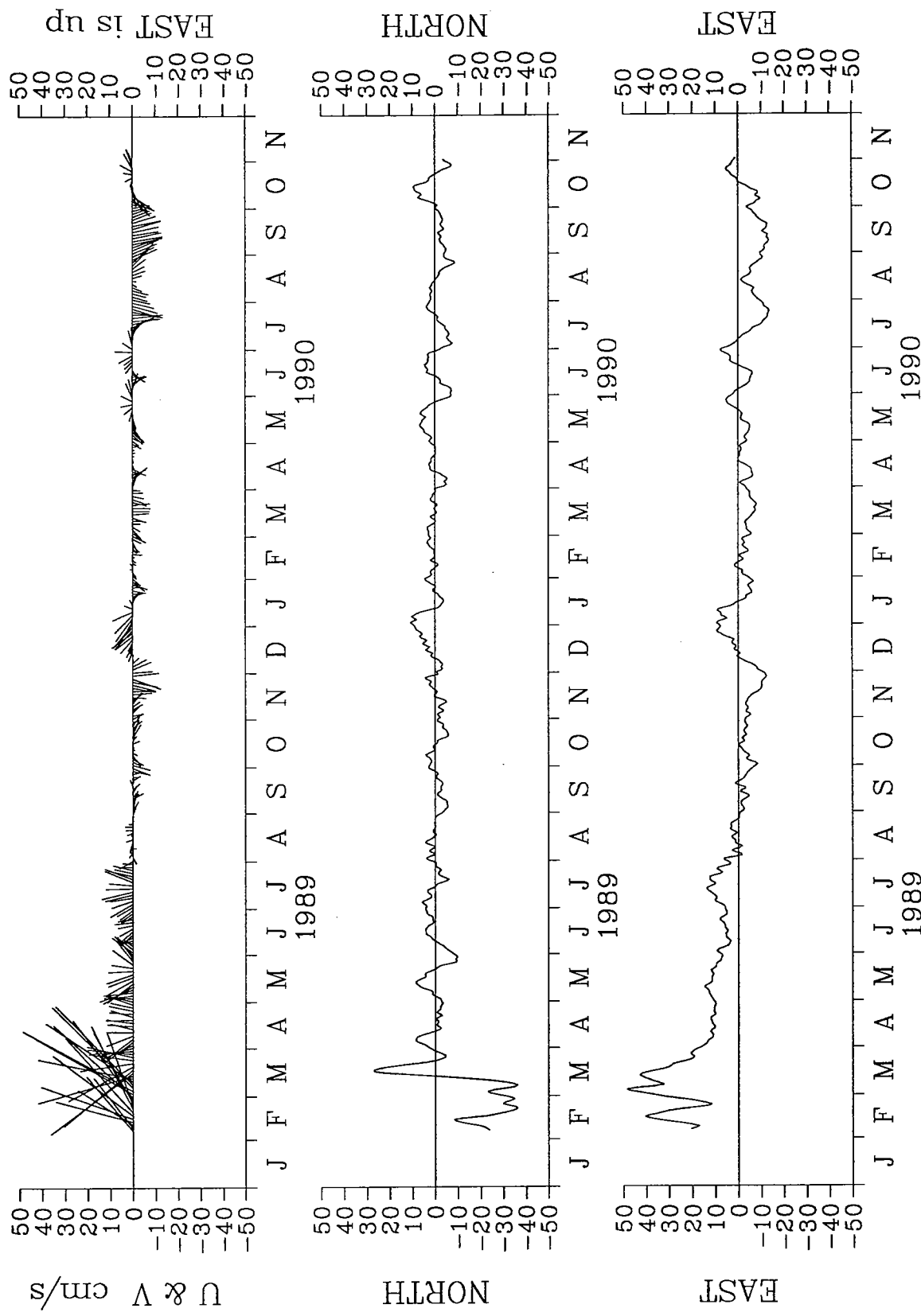


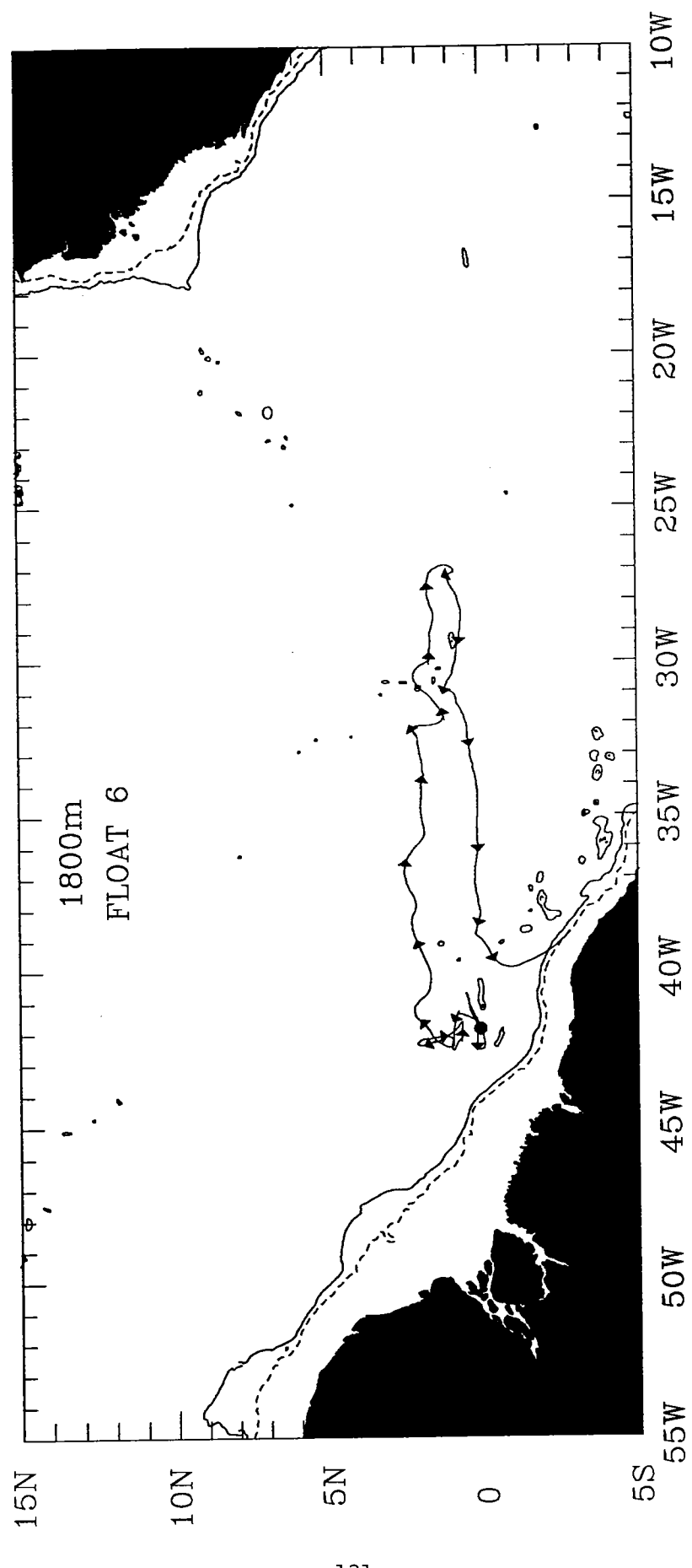


TROPICAL ATLANTIC 05

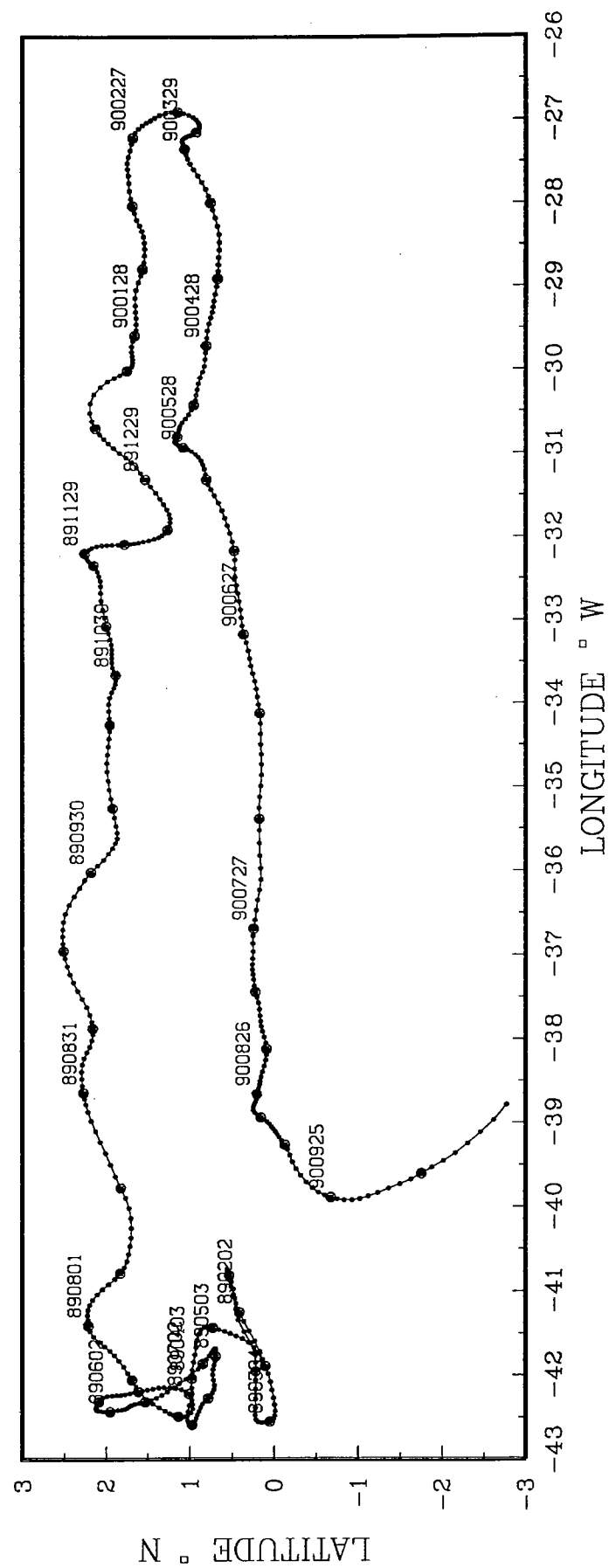


TROPICAL ATLANTIC 05
DEPTH 1800 m.

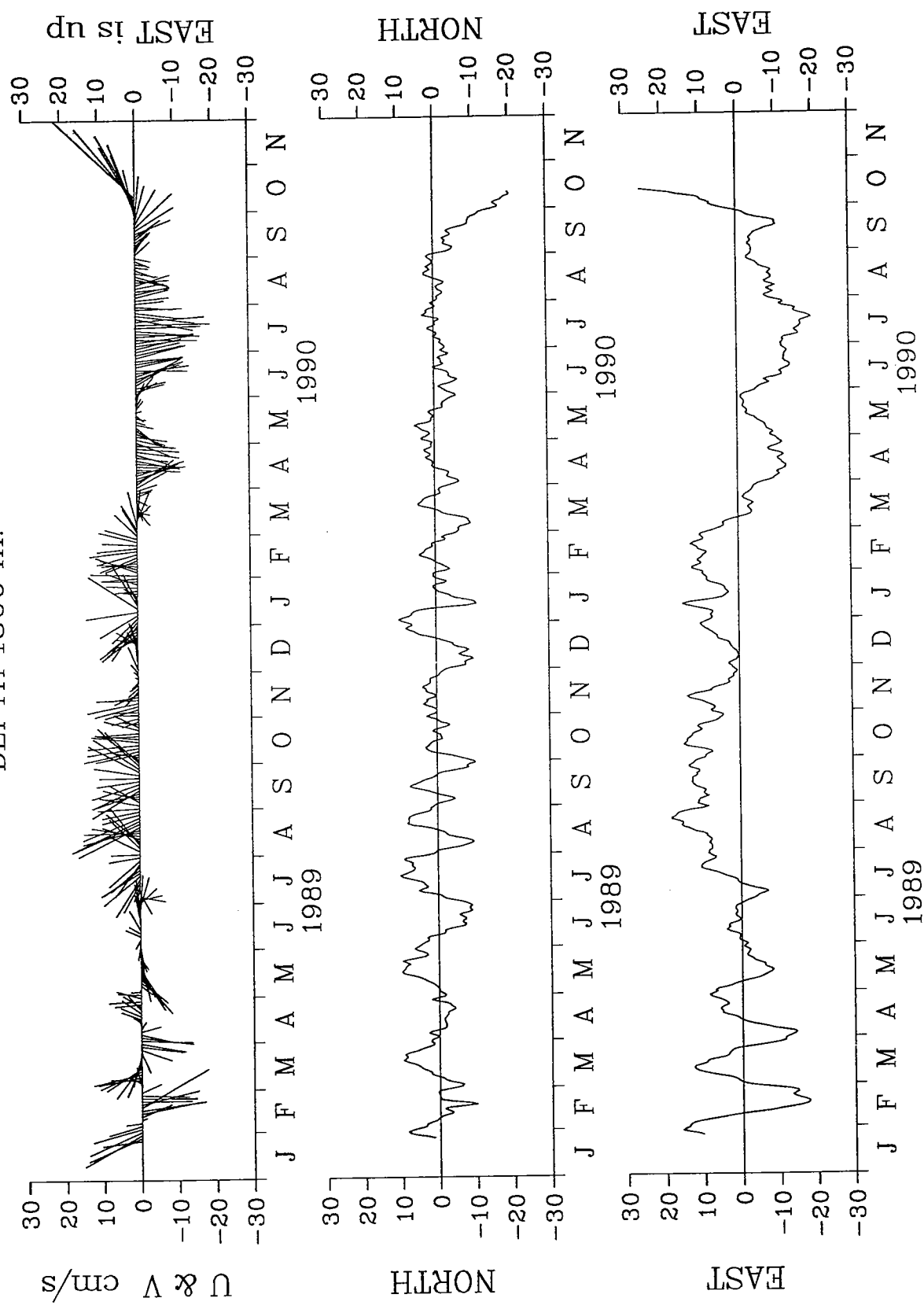


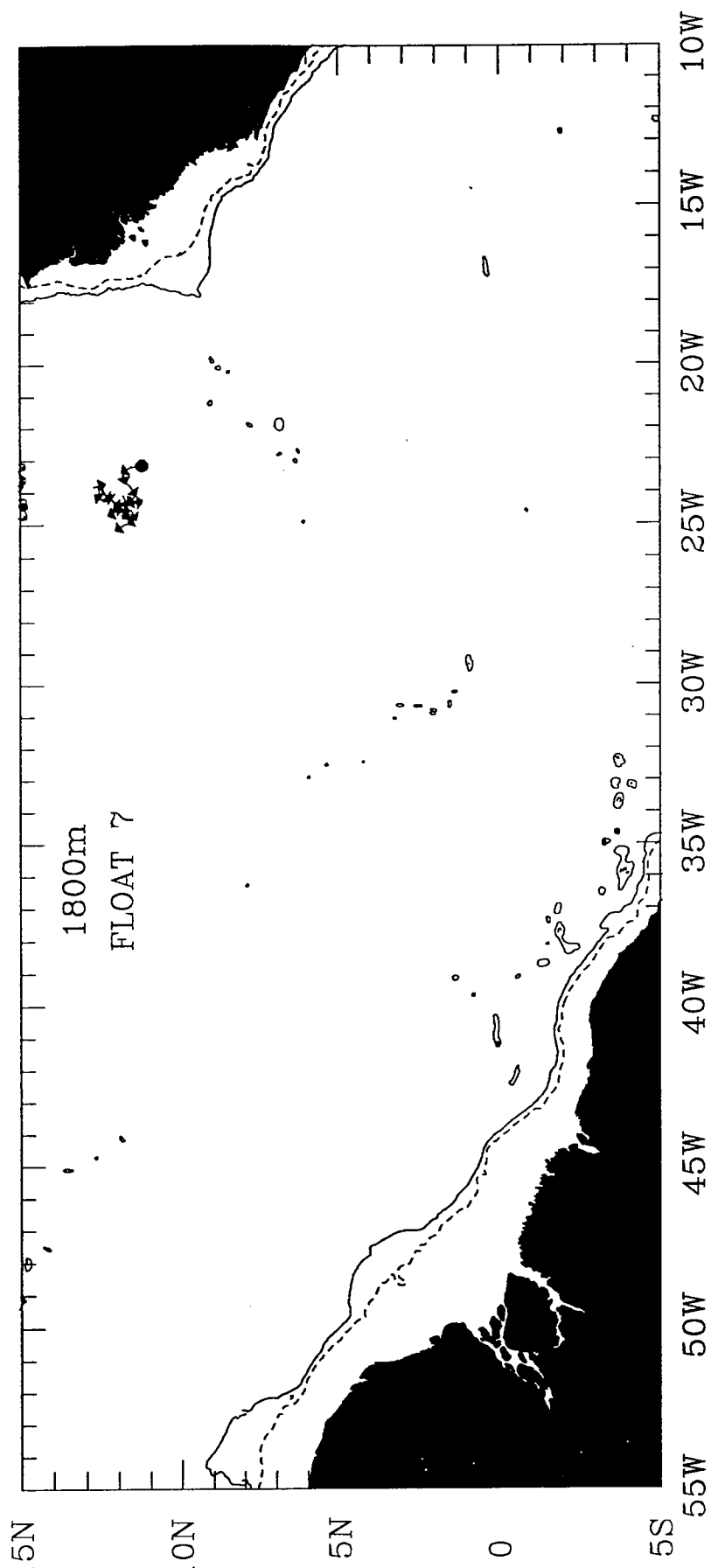


TROPICAL ATLANTIC 06

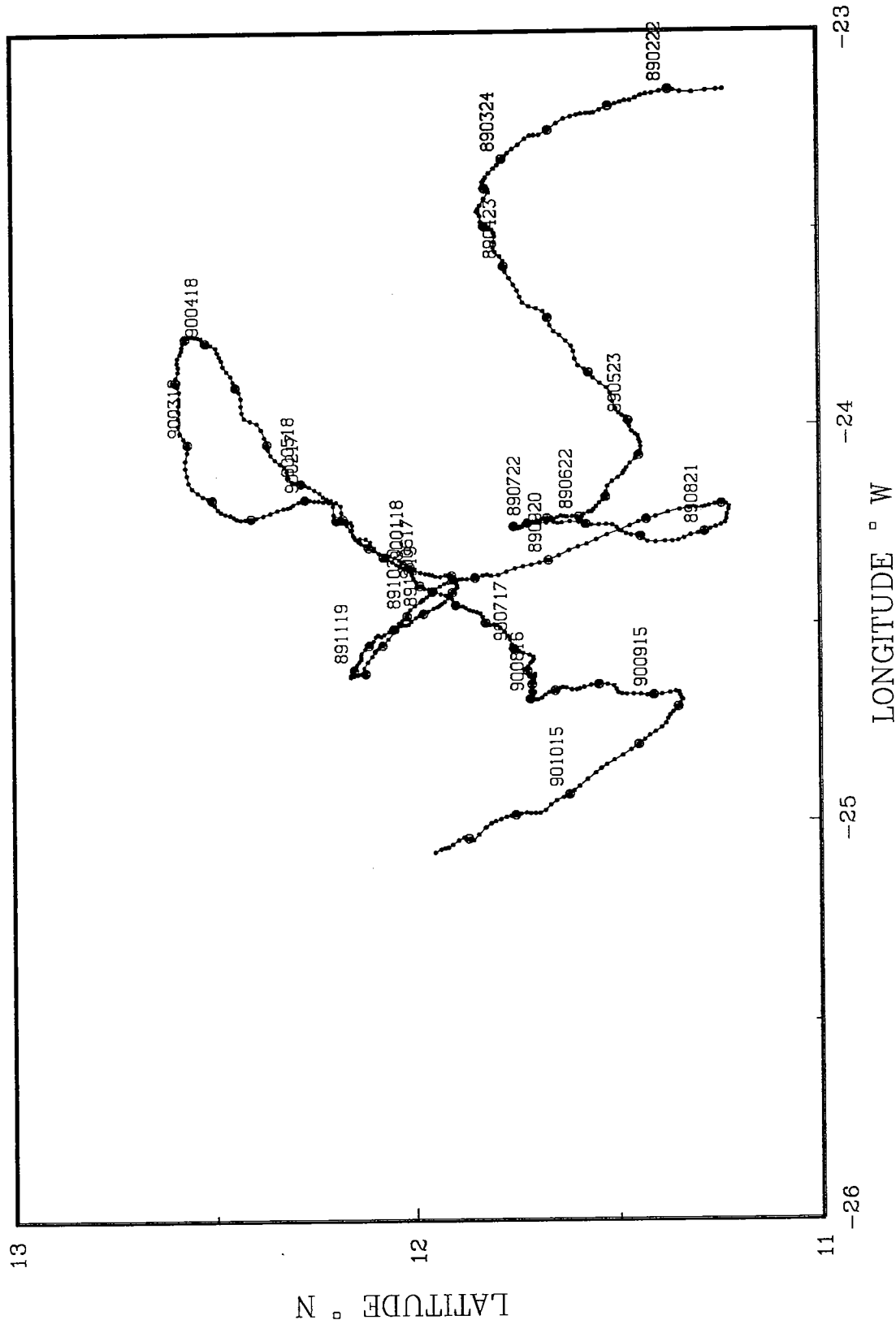


TROPICAL ATLANTIC 06
DEPTH 1800 m.

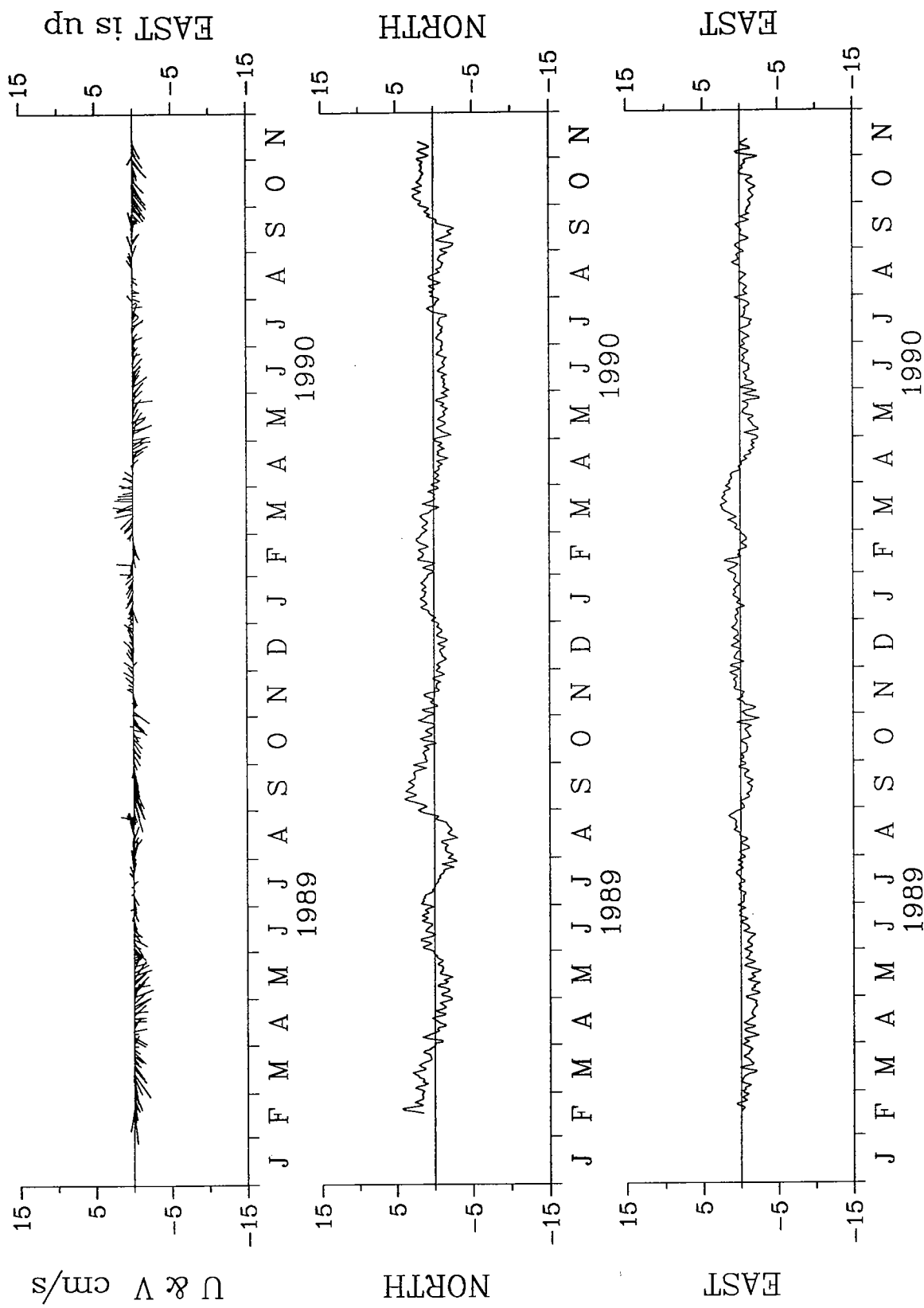


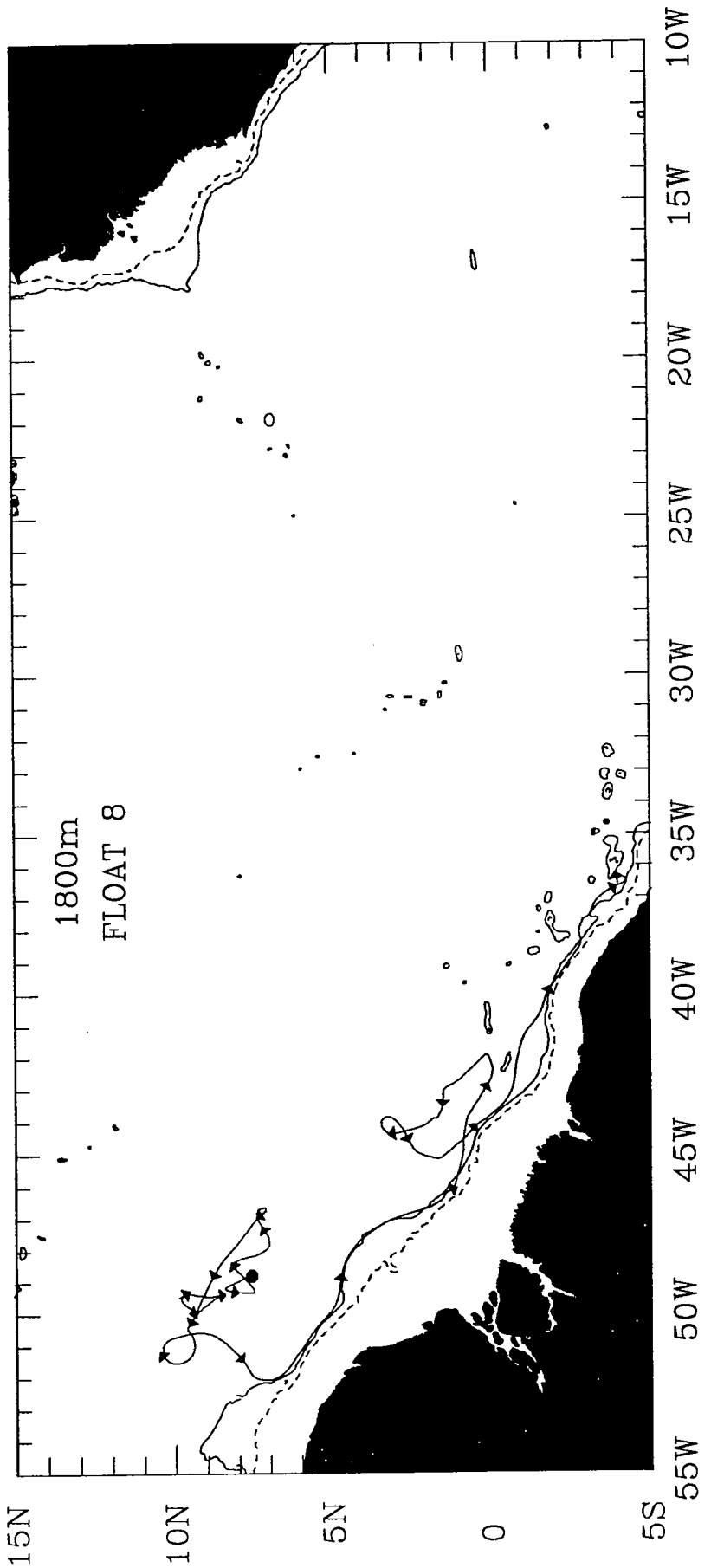


TROPICAL ATLANTIC 07

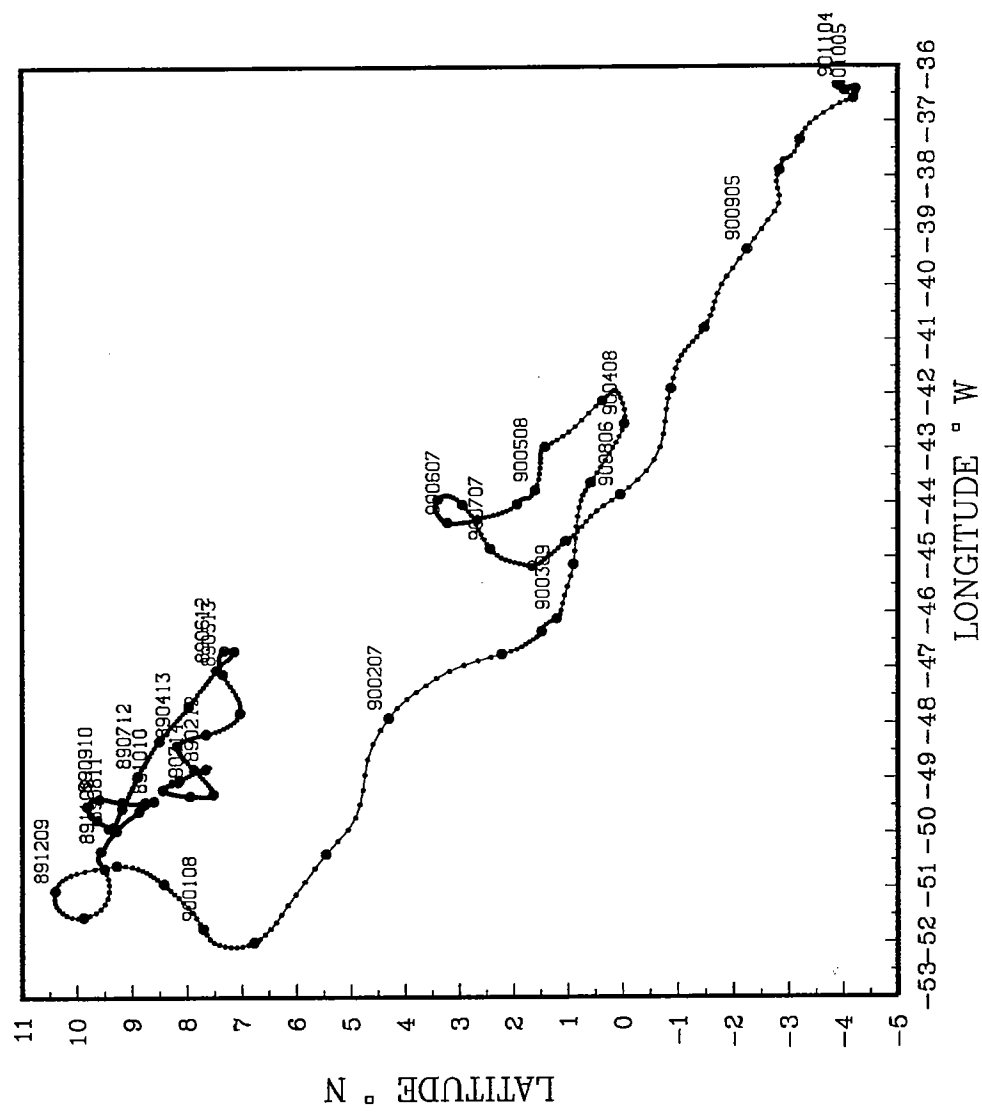


TROPICAL ATLANTIC 07
DEPTH 1800 m.

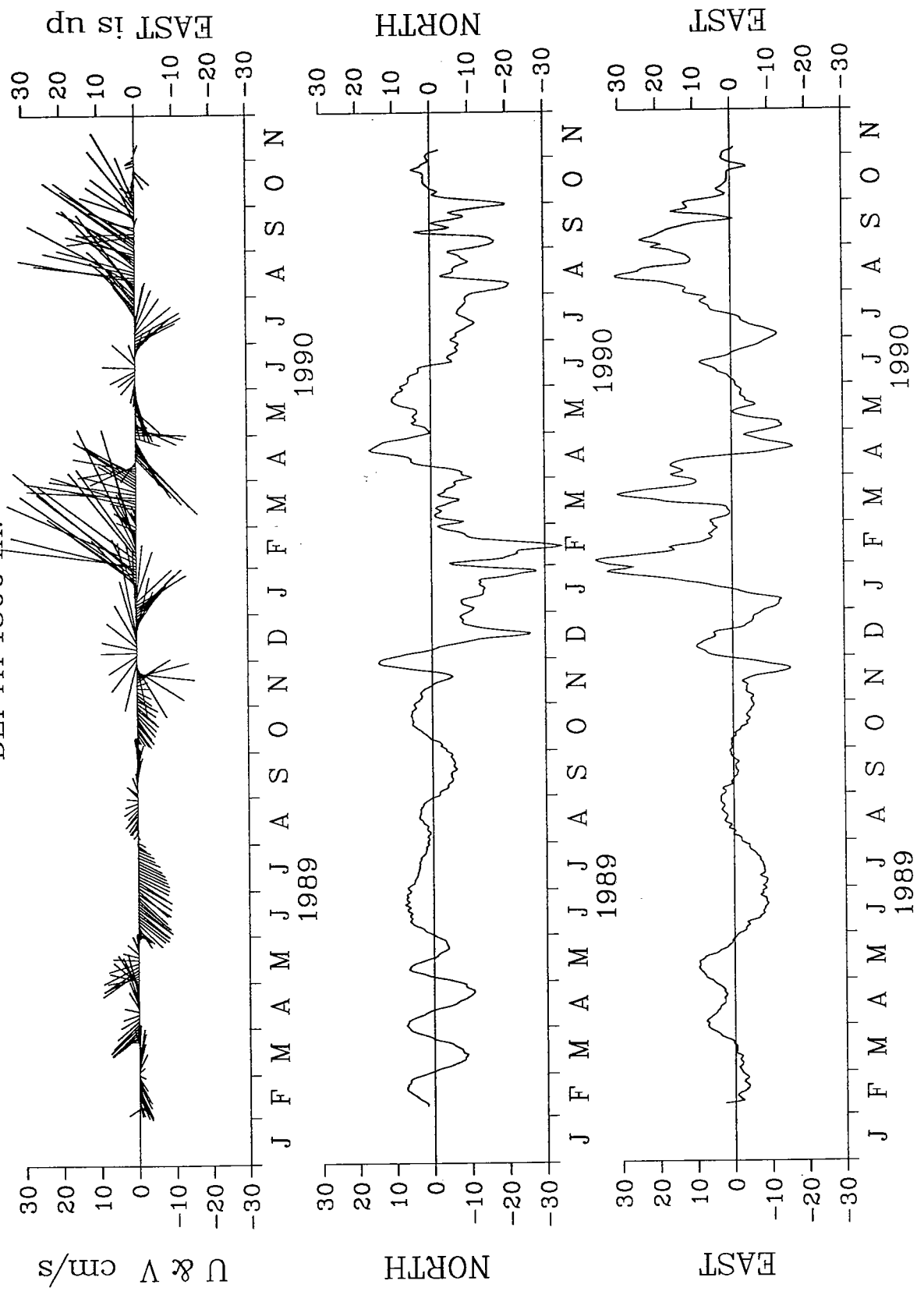


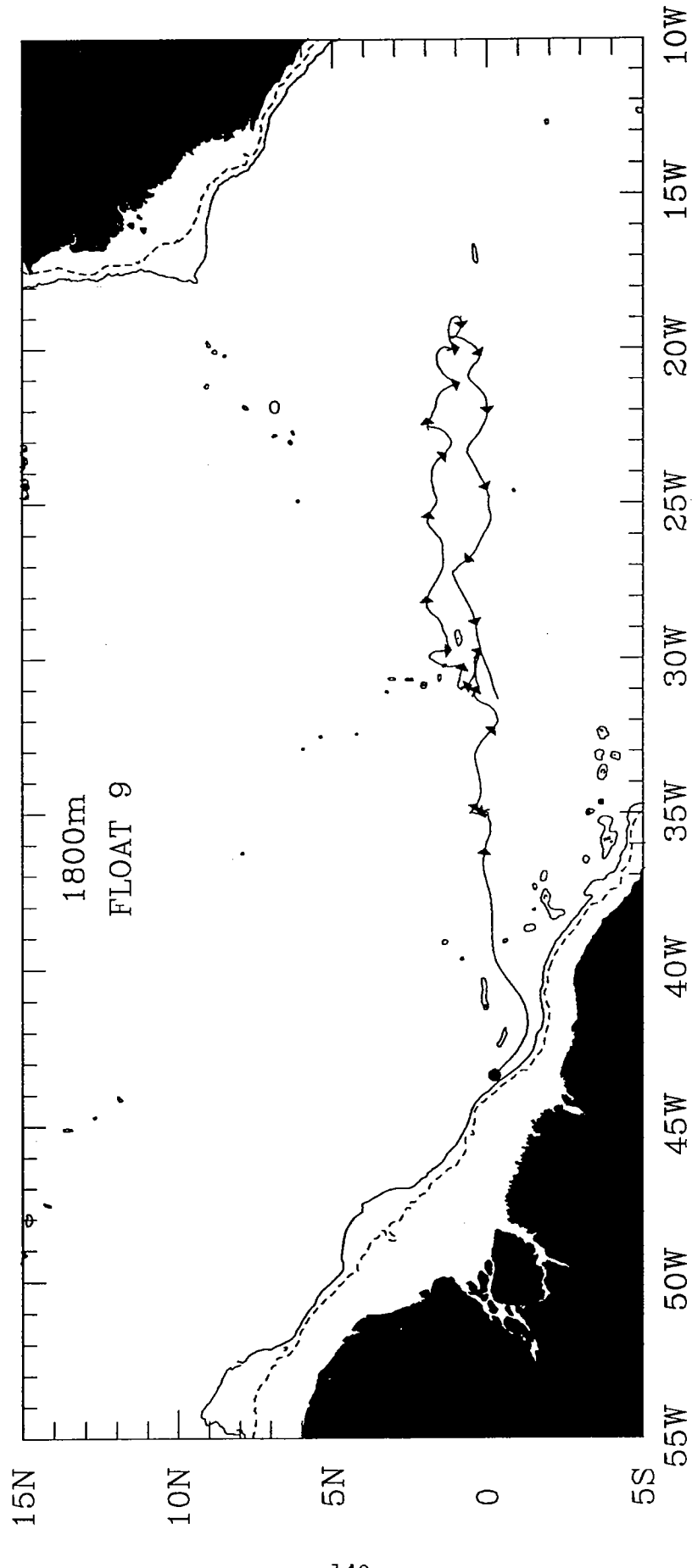


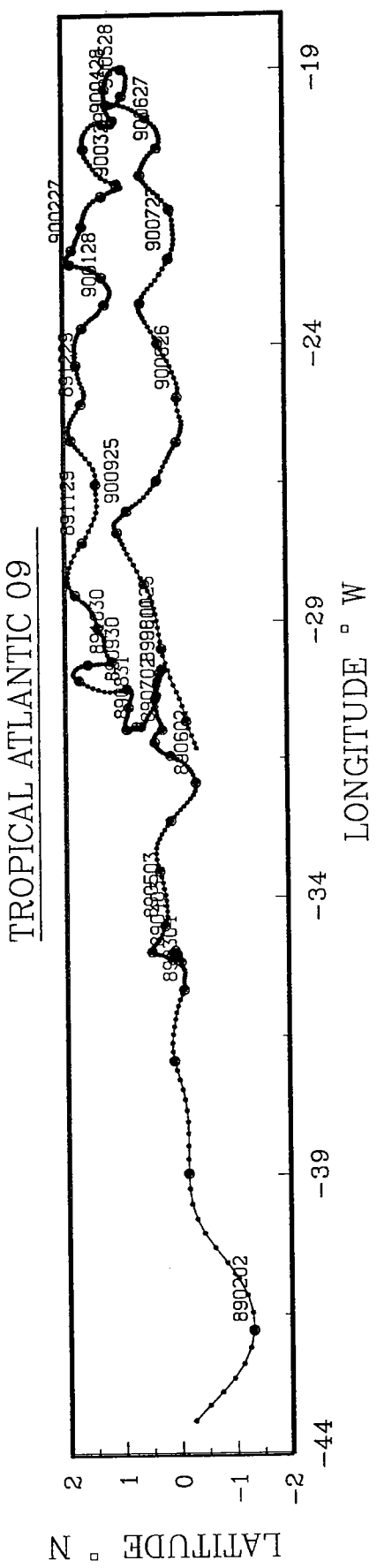
TROPICAL ATLANTIC 08



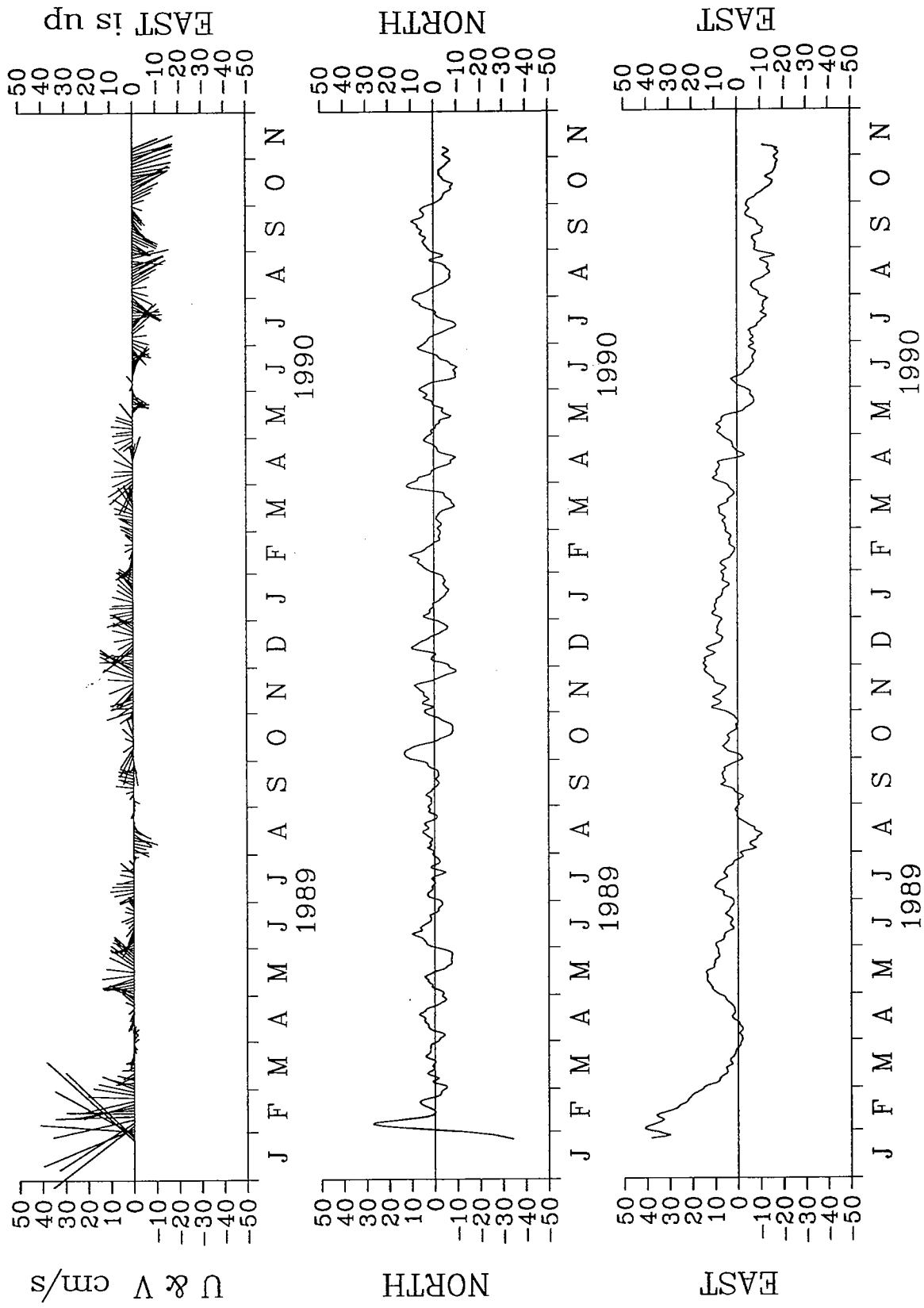
TROPICAL ATLANTIC 08
DEPTH 1800 m.

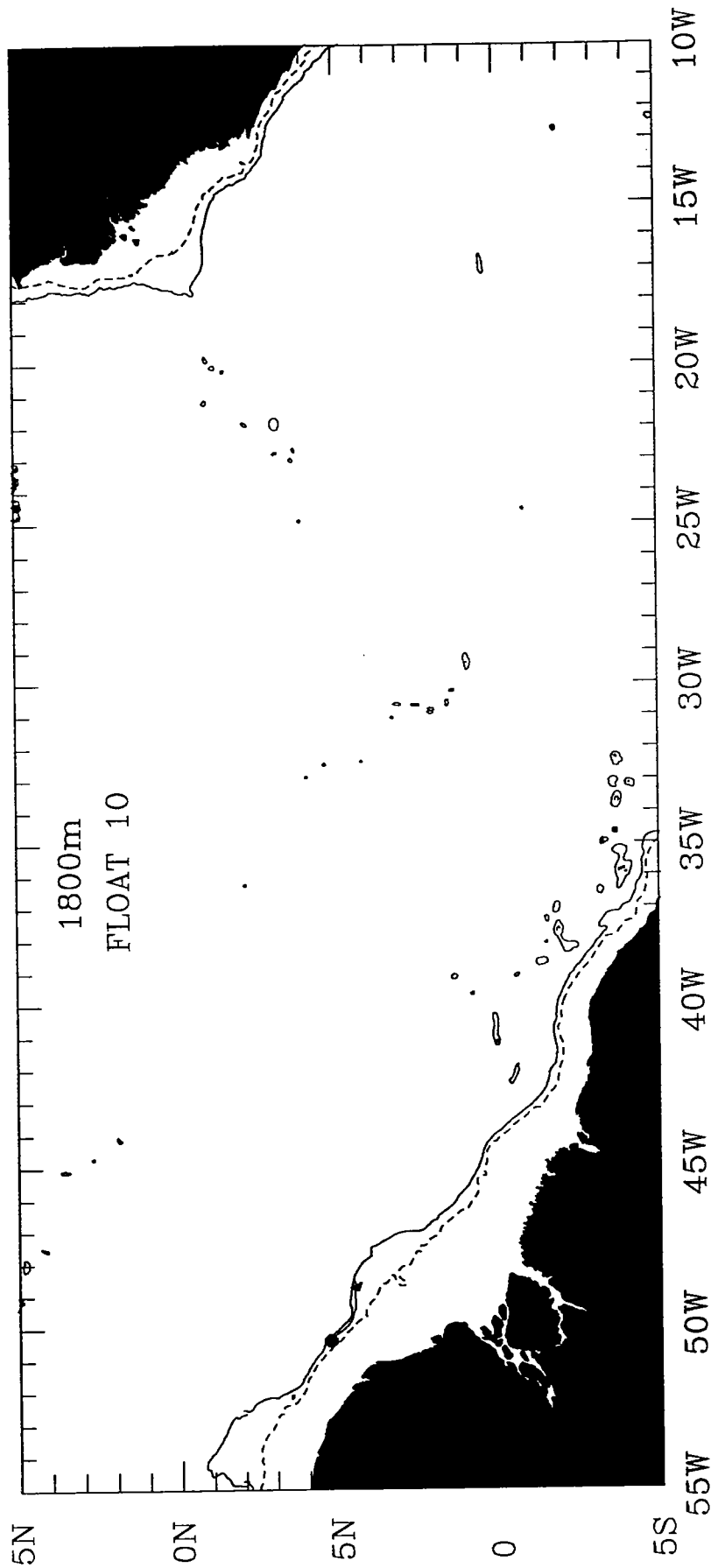




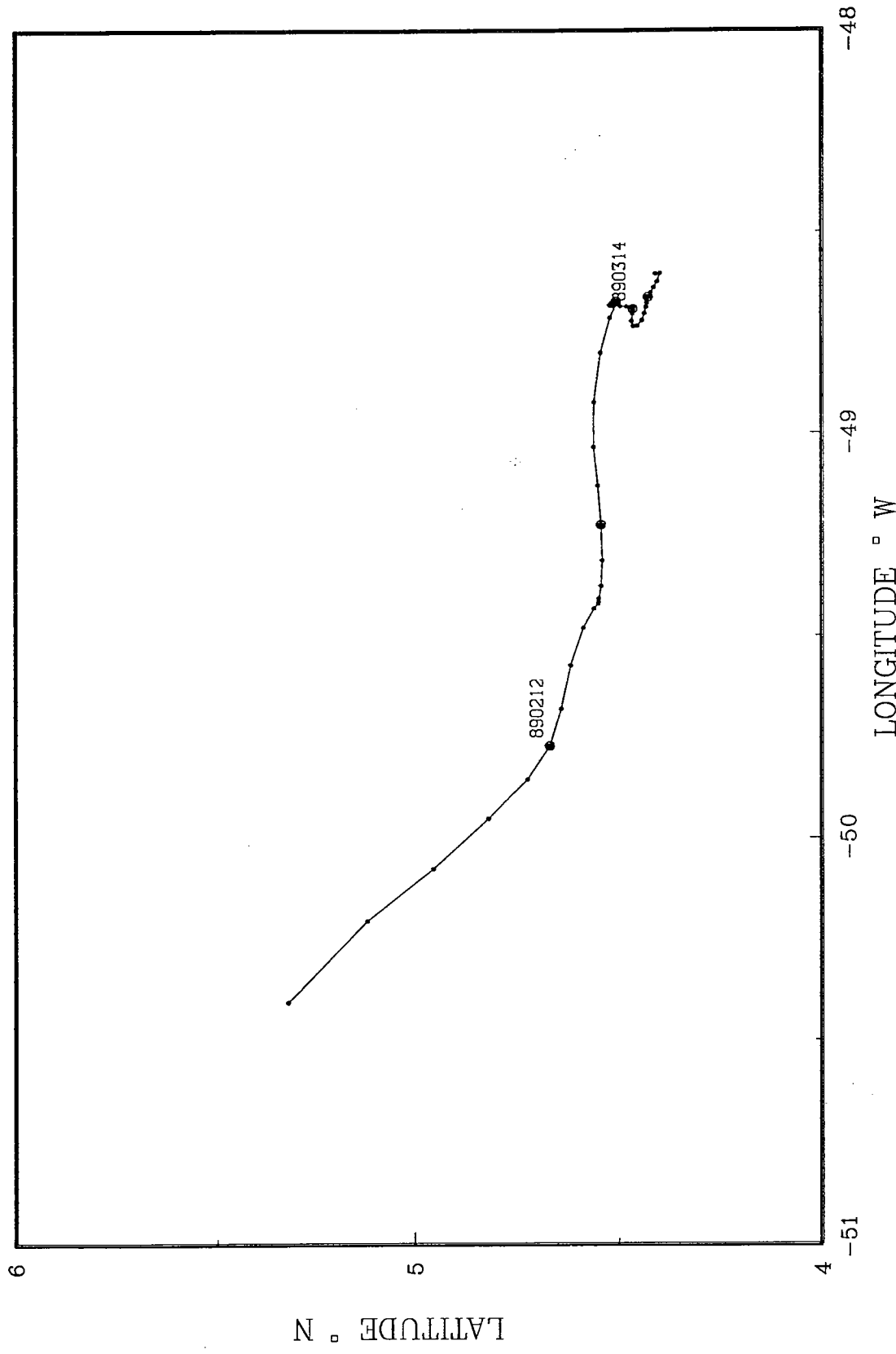


TROPICAL ATLANTIC 09
DEPTH 1800 m.

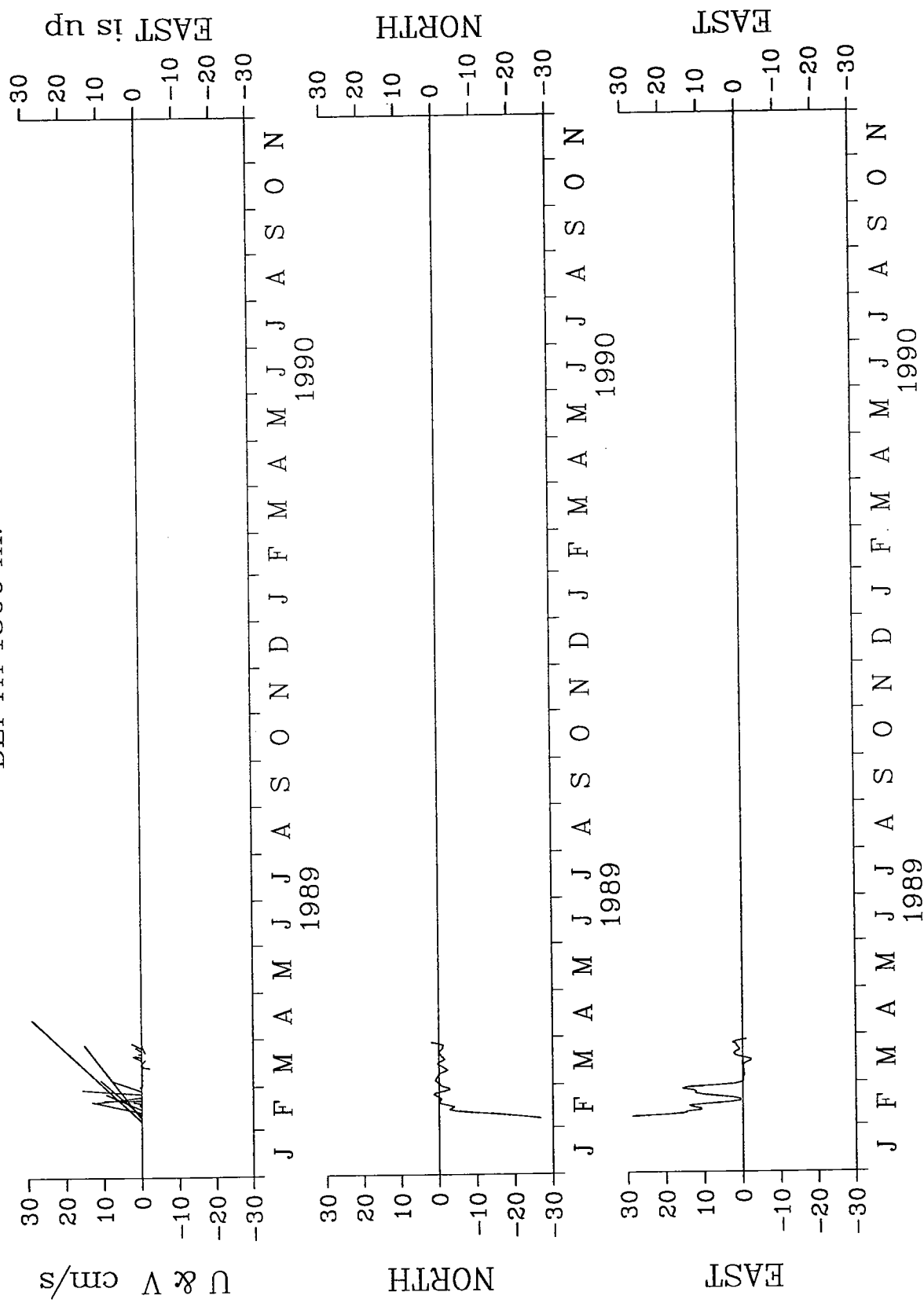


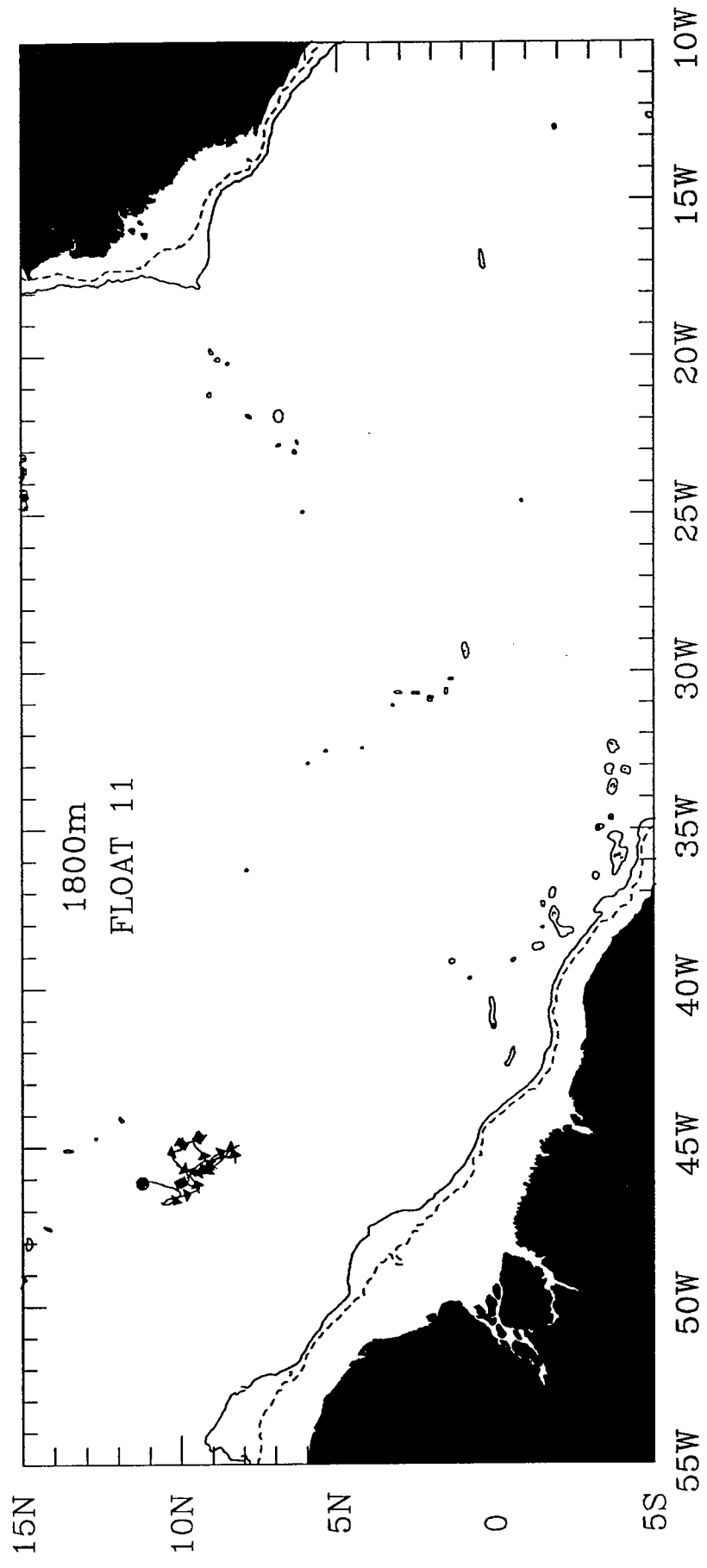


TROPICAL ATLANTIC 10

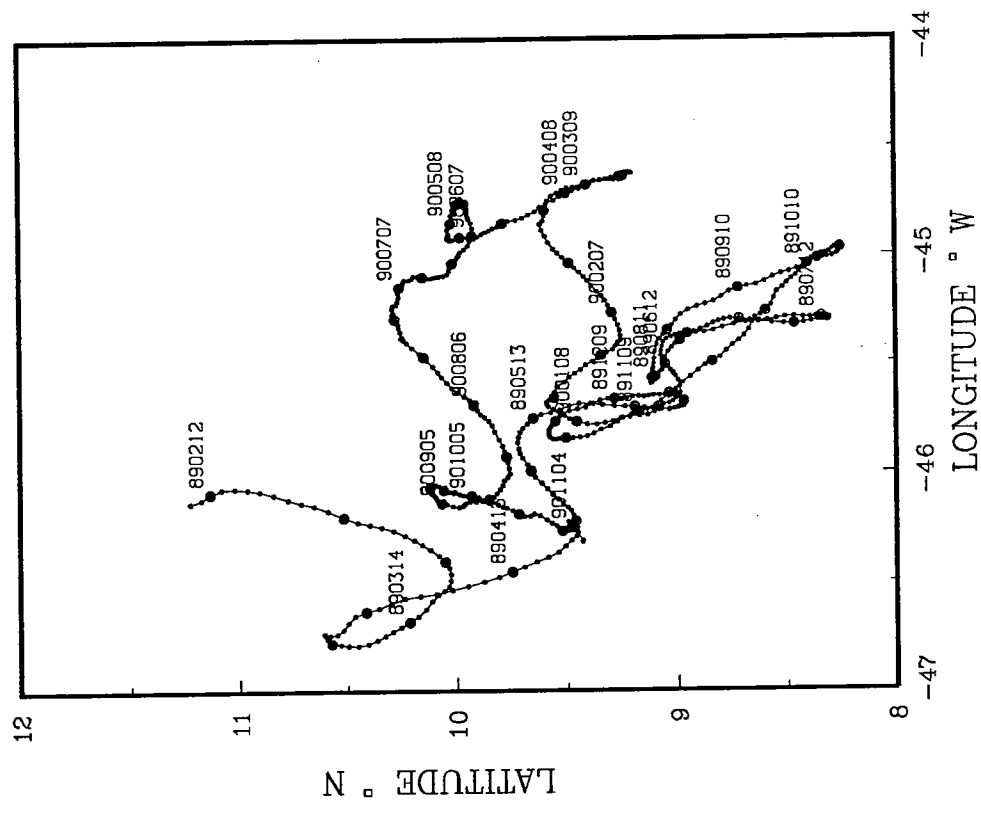


TROPICAL ATLANTIC 10
DEPTH 1800 m.

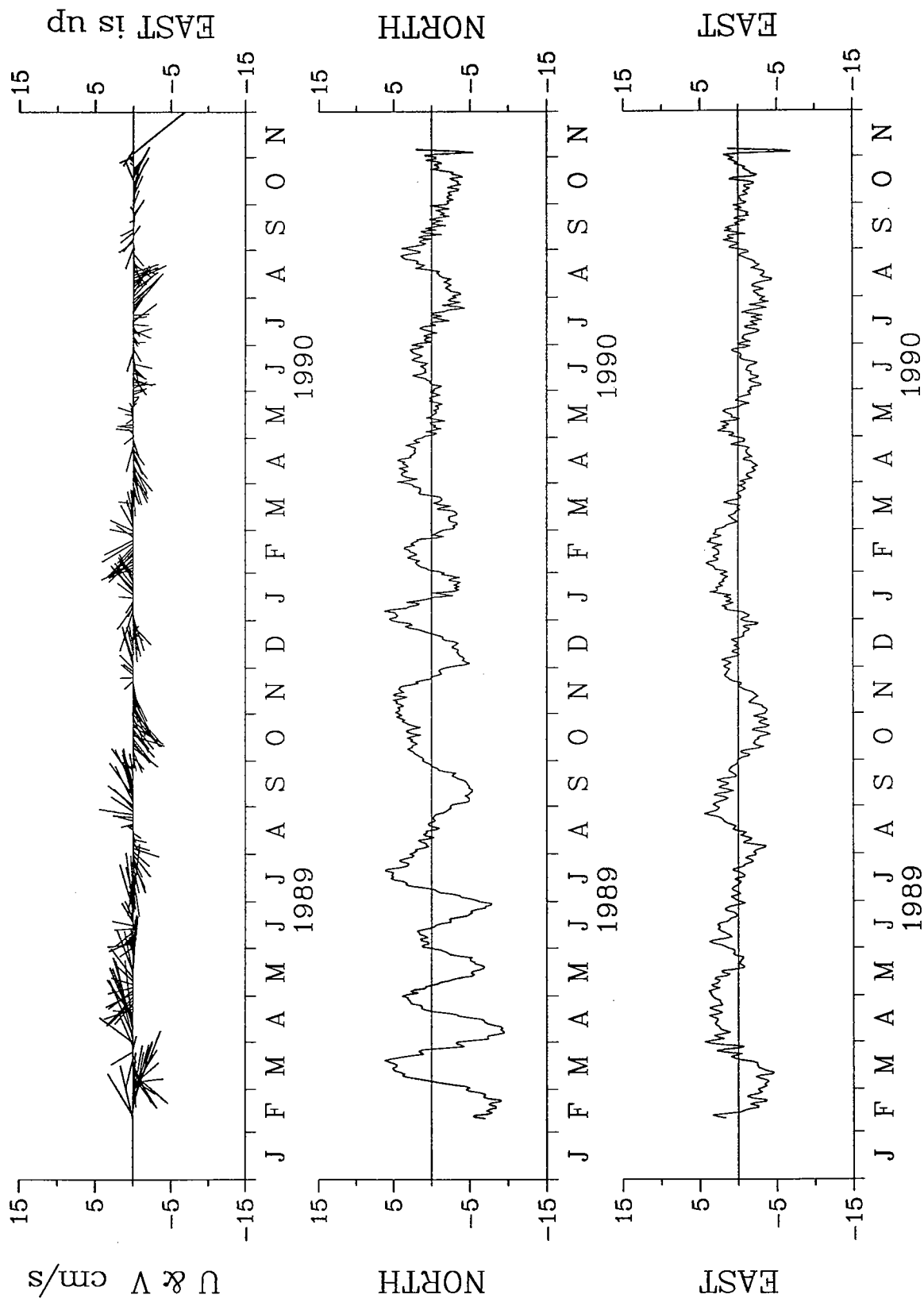


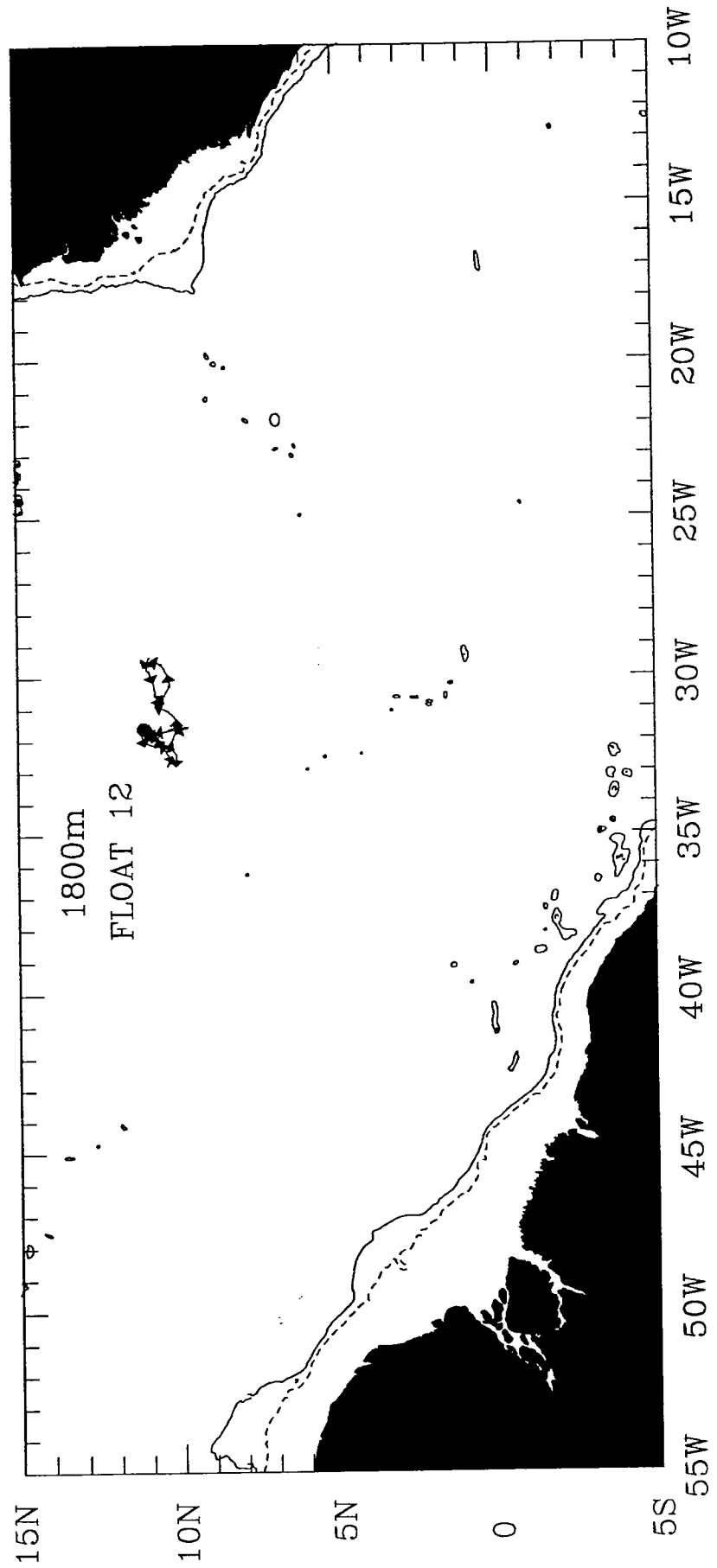


TROPICAL ATLANTIC 11

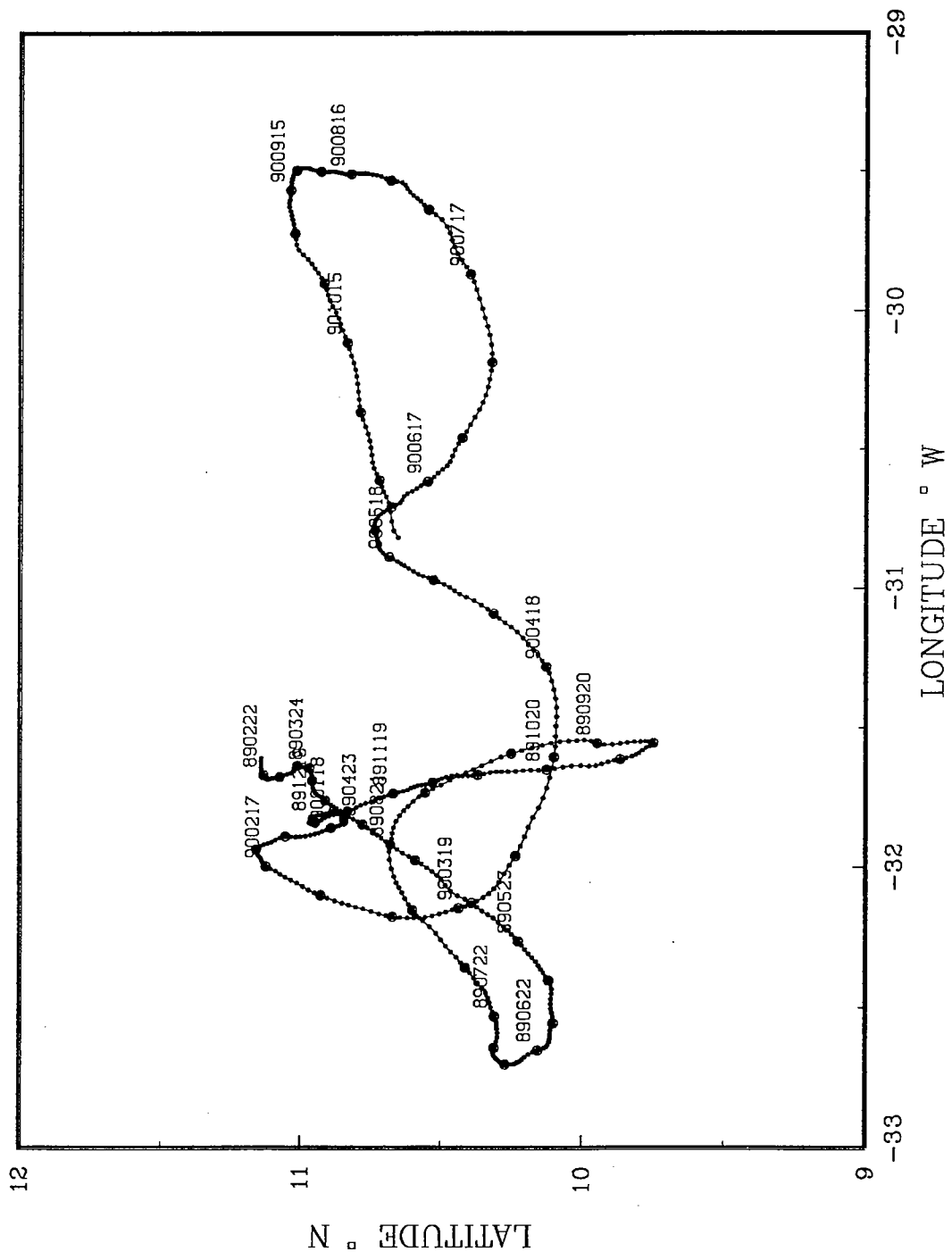


TROPICAL ATLANTIC 11
DEPTH 1800 m.

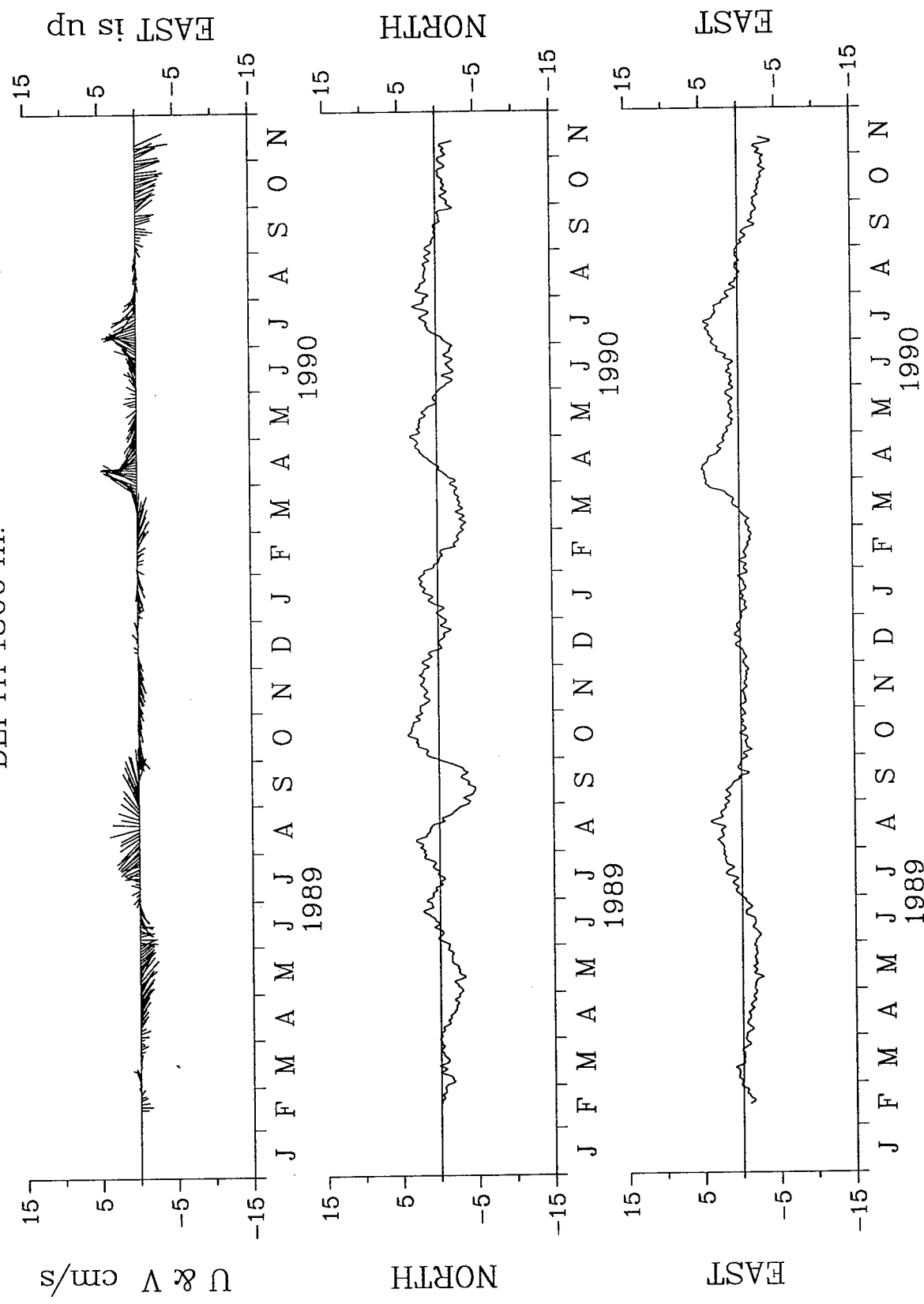


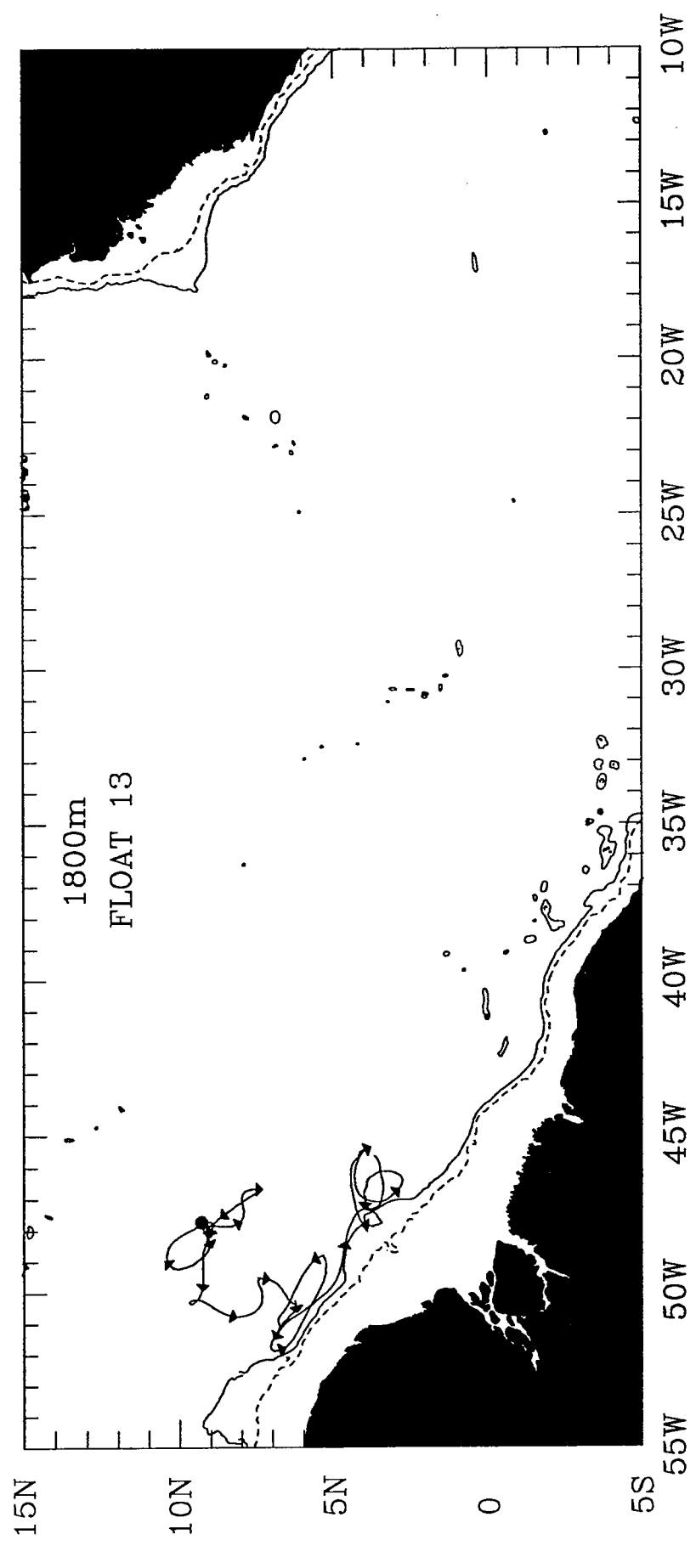


TROPICAL ATLANTIC 12

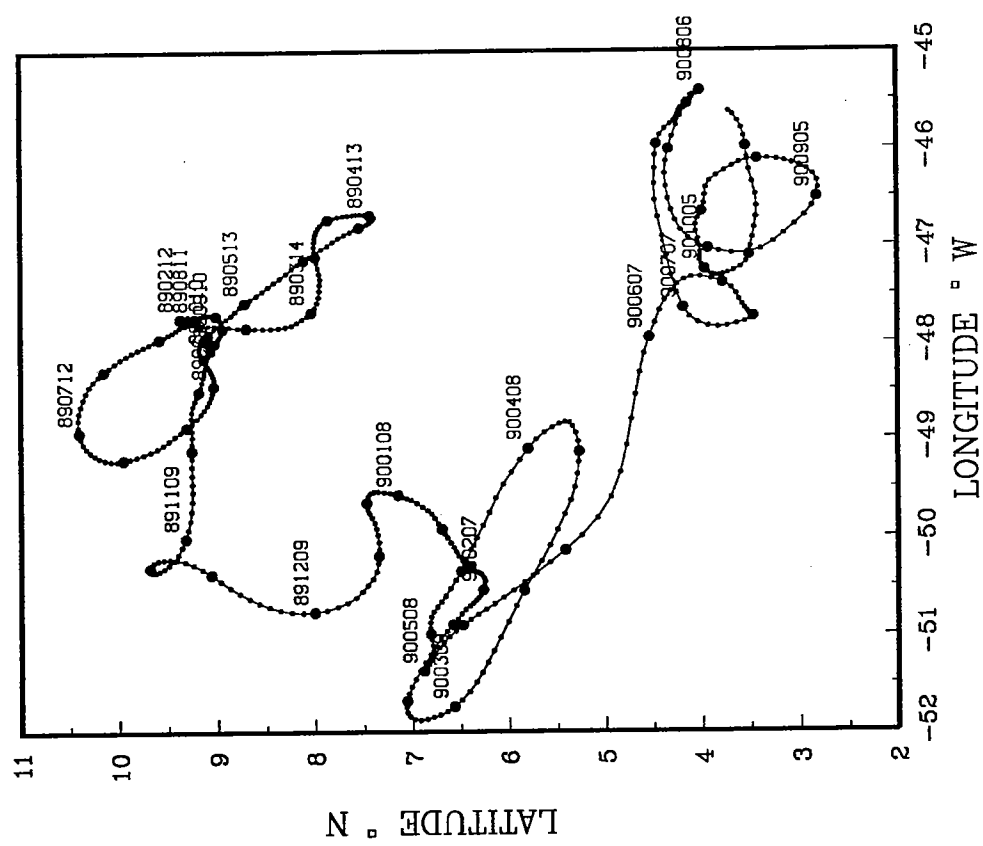


TROPICAL ATLANTIC 12
DEPTH 1800 m.

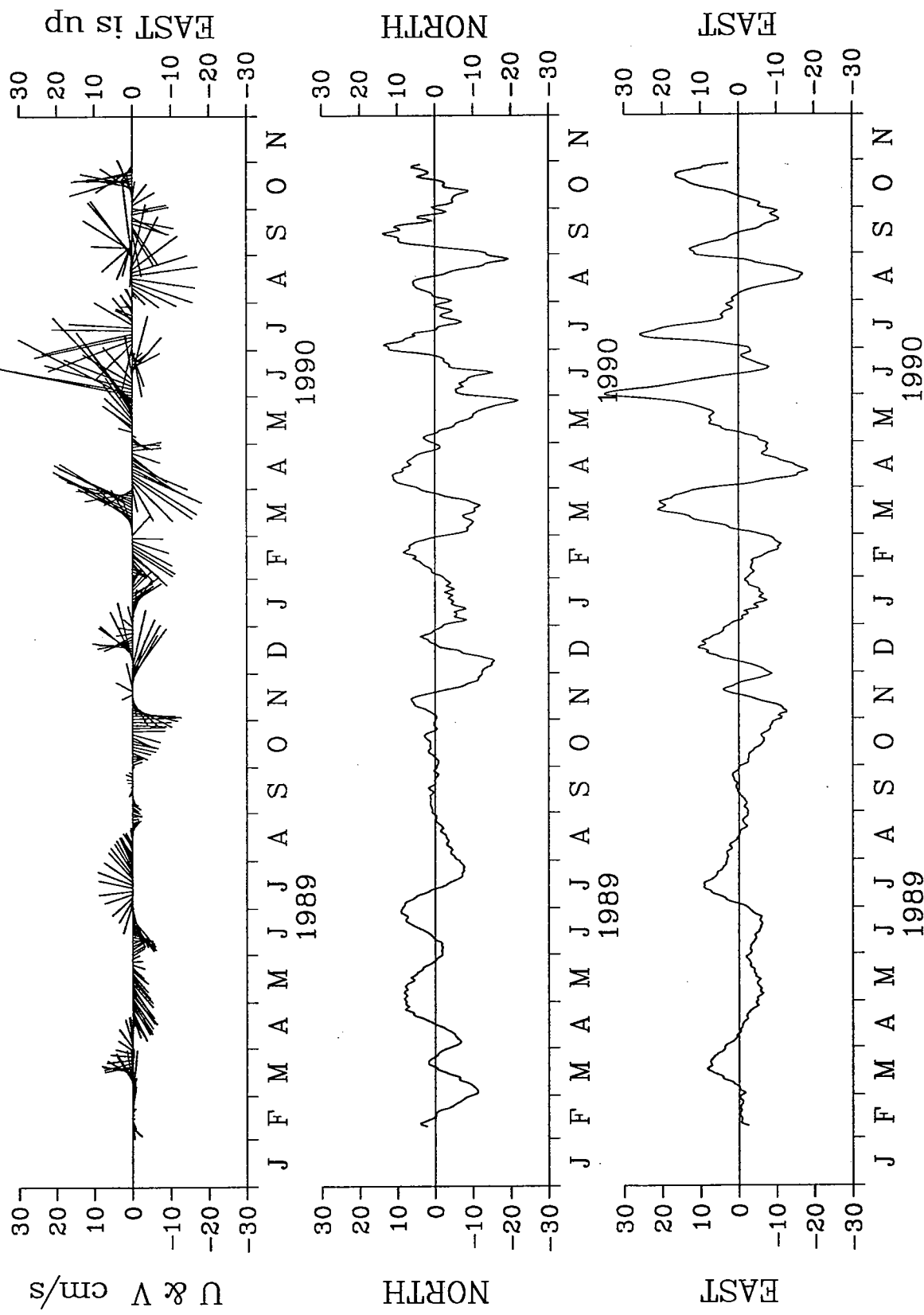


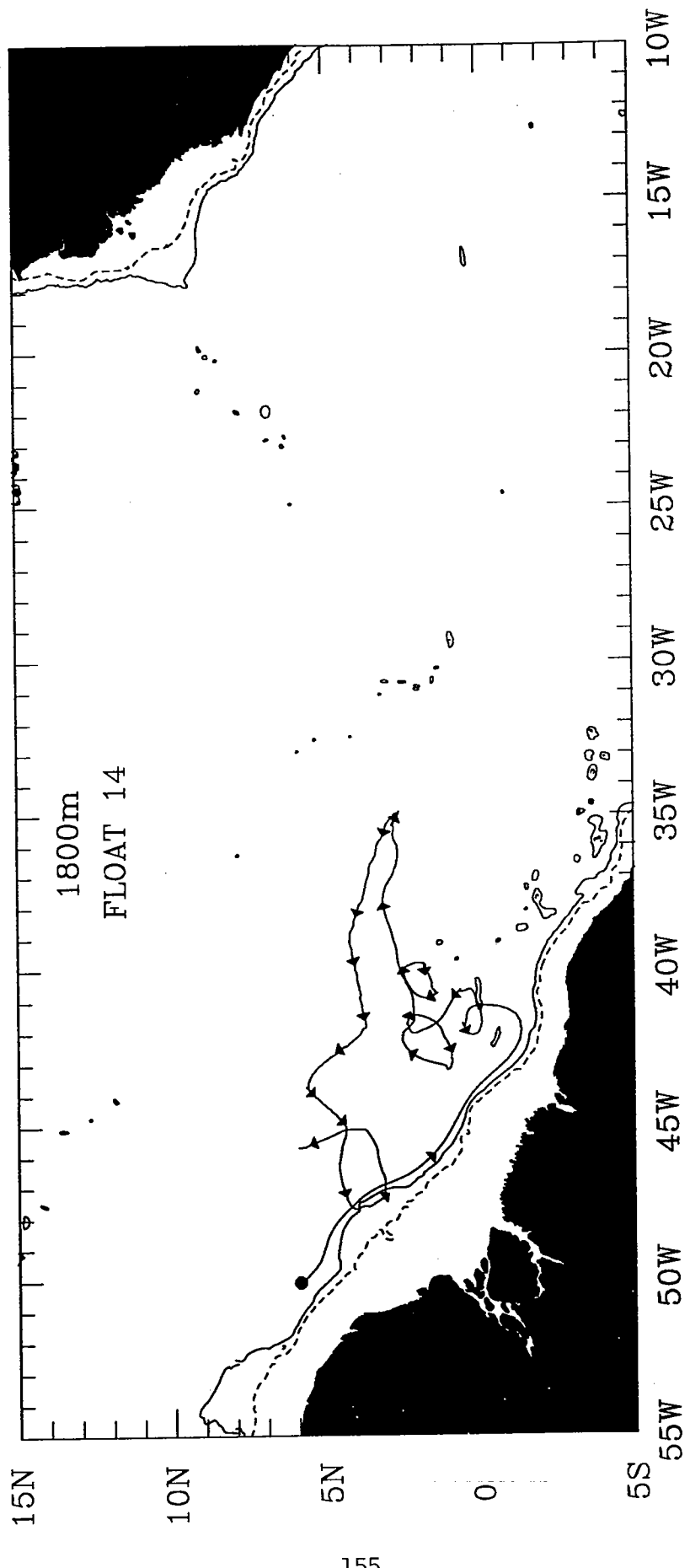


TROPICAL ATLANTIC 13

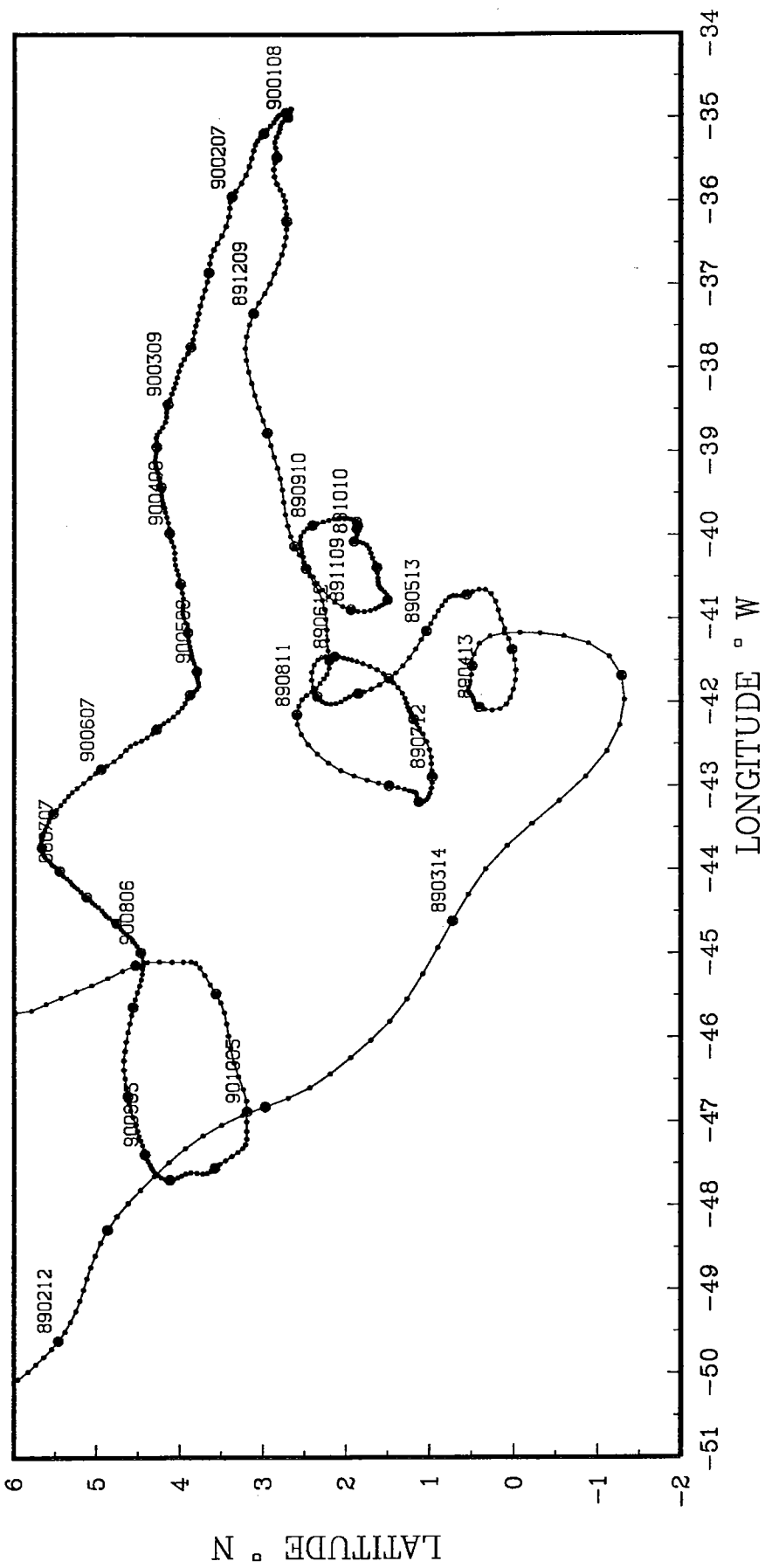


TROPICAL ATLANTIC 13
DEPTH 1800 m.

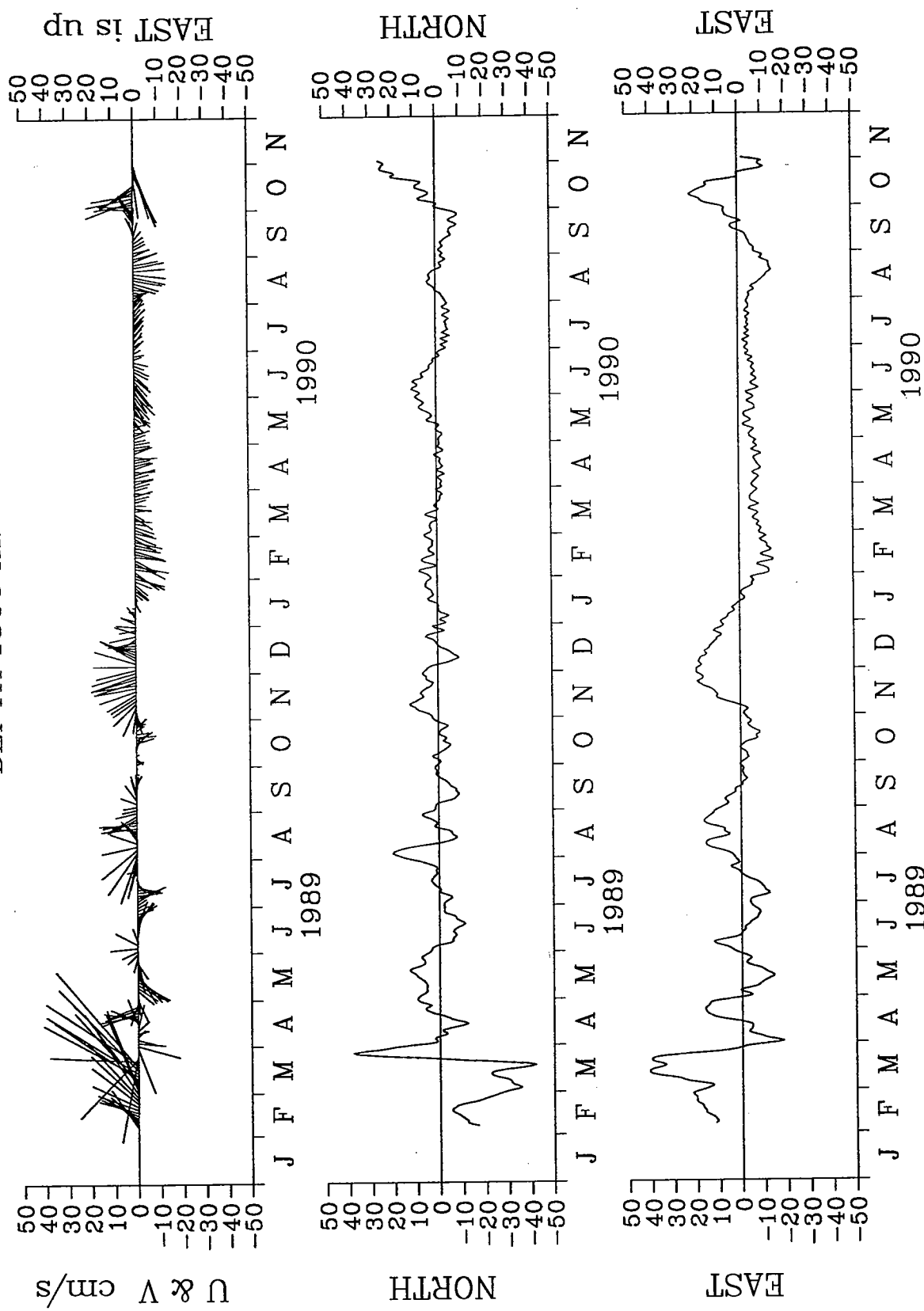


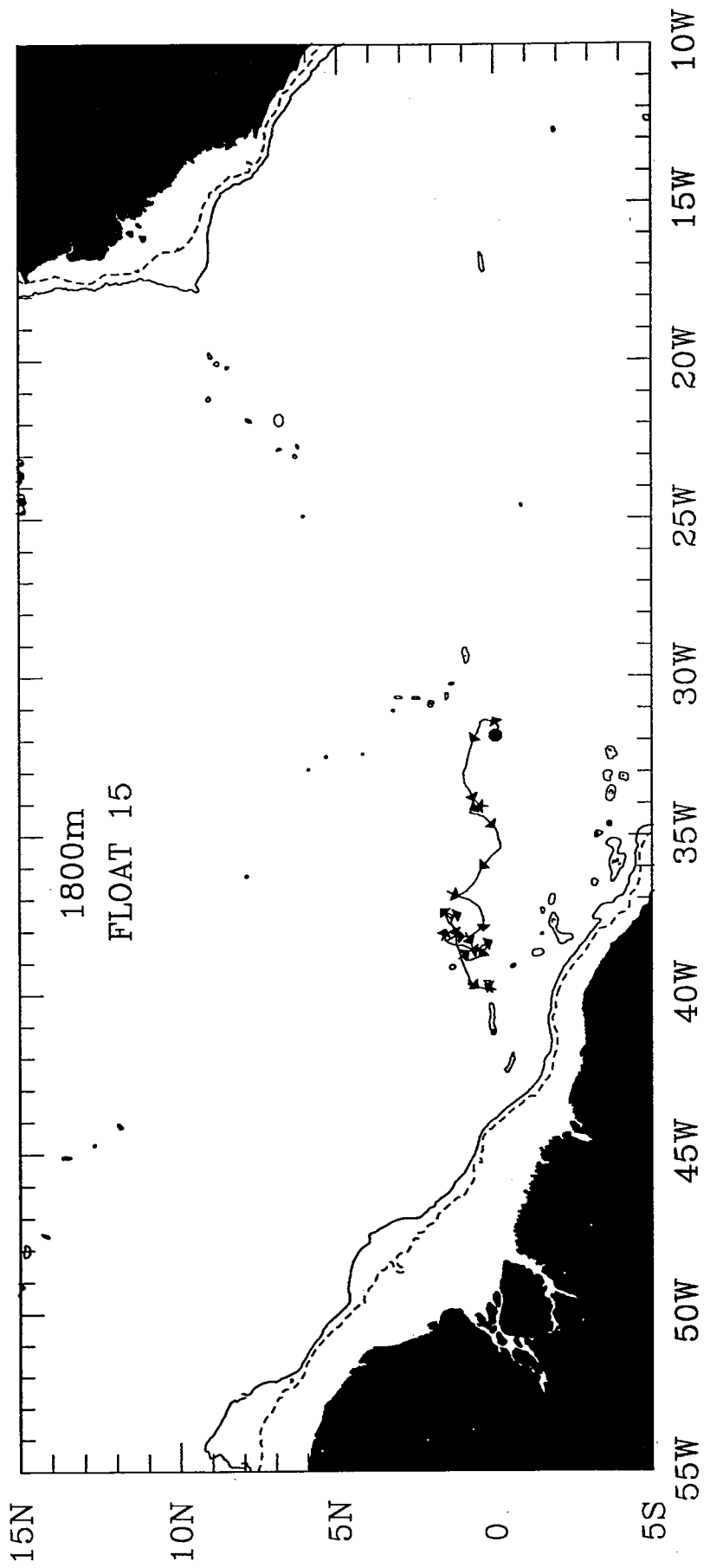


TROPICAL ATLANTIC 14

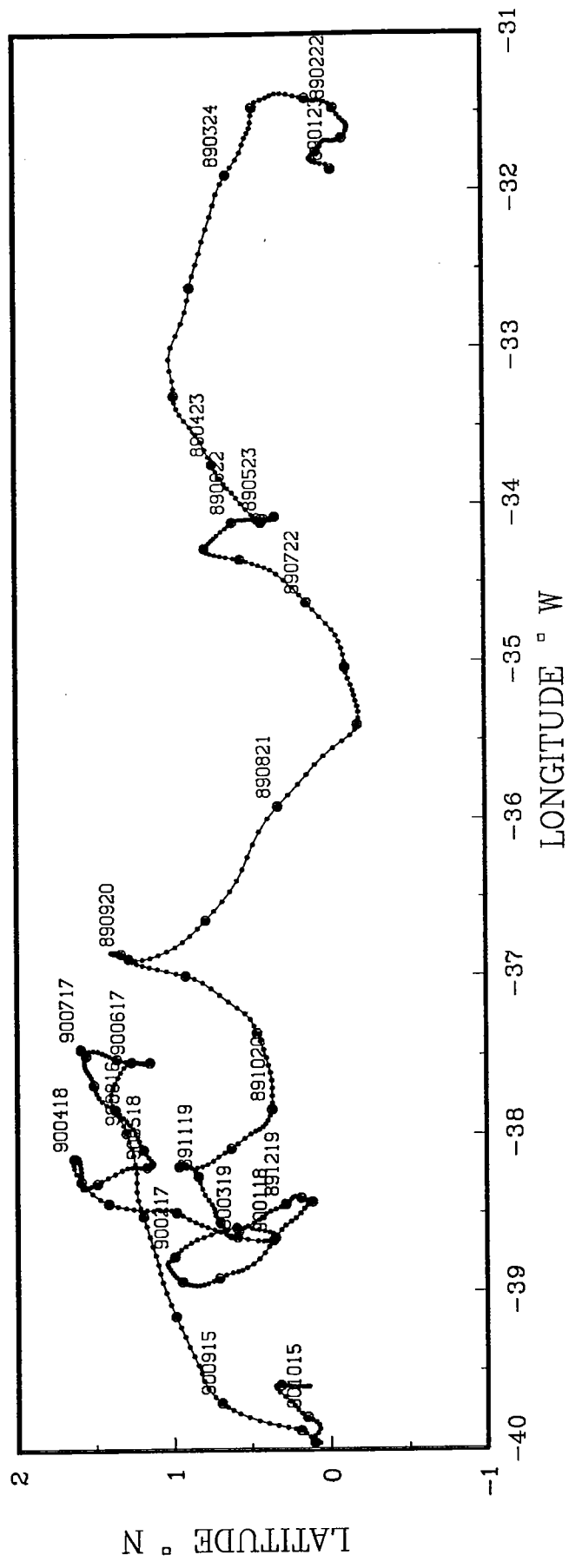


TROPICAL ATLANTIC 14
DEPTH 1800 m.

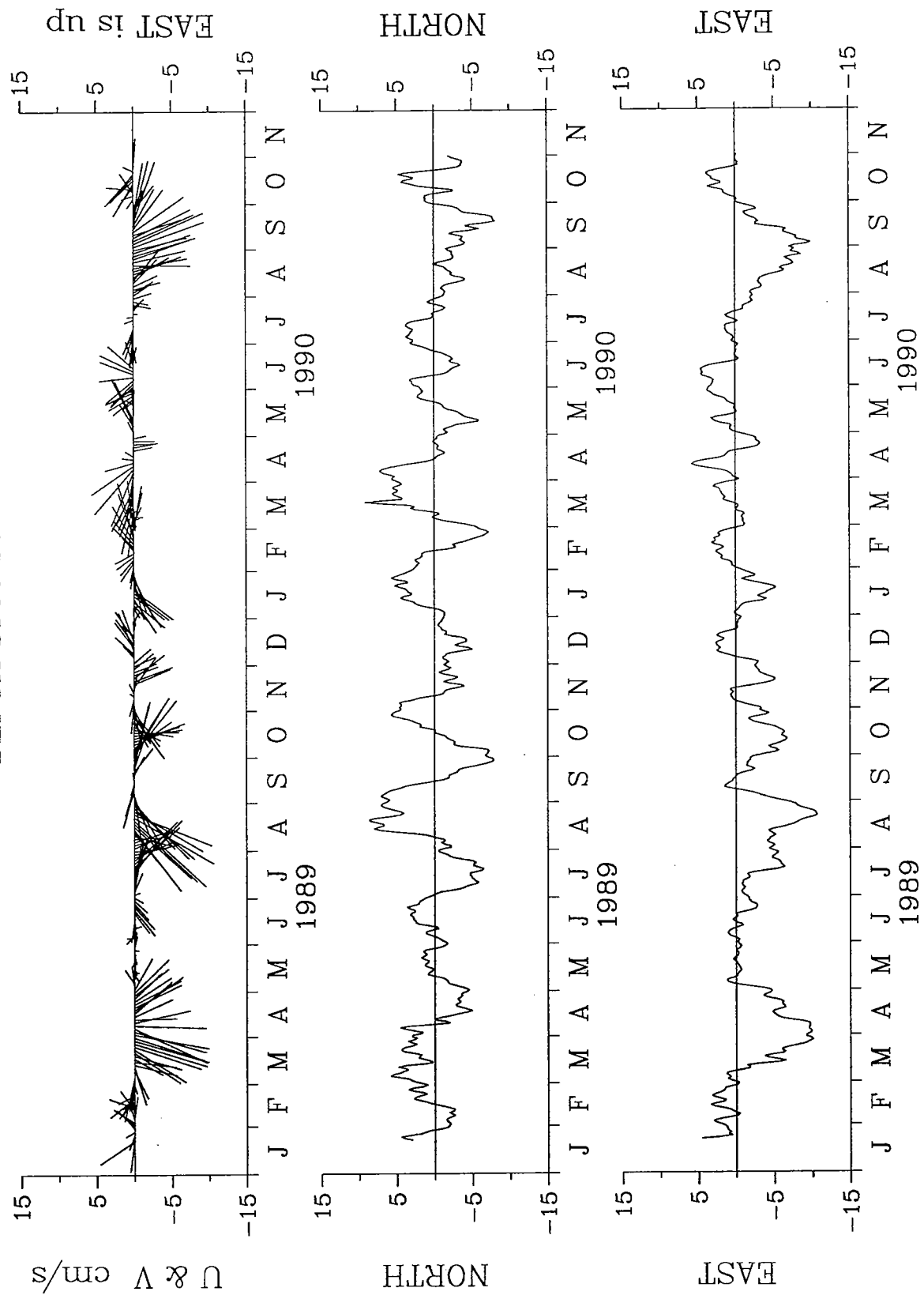


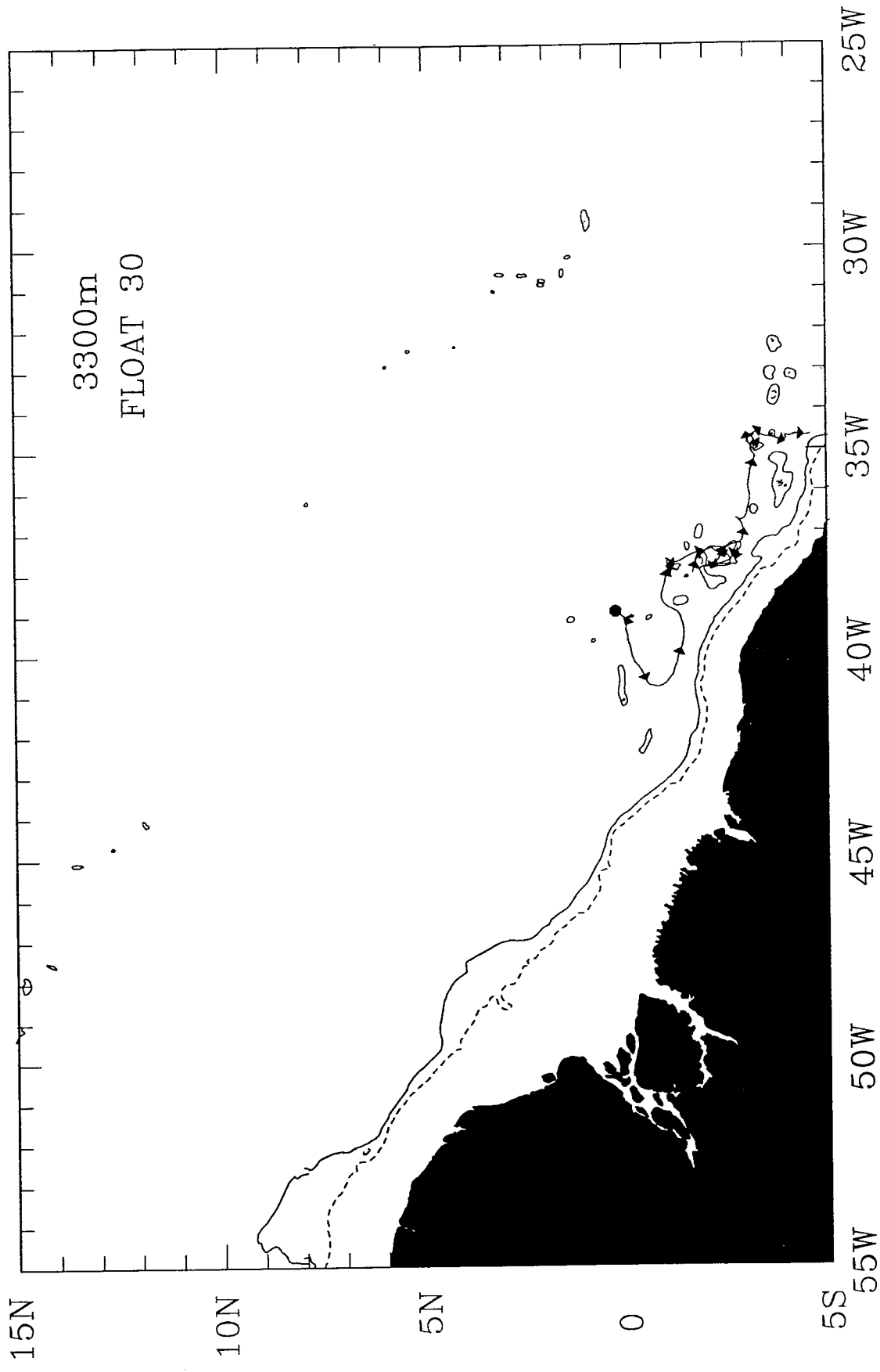


TROPICAL ATLANTIC 15

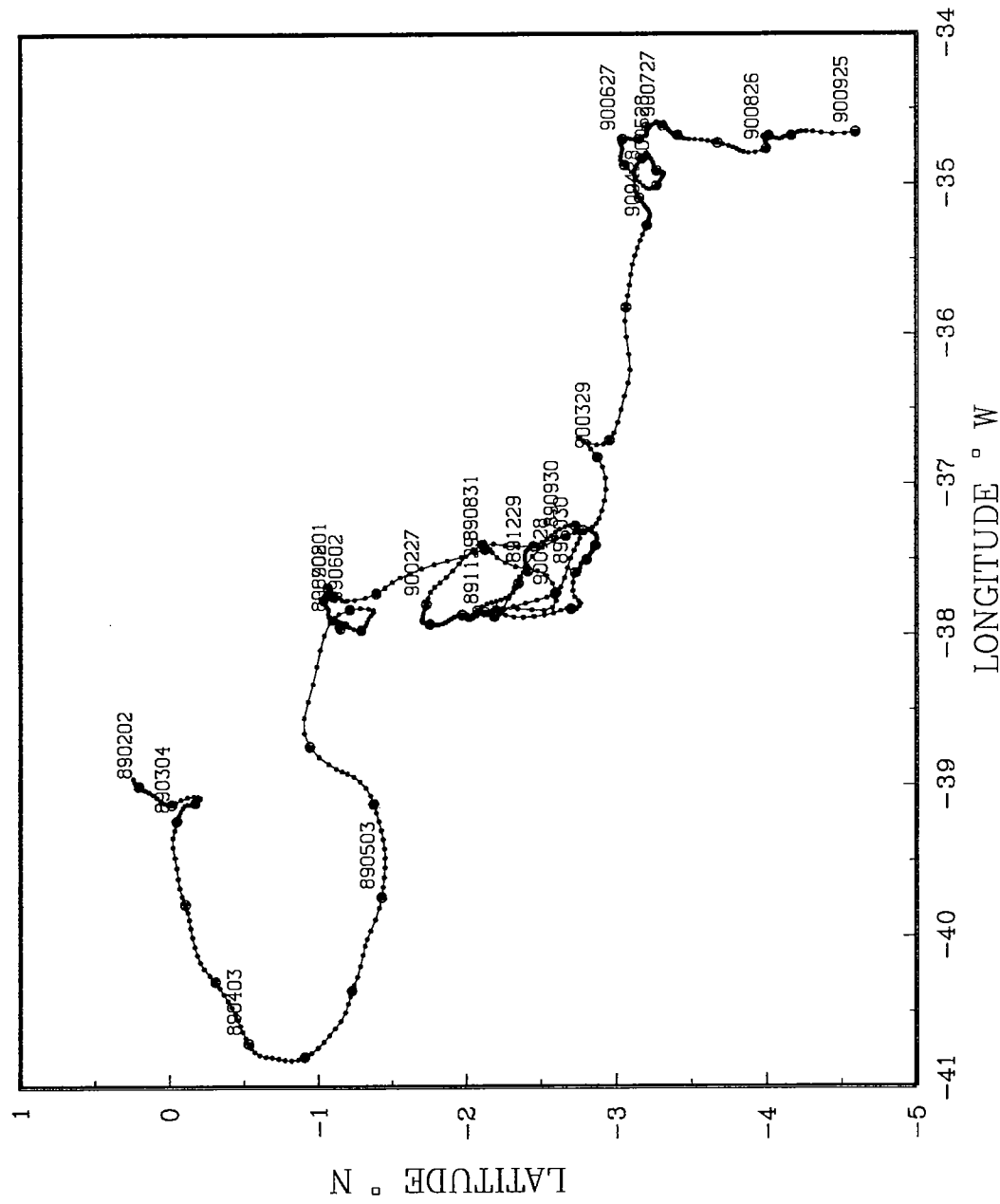


TROPICAL ATLANTIC 15
DEPTH 1800 m.

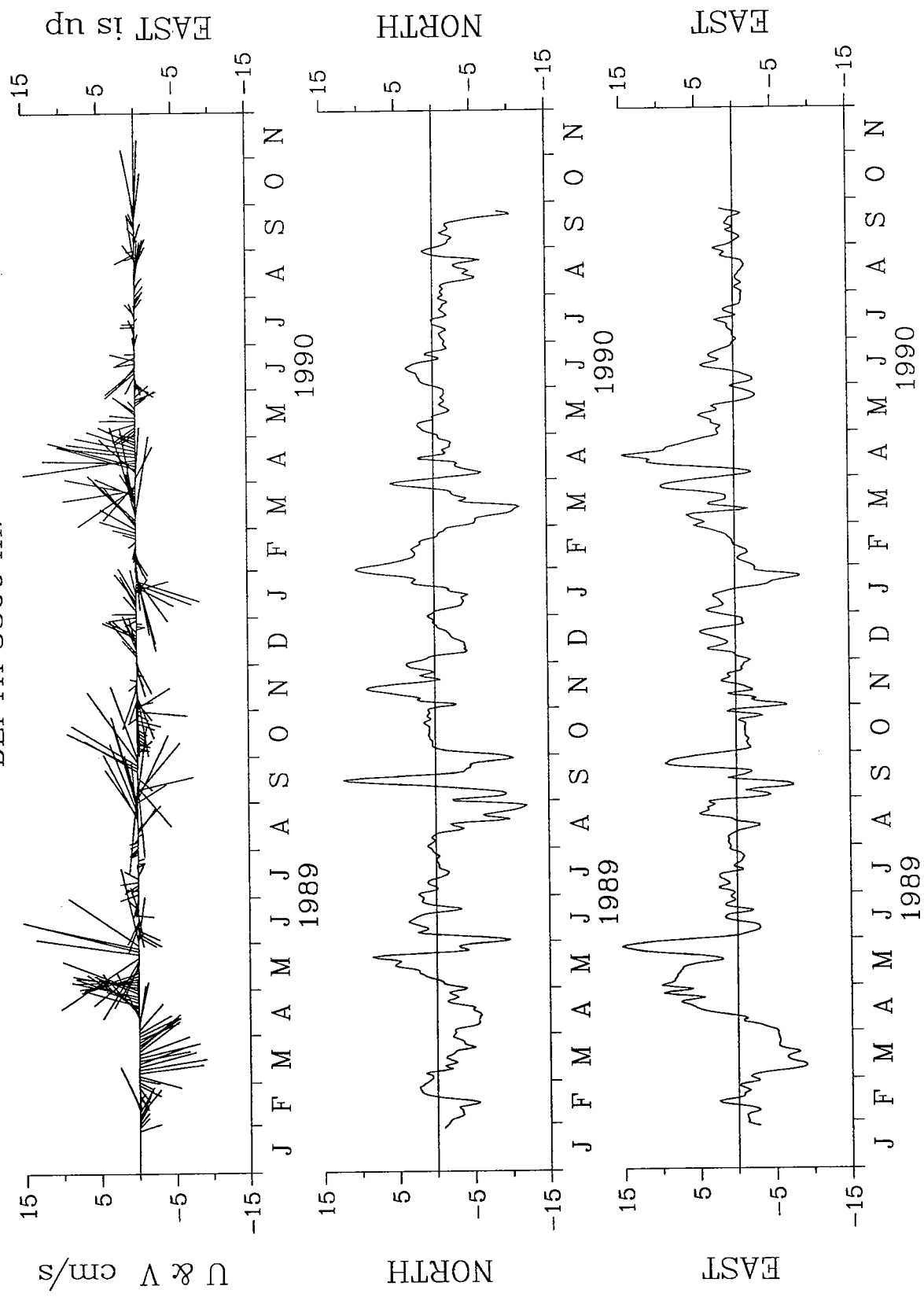


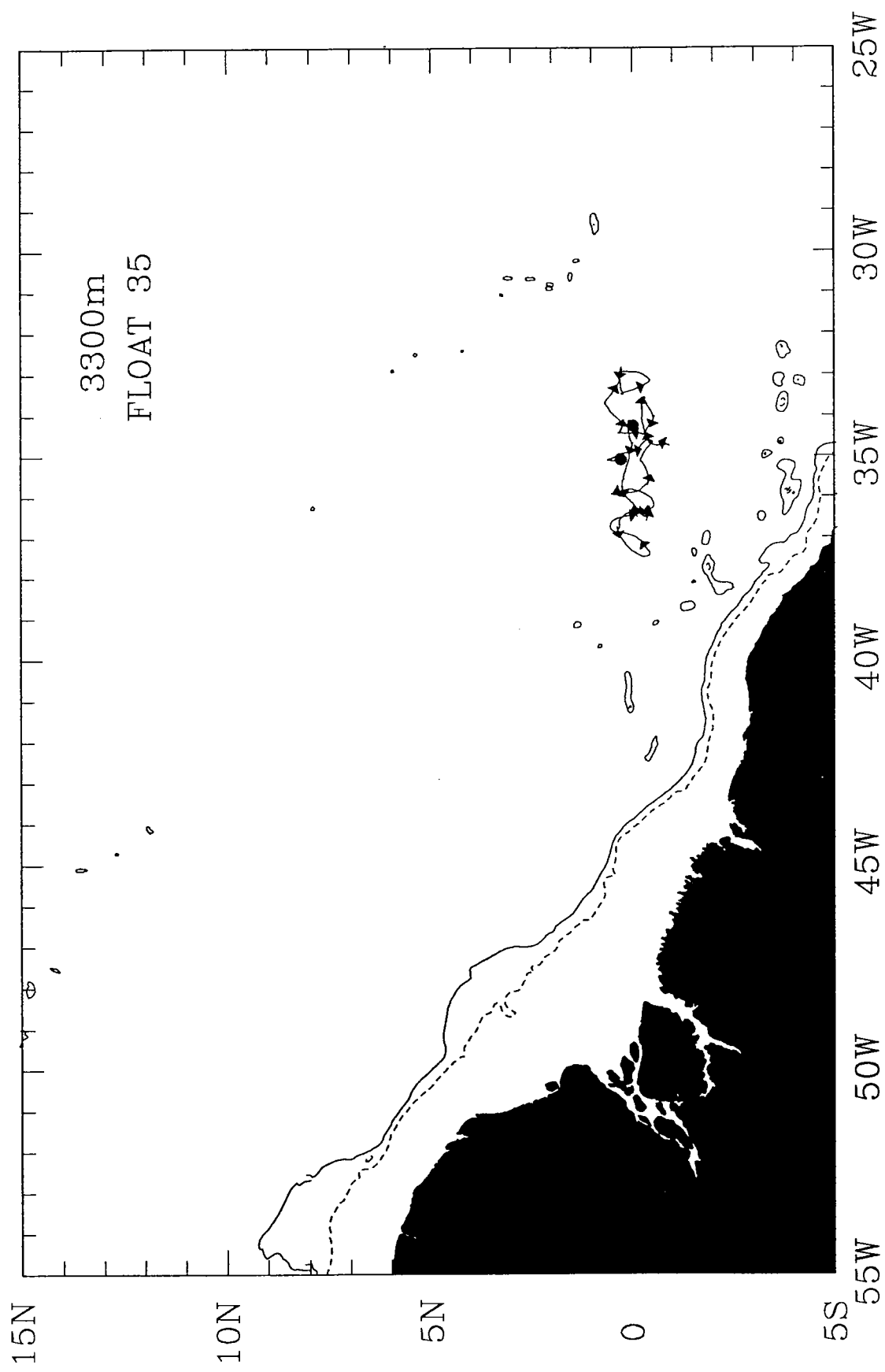


TROPICAL ATLANTIC 30

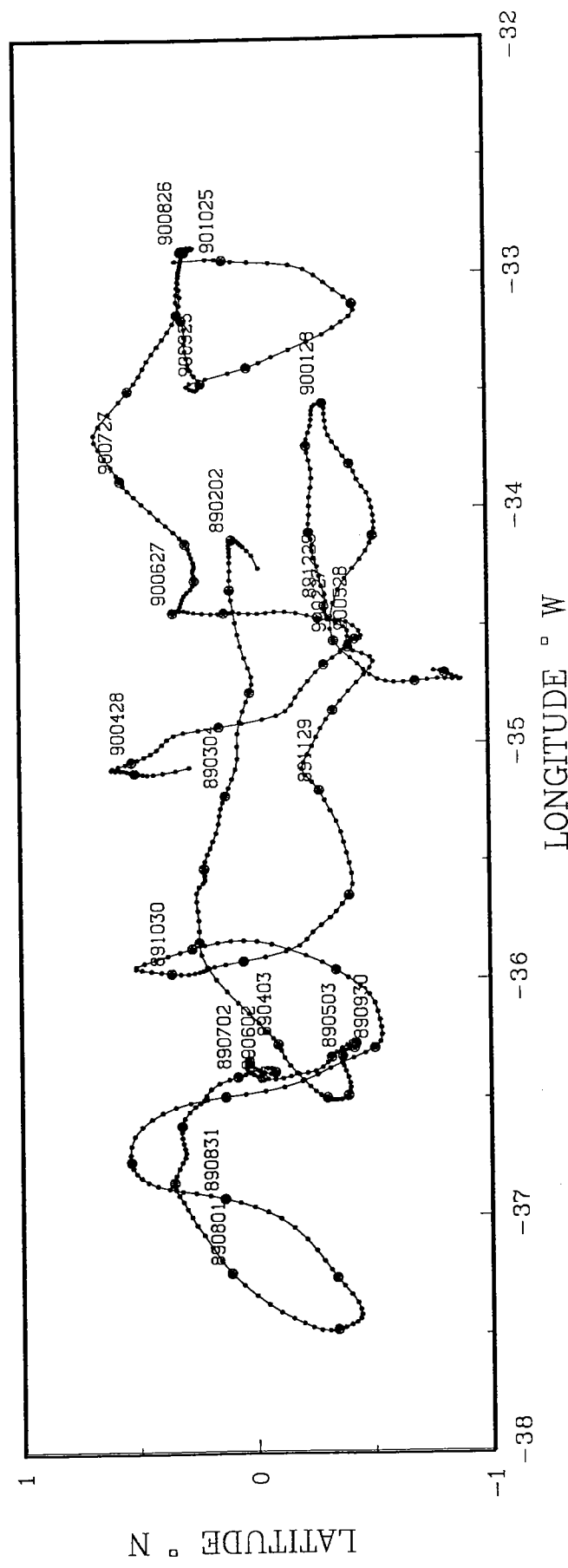


TROPICAL ATLANTIC 30
DEPTH 3300 m.

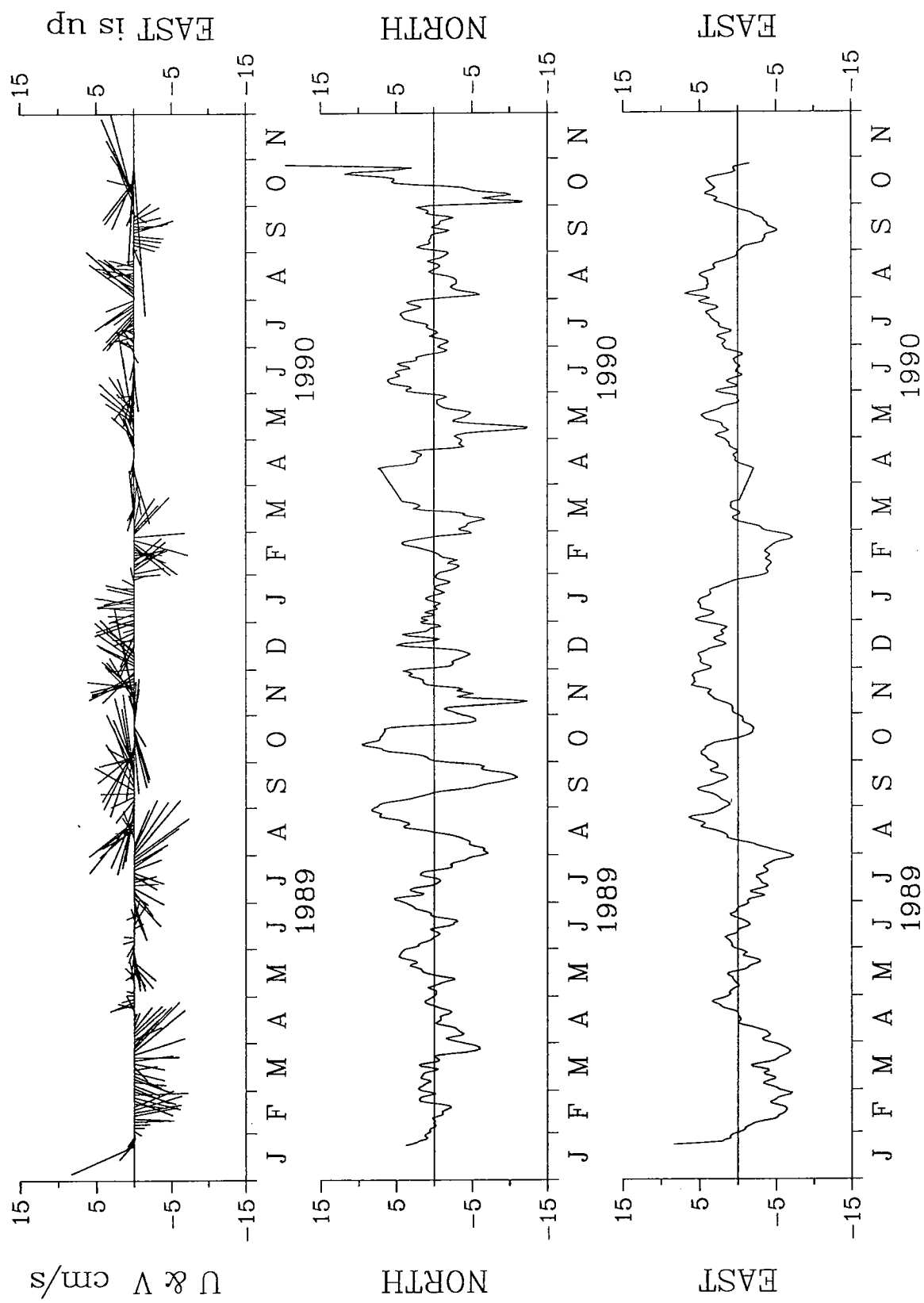


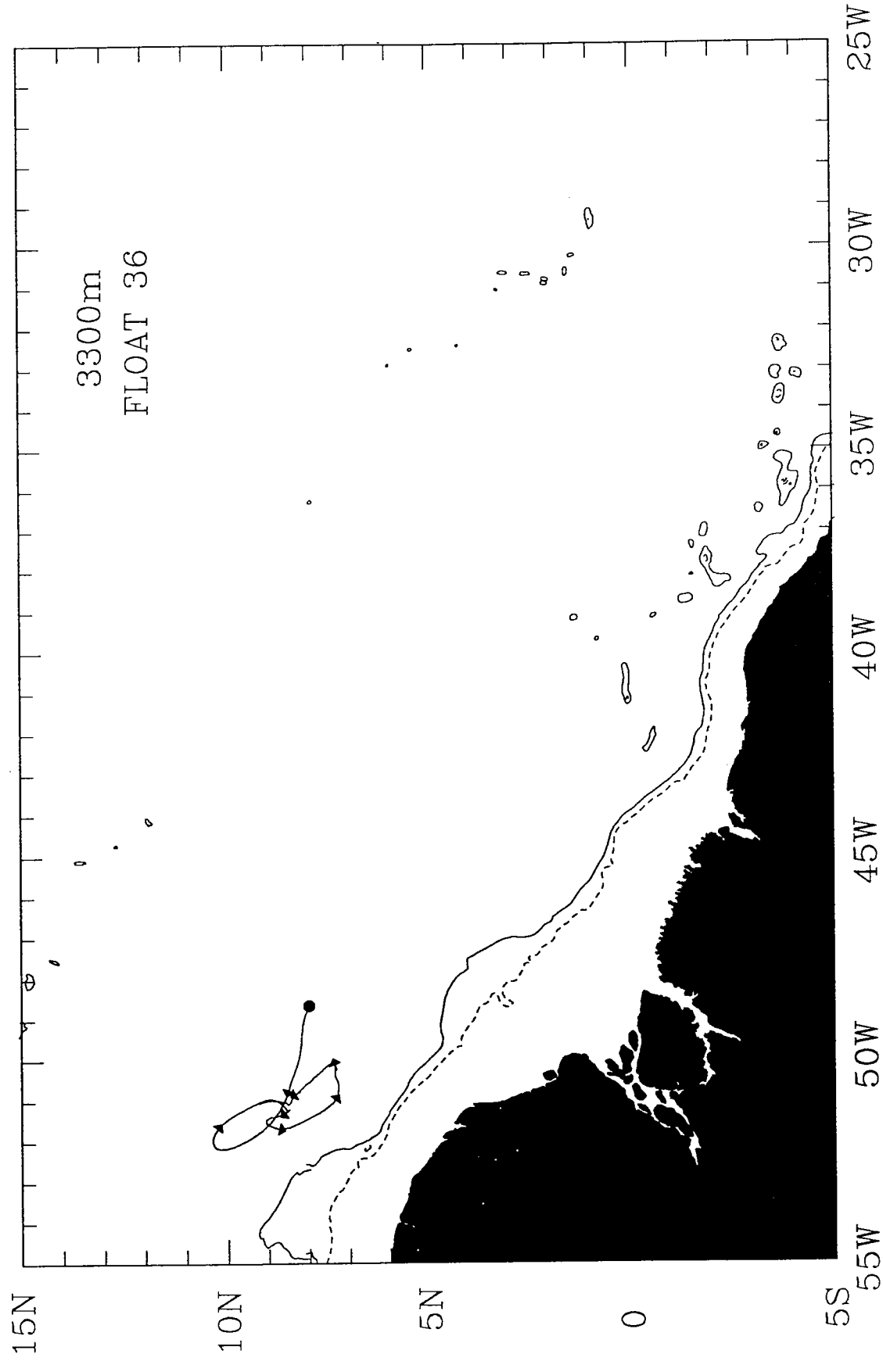


TROPICAL ATLANTIC 35

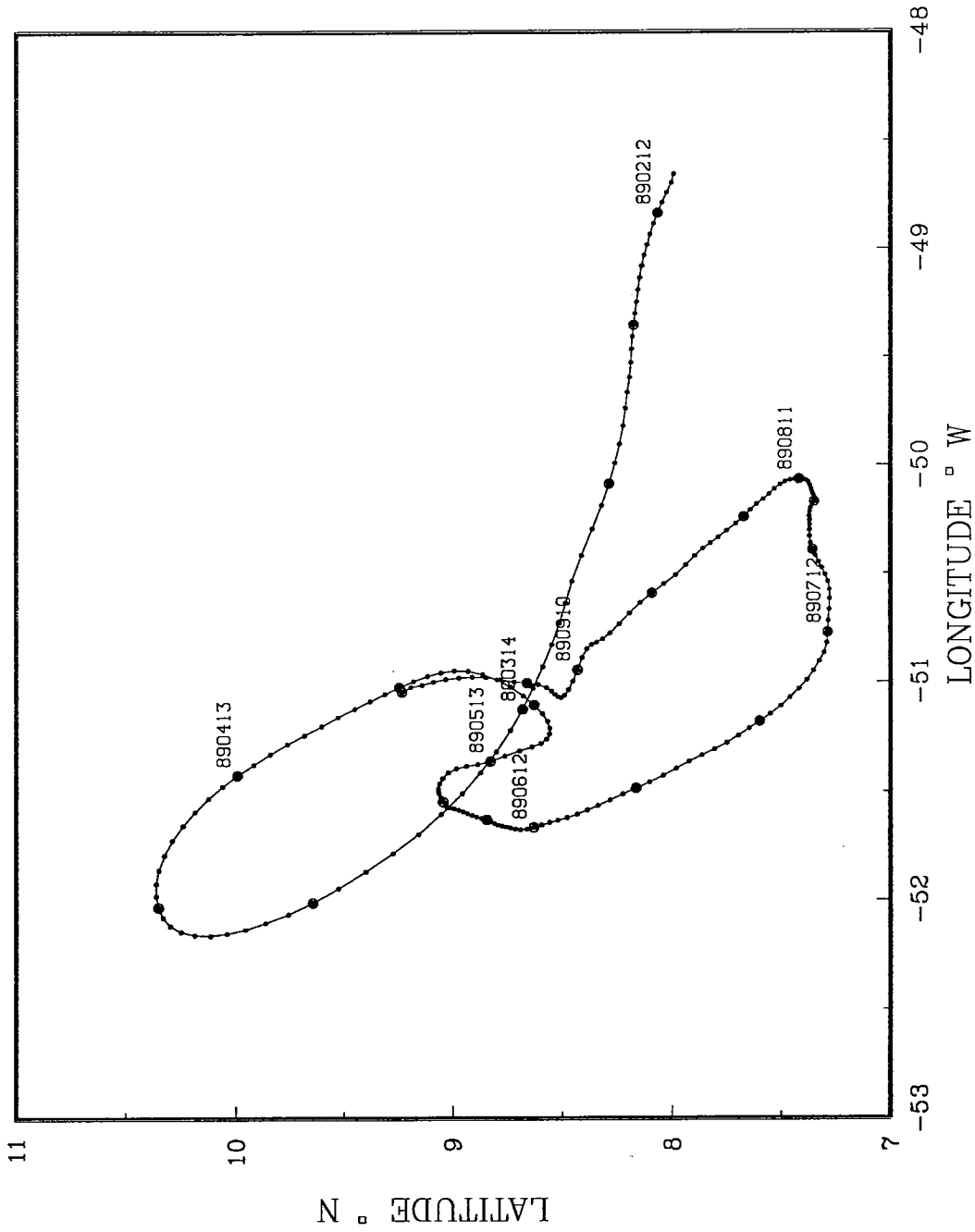


TROPICAL ATLANTIC 35
DEPTH 3300 m.

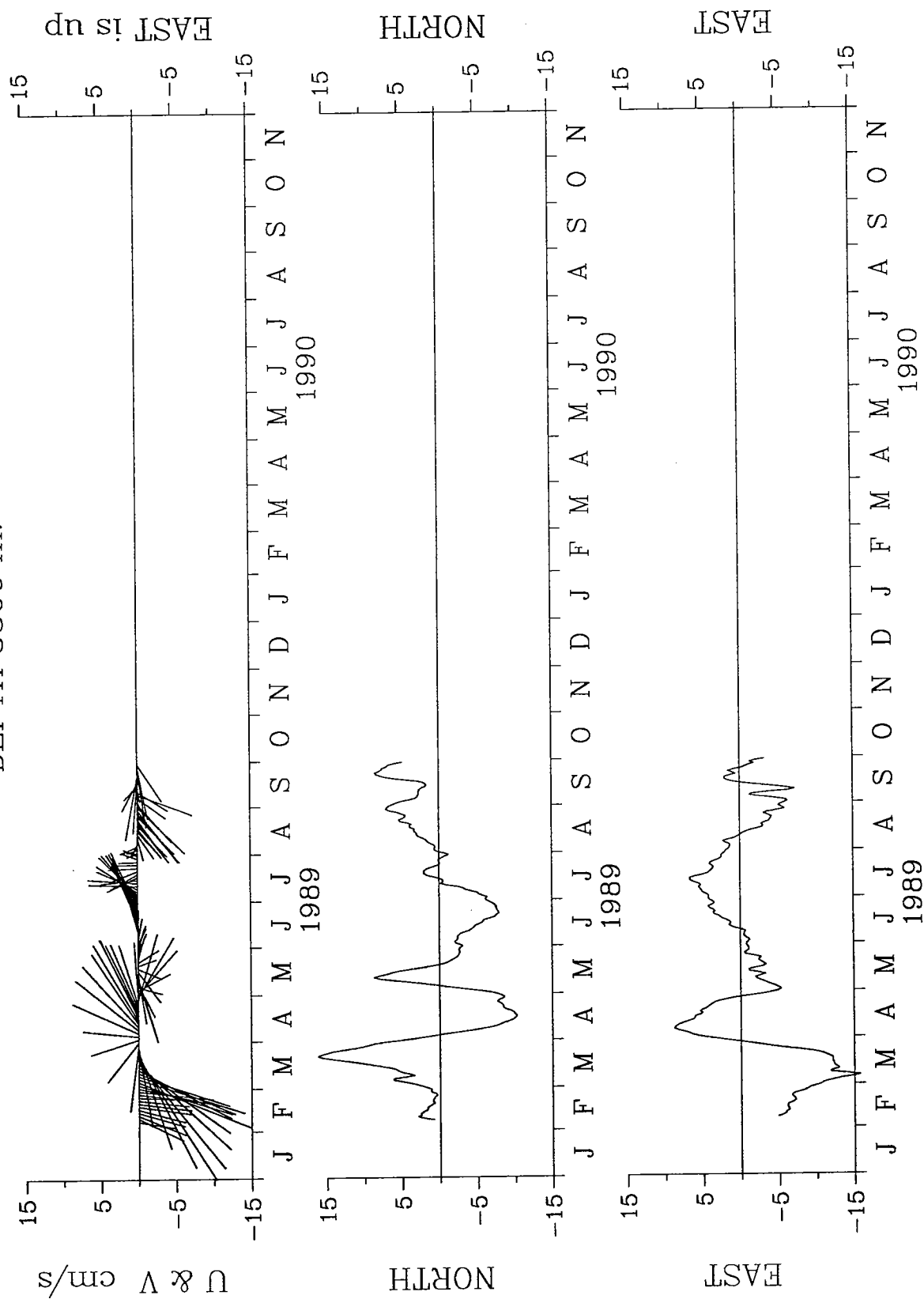


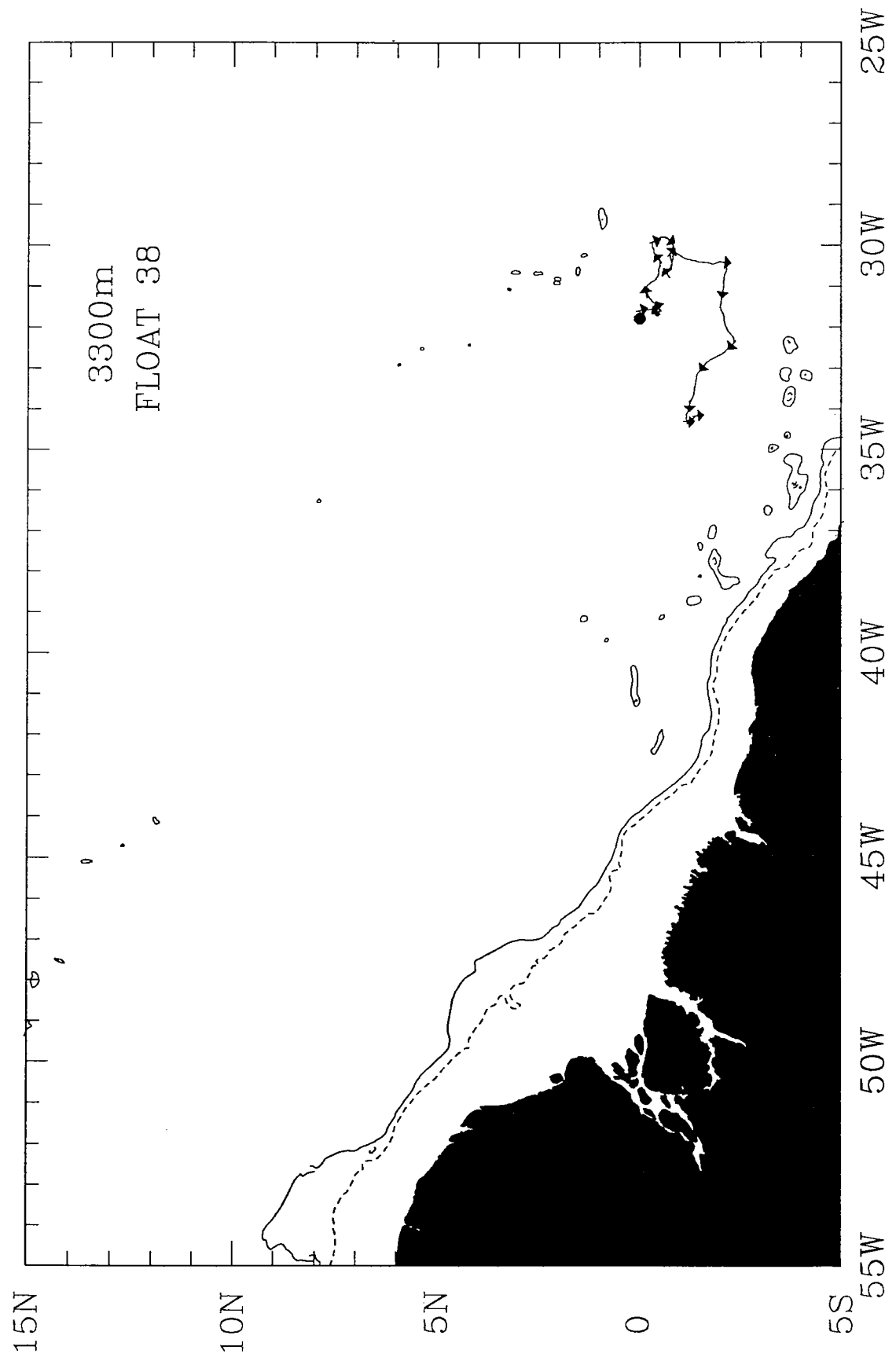


TROPICAL ATLANTIC 36

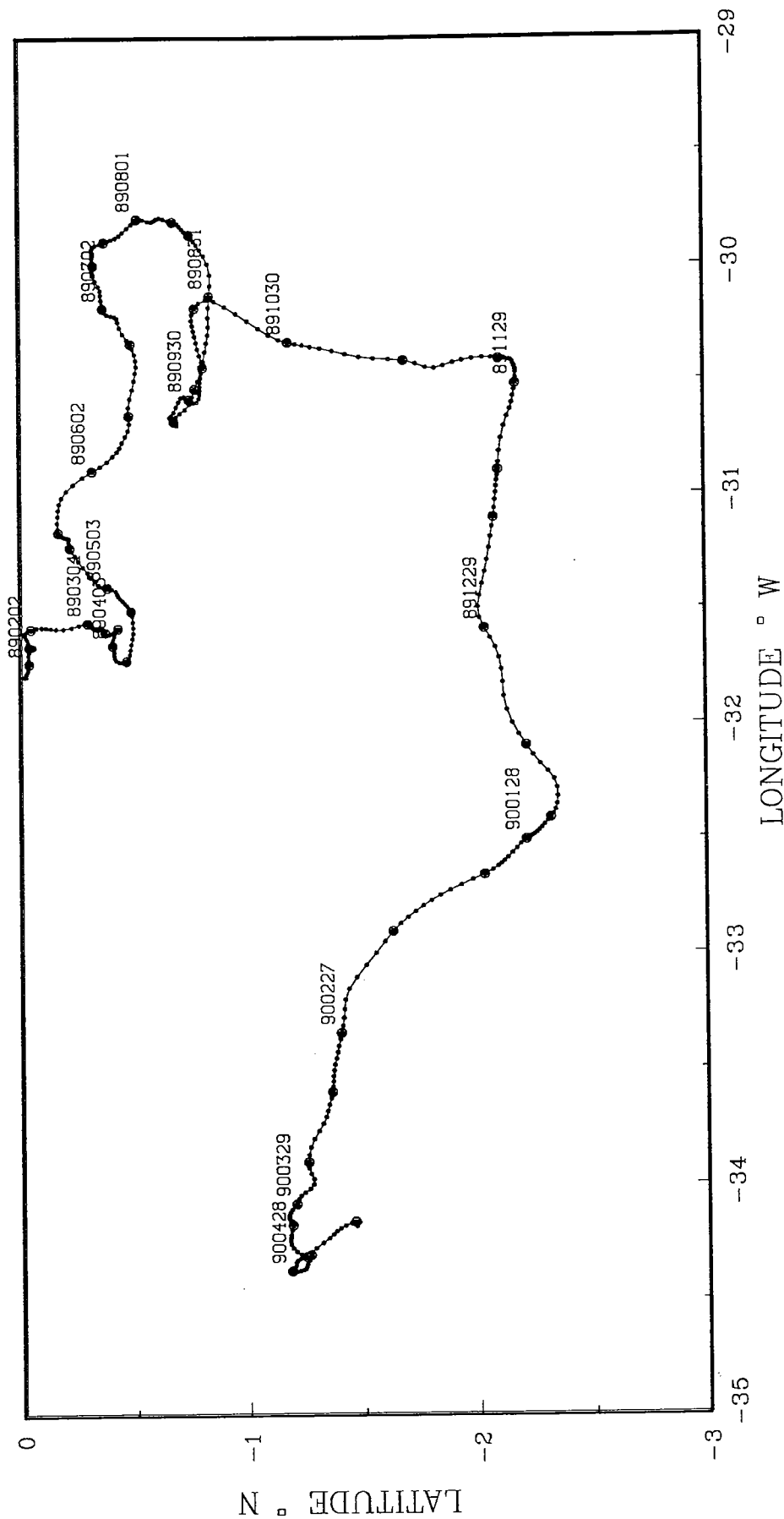


TROPICAL ATLANTIC 36
DEPTH 3300 m.

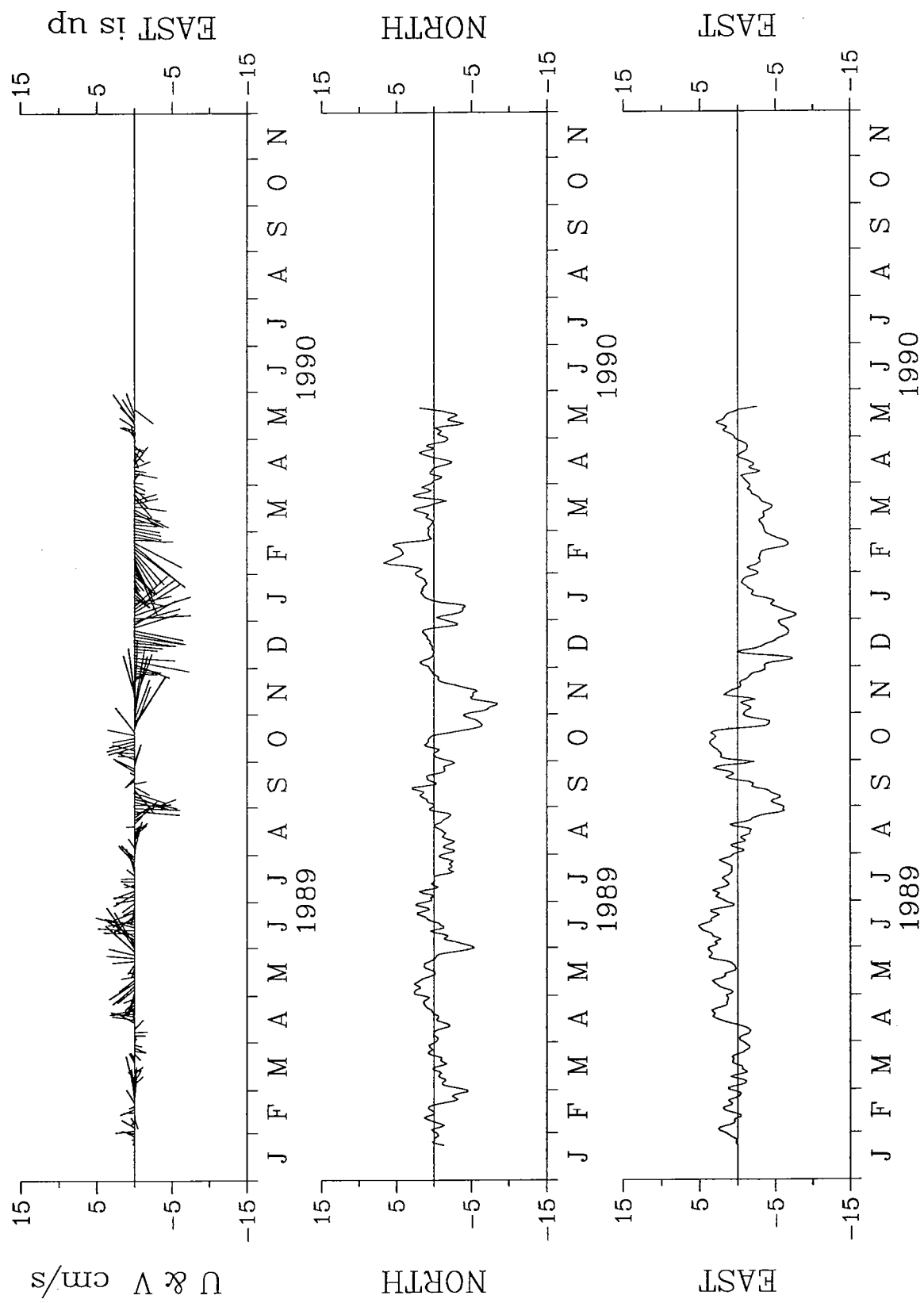


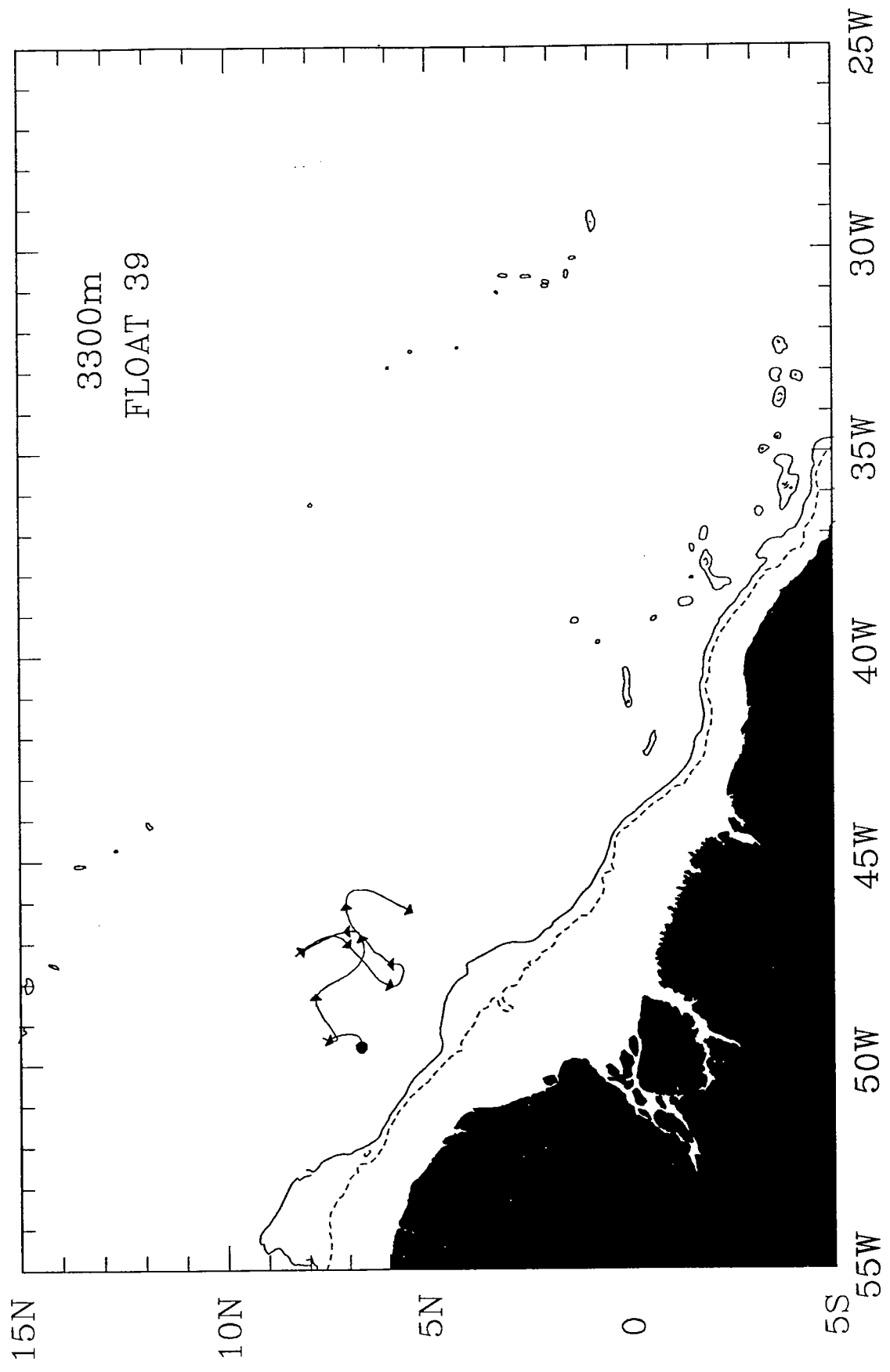


TROPICAL ATLANTIC 38

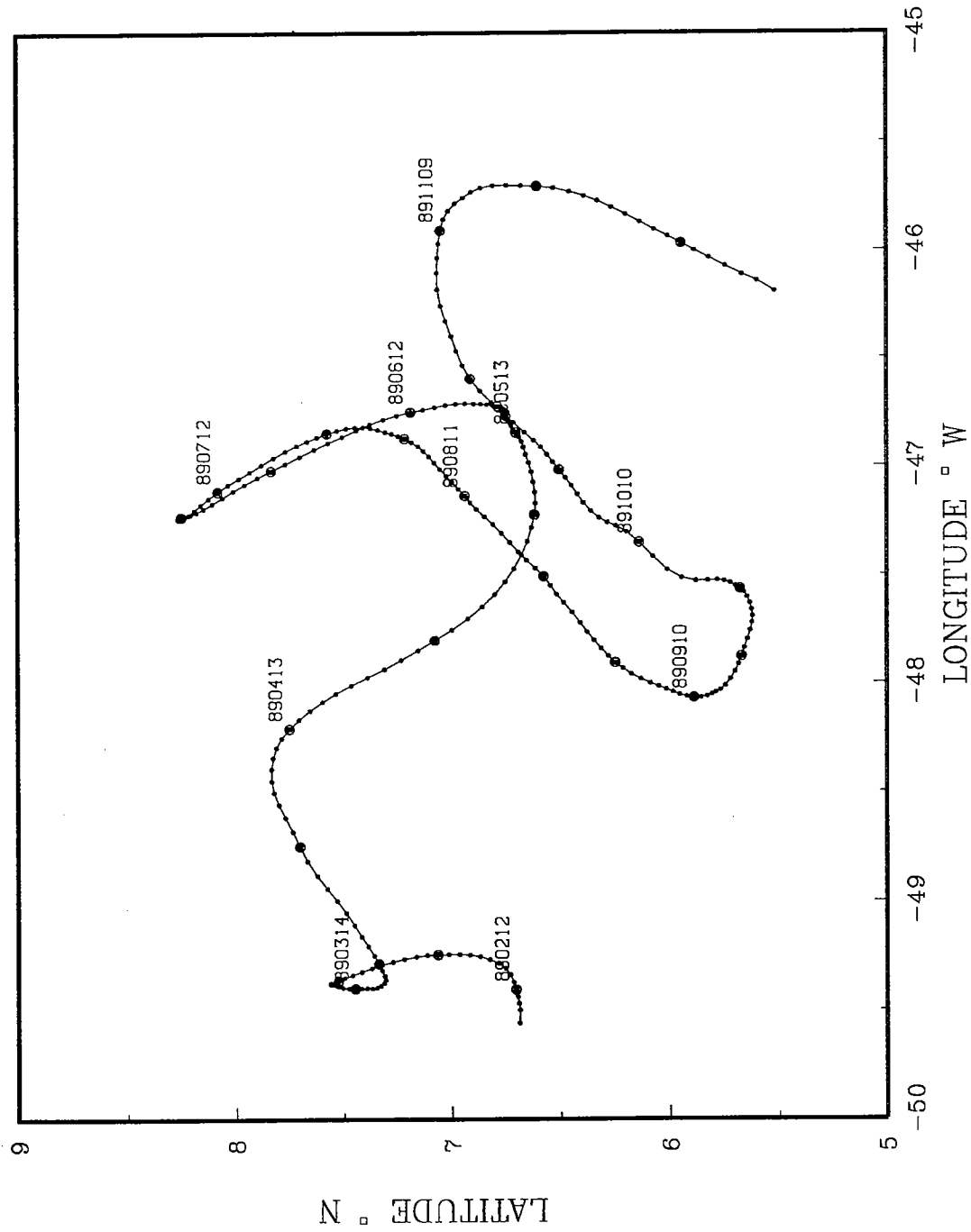


TROPICAL ATLANTIC 38
DEPTH 3300 m.

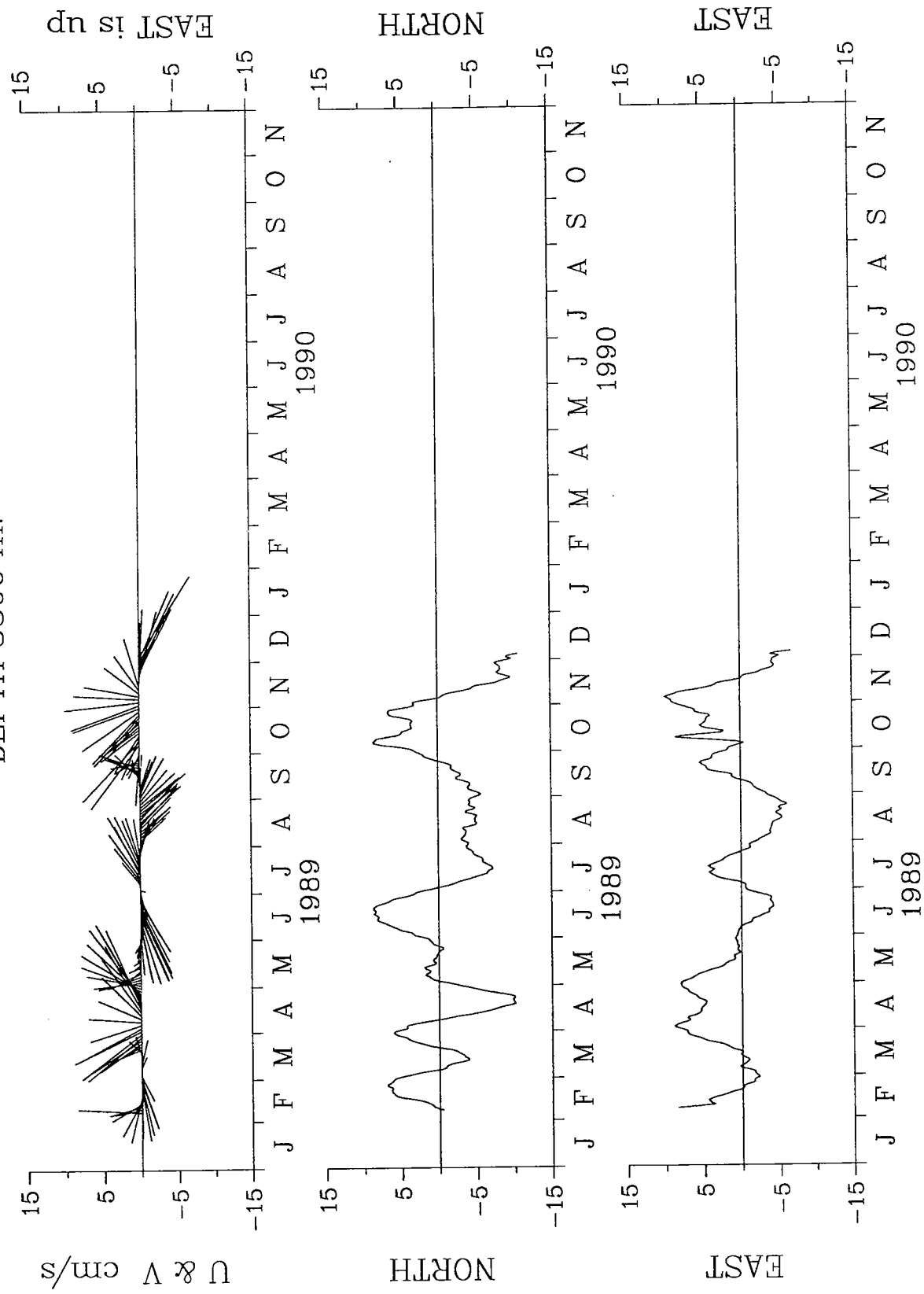


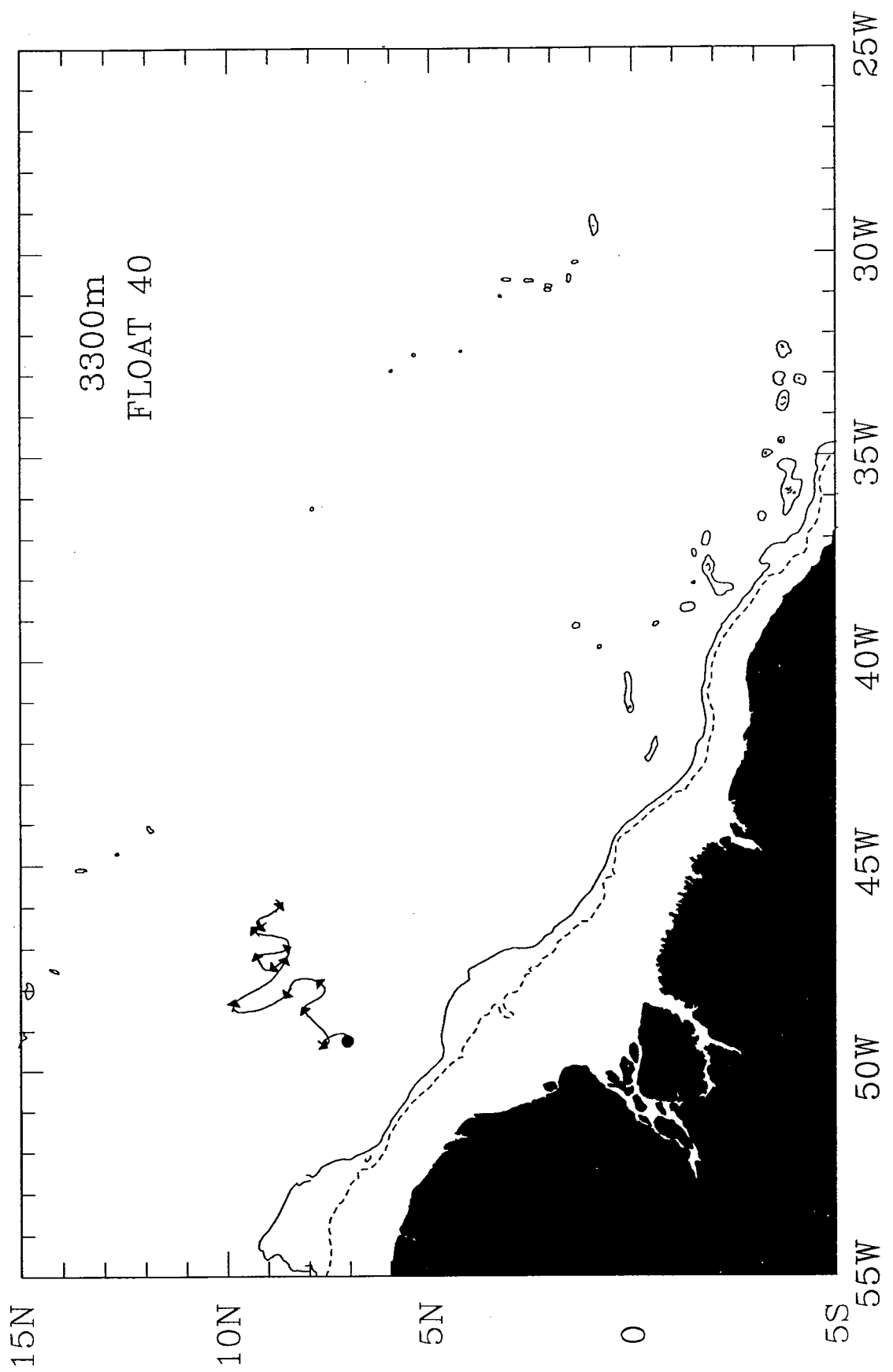


TROPICAL ATLANTIC 39

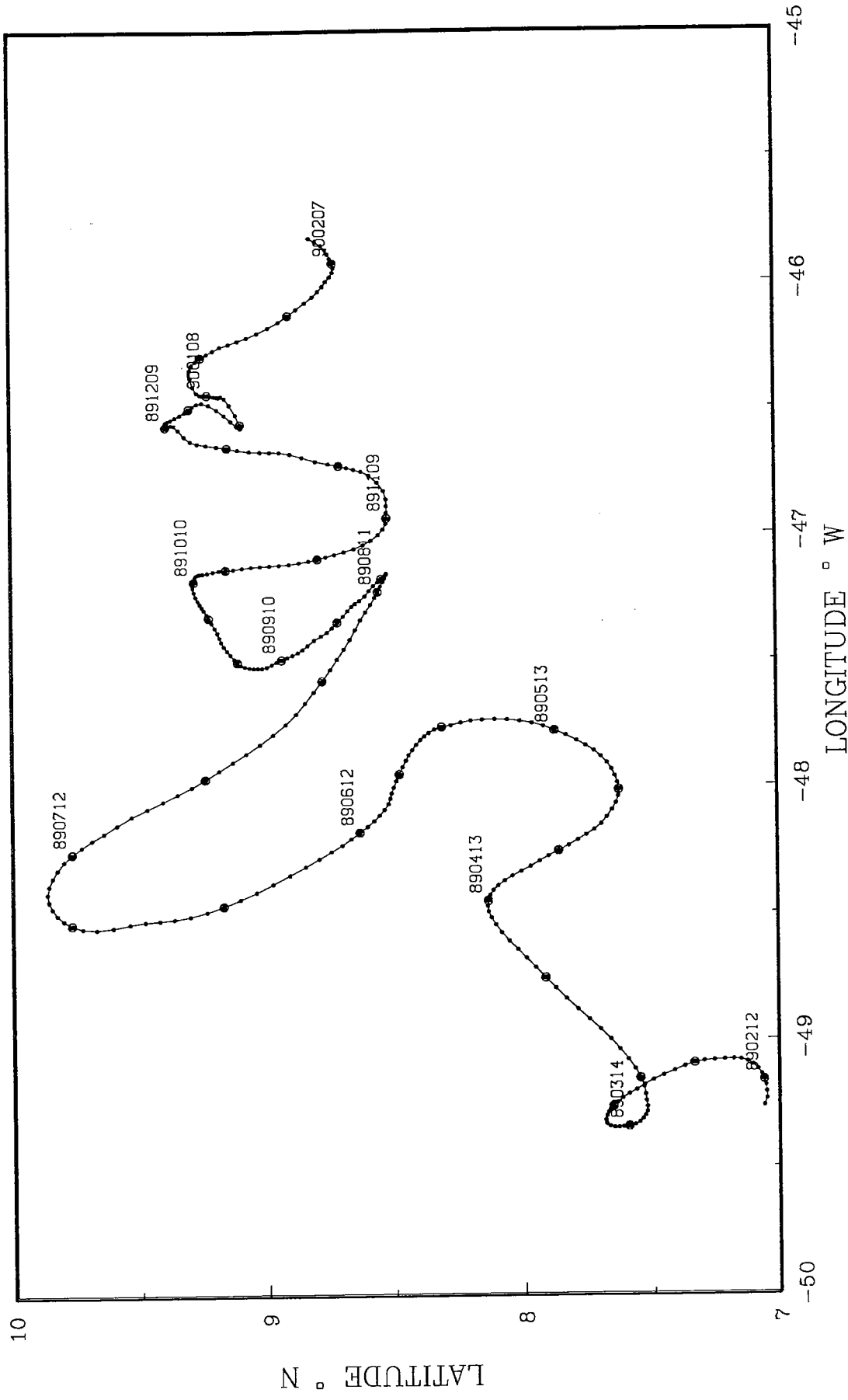


TROPICAL ATLANTIC 39
DEPTH 3300 m.

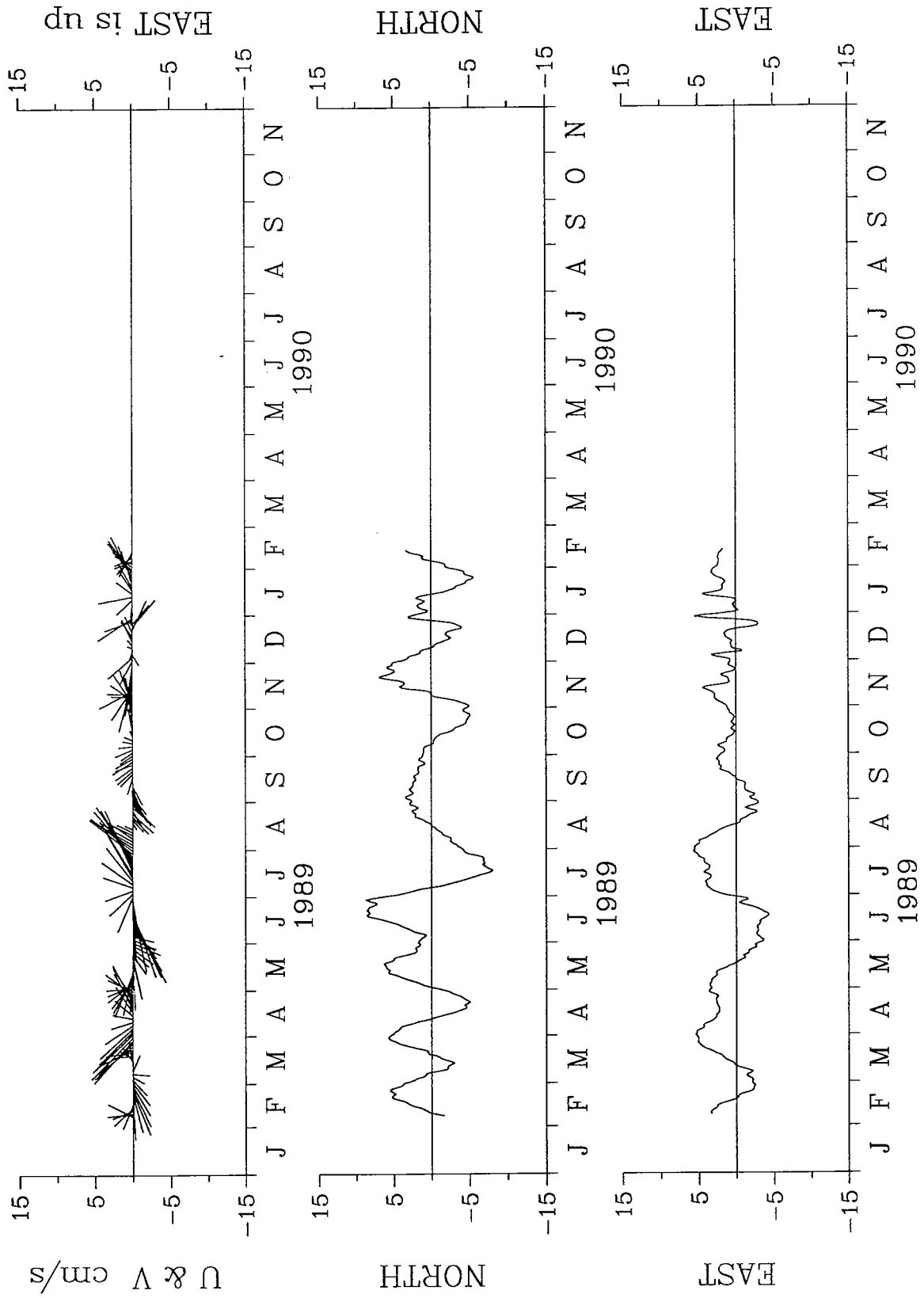


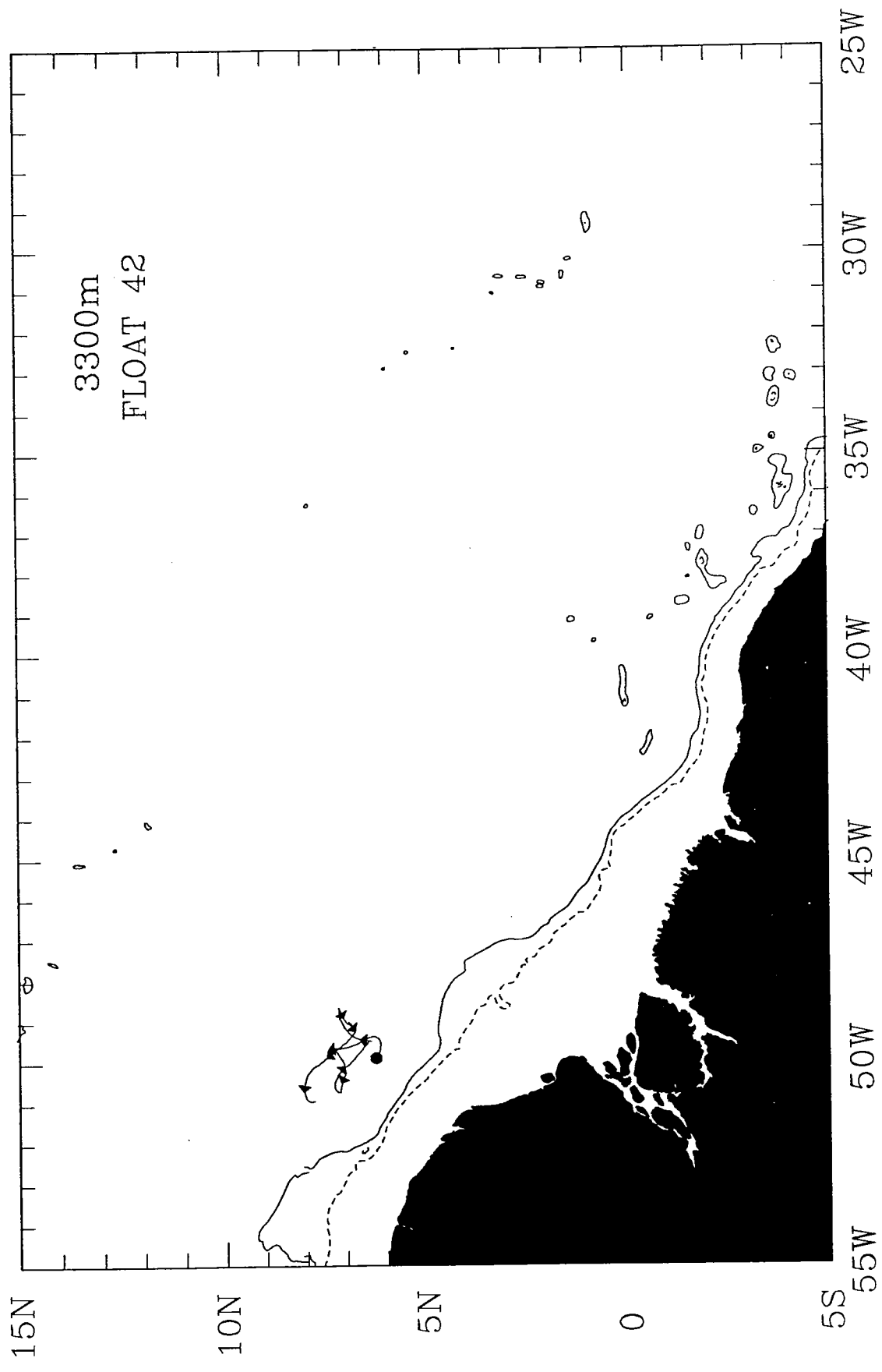


TROPICAL ATLANTIC 40

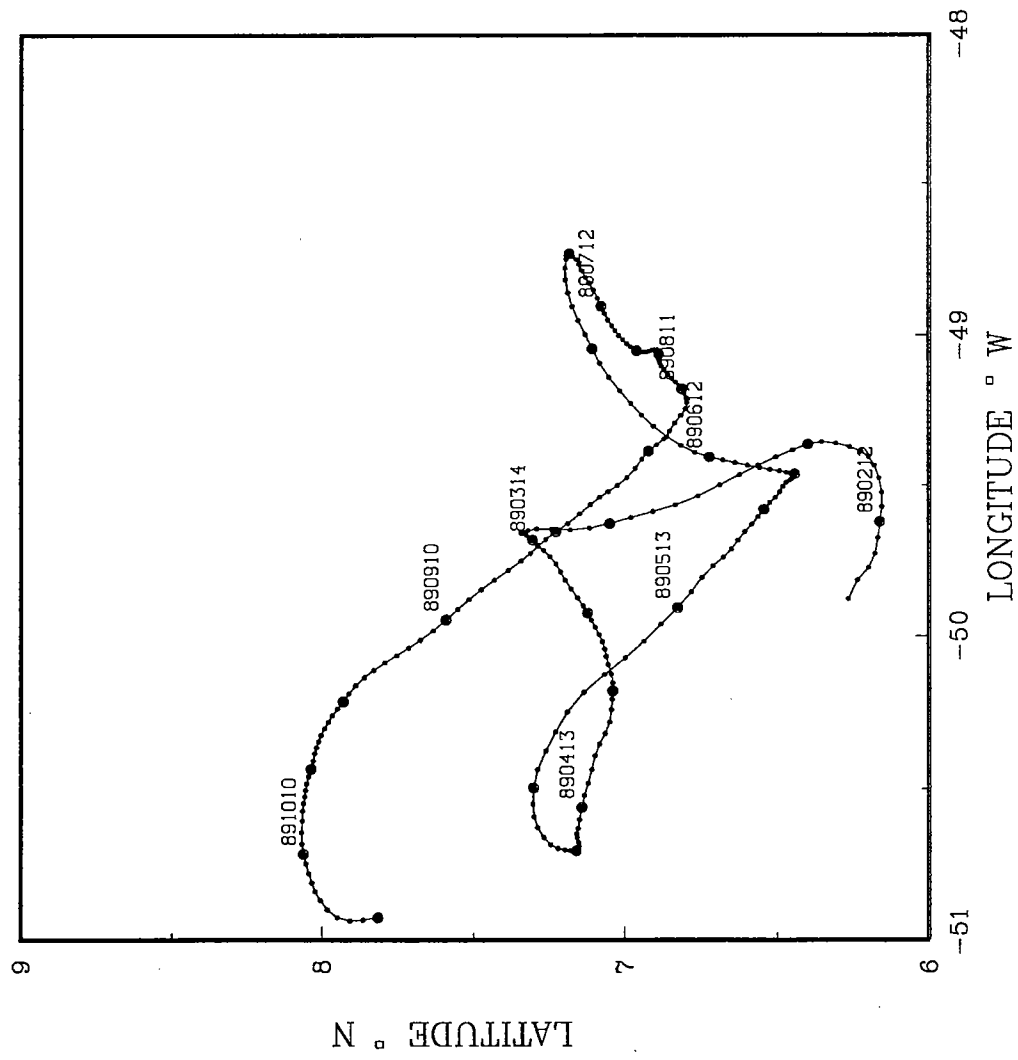


TROPICAL ATLANTIC 40
DEPTH 3300 m.

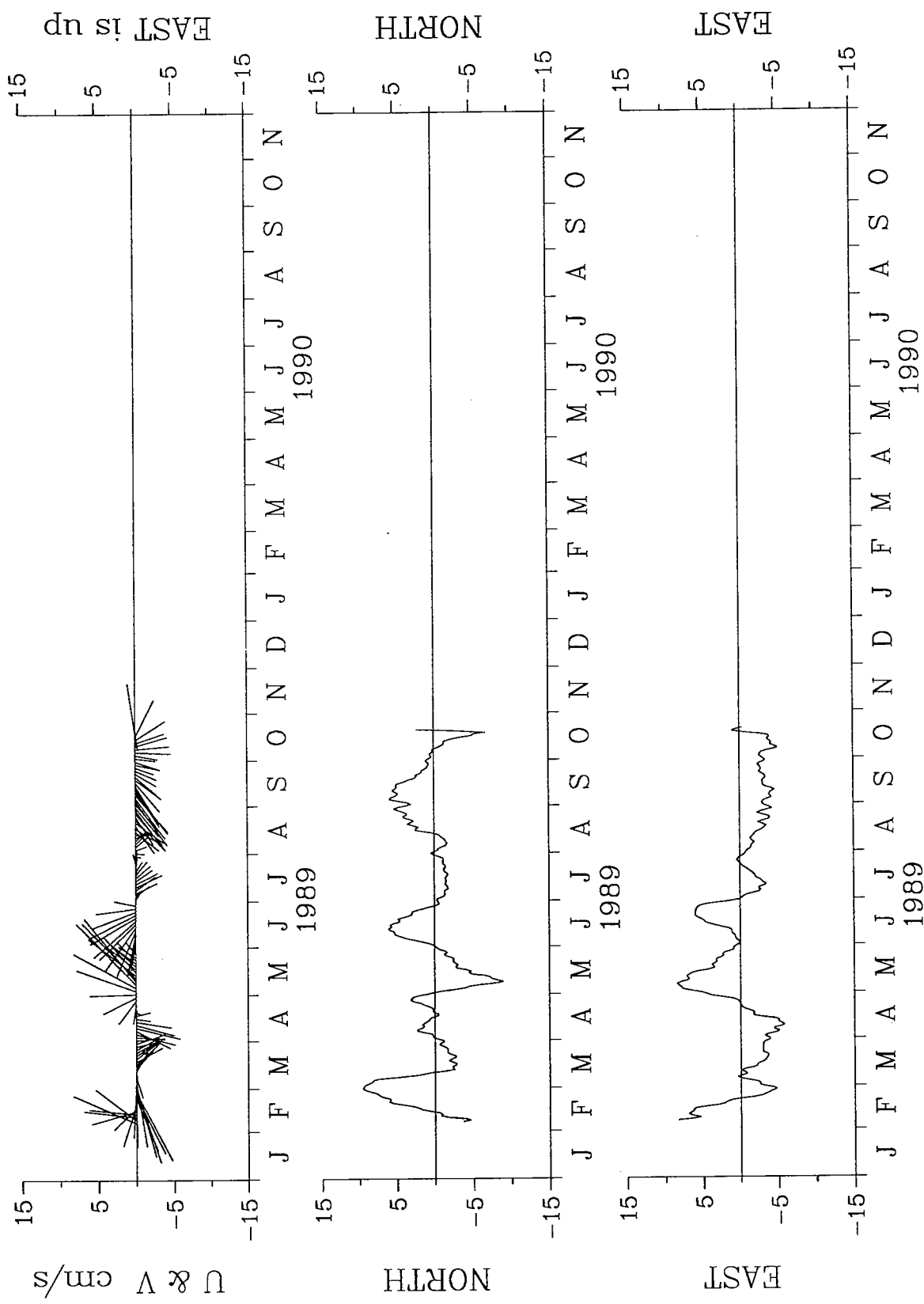


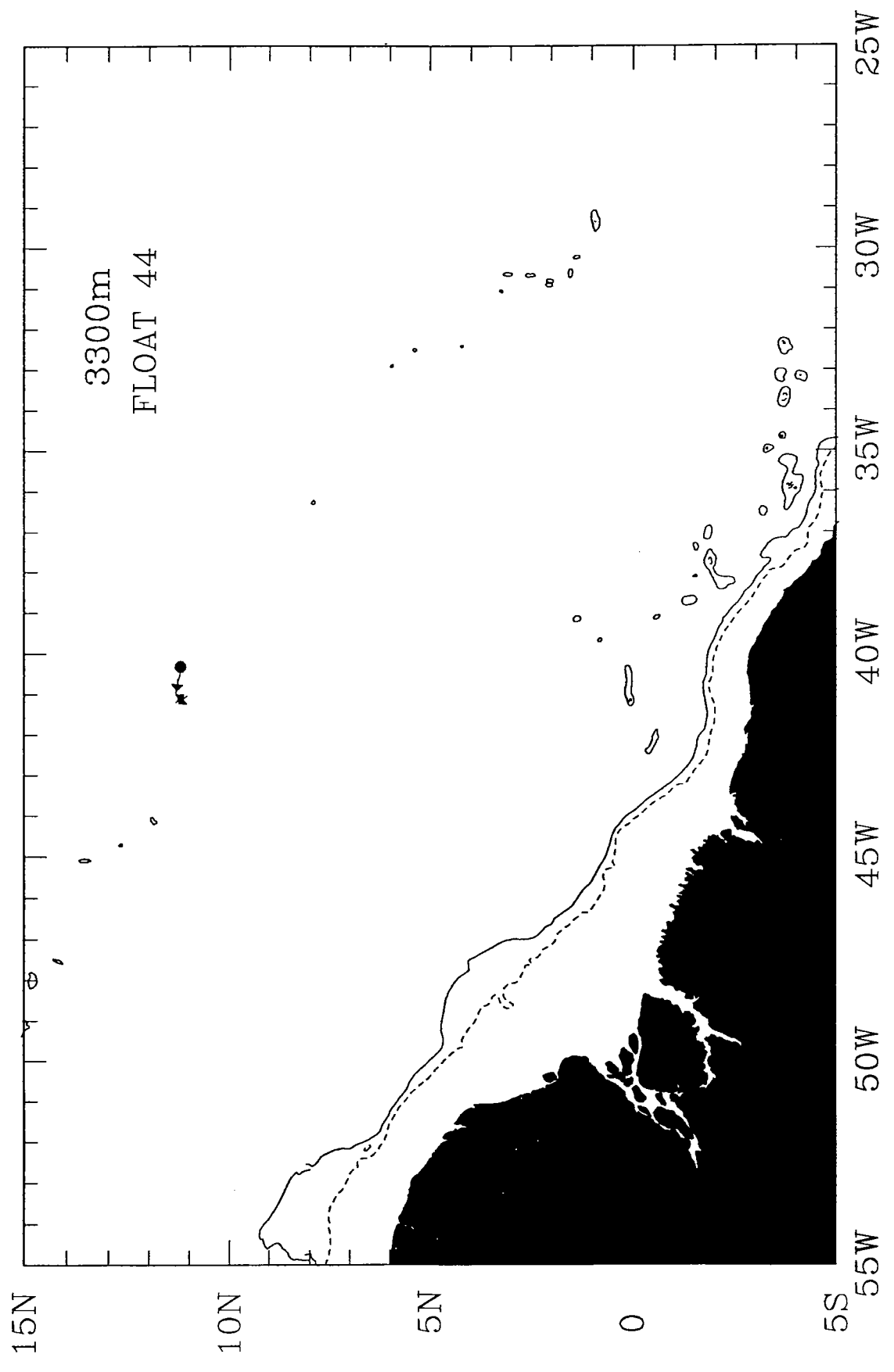


TROPICAL ATLANTIC 42

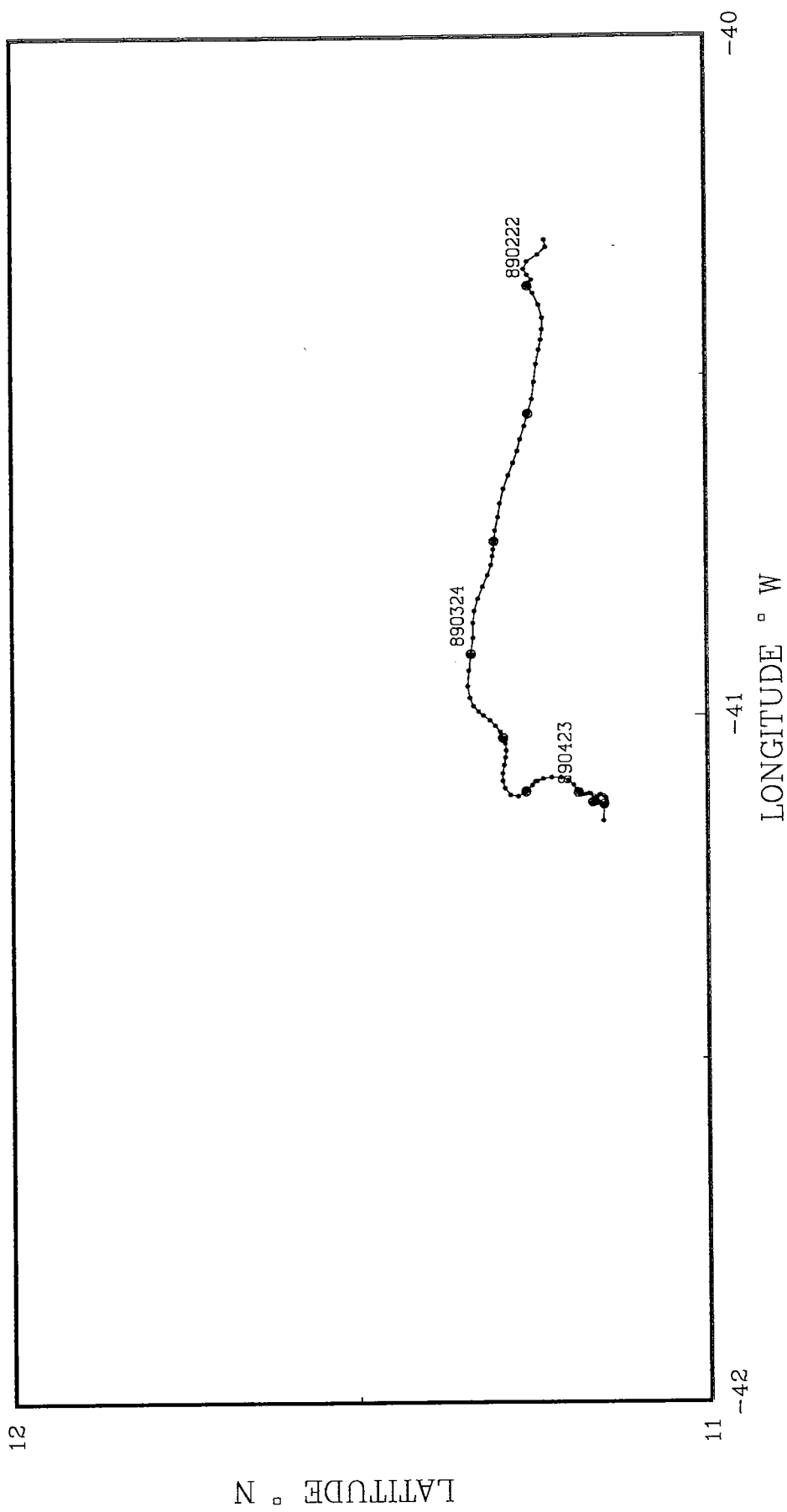


TROPICAL ATLANTIC 42
DEPTH 3300 m.





TROPICAL ATLANTIC 44



12

11

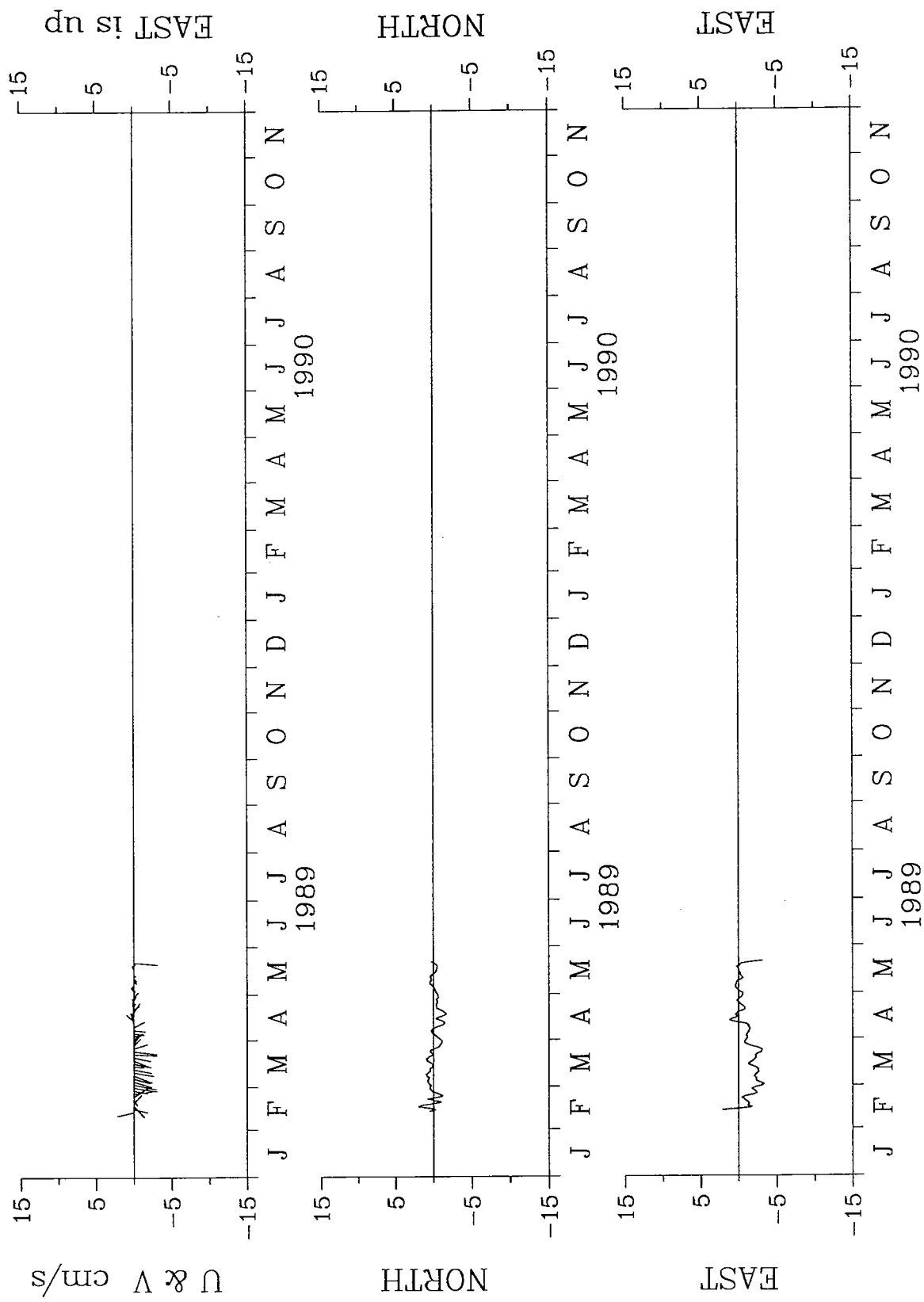
-42

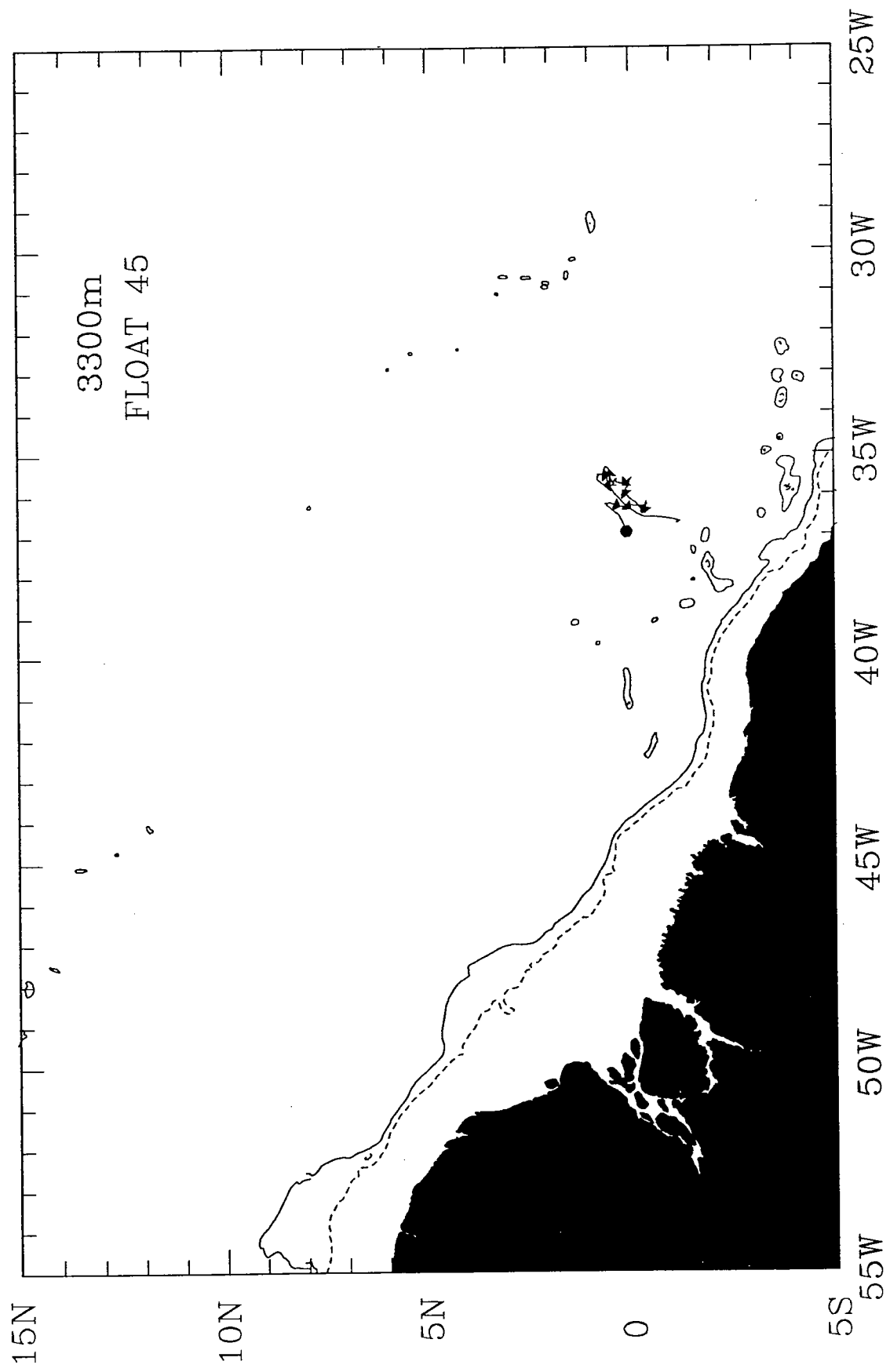
-41

LATITUDE ° N
LONGITUDE ° W

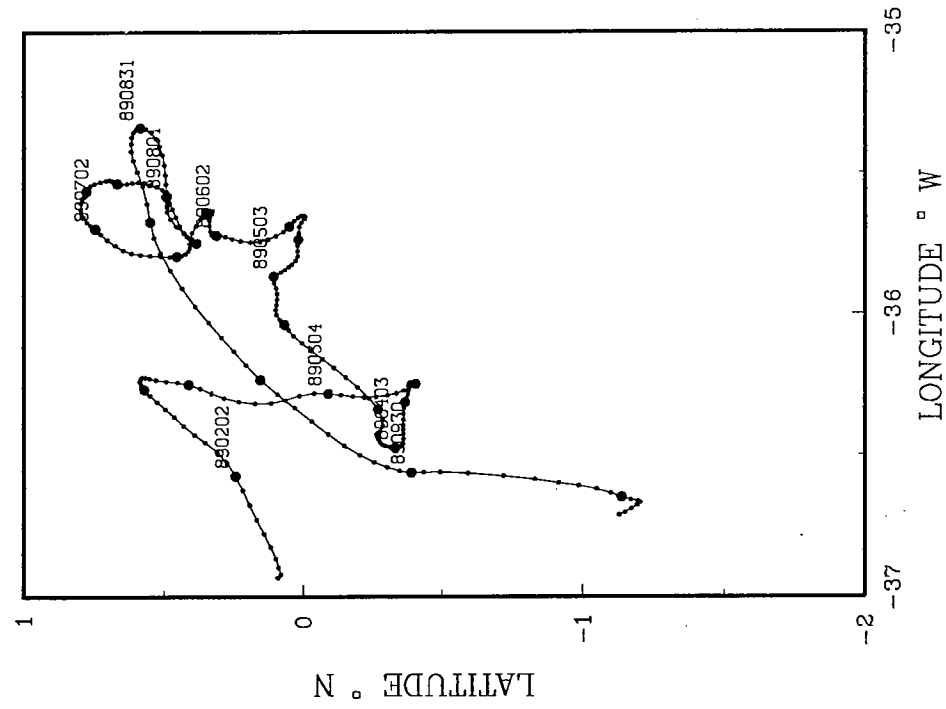
LATITUDE ° N

TROPICAL ATLANTIC 44
DEPTH 3300 m.

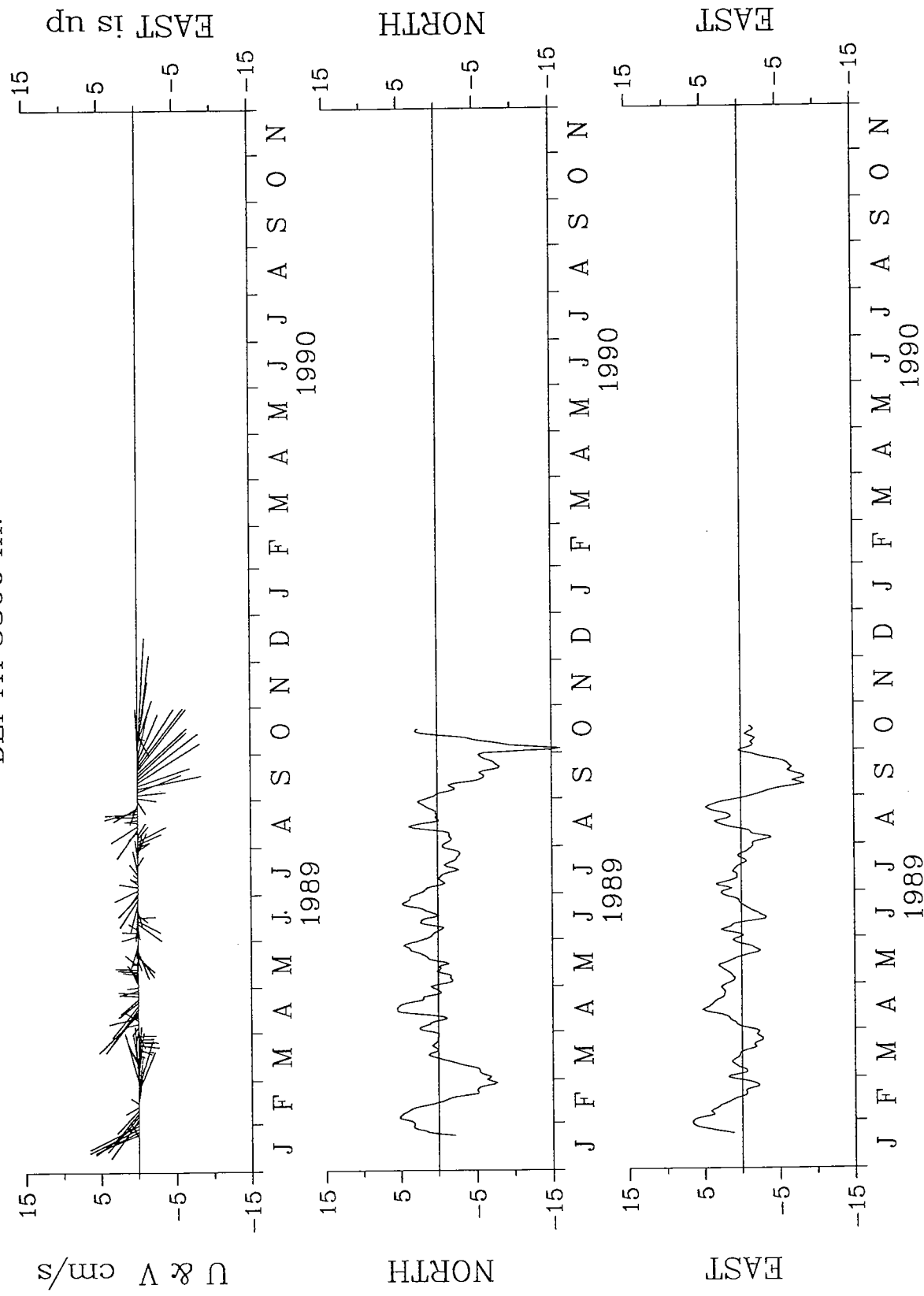




TROPICAL ATLANTIC 45



TROPICAL ATLANTIC 45
DEPTH 3300 m.



DOCUMENT LIBRARY

March 11, 1991

Distribution List for Technical Report Exchange

Attn: Stella Sanchez-Wade
Documents Section
Scripps Institution of Oceanography
Library, Mail Code C-075C
La Jolla, CA 92093

Hancock Library of Biology &
Oceanography
Alan Hancock Laboratory
University of Southern California
University Park
Los Angeles, CA 90089-0371

Gifts & Exchanges
Library
Bedford Institute of Oceanography
P.O. Box 1006
Dartmouth, NS, B2Y 4A2, CANADA

Office of the International
Ice Patrol
c/o Coast Guard R & D Center
Avery Point
Groton, CT 06340

NOAA/EDIS Miami Library Center
4301 Rickenbacker Causeway
Miami, FL 33149

Library
Skidaway Institute of Oceanography
P.O. Box 13687
Savannah, GA 31416

Institute of Geophysics
University of Hawaii
Library Room 252
2525 Correa Road
Honolulu, HI 96822

Marine Resources Information Center
Building E38-320
MIT
Cambridge, MA 02139

Library
Lamont-Doherty Geological
Observatory
Columbia University
Palisades, NY 10964

Library
Serials Department
Oregon State University
Corvallis, OR 97331

Pell Marine Science Library
University of Rhode Island
Narragansett Bay Campus
Narragansett, RI 02882

Working Collection
Texas A&M University
Dept. of Oceanography
College Station, TX 77843

Library
Virginia Institute of Marine Science
Gloucester Point, VA 23062

Fisheries-Oceanography Library
151 Oceanography Teaching Bldg.
University of Washington
Seattle, WA 98195

Library
R.S.M.A.S.
University of Miami
4600 Rickenbacker Causeway
Miami, FL 33149

Maury Oceanographic Library
Naval Oceanographic Office
Stennis Space Center
NSTL, MS 39522-5001

Marine Sciences Collection
Mayaguez Campus Library
University of Puerto Rico
Mayaguez, Puerto Rico 00708

Library
Institute of Oceanographic Sciences
Deacon Laboratory
Wormley, Godalming
Surrey GU8 5UB
UNITED KINGDOM

The Librarian
CSIRO Marine Laboratories
G.P.O. Box 1538
Hobart, Tasmania
AUSTRALIA 7001

Library
Proudman Oceanographic Laboratory
Bidston Observatory
Birkenhead
Merseyside L43 7 RA
UNITED KINGDOM

REPORT DOCUMENTATION PAGE		1. REPORT NO. WHOI-92-33	2.	3. Recipient's Accession No.
4. Title and Subtitle SOFAR Float Trajectories from an Experiment to Measure the Atlantic Cross Equatorial Flow (1989-1990)			5. Report Date August, 1992	6.
7. Author(s) Philip L. Richardson, Marguerite E. Zemanovic, Christine M. Wooding, William J. Schmitz, Jr. and James F. Price			8. Performing Organization Rept. No. WHOI 92-33	
9. Performing Organization Name and Address The Woods Hole Oceanographic Institution Woods Hole, Massachusetts 02543			10. Project/Task/Work Unit No.	
			11. Contract(C) or Grant(G) No. (C) OCE-8521082, OCE-8517375, (G) OCE-9114656	
12. Sponsoring Organization Name and Address Funding was provided by the National Science Foundation.			13. Type of Report & Period Covered Technical Report	
			14.	
15. Supplementary Notes This report should be cited as: Woods Hole Oceanog. Inst. Tech. Rept., WHOI-92-33.				
16. Abstract (Limit: 200 words) Neutrally buoyant SOFAR floats at nominal depths of 800, 1800, and 3300 m were tracked for 21 months in the vicinity of western boundary currents near 6N and at several sites in the Atlantic near 11N and along the equator. Trajectories at 1800 m show a swift (>50 cm/sec), narrow (100 km wide) southward-flowing deep western boundary current (DWBC) extending from 7N to the equator. At times (February-March 1989) DWBC water turned eastward and flowed along the equator and at other times (August-September 1990) the DWBC crossed the equator and continued southward. The mean velocity near the equator was eastward from February 1989 to February 1990 and westward from March 1990 to November 1990. Thus the cross-equatorial flow in the DWBC appeared to be linked to the direction of equatorial currents which varied over periods of more than a year. No obvious DWBC nor swift equatorial current was observed by 3300 m floats. Eight-hundred-meter floats revealed a northwestward intermediate level western boundary current although flow patterns were complicated. Three floats that significantly contributed to the northwestward flow looped in anticyclonic eddies that translated up the coast at 8 cm/sec. Six 800 m floats drifted eastward along the equator between 5S and 6N at a mean velocity of 11 cm/sec; one reached 5W in the Gulf of Guinea, suggesting that the equatorial current extended at least 35-40° along the equator. Three of these floats reversed direction near the end of the tracking period, implying low frequency fluctuations.				
17. Document Analysis a. Descriptors				
<ol style="list-style-type: none"> 1. SOFAR floats 2. Equatorial currents 3. deep western boundary current 				
b. Identifiers/Open-Ended Terms				
c. COSATI Field/Group				
18. Availability Statement Approved for publication; distribution unlimited.		19. Security Class (This Report) UNCLASSIFIED	21. No. of Pages 197	
		20. Security Class (This Page)	22. Price	

